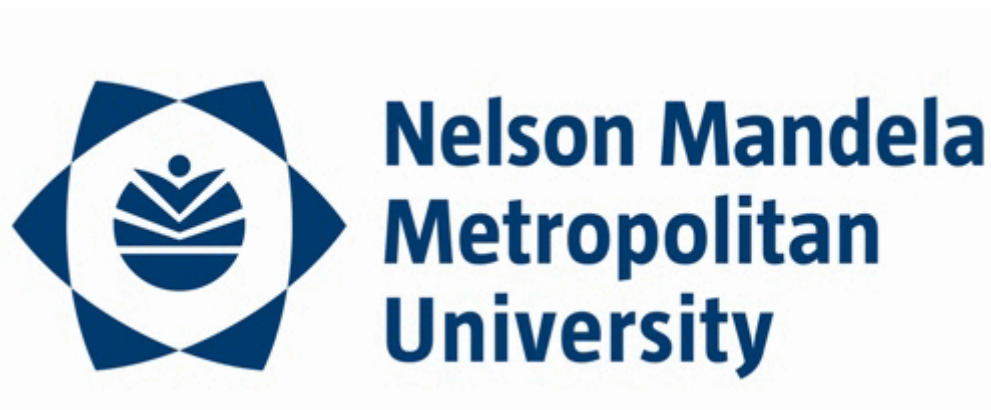


# **The Kinetics and Associated Equilibria of High Oxidation State Osmium Complexes**



by

**Belinda Julie McFadzean**

Submitted in fulfilment  
of the requirements for the degree of

**Philosophiae Doctor**

In the Faculty of Science  
at the Nelson Mandela Metropolitan University

December 2007

Supervisor: **Prof. H.E. Rohwer**

## ACKNOWLEDGEMENTS

**I would like to express my sincere thanks and acknowledgment to the following people:**

To my supervisor, Prof Hans Rohwer, for your encouragement, advice and support.

To Dr Eric Hosten and Dr Willem Gerber for your time, effort and thoughtful insight – it is much appreciated.

To my colleagues in the Chemistry department, thanks for your support – especially Lian von Wielligh for enduring arctic temperatures in the name of science and Theo Geswindt for solving a *very* long series of equations! Also to Yatish Jaganath – an unfailing source of help; Henk Schalekamp – because it was never too much effort; Lukas, Willem, Henk and Eric – my lunch buddies. And to all in the lab – Jolanda, Yolanda, Talana, Michelle, Kivara, Marissa, Diba, Zeni, Irvin – you all touched my life.

**For financial assistance my grateful thanks to:**

Anglo Platinum Research Centre

National Research Foundation

Nelson Mandela Metropolitan University and the Inorganic Chemistry Department

**And finally...**

To Mom and Dad – you are my strength and my inspiration,

To Greg – for believing in me,

And in memory of Harry, the dog – my faithful companion.

# TABLE OF CONTENTS

<b>Acknowledgements</b>	i
<b>Table of contents</b>	ii
<b>List of Figures</b>	vi
<b>List of Tables</b>	xvi
<b>Abbreviations</b>	xix
<b>Summary</b>	xx

## Chapter 1 – Introduction

1.1	History of osmium	1
1.2	Uses – past and present	2
1.3	General coordination chemistry of osmium	4
1.3.1	Oxidation states	4
1.3.2	Coordination numbers	5
1.3.3	Ligands	6
1.4	Osmium(VIII)	7
1.5	Osmium(VI)	9
1.6	Aims and objectives	11

## Chapter 2 – Experimental

2.1	Apparatus	12
2.1.1	Ultraviolet and visible spectra	12
2.1.2	Nuclear magnetic resonance spectroscopy	12
2.1.3	pH measurements	12
2.1.4	Potentiometric measurements	12
2.1.5	Potentiometric titrations	12
2.2	Computer software	13
2.3	Standardisation of reagents	14
2.3.1	Preparation of a standard iron(II) solution	14
2.3.2	Preparation of a standard hydrochloric acid solution	14

2.3.3	Preparation of a standard sodium hydroxide solution	15
2.4	Reagents used	15
2.5	Determination of potentiometric endpoints	18
2.6	Preparation and storage of osmium tetroxide	18
2.6.1	Introduction	18
2.6.2	Preparation procedure	19
2.7	Preparation of potassium osmate	22
2.8	Determining osmium concentration	22

### **Chapter 3 – The alcohol-osmium tetroxide reaction**

3.1	Introduction	24
3.2	Experimental	34
3.3	Results and discussion	36
3.4	Summary	39

### **Chapter 4 – Determining the reactants**

4.1	Introduction	40
4.2	Experimental	45
4.2.1	Osmium(VIII) – iron titrations: determining initial oxidation state	45
4.2.2	Molar extinction coefficients	45
4.2.3	Stability of osmium(VIII) in hydroxide medium	46
4.3	Results and discussion	46
4.3.1	Theoretically determined osmium(VIII) and organic reactant species	46
4.3.2	Osmium(VIII) – iron titrations: determining initial oxidation state	48
4.3.3	Molar extinction coefficients	48
4.3.4	Stability of osmium(VIII) in hydroxide medium	50
4.4	Summary	54



**Chapter 5 – Determining the products**

5.1	Introduction	55
5.2	Experimental	56
5.2.1	Osmium products	56
5.2.2	Organic products	59
5.3	Results and discussion	60
5.3.1	Osmium products	60
5.3.2	Organic products	74
5.4	Summary	82

**Chapter 6 – Equilibrium stoichiometry**

6.1	Introduction	84
6.2	Experimental	85
6.2.1	Alcohols	85
6.2.2	Ketones	85
6.3	Results	86
6.3.1	Equilibrium Reaction Model 1	86
6.3.2	Equilibrium Reaction Model 2	102
6.4	Summary	110

**Chapter 7 – Fitting the kinetic reaction model**

7.1	Introduction	112
7.2	Experimental	114
7.3	Results	115
7.3.1	Alcohol models	116
7.3.2	Ketone models	127
7.3.3	Discussion	137

**Chapter 8 – A comparative rate study**

8.1	Introduction	142
8.1.1	Varying the osmium concentration	142

8.1.2	Varying the ionic strength	143
8.1.3	Varying the pH	143
8.1.4	Varying the dielectric constant	144
8.1.5	Varying the temperature	145
8.1.6	Varying the substrate concentration	146
8.1.7	Varying the substrate	146
8.2	Experimental	148
8.2.1	Varying the osmium concentration	149
8.2.2	Varying the ionic strength	149
8.2.3	Varying the pH	149
8.2.4	Varying the dielectric constant	150
8.2.5	Varying the temperature	150
8.2.6	Varying the reducing agent	150
8.3	Results	151
8.3.1	Varying the osmium concentration	151
8.3.2	Varying the ionic strength	153
8.3.3	Varying the pH	155
8.3.4	Varying the dielectric constant	160
8.3.5	Varying the temperature	165
8.3.6	Varying the substrate and substrate concentration	179
8.4	Summary	193
	<b>Chapter 9 – Conclusion</b>	194
	<b>References</b>	205

# LIST OF FIGURES

<b>Chapter 1</b>	<b>Page</b>
Figure 1.1: A graphical representation of the electroactive species' (A) involvement in mediation of electron transfer from the electrode to the analyte in solution	3
Figure 1.2: $[\text{Os}(\text{bipy})_2\text{Cl}_2]^+$	4
<b>Chapter 2</b>	
Figure 2.1: Experimental set-up for the preparation of an organic osmium tetroxide solution	19
Figure 2.2: Plots of $\log c_{\text{org}}$ vs $\log c_{\text{aq}}$ for the extraction of osmium tetroxide from carbon tetrachloride into basic aqueous solutions.	20
Figure 2.3: A plot showing the extent of stripping of osmium tetroxide from a carbon tetrachloride solution into aqueous solutions at low hydroxide concentrations.	21
Figure 2.4: A calibration curve for the thiourea colourometric method	23
<b>Chapter 3</b>	
Figure 3.1: Generally accepted mechanism for the oxidation of alkenes to <i>cis</i> -diols	26
Figure 3.2: (a) <i>syn</i> - and (b) <i>anti</i> - dimeric monoesters (c) monomeric diester	26
Figure 3.3: Proposed pathways, a and b, for the reaction of organic reductant, R, with osmium tetroxide	27
Figure 3.4: Mechanism proposed by Sharpless <i>et al</i> involving nucleophilic attack by the C-C double bond on the electropositive osmium	28
Figure 3.5: Mechanism for the oxidation of alcohols	29
Figure 3.6: The mechanism of oxidation of alcohols by chromium trioxide	32
Figure 3.7: The change in the spectra over time of the reaction of 0.0103M ethanol with $4.40 \times 10^{-4}\text{M}$ $[\text{OsO}_4]$ in 2M NaOH. The spectra change in the direction of the solid arrows over time: from time = 0min to time = 56min37s. (Scanning 500nm to 200nm; 960nm/min; 1 cycle/min.)	37

- Figure 3.8: The progress curves of the rate of change of absorbance at 370nm at varying ethanol concentrations.  $[\text{OsO}_4] = 4.32 \times 10^{-4}\text{M}$ ;  $[\text{NaOH}] = 2\text{M}$ . 37
- Figure 3.9: The change in spectra over time up to the end of step 1. These are the spectra relating to the progress curve shown in Figure 3.9 for the following reactant concentrations:  $[\text{Ethanol}] = 0.00196\text{M}$ ;  $[\text{OsO}_4] = 4.32 \times 10^{-4}\text{M}$ ;  $[\text{NaOH}] = 2\text{M}$ . 38
- Figure 3.10: Spectra isolated at various times during the reaction of 0.0103M ethanol with  $4.40 \times 10^{-4}\text{M}$   $[\text{OsO}_4]$  in 2M NaOH. These depict, as closely as possible, species A (time = 0min), species B (time = 1min37s) and species C (time = 56min37s). 38
- Chapter 4**
- Figure 4.1: Species distribution diagram for  $[\text{OsO}_4]$  as a function of pH.  $\text{Os} = [\text{OsO}_4]$ ;  $\text{Os1H1} = [\text{OsO}_4(\text{OH})^-]$ ; and  $\text{Os1H2} = [\text{OsO}_4(\text{OH})_2]^{2-}$  41
- Figure 4.2: Potentiometric titration curves for the titration of an acidic 0.00193M iron(II) solution with a) 0.00137M osmium tetroxide in distilled water; and b) 0.00116M osmium tetroxide in 2M hydroxide. 48
- Figure 4.3: The UV-VIS spectra of osmium tetroxide solutions of varying concentration in 2M hydroxide. (a) y-axis = 0 to 2.6 (b) y-axis = 0 to 0.6 49
- (a) The progress curves of a  $4.93 \times 10^{-4}\text{M}$  osmium tetroxide solution in 2M hydroxide over time. 51
- Figure 4.4: (b) Selected spectra (corresponding to species A, B and C) taken at different times during the reaction of  $4.93 \times 10^{-4}\text{M}$  osmium tetroxide solution with 2M hydroxide.
- Figure 4.5: The progress curves of the rate of change of absorbance at 370nm at varying ethanol concentrations.  $[\text{OsO}_4] = 4.32 \times 10^{-4}\text{M}$ ;  $[\text{NaOH}] = 2\text{M}$ . Reaction with 0M ethanol;  $[\text{OsO}_4] = 4.93 \times 10^{-4}\text{M}$ ;  $[\text{NaOH}] = 2\text{M}$ . 53
- Chapter 5**
- Figure 5.1: Experimental set-up for the preparation of organic products for NMR analysis 59

- Figure 5.2: Mole ratio plot for the reaction of  $4.07 \times 10^{-4}$  M osmium tetroxide with increasing concentrations of 1-propanol in 2M hydroxide. Solutions were reacted for 3 hours at 25°C. 60
- Figure 5.3: Mole ratio plot for the reaction of  $3.97 \times 10^{-4}$  M osmium tetroxide with increasing concentrations of 2-propanol in 2M hydroxide. Solutions were reacted for 3 hours at 25°C. 61
- Figure 5.4: Potentiometric titration curves for the reaction of an acidic iron(II) solution of known concentration with an osmium solution obtained in the following manner: (a) Osmium tetroxide and ethanol of known concentrations reacted overnight in 0.1M hydroxide (b) Osmium tetroxide and acetophenone of known concentrations reacted for 10 minutes in 2M hydroxide 63
- Figure 5.5: The UV-VIS spectra of “species B’ as formed during the reaction of osmium tetroxide with selected alcohols, ketones, hexamethylphosphoramide, maleic acid or simply in hydroxide. The spectra were selected to conform as closely as possible to the maxima on a kinetic progress curve. 66
- The UV-VIS spectra of pure potassium osmate in 2M hydroxide compared to the spectra of osmium tetroxide reacted with an excess of selected alcohols or ketones (or just in hydroxide) until final equilibrium was reached. 67
- Figure 5.6: 68
- Figure 5.7: The volume corrected spectra of the titration of 2.5ml of a 0.00151M osmium tetroxide solution with a 0.00111M osmate solution in 2M hydroxide matrix. 68
- Figure 5.8: The mole ratio plot of the same titration (as Figure 5.7) at selected wavelengths with intersecting straight lines drawn through the linear portions of the curves. Also shown is the potential during the titration. 69
- Figure 5.9: The UV-VIS spectra of  $1.77 \times 10^{-4}$  M osmium tetroxide in 2M hydroxide;  $1.61 \times 10^{-4}$  M potassium osmate in 2M hydroxide; the calculated absorbance spectrum of the osmium tetroxide plus the potassium osmate; the actual absorbance spectrum at the endpoint of the reaction of  $1.77 \times 10^{-4}$  M osmium tetroxide with  $1.61 \times 10^{-4}$  M 71

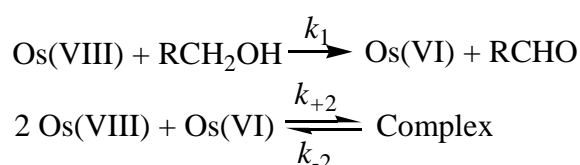
	potassium osmate in 2M hydroxide; and a sample of the absorbance spectrum for species B, from a 2-pentanone titration.	
Figure 5.10:	Absorbance at 370nm versus absorbance at 250nm taken from the spectra of the reactions of osmium tetroxide with various alcohols, ketones and hydroxide over time.	73
Figure 5.11:	The C <sup>13</sup> NMR spectrum of the final solution after reaction of osmium tetroxide with ACETONE in 2M hydroxide.	74
Figure 5.12:	The C <sup>13</sup> NMR spectrum of the final solution after reaction of osmium tetroxide with BENZYL ALCOHOL in 2M hydroxide.	75
Figure 5.13:	The C <sup>13</sup> NMR spectrum of the final solution after reaction of osmium tetroxide with 1-BUTANOL in 2M hydroxide.	75
Figure 5.14:	The C <sup>13</sup> NMR spectrum of the final solution after reaction of osmium tetroxide with 2-BUTANOL in 2M hydroxide.	76
Figure 5.15:	The C <sup>13</sup> NMR spectrum of the final solution after reaction of osmium tetroxide with ETHANOL in 2M hydroxide.	76
Figure 5.16:	The C <sup>13</sup> NMR spectrum of the final solution after reaction of osmium tetroxide with HEXAMETHYLPHOSPHORAMIDE in 2M hydroxide.	77
Figure 5.17:	The C <sup>13</sup> NMR spectrum of the final solution after reaction of osmium tetroxide with METHYL ETHYL KETONE in 2M hydroxide.	77
Figure 5.18:	The C <sup>13</sup> NMR spectrum of the final solution after reaction of osmium tetroxide with 2-PENTANONE in 2M hydroxide.	78
Figure 5.19:	The C <sup>13</sup> NMR spectrum of the final solution after reaction of osmium tetroxide with 1-PROPANOL in 2M hydroxide	78
Figure 5.20:	The C <sup>13</sup> NMR spectrum of the final solution after reaction of osmium tetroxide with 2-PROPANOL in 2M hydroxide.	79
<b>Chapter 6</b>		
Figure 6.1:	Mole ratio plot of 4.05x10 <sup>-4</sup> M osmium tetroxide with increasing concentrations; (a) methanol; and (b) ethanol; in 2M hydroxide medium	87
Figure 6.2:	Mole ratio plot of (a) 4.07x10 <sup>-4</sup> M osmium tetroxide with increasing concentrations 1-propanol; and (b) 3.97x10 <sup>-4</sup> M osmium	88

	tetroxide with increasing concentrations 2-propanol; in 2M hydroxide medium.	
Figure 6.3:	Mole ratio plot of (a) $4.14 \times 10^{-4}$ M osmium tetroxide with increasing concentrations 1-butanol; and (b) $4.28 \times 10^{-4}$ M osmium tetroxide with increasing concentrations 2-butanol; in 2M hydroxide medium	89
Figure 6.4:	Mole ratio plot of $4.07 \times 10^{-4}$ M osmium tetroxide with increasing concentrations benzyl alcohol in 2M hydroxide medium.	90
Figure 6.5:	The complete spectrum (500nm to 200nm) of each solution given by the mole ratios at each point in Figure 6.4.	90
Figure 6.6:	The spectrophotometric titration of (a) 10ml of 0.00173M osmium tetroxide in 2M hydroxide with 0.00950M ACETONE in 2M hydroxide; and (b) 10ml of 0.00154M osmium tetroxide in 2M hydroxide with 0.00856M ACETOPHENONE in 2M hydroxide.	95
Figure 6.7:	The spectrophotometric titration of (a) 10ml of 0.00149M osmium tetroxide in 2M hydroxide with 0.00558M METHYL ETHYL KETONE in 2M hydroxide; and (b) 10ml of 0.00145M osmium tetroxide in 2M hydroxide with 0.00468M 2-PENTANONE in 2M hydroxide.	96
Figure 6.8:	The complete spectrum (500nm to 200nm) after each addition of acetophenone.	97
Figure 6.9:	Theoretical and experimental curves for the reaction of increasing concentrations methanol with $4.05 \times 10^{-4}$ M osmium tetroxide in 2M hydroxide, at equilibrium.	104
Figure 6.10:	Theoretical and experimental curves for the reaction of increasing concentrations ethanol with $4.05 \times 10^{-4}$ M osmium tetroxide in 2M hydroxide, at equilibrium.	104
Figure 6.11:	Theoretical and experimental curves for the reaction of increasing concentrations 1-propanol with $4.07 \times 10^{-4}$ M osmium tetroxide in 2M hydroxide, at equilibrium.	105
Figure 6.12:	Theoretical and experimental curves for the reaction of increasing concentrations 1-butanol with $4.14 \times 10^{-4}$ M osmium tetroxide in 2M hydroxide, at equilibrium.	105

- Figure 6.13: Theoretical and experimental curves for the reaction of increasing concentrations benzyl alcohol with  $4.07 \times 10^{-4} \text{M}$  osmium tetroxide in 2M hydroxide, at equilibrium. 106
- Figure 6.14: Theoretical and experimental curves for the reaction of increasing concentrations 2-propanol with  $3.97 \times 10^{-4} \text{M}$  osmium tetroxide in 2M hydroxide, at equilibrium. 108
- Figure 6.15: Theoretical and experimental curves for the reaction of increasing concentrations 2-butanol with  $4.28 \times 10^{-4} \text{M}$  osmium tetroxide in 2M hydroxide, at equilibrium. 108

### Chapter 7

- Figure 7.1: The best theoretical fit to the experimental data for the model: 138



### Chapter 8

- Figure 8.1: Progress curves of the reaction of varying concentrations of osmium tetroxide with 0.01M ethanol in a 2M hydroxide matrix. The slopes of the tangents to the curves give the initial rate of the first and second steps of the reaction. 151
- Figure 8.2: log initial rates of the osmium tetroxide – ethanol reaction for the first and second steps, plotted versus log of the osmium concentrations used. 152
- Figure 8.3: Progress curves of  $4.23 \times 10^{-4} \text{M}$  osmium tetroxide with 0.0095M ethanol in 0.05M hydroxide matrix. Increasing concentrations of sodium perchlorate (0.01M to 0.05M) were added to each reaction without affecting the rates of the reactions. The complexation reaction model 1.2 was fitted to each progress curve using the rate constants shown in the figure. 154
- Figure 8.4: Progress curves of 0.00248M osmium tetroxide with 0.01M ethanol in a 0.1M hydroxide matrix. Increasing concentrations of sodium perchlorate were added to the reactions without affecting the rates. 154
- Figure 8.5: Progress curves of the reactions of  $4.37 \times 10^{-4} \text{M}$  osmium tetroxide 156



- with 0.0098M ethanol in varying concentrations of sodium hydroxide.
- Figure 8.6: log initial rate plotted versus log hydroxide concentration for the reactions of ethanol with osmium tetroxide in varying hydroxide concentrations. 157
- Figure 8.7: Progress curves of the reactions of  $3.45 \times 10^{-4}$ M osmium tetroxide with  $3.2 \times 10^{-4}$ M MEK in varying concentrations sodium hydroxide. 158
- Figure 8.8: log hydroxide concentration versus log initial rate for the reactions of MEK with osmium tetroxide in varying hydroxide concentrations. 158
- Figure 8.9: Progress curves of the reaction of  $4.48 \times 10^{-4}$ M osmium tetroxide with 0.01M ethanol in a 0.1M hydroxide matrix with varying tertiary butanol concentrations. 160
- Figure 8.10: Progress curves of the reaction of  $4.48 \times 10^{-4}$ M osmium tetroxide with 0.01M ethanol in a 0.1M hydroxide matrix with varying acetonitrile concentrations. 161
- Figure 8.11: The rate constant,  $k_1$ , as a function of tertiary butanol and acetonitrile concentration, respectively.  $[\text{OsO}_4] = 4.48 \times 10^{-4}\text{M}$ ;  $[\text{Ethanol}] = 0.01\text{M}$ ;  $[\text{Hydroxide}] = 0.01\text{M}$ . 162
- Figure 8.12: Progress curves of the reaction of  $2.92 \times 10^{-4}$ M osmium tetroxide with no ethanol present in a 2M hydroxide matrix with varying HMPA concentrations. 164
- Figure 8.13: Progress curves of the reaction of  $5.59 \times 10^{-4}$ M osmium tetroxide with 0.01M (a) methanol and (b) ethanol; in 2M hydroxide at various temperatures. 166
- Figure 8.14: Progress curves of the reaction of  $5.59 \times 10^{-4}$ M osmium tetroxide with 0.01M (a) 1-propanol and (b) 2-propanol; in 2M hydroxide at various temperatures. 167
- Figure 8.15: Progress curves of the reaction of  $5.59 \times 10^{-4}$ M osmium tetroxide with 0.01M (a) 1-butanol and (b) 2-butanol; in 2M hydroxide at various temperatures. 168

Figure 8.16:	The rate constants, $k_1$ , as a function of temperature.	169
Figure 8.17:	Equilibrium constant, $K_{eq}$ , as a function of temperature.	169
Figure 8.18:	Arrhenius plots for the various alcohols in 2M hydroxide medium.	171
Figure 8.19:	Progress curves of the reaction of $3.91 \times 10^{-4}$ M osmium tetroxide with $6.22 \times 10^{-4}$ M acetone in a 0.1M hydroxide medium at various temperatures.	173
Figure 8.20:	Progress curves of the reaction of $3.91 \times 10^{-4}$ M osmium tetroxide with $3.50 \times 10^{-4}$ M MEK in a 0.1M hydroxide medium at various temperatures.	173
Figure 8.21:	Progress curves of the reaction of $3.91 \times 10^{-4}$ M osmium tetroxide with $1.59 \times 10^{-4}$ M acetophenone in a 0.1M hydroxide medium at various temperatures.	174
Figure 8.22:	The relationship between the rate constant, $k_1$ , and temperature for the three ketones, acetone, MEK and acetophenone, in 0.1M hydroxide medium.	175
Figure 8.23:	The relationship between the equilibrium constant, $K_{eq}$ , and temperature for the three ketones, acetone, MEK and acetophenone, in 0.1M hydroxide medium.	176
Figure 8.24:	Arrhenius plot for acetone, MEK and acetophenone in 0.1M hydroxide medium.	176
Figure 8.25:	Progress curves of the reaction of $3.80 \times 10^{-4}$ M osmium tetroxide with increasing concentrations METHANOL in 2M hydroxide matrix.	179
Figure 8.26:	Progress curves of the reaction of $4.32 \times 10^{-4}$ M osmium tetroxide with increasing concentrations ETHANOL in 2M hydroxide matrix.	180
Figure 8.27:	Progress curves of the reaction of $4.32 \times 10^{-4}$ M osmium tetroxide with increasing concentrations 1-PROPANOL in 2M hydroxide matrix.	180
Figure 8.28:	Progress curves of the reaction of $4.32 \times 10^{-4}$ M osmium tetroxide with increasing concentrations 2-PROPANOL in 2M hydroxide matrix.	181
Figure 8.29:	Progress curves of the reaction of $3.80 \times 10^{-4}$ M osmium tetroxide	181

	with increasing concentrations 1-BUTANOL in 2M hydroxide matrix.	
Figure 8.30:	Progress curves of the reaction of $4.80 \times 10^{-4}$ M osmium tetroxide with increasing concentrations 2-BUTANOL in 2M hydroxide matrix.	182
Figure 8.31:	Progress curves of the reaction of $8.54 \times 10^{-4}$ M osmium tetroxide with increasing concentrations 2-CHLOROETHANOL in 2M hydroxide matrix.	182
Figure 8.32:	Progress curves of the reaction of $3.71 \times 10^{-4}$ M osmium tetroxide with increasing concentrations BENZYL ALCOHOL in 2M hydroxide matrix.	183
Figure 8.33:	Progress curves of the reaction of $3.45 \times 10^{-4}$ M osmium tetroxide with increasing concentrations ACETONE in 0.1M hydroxide matrix.	183
Figure 8.34:	Progress curves of the reaction of $3.76 \times 10^{-4}$ M osmium tetroxide with increasing concentrations MEK in 0.1M hydroxide matrix.	184
Figure 8.35:	Progress curves of the reaction of $3.76 \times 10^{-4}$ M osmium tetroxide with increasing concentrations 2-PENTANONE in 0.1M hydroxide matrix.	184
Figure 8.36:	Progress curves of the reaction of $3.97 \times 10^{-4}$ M osmium tetroxide with increasing concentrations ACETOPHENONE in 0.1M hydroxide matrix.	185
Figure 8.37:	Progress curves of the reaction of $3.89 \times 10^{-4}$ M osmium tetroxide with increasing concentrations MALEIC ACID in 2M hydroxide matrix.	185
Figure 8.38:	Best fit of the theoretical complexation model to the reaction of $4.93 \times 10^{-4}$ M osmium tetroxide in 2M hydroxide	188
Figure 8.39:	Comparison of the rate constants, $k_1$ , for the reaction of osmium tetroxide with alcohols and maleic acid in a 2M hydroxide matrix.	189
Figure 8.40:	Comparison of the rate constants, $k_1$ , for the reaction of osmium tetroxide with the simple alcohols, methanol to butanol, in a 2M hydroxide matrix.	189
Figure 8.41:	Comparison of the rate constants, $k_1$ , for the reaction of osmium	190

tetroxide with ketones in a 0.1M hydroxide matrix.

- Figure 8.42: Taft plot, incorporating the alcohols ethanol, 1-propanol, 2-propanol, 1-butanol and 2-butanol. 192
- Figure 8.43: Taft plot, incorporating all of the alcohols from Figure 8.46, as well as benzyl alcohol and 2-chloroethanol. 192

## Chapter 9

- Figure 9.1: Part 1 of the hydride transfer model – from the associative reaction of the primary or secondary alcohol molecule with the osmium(VIII), to formation of the osmate ion and the aldehyde or ketone. 195
- Figure 9.2: The E2 C-H bond cleavage model 196
- Figure 9.3: The hydride transfer model for benzyl alcohol showing the resonance stabilisation of the associative transition state. 199
- Figure 9.4: Proton abstraction mechanism for the reaction of 2-chloroethanol with osmium tetroxide in basic medium. 200
- Figure 9.5: Part 2 of the hydride transfer model for primary alcohols. The reaction mechanism for the reaction of an aldehyde with osmium(VIII) in basic medium. 201
- Figure 9.6: Part 2 of the hydride transfer model for secondary alcohols. The reaction mechanism for the reaction of an ketone with osmium(VIII) in basic medium. Note that the reactive organic species is the enolate ion. 202
- Figure 9.7: Trimer formation between osmium(VIII) and osmium(VI) 203

# LIST OF TABLES

---

<b>Chapter 1</b>	<b>Page</b>
Table 1.1: Unusual coordination numbers for osmium complexes	6
<b>Chapter 2</b>	
Table 2.1: Reagents used in this study	15
<b>Chapter 3</b>	
Table 3.1: Second order rate constants for the oxidation of hydroxyl compounds by Os(VIII) in alkaline medium	29
Table 3.2: Reactant volumes and concentrations for the reaction of osmium tetroxide with ethanol in 2M sodium hydroxide matrix	35
<b>Chapter 4</b>	
Table 4.1: Average acid dissociation constants calculated in a previous study by this author <sup>(31)</sup> compared to other values reported in the literature <sup>(32)</sup> .	41
Table 4.2: Percentages of the various osmium(VIII) species present in solutions of varying pH calculated from species distribution diagram, Figure 4.1	46
Table 4.3: Theoretically calculated percentages of some alcohol/alkoxide ratios in solutions of varying pH	47
<b>Chapter 5</b>	
Table 5.1: Number of equivalents Fe(II) ( $n$ ) required to reduce osmium solutions (labelled in Figures 5.2 and 5.3) to osmium(IV) and the starting oxidation state that this implies	61
Table 5.2: Number of equivalents Fe(II) ( $n$ ) required to reduce osmium solutions to osmium(IV) and the starting oxidation state that this implies	62
Table 5.3: Number of equivalents Fe(II) ( $n$ ) required to reduce osmium solutions to osmium(IV) and the starting oxidation state that this implies	64

Table 5.4:	Molar extinction coefficient ( $\epsilon$ ) at 370nm of species B as calculated from the plots in Figure 5.3.	73
Table 5.5:	The organic products of the reaction osmium tetroxide with a reducing agent in 2M hydroxide as elucidated by NMR spectroscopy	80
Table 5.6:	Organic half-reactions using the known major products of the reactants	81
<b>Chapter 6</b>		
Table 6.1:	The mole ratios are given at the endpoints of the reactions as determined by least squares analysis of the linear portions of the graphs depicted in Figures 6.5 and 6.6. Also given are the ratios of ketones to osmium(VIII) that these endpoints imply.	97
Table 6.2:	Half reactions for the oxidation of ketones	98
Table 6.3:	Conditional equilibrium constants, $K_1$ and $K_2$ , for Reaction Scheme 9	106
<b>Chapter 8</b>		
Table 8.1:	The initial rates of the first and second steps of the osmium(VIII)-ethanol reaction taken from the slopes of the tangents to the curves shown in Figure 8.1.	152
Table 8.2:	Rate constants, $k_1$ , generated by kinetic modelling software using the Complexation Reaction Model for the reactions of ethanol or MEK with osmium tetroxide in varying concentrations of hydroxide.	160
Table 8.3:	Rate constants, $k_1$ , calculated for varying concentrations of <i>t</i> -butanol and acetonitrile. All other parameters are constant: $[\text{OsO}_4] = 4.48 \times 10^{-4} \text{M}$ ; $[\text{ethanol}] = 0.01 \text{M}$ ; $[\text{hydroxide}] = 0.1 \text{M}$ .	161
Table 8.4:	Rate constants, $k_1$ , for varying concentrations of HMPA.	164
Table 8.5:	Rate constant, $k_1$ and equilibrium constant, $K_{\text{eq}}$ , obtained from the best fit of the rate modelling software. Molar extinction coefficients were held constant.	170
Table 8.6:	Activation parameters for the reduction of Os(VIII) by various alcohols in alkaline medium	172
Table 8.7:	Rate constant, $k_1$ and equilibrium constant, $K_{\text{eq}}$ , obtained from the best fit of the rate modelling software.	174

Table 8.8:	Activation parameters for the reduction of Os(VIII) by various ketones in alkaline medium	177
Table 8.9:	Parameters determined by rate modelling software for the reaction of osmium tetroxide with various substrates.	186

## ABBREVIATIONS

---

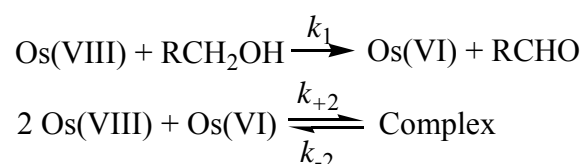
dm	decimetre
EP	end point
HCl	hydrochloric acid
m/v	mass per volume
ml	millilitre
ms	millisecond
min	minute
M	molar
NaOH	sodium hydroxide
s	second
UV-VIS	ultraviolet – visible
v/v	volume per volume
mol/l	mol per litre
MEK	methyl ethyl ketone
HMPA	hexamethyl phosphoramidate



## SUMMARY

---

The reduction of osmium tetroxide by a series of alcohols was studied spectrophotometrically. The reaction was observed to occur in two steps, unlike previously reported studies on this reaction. The identities of both reactants and products were established via a range of techniques. Equilibrium and kinetic data were gathered and reaction models were evaluated using equilibrium and kinetic modelling software. The following complexation reaction model emerged that simulates both the equilibrium and kinetic data.



Conditional rate constants and equilibrium constants were generated. Rate constants for the alcohol reactions were correlated with the Taft  $\sigma^*$  constant. The  $\rho^*$  value obtained (-1.4) is consistent with a hydride transfer mechanism coupled with synchronous removal of the hydroxyl proton. The identity of the osmium(VIII)-osmium(VI) complex has been suggested. Thermodynamic parameters were also reported.

The rate constants for benzyl alcohol and 2-chloroethanol deviated from those predicted by the Taft plot. An explanation of enhanced resonance effects is offered for benzyl alcohol and an alternative reaction mechanism, involving proton abstraction, is offered for 2-chloroethanol.

The reaction of the oxidation products of alcohols, namely ketones, with osmium tetroxide produced rate constants that were, perhaps surprisingly, far larger than those of the alcohols. A reaction mechanism for the oxidation of the ketones is suggested, which involves the enolate ion as the reactive starting reagent.

*Key words:* Osmium, spectrophotometric titration, osmium(VIII) acid, osmium(VI) acid, osmium tetroxide, potassium osmate, alcohols, ketones

# CHAPTER 1 – INTRODUCTION

## 1.1 HISTORY OF OSMIUM

Osmium, along with iridium, was discovered just over 100 years ago by Smithson Tennant, closely pursued by his French contemporaries, H.V. Collet-Descotils, A.F. de Fourcroy and L.N. Vauquelin. Smithson Tennant seems typical of the gentleman-researchers of his time. Having an independent income, he was free to pursue his studies in chemistry, which he did somewhat eccentrically it seems, not hesitating to cut off a piece of shirt in order to filter a preparation <sup>(20)</sup>.

Tennant and William Hyde Wollaston (who isolated rhodium and palladium) went into partnership to buy a large quantity of platinum ore. Wollaston worked on the portions that were soluble in *aqua regia*, while Tennant had the task of analysing the insoluble portions. He showed first that the density of this insoluble portion was 10.7 – too great for the original assertion that it was plumbago (graphite). He then took the black powder, heated it with sodium hydroxide, cooled the melt and dissolved the resulting mass in water. This probably resulted in a mixture of  $[\text{OsO}_4(\text{OH})_2]^{2-}$ ,  $[\text{OsO}_4(\text{OH})]^-$  and  $[\text{OsO}_4]$ . This mixture was then acidified and the white, volatile oxide was certainly osmium tetroxide, of which he wrote <sup>(51)</sup>:

*“It stains the skin of a dark colour which can not be effaced ... (it has) a pungent and penetrating smell... from the extrication of a very volatile metal oxide... this smell is one of its most distinguishing characters, I should on that account incline to call the metal Osmium.”*

This name is derived from the Greek οσμη – osme, smell. He obtained the metal by reducing an aqueous solution of the oxide with copper, silver or zinc.

This disregard, or rather ignorance, as to the toxicities of chemicals is typical of that era of research. Although it seems that a thorough investigation of the toxicological properties of osmium tetroxide has not been conducted, there is no doubt as to the highly toxic effects of this compound, which now carries the warning <sup>(21)</sup>

*“extremely destructive to tissue of the mucous membranes and upper respiratory tract, eyes and skin. Inhalation may result in spasm, inflammation and edema of the larynx and bronchi, chemical pneumonitis and pulmonary edema. ...sensation of seeing halos or coloured rings around lights. May be fatal if inhaled, swallowed or absorbed through the skin. Possible mutagen”*

During this study the utmost care was taken when working with osmium in all its forms since it can be oxidised to the volatile tetroxide by oxygen. This was in stark contrast to Brunot who subjected himself to the vapours in an effort to ascertain their toxicity. After 10 minutes he noticed a metallic taste in his mouth and found that smoking was unpleasant; after 30 minutes his eyes were smarting and watering; after 3 hours his chest was constricted and he had difficulty breathing; on going out into the street he noticed large haloes around the street lights<sup>(23)</sup>. These unpleasant side effects result from the reduction of [OsO<sub>4</sub>] on the eyes and lining of the lungs. Concentrations in air as low as 10<sup>-7</sup> g.m<sup>-3</sup> can cause lung congestion, skin damage, and severe eye damage<sup>(22)</sup>.

## 1.2 USES – PAST AND PRESENT

The hotly contested debate as to whether osmium or iridium is the densest metal seems now to have been solved in favour of osmium, with a density of 22.587 ±0.009g cm<sup>-3</sup>



Fountain pen nibs made from an osmium alloy

compared to that of iridium at 22.562 ±0.009g cm<sup>-3</sup> <sup>(20)</sup>. It is, therefore, used in small quantities in alloys where frictional wear must be minimised. These alloys are used in ballpoint pen tips, fountain pen tips, record player needles, electrical contacts and high-pressure bearings. It is evident from this list that the limited uses that osmium once enjoyed are rapidly being eroded, since record player needles and fountain pen tips are not in great demand these days! A less dated use for osmium is in the

platinum/osmium (90/10) alloy used in implants such as pacemakers and replacement valves<sup>(24)</sup>. This osmium alloy is a lustrous silver metal that resists corrosion better than any other, but is very difficult and costly to manufacture. Easier to manufacture is the grey osmium powder, but this is sensitive to oxidation by air to the poisonous osmium tetroxide, [OsO<sub>4</sub>]. This tetroxide was first used as a biological fixation agent (that is the preservation

of tissue and its delineation for optical and electron microscopy) in the mid-nineteenth century and its use continues to this day <sup>(20)</sup>. Probably the most useful property of osmium tetroxide is its ability to act as a catalyst in organic oxidation reactions. The most famous of these reactions is the *cis*-hydroxylation of alkenes. The groundbreaking work was performed by Criegee in 1936, in which he found that stoichiometric amounts of osmium tetroxide would selectively *cis*-hydroxylate unsaturated organic compounds <sup>(25)</sup>. Because of the expense and toxicity of the osmium tetroxide, the discovery that it could be used in conjunction with a co-oxidant in catalytic amounts was a major breakthrough <sup>(26)</sup>. The usefulness of this reaction was again recently highlighted when K. Barry Sharpless shared the 2001 Nobel Prize in Chemistry for his “development of catalytic asymmetric synthesis... on chirally catalysed oxidation reactions.” <sup>(27)</sup> These organic oxidation reactions will be discussed in great detail in Chapter 3.

Another, more recent, interest in the catalytic abilities of the lower oxidation state (II and III) osmium complexes has surfaced in the form of chemically modified electrodes. The electrode is modified either by polymerising the electroactive species onto the electrode or by placing a commercial polymer film such as Nafion onto the electrode. The electroactive species is then held within this film by electrostatic attraction. The electroactive species then mediates in electron transfer between the electrode and the analyte in solution <sup>(29)</sup>. This can best be graphically represented as in Figure 1.1 below.

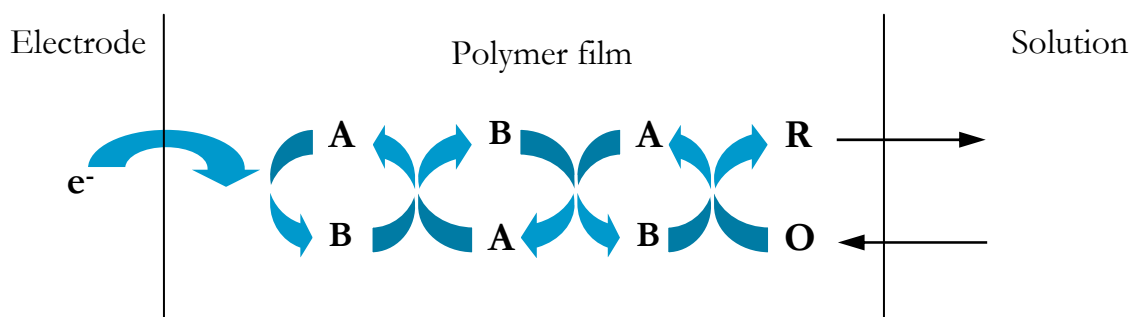


**Figure 1.1: A graphical representation of the electroactive species (A) involvement in mediation of electron transfer from the electrode to the analyte in solution.**

The catalyst is held in a fixed orientation and there is a 3D zone in which charge transfer takes place. Interest has been shown in the bipyridyl derivatives of osmium(II) and (III)<sup>(30)</sup>

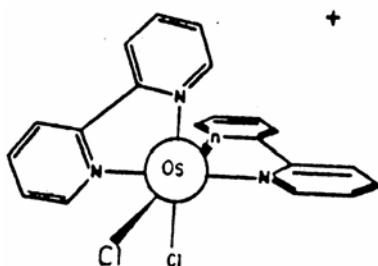


(Figure 1.2). They have been shown to increase the rate of the oxygen reduction reaction which is crucial in fuel cell operation and is an area of ongoing research since the “performance of ... fuel cells is limited primarily by the slow rate of the O<sub>2</sub> reduction half reaction...”<sup>(28)</sup>.

**Figure 1.2:** [Os(bipy)<sub>2</sub>Cl<sub>2</sub>]<sup>+</sup>

## 1.3 GENERAL COORDINATION CHEMISTRY OF OSMIUM

### 1.3.1 Oxidation states

Osmium, of all the transition metal complexes, is unique in its ability to assume a wide variety of different oxidation states. Not even ruthenium and rhenium can rival it in this, since it has representatives in all oxidation states from VIII to –II. It is a good example of a metal that adopts various oxidation states at the behest of the surrounding ligands. Thus, good  $\sigma$ - and  $\pi$ -donors such as F<sup>-</sup>, O<sup>2-</sup> and N<sup>3-</sup> are associated with the high oxidation states (VIII and VI). Strong  $\pi$  acceptors such as CO and NO<sup>+</sup> favour the low oxidation states (0, II and even –II), while conventional  $\sigma$ -donor and  $\pi$ -acceptor ligands such halides, ammonia and ethylenediamine favour the III or IV states. This diverse behaviour is due to the metal’s position as a central member of the third row of transition metals. Its 5d orbitals are exposed to the perturbing effects of the coordinating ligand, while it is capable of attaining the  $d^0$  configuration of the elements to the left of it and the  $d^{10}$  configuration of the elements to the right of it<sup>(16)</sup>.

A discussion of the more common oxidation states follows:

#### Osmium(II)

Os(II) complexes are more sensitive to oxidation by oxygen in the air than their ruthenium analogues. However, many air-stable complexes stabilised by phosphine, cyano, CO and N-heterocyclic ligands are known. Os(II) is a  $d^6$  ion and is generally low spin and octahedral although some five- and seven-coordinate complexes are known<sup>(17)</sup>.

### **Osmium(III)**

Os(III) is an octahedral, low spin  $d^5$  ion that, due to its single unpaired electron has the propensity for oxidation to the tetravalent state or reduction to the divalent state, with its filled  $t_g$  subshell. However, Os(III) is stabilised by a wide variety of strong  $\pi$ -acceptor ligands with N, O, S and P donors <sup>(18)</sup>.

### **Osmium(IV)**

Os(IV) is the most common oxidation state but it requires the stability of a good  $\sigma$ -donor,  $\pi$ -acceptor ligand – often forming halo- or oxo- complexes. Most Os(IV) complexes are low spin and octahedral. Although they have two unpaired electrons they may have anomalous magnetic properties due to the quenching of electron spin by the orbital spin. Some diamagnetic and square-planar complexes have also been found <sup>(17)</sup>.

### **Osmium(VI)**

This oxidation state requires the stability of at least two strong  $\pi$  bases. The chemistry is dominated by the osmyl species, which consists of the *trans*-dioxo moiety. However, there are a number of different combinations of ligands that have been studied and, increasingly, five-coordinate, tetrahedral and even trigonal-planar complexes have been discovered <sup>(17)</sup>.

### **Osmium(VIII)**

Os(VIII) is a strong oxidising agent, but not nearly as strong as its ruthenium analogue. The most important complex is the stable, tetrahedral osmium tetroxide, which can form five- or six-coordinate adducts with a variety of ligands <sup>(16)</sup>.

#### **1.3.2 Coordination numbers**

The vast majority of the osmium complexes are octahedral, although deviations from this have been discussed above. There are a few examples of eight- and seven-coordination. Nine-coordinate geometry has not been observed, but has been discussed <sup>(16)</sup>. There are examples of square-based pyramidal for the higher oxidation states and trigonal bipyramidal geometry for the lower oxidation states. Although tetrahedral geometry is rare it is found in the important osmium tetroxide and in osmium(-II). Table 1.1 lists some of the more unusual coordination numbers.

**Table 1.1: Unusual coordination numbers for osmium complexes** <sup>(16)</sup>

Coordination number	Examples	Geometry
8	$\text{Os}(\text{PMe}_2\text{Ph})_2\text{H}_6$	Unknown
7	$\text{Os}(\text{edta})(\text{H}_2\text{O})$ $\text{OsF}_7$	Monocapped octahedron Pentagonal bipyramidal
5	$\text{OsO}(\text{O}_2\text{R})_2$ , $\text{Os}_2\text{O}_4(\text{O}_2\text{R})_2$ $\text{OsOCl}_4$ $\text{Os}(\text{CO})_5$	Square-based pyramidal Square-based pyramidal Trigonal bipyramidal
4	$[\text{OsO}_4]$ , $[\text{OsO}_4]^-$ $\text{Os}(\text{NO})_2(\text{PPh}_3)_2$	Tetrahedral Distorted tetrahedral

### 1.3.3 Ligands

#### Group IV donors

The osmium carbonyl cluster chemistry dominates this group. Cyanide, being a good  $\sigma$ -donor, medium  $\pi$ -acceptor ligand, forms its most stable complex with the +2 oxidation state –  $[\text{Os}(\text{CN})_6]^{4-}$ . In *trans*- $[\text{OsO}_2(\text{CN})_4]^{2-}$  the high oxidation state is likely maintained by the strong  $\sigma$ -donor,  $\pi$ -donor oxo ligands <sup>(16)</sup>.

#### Group V donors

There has been considerable work done with all the Group V donors. One of the most interesting of these is the stable osmium nitrido complex with a metal-nitrogen triple bond. Ethylenediamine and ammonia, having no  $\pi$ -acceptor capabilities, form stable complexes with oxidation states IV and III. Phosphorus, arsenic and antimony, on the other hand, having good  $\pi$ -acceptor capabilities, form stable complexes with osmium(III) and (II) <sup>(18)</sup>.

#### Group VI donors

This group is dominated by a number of high oxidation osmium complexes stabilised by the oxo ligand, among them the important osmium tetroxide,  $[\text{OsO}_4]$ . There are a wide variety of very stable osmium(VI) complexes containing the osmyl ( $\text{O}=\text{Os}=\text{O}$ ) moiety. Also important and pertinent to this study is the unique cyclic oxo-ester chemistry, which will be discussed in much more detail in Chapter 3 <sup>(16 & 18)</sup>.

### Group VII donors

All four halide ions form octahedral complexes with osmium. Fluorides form complexes with osmium (VIII) to (IV). The other halides prefer oxidation states IV and III<sup>(16)</sup>, with a tendency for the hexachloro species to predominate in a manner similar to the other precious group metals. One reviewer reports little work on the kinetics of the hexahalogenes<sup>(18)</sup>.

---

---

## 1.4 OSMIUM(VIII)

---

---

Since the emphasis of this work is on the high oxidation state osmium complexes, it is fitting to go into a more detailed discussion of this oxidation state, with special focus on osmium tetroxide and its alkaline derivatives.

Osmium tetroxide is chemically quite stable and, for an octavalent element, is a relatively mild oxidising agent. Its ability to successfully stabilise its octavalent state is through its central position in the 3d elements and with the help of pi-donor ligands. RuO<sub>4</sub> being a 2d element, is barely able to sustain its octavalent state and FeO<sub>4</sub> is unknown<sup>(16)</sup>.

[OsO<sub>4</sub>] can easily be prepared by oxidising almost any source of osmium with a wide variety of oxidising agents. It is very volatile and can be distilled off – a property used in its preparation. The toxic vapour has a high vapour pressure at room temperature and should be stored in stoppered flasks or sealed ampoules. A range of [OsO<sub>4</sub>L] complexes, where L is an amine ligand or an N-heterocyclic ligand, have been investigated for their thermodynamic stability<sup>(18)</sup>. The ligand reduces the volatility of the [OsO<sub>4</sub>] and is a “safe” way of storing [OsO<sub>4</sub>] in solution.

Osmium tetroxide is sparingly soluble in water, giving a colourless solution. The solubilities, in grams of tetroxide per 100 grams water, are 5.3 at 0°, 6.47 at 18° and 7.24 at 25°. It is much more soluble in organic solvents (polar or nonpolar) - 250g osmium tetroxide per 100g carbon tetrachloride at 20°C<sup>(18)</sup>. Extensive use of these properties was made during this study.



There is much debate as to the equilibrium reactions in aqueous solution and was the subject of a previous study by this author. Although Griffith <sup>(18)</sup> speaks of “frequent references in the literature” to osmic acid,  $H_2[OsO_5]$ , which is supposed to exist in aqueous solutions, he maintains that these complexes are more likely to be  $[OsO_4(H_2O)_2]$  or  $[OsO_4(OH)_2]^{2-}$ . He continues that the Raman spectrum of  $[OsO_4]$  in aqueous solutions suggests that the major species present is  $[OsO_4]$ . It was previously shown by this author that the absorption spectrum of  $[OsO_4]$  in water is the same as in hexane indicating that it is still tetrahedral <sup>(31)</sup>. Acid dissociation constants of  $8.8 \times 10^{-13}$  and  $7.5 \times 10^{-15}$  were obtained and have proved valuable in the current study. Galbacs *et al* agree that  $[OsO_4]$  behaves as an acid in aqueous solution, with acidic constants of  $6.3 \times 10^{-13}$  and  $\sim 4 \times 10^{-15}$  <sup>(32)</sup>.

In a basic solution osmium tetroxide reacts with hydroxide ions to form the “perosmate” ion ( $[OsO_4(OH)_2]^{2-}$ ) <sup>(16)</sup>. This was found to occur in a two-step process with formation constants  $\beta_1$  and  $\beta_2$  of 88 and 66, respectively <sup>(31)</sup>. The perosmate is easily reduced with heating or alcohol to “osmate” ( $[OsO_2(OH)_4]^{2-}$ ) <sup>(16)</sup>. Various different salts have been reported to have been isolated by early workers:  $M_2[OsO_4(OH)_2]$  where  $M = K^{(33 \ \& \ 34)}$ ,  $Rb^{(34)}$ ,  $Cs^{(33 \ \& \ 34)}$  and  $Ba[OsO_4(OH)_2]$  <sup>(33)</sup>. By using a deficiency of MOH with  $[OsO_4]$ ,  $M[OsO_4(OH)]$  ( $M = Rb, Cs^{(33)}$ ) was claimed. More recent X-ray work has shown the existence of *cis*- $[OsO_4(OH)_2]^{2-}$ ,  $[Os_2(OH)O_8]^-$  and  $[OsO_5(H_2O)]^-$  <sup>(16)</sup>.

A common problem in studies with osmium is in determining its oxidation state since it is so easily oxidised and reduced. A titration with Fe(II) (followed potentiometrically and/or spectrophotometrically) was developed in a previous study <sup>(31)</sup> and was valuable in determining the oxidation state of the osmium.

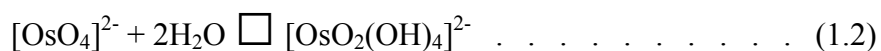
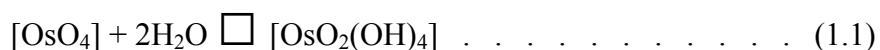
The volatility of osmium tetroxide in an aqueous solution was observed semi-quantitatively. In a basic solution of sufficient concentration, the osmium tetroxide is “anchored” and is not volatile. The threshold concentration was not determined but could be inferred from the species distribution diagram and was shown empirically to be above 0.02M (pH 12.3). Osmium tetroxide is only entirely absent from solutions above pH 14 (1M). In addition, it was shown that the osmium tetroxide underwent gradual reduction in a basic medium. Those open to the atmosphere underwent reduction faster than those in a closed vessel <sup>(31)</sup>.

## 1.5 OSMIUM(VI)

In addition to a strong focus on osmium tetroxide in this study, there is also a focus on its reduction product, osmium (VI) or  $[\text{OsO}_2(\text{OH})_2]^{2-}$ . Therefore, the chemistry of this complex is also discussed.

The high oxidation state osmium(VI), like the osmium tetroxide, is stabilised by strong  $\sigma$ -donor,  $\pi$ -donor ligands. The chemistry of the osmium(VI) complexes is dominated by the osmyl species,  $\text{O}=\text{Os}=\text{O}$ . Whereas osmium tetroxide is unique in being a stable, neutral complex of an element in oxidation state eight, there are analogues to the “osmyl” complexes in other elements capable of attaining the  $d^2$  configuration. However, only the uranyl system can rival the *trans*- $[\text{Os}^{\text{VI}}\text{O}_2\text{X}_4]^{n-}$  in its diversity of co-ligands<sup>(16)</sup>.

The osmium(VI) salt, potassium osmate –  $\text{K}_2[\text{OsO}_2(\text{OH})_4]$  – has long been known but, previous to the work of Lott and Symons in 1960<sup>(35)</sup>, was considered to be the tetrahedral  $\text{K}_2[\text{OsO}_4] \cdot 2\text{H}_2\text{O}$ . However, all of the osmyl complexes are diamagnetic, which led Lott and Symons to conclude that they were almost all octahedral. The *trans* bonds cause large tetragonal compression of the Os-OH bonds, causing the two  $d$  electrons to pair up in the  $d_{xy}$  orbital (assuming the oxo ligands lie on the  $z$  axis). An additional explanation is given in terms of a comparison of the ease of hydration between osmium tetroxide and the osmium(VI) anion.



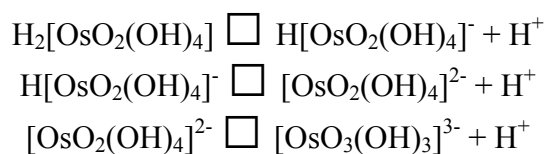
The equilibrium in Equation 1.1 lies far to the left, whereas for Equation 1.2 it lies far to the right. The generalisation is made that the closed shell tetrahedral complex has a smaller tendency to hydrate than those with one or two outer electrons. It is approximated that the two outer electrons reside in the  $d_{z^2}$  and  $d_{x^2-y^2}$  orbitals in the tetrahedral  $[\text{OsO}_4]^{2-}$  and in the  $d_{xy}$  orbital in  $[\text{OsO}_2(\text{OH})_4]^{2-}$ . As the extent of the overlap between the ligand  $p$ - $\pi$  orbitals and the metal  $d$  orbitals increases, so the stability of the outer orbitals decreases. The extent of  $\pi$ -overlap will be greater for an oxo than a hydroxo ligand and, therefore, will be of lowest energy for the  $d_{xy}$  orbital in  $[\text{OsO}_2(\text{OH})_4]^{2-}$ <sup>(35)</sup>.

Most of the osmyl complexes have linear or almost linear units, and most are mononuclear but there are some binuclear exceptions with a  $\mu\mu'$  dioxo bridge. Potassium osmate has a linear O=Os=O unit, the Os–OH bond angles are  $90^\circ$ , the Os–O bond distance is 1.77 angstrom and the Os–OH bond distance is 2.03 angstrom<sup>(16)</sup>.

Galbacs *et al* <sup>(32)</sup> determined acid dissociation constants for the hypothetical osmium(VI) acid,  $H_2[OsO_2(OH)_4]$ , to be  $3.2 \times 10^{-9}$  and  $4.0 \times 10^{-11}$ . Prior to that, researchers claimed to have provided the first evidence for the acid-base characteristics of the osmate ion ( $[OsO_2(OH)_4]^{2-}$ ) <sup>(36)</sup>. They calculated an equilibrium constant of  $0.96 \times 10^{-15}$  for the reaction



and maintained that  $[OsO_2(OH)_4]^{2-}$  was the predominant ion in less basic solutions. If these studies are assumed correct, when taken together they presume the osmate ion to be a triprotic acid according to the following equations:



However, later research <sup>(31)</sup> found only two acid dissociation constants ( $K_1$  and  $K_2$ ) of  $2.2 \times 10^{-10}$  and  $2.9 \times 10^{-10}$ , which favours the results found by Galbacs *et al*.

The study of the acidic constants of the osmate ion is complicated by the fact that osmium(VI) is oxidised by dioxygen to osmium(VIII) and that in a medium more acidic than pH 10 osmium(VI) disproportionates at a rate dependent on pH<sup>(32)</sup>.

Potassium osmate is a useful starting material for a variety of other “osmyl” complexes. It reacts with halogen acids to give  $K_2[OsO_2(OH)_2X_2]$  or  $K_2[OsO_2X_4]$  ( $X = Cl$  or  $Br$ )<sup>(18)</sup>.  $[OsO_2Cl_3H_2O]^-$  is thought to exist in equilibrium with  $[OsO_2Cl_4]^{2-}$ . An equilibrium constant of 1.31 has been calculated, as well as the spectrum of each complex<sup>(36)</sup>.

Osmium(VI) has an extensive oxo chemistry. It encompasses the hexa-oxo to mono-oxo species and everything in between. The hexa-, penta- and tetra-oxo species have been reported, but it is not certain whether these are mononuclear species or not. Examples are

$\text{Li}_6[\text{OsO}_6]$ ,  $\text{Na}_4[\text{OsO}_5]$  and  $\text{Ba}[\text{OsO}_4]n\text{H}_2\text{O}$  <sup>(16)</sup>. The trioxo species is not as common. Many reports in the earlier literature claimed trioxo mononuclear species. These are now known to be dimers although some exhibit a monomer-dimer equilibrium in solution. There are many dioxo species – as mentioned earlier the osmyl species dominates the osmium(VI) chemistry. Two mono-oxo halide complexes are known – the oxotetrafluoride and the oxotetrachloride. There is an extensive body of osmium(VI) mono-oxo cyclic esters, mostly formed through the reaction of osmium tetroxide with an alkene. These will be discussed extensively in later chapters.

---

## 1.6 AIMS AND OBJECTIVES

---

Although osmium is not as valuable as the other platinum group metals, the mining industry must separate and stabilise osmium during the refining processes associated with the procurement of, amongst others, platinum and palladium. In this regard, potential environmental and occupational health hazards must also be dealt with. Not all aspects of osmium chemistry are well understood and in order to be of assistance to the mining industry, it is necessary to acquire experience and knowledge in the behaviour and handling of osmium.

That having been done, it is important to have an understanding of the kinetics and mechanisms at work during the refining process. In addition to this, the osmium tetroxide catalysed oxidations of organic molecules are industrially important in many organic syntheses. Although these reactions have received attention in the past there does not seem to be consensus as to the mechanisms associated with the reactions.

The study focuses on reduction of osmium tetroxide to osmium(VI) by alcohols in a basic medium. Through kinetic and stoichiometric studies in which parameters were exhaustively varied, a mechanism explaining the resulting data is proposed. At the same time a better understanding of the fundamental chemical behaviour associated with these complexes is gained.

# CHAPTER 2

## EXPERIMENTAL

---

### 2.1 APPARATUS

---

#### 2.1.1 Ultraviolet and visible spectra

Spectra were measured with a Perkin Elmer UV-VIS Lambda 12 Spectrometer. Quartz cuvettes with a 1cm or 1mm path length were used. The Perkin Elmer UV WinLab Version 1.22 software package was used for instrument control.

#### 2.1.2 Nuclear magnetic resonance spectroscopy

The 300.13MHz  $^{13}\text{C}$ -NMR spectra were recorded on a Bruker 300MHz spectrometer using  $\text{SiMe}_4$  as an internal standard. Generally the spectra were run overnight, i.e. approximately 15000 cycles, since the solutions were too dilute to obtain a signal in a shorter time. Deuterated water was used as the reference solvent.

#### 2.1.3 pH measurements

pH was measured with a Metrohm 780 pH meter using a Metrohm 6.0232.100 combined pH glass electrode. The electrode was calibrated with pH 4 and 7 Metrohm buffer solutions.

#### 2.1.4 Potentiometric measurements

Potential was measured with a Metrohm 780 pH meter using a Metrohm 6.0402.100 combined platinum-wire electrode.

#### 2.1.5 Potentiometric titrations

Titrations were performed and recorded using a Metrohm 780 pH meter with a Metrohm 665 Dosimat and stirrer. The titrations were performed manually (with titrant being delivered by hand) or automatically (with measured aliquots of titrant being delivered by dosimat) as described in each experimental section.

---

---

## 2.2 COMPUTER SOFTWARE

---

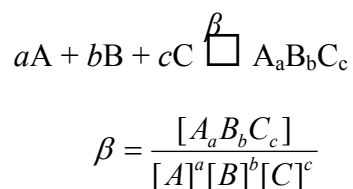
---

All apparatus utilised their own software packages as detailed in 2.1 above.

### Equilibrium and kinetic data analysis

Two different computer programmes were used to model absorbance changes observed during titrations. Different reaction models could be simulated and formation constants and molar extinction values calculated from the experimental data. The first programme was written by Dr E. Hosten using Borland Turbo Pascal V6.0<sup>(6)</sup>. The programme can simulate one or more equilibria. From estimates of the formation constants of each equilibrium and the total reagent concentrations, the programme uses an iterative Gauss-Newton algorithm<sup>(7)</sup> to calculate the free reagent (unreacted) concentrations. Together with the free reagent concentrations, the estimated formation constants and the molar extinction values, the programme can then calculate the total absorbance. By comparing the calculated absorbance with the experimental absorbance, the programme uses another iterative Gauss-Newton algorithm to calculate better estimates for reagent concentrations, formation constants and molar extinction values. These iterative cycles then continue till the changes to all the constants become negligible. During all the calculations the change in volume during the titrations due to the addition of titrant, is taken into account.

The SPC-V-MR programme was used to simulate mole ratio titrations where the mole ratios between various reagents change. This programme simulates the following type of equilibria:



This programme was used to simulate the redox and complexation reactions undergone by osmium and substrate. Although the type of equilibrium modelled is not a redox equilibrium, it does enable one to test various models to determine the stoichiometry at the photometric endpoints.

The second programme used for the modelling of equilibrium and kinetic data was a commercially available software programme distributed by Biokin Ltd and known as Dynafit<sup>(43)</sup>.

The programme ComplexSpecies was also used to draw up species distribution plots / concentration graphs from formation constants and reagent concentrations. This is a Windows programme written by Dr E Hosten using Borland Delphi V5.0.

### **Other software**

Microsoft Word Version 2000

Microsoft Excel Version 2000

Spectra Calc: Arithmetic A2.12, copyright 1988, Galactic Industries Corp

---

## **2.3 STANDARDISATION OF REAGENTS**

---

### **2.3.1 Preparation of a standard iron(II) solution**

The Fe(II) solutions were prepared with the iron(II) sulfate heptahydrate salt ( $\text{FeSO}_4 \cdot 7\text{H}_2\text{O}$ ) dissolved in a 10%(v/v)  $\text{H}_2\text{SO}_4$  solution. Potassium dichromate was dried in an oven at 120°C for about one hour and then allowed to cool in a desiccator. A standard potassium dichromate solution was then prepared in distilled water. 20ml of the Fe(II) solution to be standardised was pipetted into a beaker and 5ml  $\text{H}_3\text{PO}_4$  was added immediately prior to titration with the standard potassium dichromate solution. The titration was performed until concurrent results were obtained with a Metrohm 780 pH meter using a Metrohm 6.0402.100 combined platinum-wire electrode.

### **2.3.2 Preparation of a standard hydrochloric acid solution**

An HCl solution was made up in distilled water. A standard sodium tetraborate (borax) solution was prepared in distilled water. The borax solution was then automatically titrated against the HCl solution until concurrent results were obtained using a Metrohm 780 pH meter with combination glass electrode.

### 2.3.3 Preparation of a standard sodium hydroxide solution

NaOH pellets were dissolved in distilled water and the freshly prepared solutions were titrated against the standardised HCl solutions until concurrent results were obtained using a Metrohm 665 Dosimat and stirrer with combination glass electrode.

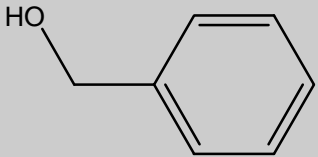
## 2.4 REAGENTS USED

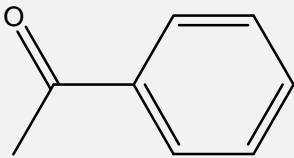
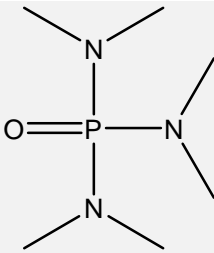
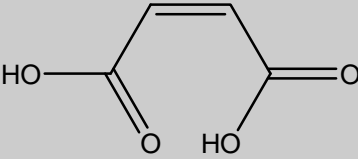
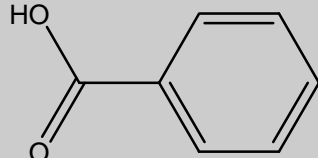
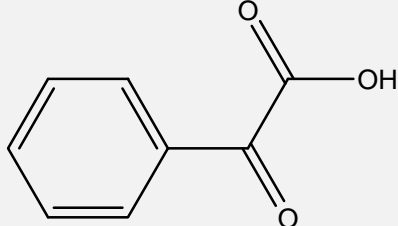
Osmium was obtained as a crude salt, potassium osmate ( $K_2[OsO_2(OH)_4]$ ), from the Anglo Platinum Research Centre. The crude potassium osmate was used as an osmium source in the preparation of a pure osmium tetroxide solution. It was oxidised to the tetroxide, which then vapourised, and was trapped in carbon tetrachloride. If a pure potassium osmate salt was required, it was recrystallised as described in Chapter 2.7.

**Table 2.1: Reagents used in this study**

Reagent	Chemical formula	Percentage purity (salt) / Percentage composition (liquid)	Supplier
Sodium hydroxide	NaOH	98	Merck Chemicals (Pty) Ltd
Potassium hydroxide	KOH	85	Minema Laboratory Supplies (Pty) Ltd
Ferrous sulfate heptahydrate	$FeSO_4 \cdot 7H_2O$	99	Associated Chemical Enterprises (Pty) Ltd
Sodium chloride	NaCl	99.5	Associated Chemical Enterprises (Pty) Ltd
Thiourea	$CH_4NS_2$	98	Associated Chemical Enterprises (Pty) Ltd
Potassium dichromate	$K_2Cr_2O_7$	99.5	Saarchem (Pty) Ltd
Sodium tetraborate	$Na_2B_4O_7 \cdot 10H_2O$	99	May & Baker



Orthophosphoric acid	$\text{H}_3\text{PO}_4$	85	Associated Chemical Enterprises (Pty) Ltd
Sulfuric acid	$\text{H}_2\text{SO}_4$	98	SMM Chemicals (Pty) Ltd
Hydrochloric acid	$\text{HCl}$	32	SMM Instruments (Pty) Ltd
Nitric acid	$\text{HNO}_3$	55	Associated Chemical Enterprises (Pty) Ltd
Ethanol	$\text{CH}_3\text{CH}_2\text{OH}$	99.9	Minema Laboratory Supplies (Pty) Ltd
Diethyl ether	$\text{CH}_3\text{CH}_2\text{OCH}_2\text{CH}_3$		SMM Chemicals (Pty) Ltd
Carbon tetrachloride	$\text{CCl}_4$		Riedel deHaën
Propan-1-ol	$\text{CH}_3\text{CH}_2\text{CH}_2\text{OH}$	99	Merck Chemicals (Pty) Ltd
Propan-2-ol	$\text{CH}_3\text{CH}(\text{OH})\text{CH}_3$	99	Merck Chemicals (Pty) Ltd
Methyl Ethyl Ketone (MEK)	$\begin{array}{c} \text{O} \\    \\ \text{CH}_3\text{CCH}_2\text{CH}_3 \end{array}$	99	Holpro Analytics (Pty) Ltd
Acetone	$\begin{array}{c} \text{O} \\    \\ \text{CH}_3\text{CCH}_3 \end{array}$	99.5	Fluka Chemie AG
Benzyl alcohol		99	Associated Chemical Enterprises cc
2-Pentanone	$\begin{array}{c} \text{O} \\    \\ \text{CH}_3\text{CCH}_2\text{CH}_2\text{CH}_3 \end{array}$	99	Fluka Chemie AG
Formic acid	$\text{O}=\text{CH}(\text{OH})$	85%AR	Associated Chemical Enterprises cc
Butan-1-ol	$\text{CH}_3\text{CH}_2\text{CH}_2\text{CH}_2\text{OH}$	99	Merck Chemicals (Pty)

Butan-2-ol	$\text{CH}_3\text{CH}(\text{OH})\text{CH}_2\text{CH}_3$	99	Hopkin and Williams
Acetophenone		98	Carlo Erba
Butyric acid	$\text{CH}_3\text{CH}_2\text{CH}_2\text{COOH}$	99.5	Hopkin and Williams
<i>t</i> -Butanol	$\text{C}(\text{CH}_3)_3(\text{OH})$	99	Fluka Chemie AG
2-chloroethanol	$\text{ClCH}_2\text{CH}_2\text{OH}$	99	Hopkin and Williams
Hexamethylphosphoramide		99	Fluka Chemie AG
Maleic acid		-	Hopkin and Williams
Chloroacetic acid	$\text{ClCH}_2\text{COOH}$	-	Hopkin and Williams
Benzoic acid		-	Holpro Analytics (Pty) Ltd
Phenylglyoxylic acid		-	Fluka Chemie AG
Propionic acid	$\text{CH}_3\text{CH}_2\text{COOH}$	99	Unilab (Pty) Ltd

## 2.5 DETERMINATION OF POTENTIOMETRIC ENDPOINTS

The endpoints of the Fe(II) potentiometric titrations were determined by the Hahn and Weiler method. This involves the use of the following equation:

$$V = V_1 + (V_2 - V_1) \times \frac{(d^2E/dV^2)_1}{[(d^2E/dV^2)_1 + (d^2E/dV^2)_2]}$$

At each titration point,  $dE/dV$  and  $d^2E/dV^2$  are calculated. The end point,  $V$ , lies between the two volumes,  $V_1$  and  $V_2$ , that show the largest value for  $d^2E/dV^2$ .

## 2.6 PREPARATION AND STORAGE OF OSMIUM TETROXIDE

### 2.6.1 Introduction

Pure solutions of osmium tetroxide were prepared by oxidising an osmium source to form the volatile osmium tetroxide, which was then bubbled through a carbon tetrachloride scrub solution. The osmium tetroxide is far more soluble in carbon tetrachloride than in water<sup>(18)</sup>. The set-up consisted of two Dreschel flasks attached to one another via glass tubes. Initially plastic tubing was used. However, it immediately turned black in the presence of  $[\text{OsO}_4]$  due to the  $[\text{OsO}_4]$ –alkene reaction occurring on the plastic surface.

It was found that for the preparation of a pure solution of osmium tetroxide, only a limited number of oxidising agents are suitable. This was due to the fact that the reduced product of the oxidising agent (or the oxidising agent itself) distilled off into the scrub solution and contaminated it. For example, when  $\text{NaClO}_3$  or  $\text{Cl}_2$  was used as the oxidising agent, chlorine species were found in the scrub solution. The presence of the oxidising agent in the osmium tetroxide solution resulted in the increased oxidising capacity of the solution<sup>(31)</sup>.

### 2.6.2 Preparation procedure

Approximately 240ml carbon tetrachloride was added to Flask 2 (see Figure 2.1). Approximately 5g crude potassium osmate was placed in Flask 1 and 100ml of a hydrogen peroxide made up as follows

45ml water

45ml phosphoric acid

10ml 30% hydrogen peroxide

was carefully added. The connecting tubes were quickly joined and the flasks placed on stirrers. The potassium osmate was oxidised to the volatile osmium tetroxide by the hydrogen peroxide. A stream of air then forced the osmium tetroxide vapour in Flask 1 to bubble through the carbon tetrachloride trap in Flask 2. The resulting osmium tetroxide solution in Flask 2 was stored in a brown glass stoppered container. The preparation time was approximately 8 hours.

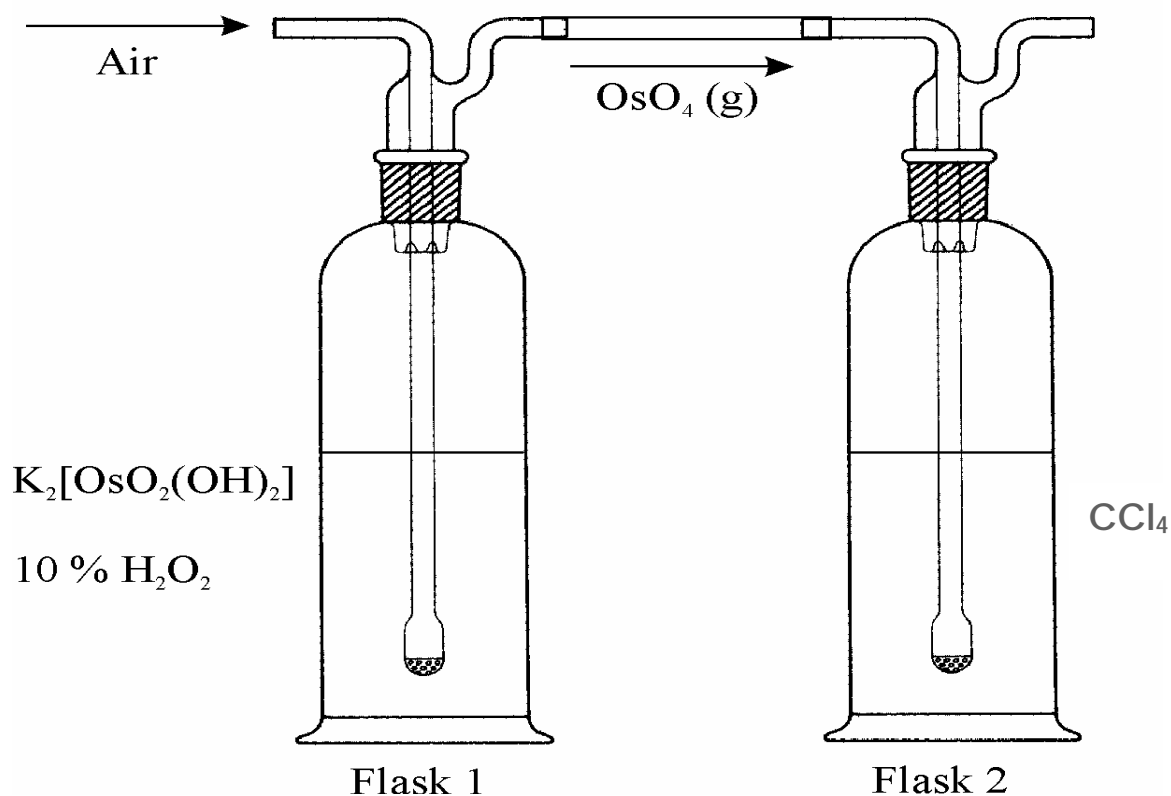


**Figure 2.1: Experimental set-up for the preparation of an organic osmium tetroxide solution**

Aqueous solutions of osmium tetroxide were then prepared as needed by extracting the osmium tetroxide into the required pH solution. Extraction isotherms were plotted for various pH solutions as shown in Figure 2.2.

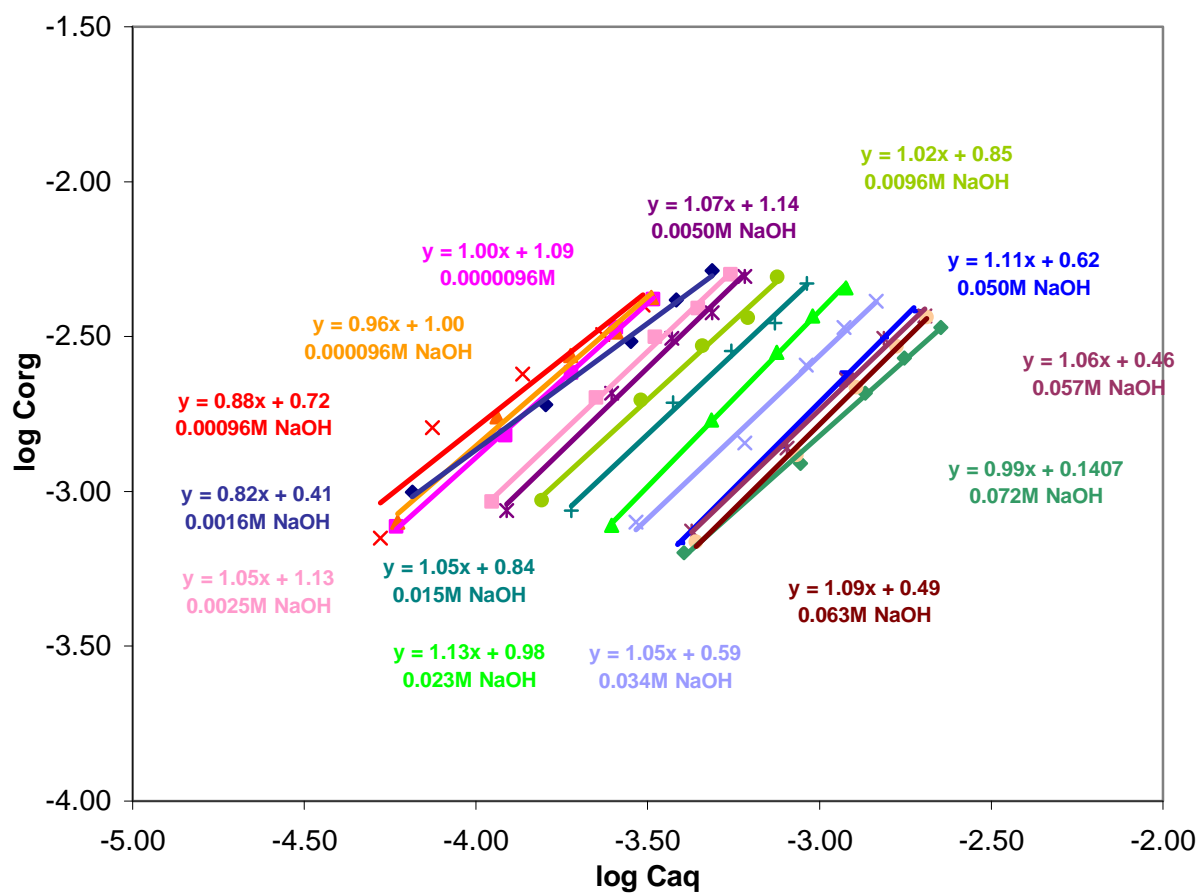


**Figure 2.2:** Plots of  $\log c_{org}$  vs  $\log c_{aq}$  for the extraction of osmium tetroxide from carbon tetrachloride into basic aqueous solutions.

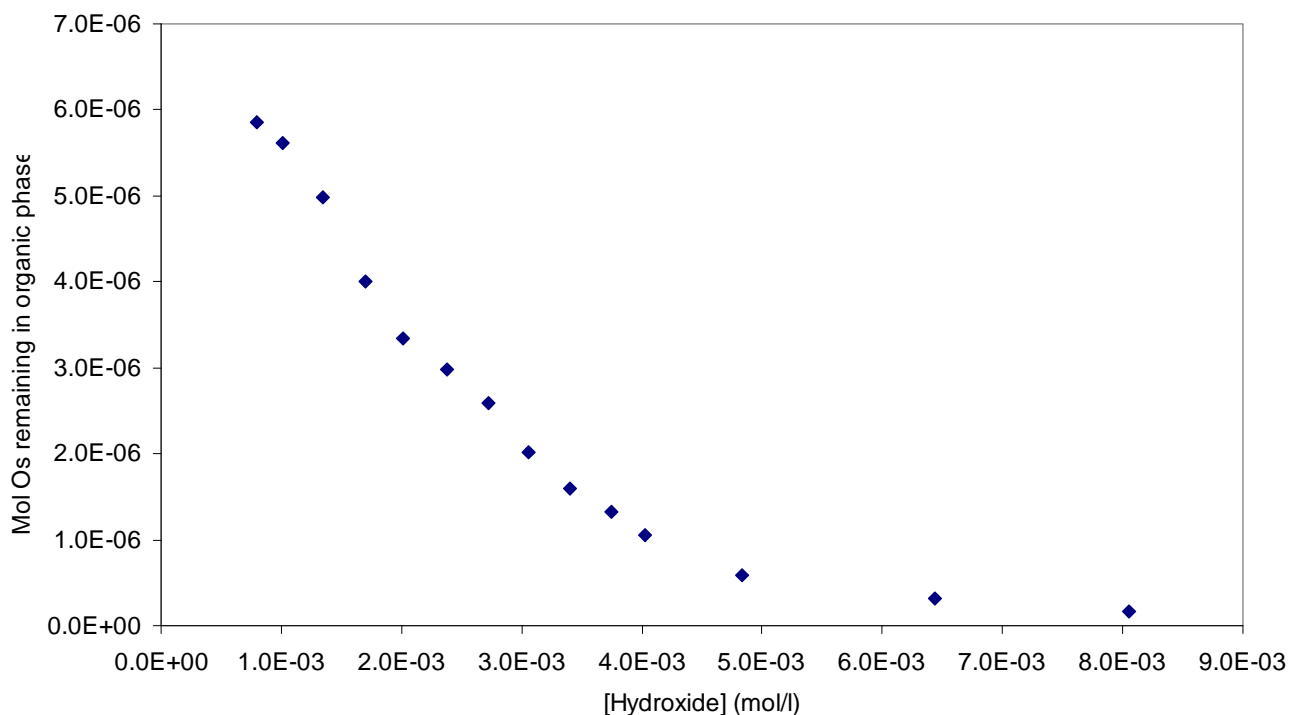


**Figure 2.3: A plot showing the extent of stripping of osmium tetroxide from a carbon tetrachloride solution into aqueous solutions at low hydroxide concentrations.**

The distribution ratio,  $D$ , is defined as the ratio of an analyte's analytical concentrations in the organic and aqueous layers:

$$D = \frac{c_{org}}{c_{aq}}$$

Therefore,

$$\log D + \log c_{aq} = \log c_{org}$$

The y-intercept of Figure 2.2, therefore, gives the distribution ratio of the osmium tetroxide at that pH. The distribution ratio was a useful tool in calculating the ratio of organic to aqueous to react in order to prepare solutions for subsequent experiments. Figure 2.3 shows the extent of stripping from a carbon tetrachloride solution into a basic solution. Above hydroxide concentrations of about 0.1mol/l, stripping becomes complete and the reaction is no longer reversible. However, at hydroxide concentrations as low as 0.01mol/l the mole osmium remaining in the organic layer begins to approach zero.

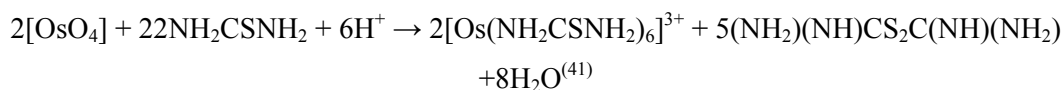
## 2.7 PREPARATION OF POTASSIUM OSMATE

The potassium osmate used in this study was obtained in a crude form. It was dissolved in a minimum of a warm 10%(m/v) KOH solution, filtered and reprecipitated with KOH to obtain pure potassium osmate.

It was also prepared according to the classical method of reducing an aqueous solution of  $[\text{OsO}_4]$  in excess KOH with ethanol<sup>(21)</sup>.

## 2.8 DETERMINING OSMIUM CONCENTRATION

Osmium concentration was determined using a modification of the classic thiourea colourimetric method. Chugaev found in 1918 that solutions of osmium tetroxide treated with thiourea and hydrochloric acid gave a brilliant rose red solution. The red solid crystallised from the reaction mixture gave a percentage composition that corresponded to the trivalent  $[\text{Os}(\text{NH}_2\text{CSNH}_2)_6]\text{Cl}_3\cdot\text{H}_2\text{O}$  or to the tetravalent  $[\text{Os}(\text{NH}_2\text{CSNH}_2)_6]\text{OHCl}_3$ . Chugaev first accepted the former but later rejected it in favour of the latter<sup>(40)</sup>. Not until 1953 did Sauerbrunn and Sandell prove conclusively that the composition of the complex in solution was the trivalent  $[\text{Os}(\text{NH}_2\text{CSNH}_2)_6]^{3+}$ <sup>(41)</sup> and reacted with osmium tetroxide according to the following equation:



The formation and stability of the osmium-thiourea complex was investigated in a previous study by this author with the following findings<sup>(31)</sup>:

- In accordance with the equation above, a vast excess of thiourea and acid is required. A 5% (m/v) thiourea solution in 50% (v/v) HCl was found to be optimum.
- Osmium tetroxide and potassium osmate should be allowed to equilibrate for 48 hours prior to reading their absorbance at 490nm. Ammonium hexachlorosmium(IV) requires an equilibration time of 7 days before reading.

- The linear range was found to extend from  $1.05 \times 10^{-5}$  to  $2.10 \times 10^{-4}$  mol/l (Figure 2.4) with a molar extinction coefficient at 490nm of  $3760 \text{ l mol}^{-1} \text{ cm}^{-1}$ .
- The standards were made using a Spectrascan element standard for spectroscopy by Teknolab A/S.

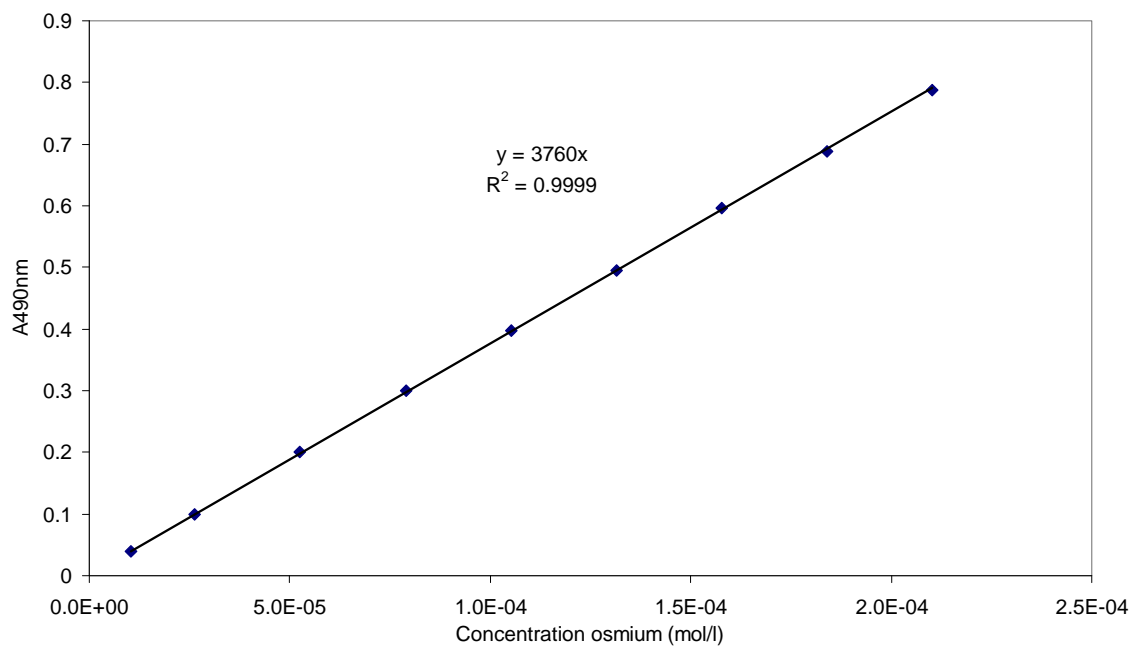


**Figure 2.4: A calibration curve for the thiourea colorimetric method**



## CHAPTER 3

# THE ALCOHOL – OSMIUM TETROXIDE REACTION

### 3.1 INTRODUCTION

There is fairly extensive literature covering the use of osmium tetroxide as an oxidant for organic molecules<sup>(2-6, 8, 11, 12-14, 16)</sup>. In many cases the osmium tetroxide acts a catalyst with the use of some co-oxidant to regenerate the reduced osmium product back to the osmium(VIII). However, much of the literature centres on the economically important oxidation of alkenes to *cis*-diols. There has been renewed interest in this of late due to the awarding of the 2001 Nobel Prize in Chemistry to Barry Sharpless, among others, for his work on “chirally catalyzed oxidation reactions”<sup>(27)</sup>, of which the catalysis by osmium tetroxide of an asymmetric dihydroxylation is of interest here. Much of the literature on the oxidation of alcohols and carbonyl compounds is rather dated. This, together with the interesting nature of some of the preliminary data, prompted us to take a fresh look at this reaction.

This study was initially undertaken from the point of view of understanding the equilibria and kinetics of the osmium species in solution, rather than from an understanding of the organic molecules that play a role in the reaction. The study focussed on a process used in the platinum refining industry during which osmium tetroxide is reduced in a basic medium to osmium(VI) using ethanol. A detailed understanding of the kinetics and equilibria of the osmium species in solution is of interest to this industry. However, in order to have a detailed understanding of the reaction, one needs to have an understanding of the behaviour of the organic molecules in solution and the study was therefore broadened to encompass this area.

This chapter serves as a general introduction to the chapters that follow. Here, a broad background is given into the osmium tetroxide–alcohol reaction by discussing previous studies in this field as well as related studies into the oxidation of other organic molecules by osmium tetroxide. The reader will be introduced to experimental results featuring the

osmium tetroxide–ethanol reaction in order to become familiar with a typical example of the reactions in question. Subsequent chapters will firstly deal with the determination of the reactants and their stability and, secondly, with attempts at determining the products of the reactions. Thereafter, the equilibrium stoichiometry of these reactants and products is discussed. This is followed by a discussion of the difficulties and final fitting of a kinetic reaction model to the empirical data. Finally, mechanistic inferences are made by measuring the rates of the reactions while changing various experimental parameters.

There is fairly extensive literature on the use of osmium tetroxide as an oxidant. In particular, the oxidation of alkenes to *cis*-diols by osmium tetroxide has received much attention for its industrial importance. There is not, however, as extensive a literature on the reaction between the osmium tetroxide and alcohols. However, Singh *et al* made a comprehensive study of the use of osmium tetroxide as a catalyst in conjunction with the co-oxidant hexacyanoferrate(III) with such varying substrates as alcohols, diols, carboxylic acids and ketones<sup>(2-6, 11, 16-18)</sup>. In light of fairly extensive literature coverage, it is therefore surprising that there does not seem to be consensus as to the mechanisms of either the alkene or alcohol/carbonyl reactions. Most of the debate centres on the mechanism of formation of an osmium-substrate complex, and the nature of this complex, although other details such as the dependence on hydroxide concentration are also at issue. A discussion on the alkene hydroxylation reaction serves to initiate the investigation into this divergence of opinion.

Criegee performed the ground-breaking work for this important reaction in which it was shown that alkenes would react with osmium tetroxide to give the osmium(VI) complexes,  $[\text{OsO}_2(\text{O}_2\text{R})]$  and, in some cases  $[\text{OsO}(\text{O}_2\text{R})_2]$ . Subsequent IR and x-ray crystallographic studies formulated these complexes as dimers<sup>(37)</sup>. The rate of the reaction was increased by the addition of bases such as pyridine. This is an early example of ligand accelerated catalysis<sup>(26)</sup>. Hydrolysis of any of these complexes gave the *cis*-diol,  $\text{R}(\text{OH})_2$ <sup>(16)</sup>.

A generally favoured mechanism for this reaction is attack by the oxygen attached to the osmium(VIII) centre on the unsaturated double bond of the alkene leading to a six-electron transition state<sup>(11, 13, 38)</sup>. This, then, proceeds to a five-membered ring that, upon hydrolysis, accounts for the exclusively *cis*-product.

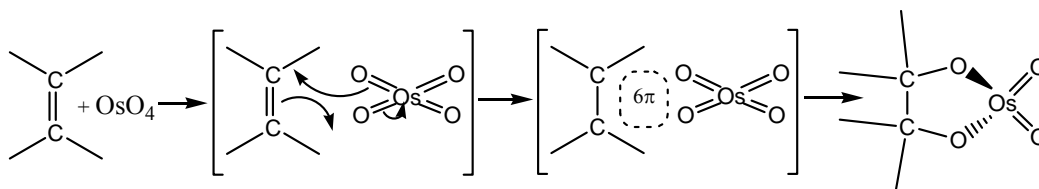


**Figure 3.1: Generally accepted mechanism for the oxidation of alkenes to *cis*-diols**

Veerasomaiah *et al*<sup>(13)</sup> conducted a kinetic study of the oxidation of unsaturated organic compounds by osmium tetroxide in a sulphuric acid/acetic acid medium. They found evidence of a single reaction with a single rate constant and proposed a mechanism similar to Figure 3.1 in which the six-electron complex is an ephemeral transition state. There is no evidence of the formation of a stable five-membered ring. Singh<sup>(11)</sup> agrees, since the five-membered ring proposed in Figure 3.1 would at best be transient, if formed at all, since third row transition metals have no  $d^2$  tetrahedral stereochemistry. In addition, there is unfavourable angular strain on the five-membered ring.

It seems that only in non-reducing organic solvents could one expect to find a stable intermediate osmium(VI)-ester complex. Tetra-substituted alkenes, or those having electron-withdrawing groups, generally form monomeric diester complexes in such solutions. Alkenes such as cyclohexene and ethylene form dimeric monoester complexes<sup>(11)</sup>.

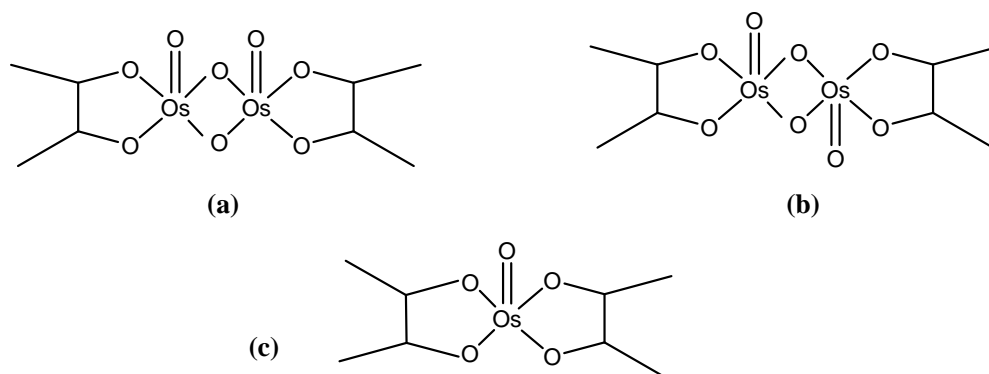


**Figure 3.2: (a) *syn*- and (b) *anti*- dimeric monoesters (c) monomeric diester**

Contrary to the above-stated belief that one would only see the production of a stable osmate ester in organic medium, Subbaraman *et al* claimed to have followed the kinetics of formation of this ester in aqueous medium. They published two separate rate constants – one for the formation of an osmate ester and one for the hydrolysis of the ester <sup>(7)</sup>. The results were obtained in three independent steps: (1) the kinetics of formation of the ester was followed spectrophotometrically in basic medium; (2) the osmate ester was prepared in organic medium, and (3) the kinetics of the ester's hydrolysis was followed in basic aqueous medium. Another aspect of this study worthy of mention is the monodentate nature of the organic moiety of the osmate esters, which were formulated as  $[(RO)_2OsO_2L_2]$  where L represents various monodentate ligands. The authors did not postulate on a reaction mechanism.

Sharpless *et al* <sup>(8)</sup> challenged the conventionally accepted mechanism given in Figure 3.1. Low temperature experiments with chromyl chloride oxidation of olefins yielded organic products that were not easily accounted for by the previously accepted mechanism. These authors tendered a new reaction mechanism for this reaction and extended it to include other  $d^0$  oxo-transition metal species. They argued that by the conventionally accepted mechanism, the reaction must proceed via direct attack by the organic reductant on the oxygen end of the oxo moiety (path b below) implying the resonance form indicated in 2. However, the resonance structure is clearly better represented by 1 below, indicating the preferred reaction pathway, a.

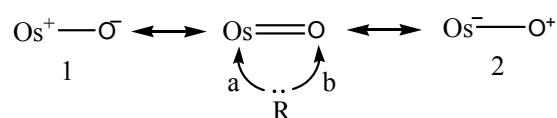


**Figure 3.3: Proposed pathways, a and b, for the reaction of organic reductant, R, with osmium tetroxide**

This is analogous to nucleophilic attack in carbonyl compounds that occurs exclusively at the electropositive carbon atom, and not the oxygen atom. This implies the formation of an organometallic osmium(VIII) intermediate. This intermediate then undergoes rearrangement during the rate-determining step (possibly to a dimeric cyclic ester), which on rapid hydrolysis gives the product. As opposed to the alternative mechanism, this scheme alleviates the uncomfortable angular strain on the intermediate ester ring in the

first step in the absence of pyridine. Attack by the pyridine results in a reductive insertion of the Os-C bond of the metallacycle into an oxo group giving an ester which then reacts with more pyridine giving  $[\text{OsO}_2(\text{O}_2\text{R})\text{L}_2]$ . This mechanism has yet to be conclusively proven.

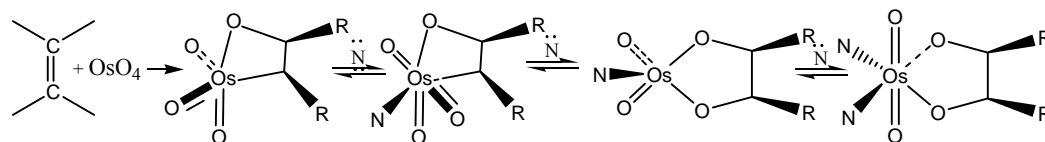


**Figure 3.4: Mechanism proposed by Sharpless *et al* involving nucleophilic attack by the C-C double bond on the electropositive osmium.**

Thus, essentially two mechanisms are proposed (with some variation on the former). Each involves the formation of intermediates, the composition of which is not agreed upon.

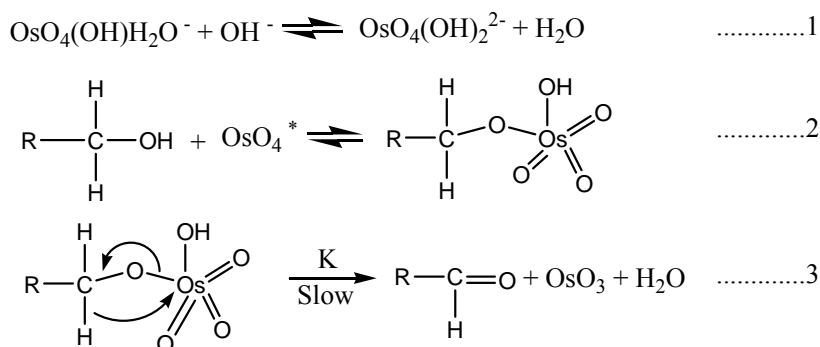
There is similar confusion relating to the oxidation of alcohols by osmium tetroxide. A study into the kinetics of oxidation of alcohols, diols and  $\alpha$ -hydroxy acids by osmium tetroxide in alkaline medium conducted by VeeraSomaiah *et al* <sup>(14)</sup> concluded that the reaction was first order in osmium and substrate. While they found that there was no evidence for a stable intermediate complex formation, they proposed a mechanism involving an osmium(VIII)-alcohol transition state, followed by hydride ion abstraction by the osmium(VIII) in a slow step (Figure 3.5). They found that an increase in hydroxide concentration caused an increase in the rate of the reaction and that the order of the reaction in hydroxide concentration was less than unity. They identified the products of oxidation of the substrates as the corresponding aldehydes and ketones. Rate constants for the various alcohols were determined and a selection is reproduced in Table 3.1.

**Table 3.1: Second order rate constants for the oxidation of hydroxyl compounds by Os(VIII) in alkaline medium<sup>(14)</sup>.**

$$[\text{Os(VIII)}] = 3.16 \times 10^{-4}; [\text{OH}^-] = 0.05\text{M}; \text{temp} = 305\text{K}$$

Substrate	$k$ ( $\times 10^3 \text{ dm}^3 \text{ mol}^{-1} \text{ s}^{-1}$ )
Methanol	4.85
Ethanol	51.2
Chloroethanol	15.3
<i>n</i> -propanol	54.8
2-propanol	69.8
<i>n</i> -butanol	102.3
Isobutanol	83.4
Benzyl alcohol	16100

The trend in the rates of the reactions with various alcohols was used to substantiate the authors' theory of a hydride ion abstraction mechanism by osmium tetroxide. In this theory electron-releasing substituents at the  $\alpha$ -carbon should increase the rate of oxidation, while electron-withdrawing substituents should retard it. This theory was backed by a Taft plot with  $\rho^* = -1.91$ , which negative value the authors claim supports their hydride ion transfer mechanism. It is worthwhile to reproduce the reaction scheme here for greater clarity, since this reaction mechanism is fairly representative of others.



\*  $[\text{OsO}_4(\text{OH})_2]^{2-}$  written as  $[\text{OsO}_4]$  for simplicity (as per the original authors)

**Figure 3.5: Mechanism for the oxidation of alcohols<sup>(14)</sup>**

The same authors found that, although in acidic medium all organic substrates with double bonds reacted smoothly, there was no reaction between osmium tetroxide and alcohols. They did not, however, put forward any explanation for this <sup>(13)</sup>.

H.S Sing *et al* <sup>(2)</sup>, who performed much of the early work on the kinetics of osmium tetroxide catalysed oxidation of alcohols by hexacyanoferrate(III), also found evidence for the occurrence of only a single reaction with a single rate constant. The flaw in many of these early works was the fact that the first concentration readings were made only approximately 5 to 10 (and sometimes as much as 20) minutes into the experiment, thus missing any reactions that may have been occurring in these first crucial minutes. They found that the order of the reaction with respect to osmium, 1- and 2-propanol and hydroxide (at hydroxide concentrations lower than 0.01M) was unity. At hydroxide concentrations greater than 0.01M the rate became independent of hydroxide concentration. These authors based their reaction scheme on the observation quoted from Cotton and Wilkinson <sup>(50)</sup>, that “[OsO<sub>4</sub>(OH)<sub>2</sub>]<sup>2-</sup> is the only reactive species”. However, at the low hydroxide concentrations at which they were working there would be no [OsO<sub>4</sub>(OH)<sub>2</sub>]<sup>2-</sup> present. Even at the highest hydroxide concentration of 0.01M there would be approximately equal quantities of [OsO<sub>4</sub>(OH)]<sup>-</sup> and [OsO<sub>4</sub>], but no [OsO<sub>4</sub>(OH)<sub>2</sub>]<sup>2-</sup> <sup>(31)</sup>. No attempt is made to explain why the [OsO<sub>4</sub>(OH)<sub>2</sub>]<sup>2-</sup> is the only reactive species. This assertion is repeated without explanation in other studies <sup>(10, 5)</sup>. The proposed reaction scheme involves a seven-coordinate osmium(VIII)-propanol transition state (rare, in itself), which decomposes to the aldehyde and [OsO<sub>2</sub>(OH)<sub>4</sub>]<sup>2-</sup>. The aldehyde is subsequently oxidised to the carboxylic acid.

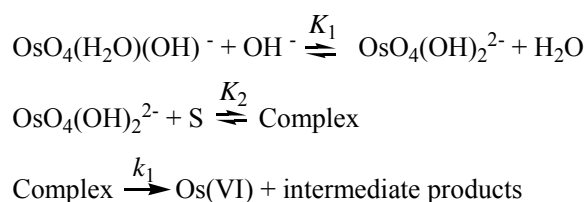
These authors extended their work from propanol to cover many of the alcohols, with similar results and conclusions to the above study <sup>(3, 4, 11)</sup>. The derived rate laws were similar for all these studies:

$$\frac{d[\text{Fey}]}{dt} = \frac{2k_1 K_1 K_2 [\text{S}][\text{OH}^-][\text{Os(VIII)}]_{\text{T}}}{1 + K_1 [\text{OH}^-]}$$

where Fey is the hexacyanoferrate(III) co-oxidant;

S is the alcohol substrate; and

the rate and equilibrium constants refer to the following reaction scheme:



Work with diethylene glycol monomethyl ether, diethylene glycol monoethyl ether, methoxyethanol and ethoxyethanol<sup>(11)</sup> prompted them to conclude that the reaction may proceed either by

- activated complex formation between osmium tetroxide and the organic substrate as discussed above; or
- activated complex formation between osmium tetroxide and an anion derived from the alcohol molecule.

The same authors published work on the oxidation of ketones and even carboxylic acids<sup>(5, 6)</sup>. It is worth mentioning the ketone study at more length since the present study also deals with this class of molecule. The study was carried out using acetone and methyl ethyl ketone (MEK) in an aqueous alkaline buffer solution of carbonate and bicarbonate ions (this could have had implications for the reaction rate if a product of the reactions was CO<sub>2</sub>). They found that the reaction rate decreased with increasing ketone concentration (which was varied between 0.025 and 0.4M) and attributed this to a decrease in dielectric constant. They, therefore, continued to ascribe a first order rate dependence to the ketone concentration. The same held true for the rate dependence on osmium tetroxide concentration. It, too, decreased with increasing osmium tetroxide concentration, but was held to be directly proportional to the reaction rate at low osmium tetroxide concentrations. They also found that the reaction rate was first order in hydroxide concentration. On the basis of these assumptions, they found the rate constant,  $k$ , for the reaction

$$-\frac{d[\text{Fey}]}{dt} = k[\text{ketone}][\text{OH}^-][\text{OsO}_4]$$

at 25°C to be 44.9 mol<sup>-2</sup>l.<sup>2</sup>sec.<sup>-1</sup> for acetone and 1111 mol<sup>-2</sup>l.<sup>2</sup>sec.<sup>-1</sup> for MEK for a given set of conditions. Paper chromatographic analysis showed oxalic acid to be the product of both reactions. They proposed a reaction mechanism in which the ketone is in equilibrium with the enolate ion and it is this enolate that forms a complex through the enolate's



negatively charged oxygen atom with the osmium tetroxide. This complex then decomposes rapidly to give osmium(VI) and organic products.

None of these studies found evidence for a *stable* osmium-alcohol complex although the olive-green osmium(VI) complex,  $K_2[OsO_2(Ome)_4]$ , has been characterised by infra-red and UV-VIS spectroscopy. This was synthesised by the reaction of osmium tetroxide and potassium hydroxide in methanol <sup>(16)</sup>. In addition, Subbaraman *et al* found evidence for the formation of an osmium(VI)-thymine glycol complex upon reaction of osmium(VI)-pyridine complexes with thymine glycols <sup>(12)</sup>. Glycols, however, would be expected to form more stable esters with osmium(VI) than alcohols because of the cyclic, bidentate nature of the ester.

At this stage it may be instructive to look at the mechanism of oxidation of alcohols by other oxidants. In particular, it is of interest to determine whether the reaction is initiated by C-H or O-H bond cleavage. For example, it was established by Westheimer and proven by subsequent researchers that the oxidation of alcohols by chromic acid required the initial participation of the O-H bond – that is chromate ester formation <sup>(1)</sup>. This led from the observation that the rate of oxidation of 2-propanol is approximately 1500 times faster than that of diisopropyl ether.

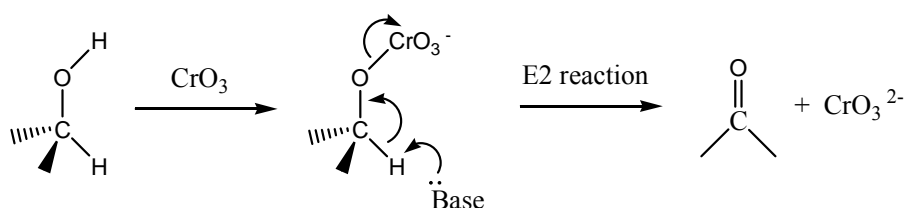


**Figure 3.6: The mechanism of oxidation of alcohols by chromium trioxide**

On the other hand, ruthenium tetroxide is assumed, on the basis of experimental evidence, to proceed via abstraction of the  $\alpha$ -hydrogen without interaction with the O-H bond <sup>(9)</sup>. In addition it reacts with alcohols and ethers at approximately the same rate, which is taken as further confirmation of the above mechanistic interpretation.

The same argument was used by Rankin *et al* <sup>(1)</sup> for the oxidation of alcohols by permanganate. The proposed mechanism involved C-H bond cleavage on the basis of a

similarity in rates of variously substituted benzyl alcohols and their equivalent benzyl methyl ethers. The rationale behind these assumptions is that oxidants that utilise a C-H bond cleavage mechanism should exhibit similar rates for equivalent alcohols and ethers, since the  $\alpha$ -hydrogens in alcohols and ethers are electronically similar (each is attached to a carbon atom that is attached to an oxygen and other carbons or hydrogens).

In passing, it is interesting to note a recent publication<sup>(39)</sup> on the oxidation of saturated alkanes by aqueous alkaline osmium tetroxide at 85°C. A concerted [3+2] mechanism is suggested, analogous to the dihydroxylation pathway of alkenes that is the generally favoured mechanism.

This concludes a fairly detailed review of the literature on the oxidation of alcohols and ketones by osmium tetroxide, including a small variety of similar studies into closely related reactions in order for comparative conclusions to be drawn.

## 3.2 EXPERIMENTAL

This section will introduce a typical osmium tetroxide–alcohol kinetic reaction, using ethanol as a representative alcohol.

The progress of the reaction was followed using a Perkin Elmer UV-VIS Lambda 12 Spectrometer. The reactants were mixed in a 1cm pathlength cuvette with built-in stirrer. The reaction time was started at the time of addition of the ethanol. The reaction progress was followed in one of two ways. For the first reaction, a small concentration of ethanol was added, such that the reaction progress was slow. The reaction was then followed by scanning the spectral range from 500nm to 200nm every 50 seconds at a scan speed of 960nm/min. The first spectrum was read before the addition of ethanol. This spectrum was volume corrected to the same volume as the other spectra (multiply absorbance by (total volume – ethanol volume) / total volume). A measured volume of known concentration ethanol was added immediately prior to the start of the second scan.

Subsequent experiments involved the addition of increasingly greater volumes of ethanol to produce a greater final concentration. These reactions were followed at a single wavelength – 370nm, which was determined during the spectral scans to produce the optimum progress curves. A reading was taken every 0.5 seconds. The initial absorbance at 370nm was read before the addition of any ethanol and was volume corrected as for the spectrum mentioned above.

The osmium tetroxide was obtained as a freshly prepared aqueous solution as described in Chapter 2.6. The osmium tetroxide was extracted from carbon tetrachloride into distilled water. The concentration of this stock osmium tetroxide solution was determined by the thiourea method.

The reaction was run in a 2M sodium hydroxide medium. This concentration was achieved by adding a measured volume of 6M sodium hydroxide to the reaction vessel.



### 3.3 RESULTS AND DISCUSSION

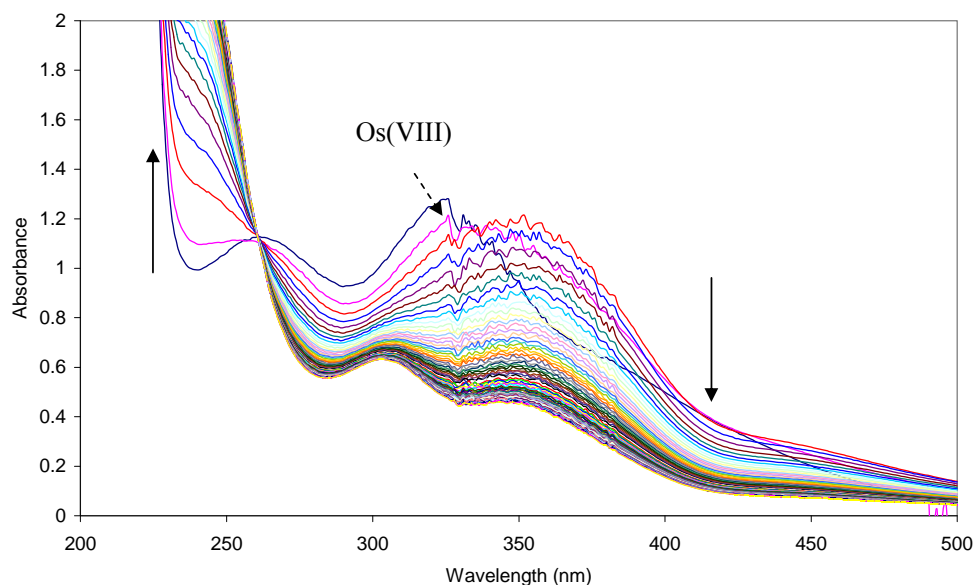
Figure 3.7 shows the change in spectra over time of a typical osmium tetroxide–ethanol reaction. The dashed arrow points to the initial osmium(VIII) spectrum, while the solid arrow indicates the direction of increasing time. This figure is shown to give a broad overview of the shape of the various spectra, from the initial osmium(VIII) spectrum, to the final spectrum once the solution had reached equilibrium. Note the isosbestic point at 261nm.

It should be noted here that there is noise visible on the spectra between the wavelengths of approximately 329nm and 382nm. This is evident throughout the results that follow and is due to a damaged filter on the Perkin Elmer instrument. It does not impact on the validity of the results in any way.

Figure 3.8 shows the progress curves of the reactions in Table 3.2. The data from all reactions, except the lowest ethanol concentration (0.00196M), were collected at a fixed wavelength (370nm) and at a fixed interval of 0.5 seconds. Data from the 0.00196M ethanol reaction was collected by scanning the spectral range. From Figure 3.8 it is clear that the absorbance increases to a maximum and then decreases until it begins to level out once the reaction has reached equilibrium. This illustrates the first important point to be made – the reaction seems to be following a clearly distinct two-step process. These will be referred to as “step one” and “step two”. To expand on this point, different osmium species will have different molar extinction coefficients at 370nm. Therefore, formation of an intermediate species, with a larger molar extinction coefficient than the initial osmium reactant species, will result in an increase in absorbance. A third species with a smaller molar extinction coefficient results in a decrease in absorbance as shown in Figure 3.8. This is the “step one” and “step two” of the reaction process.

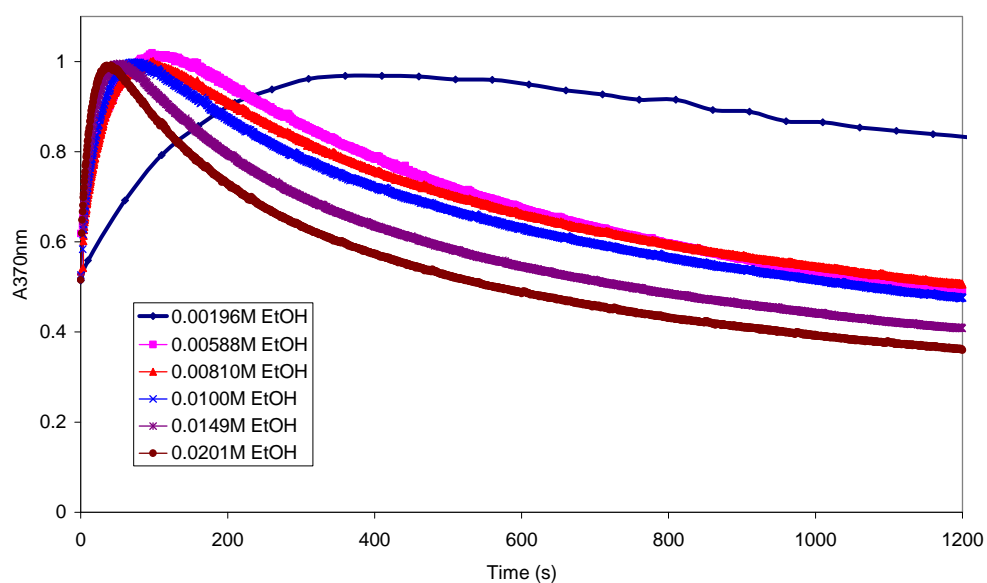
Figure 3.9 is a slower reaction than that shown in Figure 3.7. It does not reach equilibrium, but shows in detail the change in shape of the spectra for step one only.

Figure 3.10 shows individual spectra isolated at a time where they most closely resemble the initial osmium species, the product/s of step one and the product/s of step two, respectively.



**Figure 3.7:** The change in the spectra over time of the reaction of 0.0103M ethanol with  $4.40 \times 10^{-4} \text{M}$   $[\text{OsO}_4]$  in 2M NaOH. The spectra change in the direction of the solid arrows over time: from time = 0min to time = 56min37s. (Scanning 500nm to 200nm; 960nm/min; 1 cycle/min.)

Formatted: Bullets and Numbering



**Figure 3.8:** The progress curves of the rate of change of absorbance at 370nm at varying ethanol concentrations.  $[\text{OsO}_4] = 4.32 \times 10^{-4} \text{M}$ ;  $[\text{NaOH}] = 2 \text{M}$ .

Formatted: Bullets and Numbering

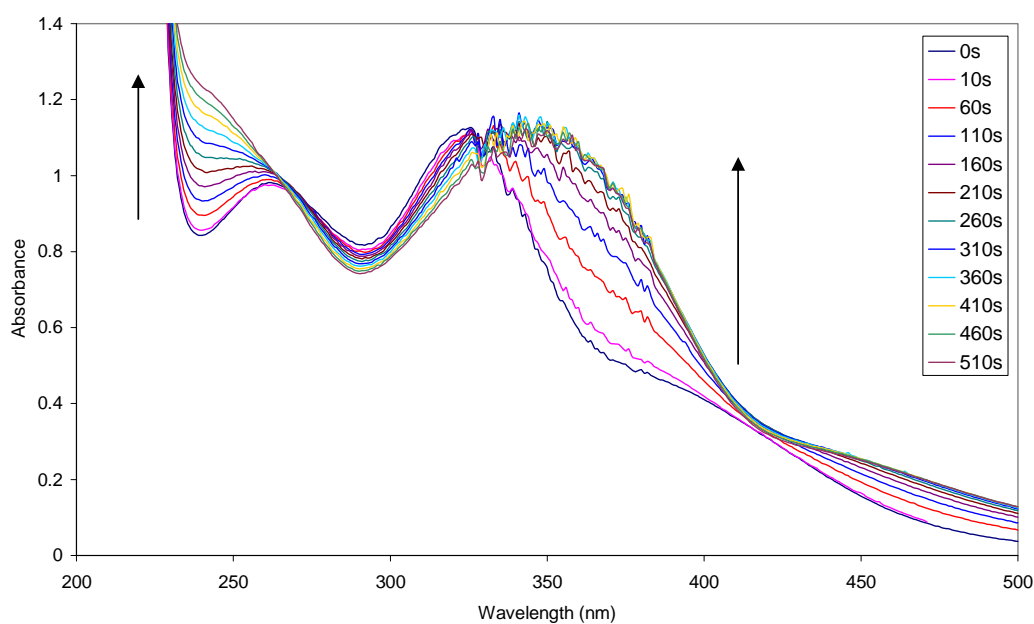


**Figure 3.9:** The change in spectra over time up to the end of step 1. These are the spectra relating to the progress curve shown in Figure 3.9 for the following reactant concentrations: [Ethanol] = 0.00196M; [OsO<sub>4</sub>] = 4.32 x 10<sup>-4</sup>M; [NaOH] = 2M. The spectra change in the direction of the arrows over time. (Scanning 500nm to 200nm; 960nm/min; 1 cycle/50s)

Formatted: Bullets and Numbering

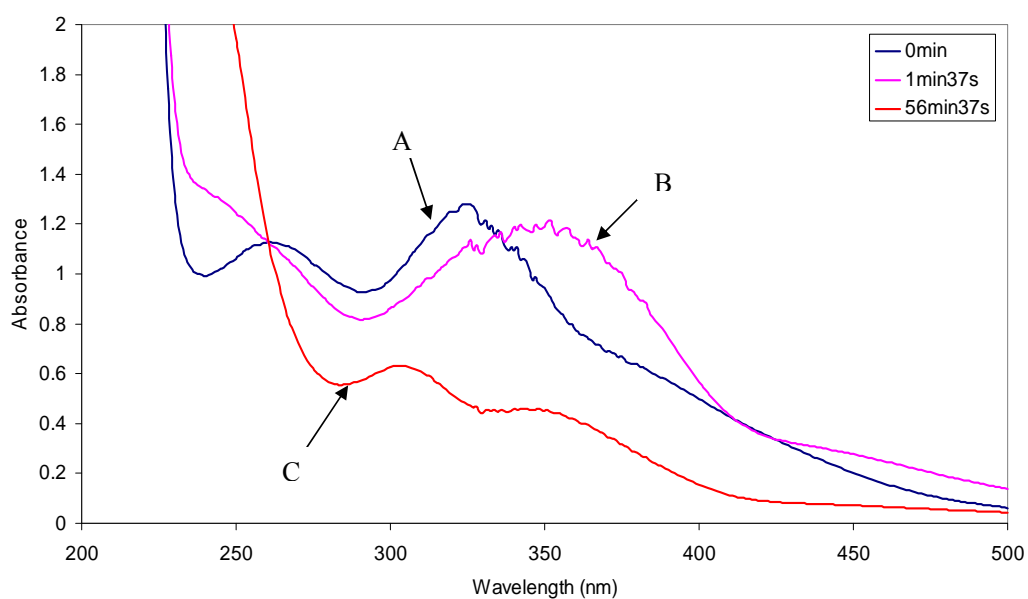


**Figure 3.10:** Spectra isolated at various times during the reaction of 0.0103M ethanol with 4.40 x 10<sup>-4</sup>M [OsO<sub>4</sub>] in 2M NaOH. These depict, as closely as possible, species A (time = 0min), species B (time = 1min37s) and species C (time = 56min37s).

Formatted: Bullets and Numbering

According to the data laid out thus far, it is clear that there must be at least three absorbing species, which for the sake of clarity will be labelled species A, species B and species C:

- 1) the initial osmium(VIII) species (species A);
- 2) the product of step one (species B); and
- 3) the final product of the reaction (species C).

The spectra of these species have been isolated. They could immediately be identified as osmium species, since the possibility of any of the organic species present in the solution (reactants or products) showing absorbance at 370nm was discounted. The labelling of the species as A, B and C does not discount the fact that there may be more than one osmium species present in the solutions with spectra marked A, B and C or that there may be more than two steps involved in the reaction mechanism. Later chapters will look at these aspects in more detail. It will become apparent in later chapters that both the spectra and the progress curves that are shown here for ethanol are not unique to the osmium-ethanol reaction, but are common to every substrate that will be discussed.

---

## 3.4 SUMMARY

---

- 1) The reaction between osmium (VIII) and ethanol follows a two-step process – “step one” and “step two” – which is visible by following the progress of the reaction with UV-VIS spectrophotometry.
- 2) This implies at least three absorbing osmium species:
  - a. Species A (which is the initial osmium(VIII) species);
  - b. Species B (which is the intermediate species); and
  - c. Species C (which is the final osmium product of the reaction).
- 3) This does not discount the possibility that there may be more than two steps to the process or that there may be more than three absorbing osmium species present in the solution.



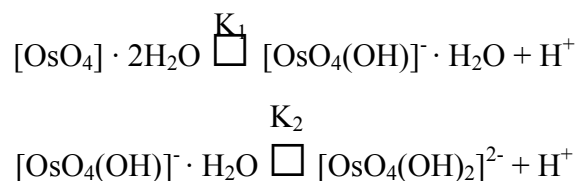
## CHAPTER 4

### DETERMINING THE REACTANTS

#### 4.1 INTRODUCTION

At face value, the identity of the reactants may appear self-evident. However, since one might describe osmium as the schizophrenic of the periodic table due to its placing in the middle of the 3<sup>rd</sup> row of transition metals, it turned out to be fitting that its stability and identity, as well as those of the reacting organic molecules, be investigated.

A previous study by this author <sup>(31)</sup> established the reaction equilibria for the interaction of osmium tetroxide with hydroxide. The reaction equilibria were modelled to the experimental data and a good simulation obtained for the following equilibria:



Acid dissociation constants for the osmium(VIII) acid, written as  $[\text{OsO}_4] \cdot 2\text{H}_2\text{O}$ , were calculated as  $8.69 \times 10^{-13}$  ( $K_1$ ) and  $7.58 \times 10^{-15}$  ( $K_2$ ) and a species distribution diagram was calculated (Figure 4.1). Therefore, since the pH of the solutions in the current study were known, this enabled the prediction of which osmium(VIII) species would be present in solution.

The acid dissociation constants calculated above were compared with acid dissociation constants found from previous studies, <sup>(32)</sup> as shown in Table 4.1. On average, the results compared quite favourably with one another, with the exception of the constants calculated for the tetraprotic osmium acid,  $\text{H}_4[\text{OsO}_6]$ .

**Table 4.1: Average acid dissociation constants calculated in a previous study by this author <sup>(31)</sup> compared to other values reported in the literature <sup>(32)</sup>.**

	$K_1$	$K_2$	$K_3$	$K_4$
<b>Os(VIII) acid</b> <sup>(31)</sup>	$8.8 \times 10^{-13}$	$7.5 \times 10^{-15}$	-	-
$[\text{OsO}_2(\text{OH})_4]$ <sup>(32)</sup>	$6.3 \times 10^{-13}$	$\sim 4 \times 10^{-15}$	-	-
$\text{H}_2[\text{OsO}_5]$ <sup>(32)</sup>	$8.0 \times 10^{-13}$	-	-	-
$\text{H}_{2n}[\text{OsO}_{4+n}]$ <sup>(32)</sup>	$1.0 \times 10^{-12}$	$3.0 \times 10^{-15}$	-	-
$\text{H}_4[\text{OsO}_6]$ <sup>(32)</sup>	$6.3 \times 10^{-8}$	$6.3 \times 10^{-13}$	$1.1 \times 10^{-14}$	$2.0 \times 10^{-15}$
$\text{H}_2[\text{OsO}_5 \cdot \text{H}_2\text{O}]$ <sup>(32)</sup>	$3.2 \times 10^{-13}$			
$\text{H}_2\text{OsO}_5$ <sup>(32)</sup>	$6.4 \times 10^{-13}$	-	-	-

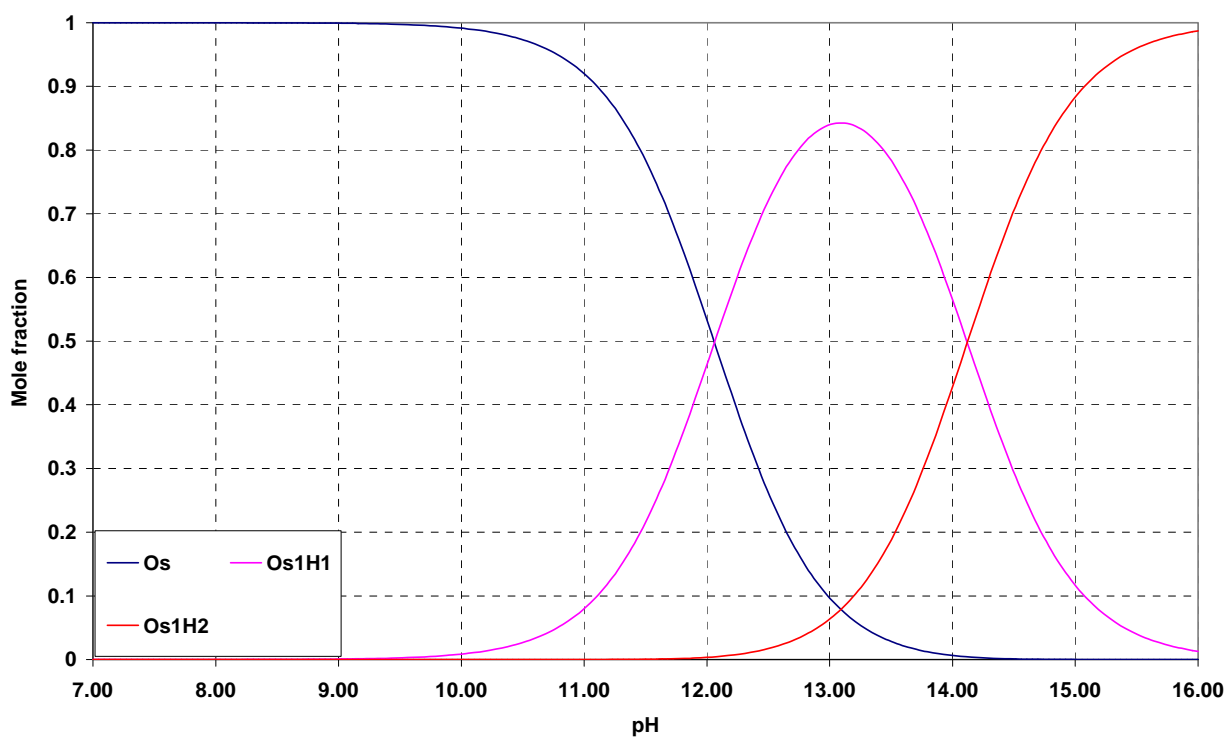
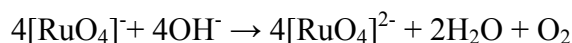
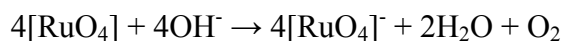


**Figure 4.1: Species distribution diagram for  $\text{OsO}_4$  as a function of pH <sup>(31)</sup>.  $\text{Os} = [\text{OsO}_4] \cdot 2\text{H}_2\text{O}$ ;  $\text{Os1H1} = [\text{OsO}_4(\text{OH})^-] \cdot \text{H}_2\text{O}$ ; and  $\text{Os1H2} = [\text{OsO}_4(\text{OH})_2]^{2-}$**

This species distribution diagram (plotted based on dissociation constants  $8.69 \times 10^{-13}$  ( $K_1$ ) and  $7.58 \times 10^{-15}$  ( $K_2$ )) was based on the rapid two-step equilibria between osmium tetroxide and

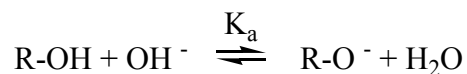
hydroxide, with the hydroxide acting as the coordinating ligand. However, in light of the fact that ruthenium tetroxide is said to be reduced in a two-step process in basic medium, <sup>(42)</sup> the stability of the osmium tetroxide under these conditions was investigated. The ruthenium tetroxide is said to be reduced to the ruthenate(VI) ion via the perruthenate(VII) ion.



By virtue of its status as a *2d* transition metal, ruthenium tetroxide is a stronger oxidising agent than osmium tetroxide but is similar in many other respects, including its tetrahedral structure and their solid states which are yellow, volatile, toxic and smell like ozone. According to the same source <sup>(42)</sup>, osmium tetroxide is stable and is not reduced in basic medium but forms the perosmate ion,  $[\text{OsO}_4(\text{OH})_2]^{2-}$ .

During the course of this investigation, a number of different alcohols were used in comparative studies. Since the first oxidative product of an alcohol is the corresponding ketone or aldehyde, these were also reacted with osmium (VIII) in order to do comparative assessments.

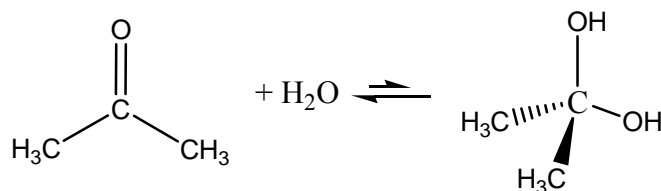
The position with respect to alcohols is fairly straightforward. They are weak acids whose  $\text{pK}_a$ 's are generally known. It is therefore a simple matter to calculate the relative percentages of alcohol and alkoxide ion in solution. The acidity of an alcohol is related primarily to the solvent stabilisation of the alkoxide ion that results from the dissociation. Therefore, the more easily accessible oxygen atom of the methoxide ion is more readily solvated by water than the more sterically hindered *t*-butoxide. Therefore, methanol is a stronger acid than *t*-butanol. The generalised equation in basic medium is:



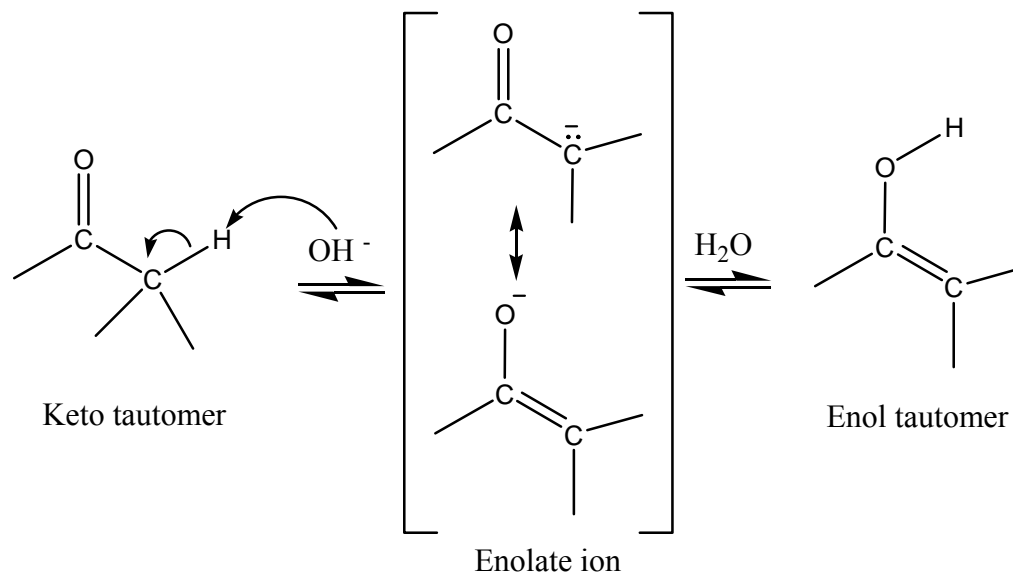
Inductive effects are also important in determining alcohol acidities. Electron-withdrawing substituents such as halogens spread the electron density over a larger area, making the alkoxide ion more stable and, hence, more acidic <sup>(38)</sup>.

The oxidation of alcohols should get a brief mention here. Primary alcohols are oxidised to aldehydes or carboxylic acids, secondary alcohols yield ketones, and tertiary alcohols are unreactive to most oxidising agents.

The position with respect to aldehydes and ketones is somewhat more complex. Aldehydes are generally more reactive to oxidation than ketones due to the  $-CHO$  proton that can be abstracted during oxidation. Ketones are generally inert to oxidation. The oxidation occurs via the formation of a 1,1 diol which is, to a varying degree, a reversible reaction common to all aldehydes and ketones. In aqueous solution, water adds to the aldehyde or ketone in a base-catalysed reaction as shown below for acetone. In the case of acetone, the percentage diol at equilibrium is only 0.1%, whereas the percentage of diol of an aqueous solution of formaldehyde at equilibrium would be 99.9%. As can be seen, the formation of the gem diol of a ketone results in a tertiary alcohol, which is unreactive to oxidation.

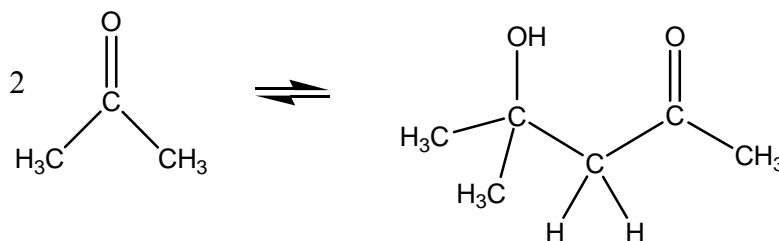


Ketones and aldehydes have the added complication of existing in equilibrium with their enols and enolates to greater or lesser extents. Whereas 0.0001% cyclohexanone exists as its enol at equilibrium, only 0.000001% of acetone exists as the enol. The enols and enolates exist by virtue of the fact that the  $\alpha$ -hydrogens of ketones and aldehydes are acidic and can be removed by a base. The mechanism of the base-catalysed formation of an enol is shown below.



Enolate ions are more stable and can be produced in higher yield in basic solution than the enol tautomer due to the resonance stabilisation of the two enolate forms. Enolates are also more reactive than enols thanks to their negative charge, which makes them better nucleophiles. They can react either at the negatively charged oxygen or carbon atoms.

One final aspect of carbonyl chemistry that needs to be mentioned is the carbonyl condensation reaction. The negatively charged carbon atom of an enolate ion launches a nucleophilic attack on the electrophilic carbonyl group to produce a condensation product as shown below.



Mono-substituted acetaldehydes ( $\text{RCH}_2\text{CHO}$ ) favour the product, but di-substituted acetaldehydes ( $\text{R}_2\text{CHCHO}$ ) and ketones favour the starting material. In the example above for acetone, approximately 5% condensation product is formed. But phenylacetaldehyde ( $\text{Ph-CH}_2\text{CHO}$ ) yields 90% condensation product in sodium hydroxide medium.

Therefore, there is a range of possibilities as starting materials for the organic products: for the alcohols – mostly alcohol with a small percentage alkoxide ion; for the ketones and aldehydes – a mixture of ketone/aldehyde; 1,1 diol; enolate; enol and aldol.

---

---

## **4.2 EXPERIMENTAL**

---

---

### **4.2.1 Osmium(VIII) – iron titrations: determining initial oxidation state**

This method of determining the oxidation state of the osmium was successfully used in a previous study <sup>(31)</sup>. High oxidation state osmium complexes are reduced in acidic media by iron(II) to osmium(IV).

Potentiometric titrations were performed on osmium tetroxide dissolved both in distilled water and in 2M hydroxide medium. A measured volume of standardised iron(II) solution in 10% (v/v) sulfuric acid was added to a beaker along with 25% (v/v) phosphoric acid and enough distilled water to cover the electrode. This was titrated with the aqueous or basic osmium solution of known concentration. The endpoint was calculated using the Hahn and Weiler method as explained in Chapter 2.

### **4.2.2 Molar extinction coefficients**

The absorbance dependence on osmium concentration was investigated in order to confirm adherence to Beer's law and to determine molar extinction coefficients, which could later be used in equilibrium and kinetic modelling programmes.

A stock osmium tetroxide solution was prepared in distilled water according to the method in Chapter 2. The concentration of the stock solution was determined using the thiourea method. Various dilutions of the stock solution were then made up in 2M sodium hydroxide such that the final concentrations of the nine solutions were between  $9.19 \times 10^{-6} \text{M}$  and  $9.18 \times 10^{-4} \text{M}$ . Their UV-VIS spectra were read across the range 500 to 200nm.

### 4.2.3 Stability of osmium(VIII) in hydroxide medium

A simple kinetic study was run that was basically a blank of the osmium(VIII) - alcohol/ketone reactions.

An osmium tetroxide solution in distilled water was freshly prepared and its concentration determined by the thiourea method. This was mixed with sodium hydroxide at time equals zero minutes to give a final hydroxide concentration of 2M. Thereafter, the spectrophotometer was set to scan the range 500nm to 200nm at set cycle intervals. The reaction was stopped after 4380 minutes (73 hours).

## 4.3 RESULTS AND DISCUSSION

### 4.3.1 Theoretically determined osmium(VIII) and organic reactant species

#### 4.3.1.1 Osmium(VIII)

The percentages of the various osmium(VIII) species theoretically present in solutions of varying pH were calculated from the species distribution diagram in Figure 4.1. The pH's represent those that were utilised during this study.

**Table 4.2: Percentages of the various osmium(VIII) species present in solutions of varying pH calculated from species distribution diagram, Figure 4.1 <sup>(31)</sup>**

[Hydroxide] (mol/l)	pH	% [OsO <sub>4</sub> ]	% [OsO <sub>4</sub> (OH)] <sup>-</sup>	% [OsO <sub>4</sub> (OH) <sub>2</sub> ] <sup>2-</sup>
0.025	12.40	29.5	69.5	1.00
0.05	12.70	17.9	79.3	2.90
0.1	13.00	10.0	83.9	6.10
0.5	13.70	1.50	71.4	27.1
1	14.00	0.70	57.2	42.1
2	14.30	0	40.0	60.0
3	14.48	0	29.5	70.5

At pH 14.3, at which most the alcohol experiments were performed, the ratio of osmium species would be 40%  $[\text{OsO}_4(\text{OH})]^-$  and 60%  $[\text{OsO}_4(\text{OH})_2]^{2-}$ .

#### 4.3.1.2 Organic

Apart from methanol, the non-aromatic alcohols can be represented by generic  $\text{pK}_a$ 's for primary, secondary and tertiary alcohols, respectively <sup>(19)</sup>.

**Table 4.3: Theoretically calculated percentages of some alcohol/alkoxide ratios in solutions of varying pH**

	pH	12.40	12.70	13.00	13.70	14.00	14.30	14.48
<b>Methanol</b> ( $\text{pK}_a = 15.54$ <sup>(38)</sup> )	% $\text{RO}^-$	0.07	0.14	0.29	1.45	2.88	5.75	8.71
	% $\text{ROH}$	99.93	99.86	99.71	98.55	97.12	94.25	91.29
<b>RCH<sub>2</sub>OH</b> ( $\text{pK}_a = 16.00$ <sup>(19)</sup> )	% $\text{RO}^-$	0.03	0.05	0.10	0.50	1.00	2.00	3.02
	% $\text{ROH}$	99.97	99.95	99.90	99.50	99.00	98.00	96.98
<b>R<sub>2</sub>CHOH</b> ( $\text{pK}_a = 17.00$ <sup>(19)</sup> )	% $\text{RO}^-$	0.00	0.01	0.01	0.05	0.10	0.20	0.30
	% $\text{ROH}$	100.00	99.99	99.99	99.95	99.90	99.80	99.70
<b>R<sub>3</sub>COH</b> ( $\text{pK}_a = 18.00$ <sup>(19)</sup> )	% $\text{RO}^-$	0.00	0.00	0.00	0.01	0.01	0.02	0.03
	% $\text{ROH}$	100	100	100	99.99	99.00	99.98	99.97
<b>Benzyl alcohol</b> ( $\text{pK}_a = 15.2$ <sup>(15)</sup> )	% $\text{RO}^-$	0.16	0.32	0.63	3.16	6.31	12.59	19.05
	% $\text{ROH}$	99.84	99.68	99.37	96.84	93.69	87.41	80.95

Therefore, at the pH at which most of the alcohol experiments were conducted (pH 14.3), the alcohols range from negligible dissociation (*t*-butanol at 0.02%) to significantly dissociated (benzyl alcohol at 12.59%). Ethanol, the only alcohol that we have discussed in any detail so far, is 2% dissociated at pH 14.3.



### 4.3.2 Osmium(VIII) – iron titrations: determining initial oxidation state

Figure 4.2 shows the potentiometric titration curves for the titration of acidic iron(II) by osmium tetroxide in a) distilled water; and b) 2M hydroxide. Using the Hahn and Weiler method to determine the endpoint, resulted in endpoints of a) 3.95 and b) 4.09 (mol Fe / mol Os). If one assumes the final osmium oxidation state to be +4<sup>(31)</sup>, this essentially means that the osmium has undergone a 4-electron reduction, which confirms that it was in the +8 oxidation state to begin with.

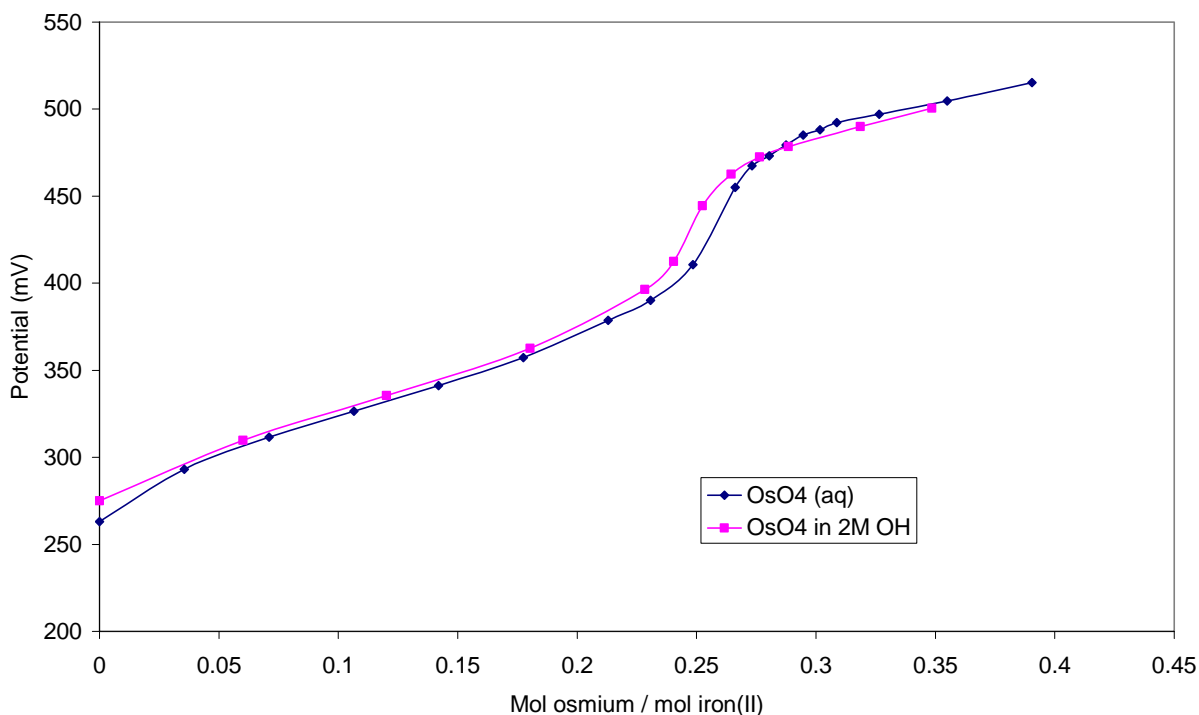
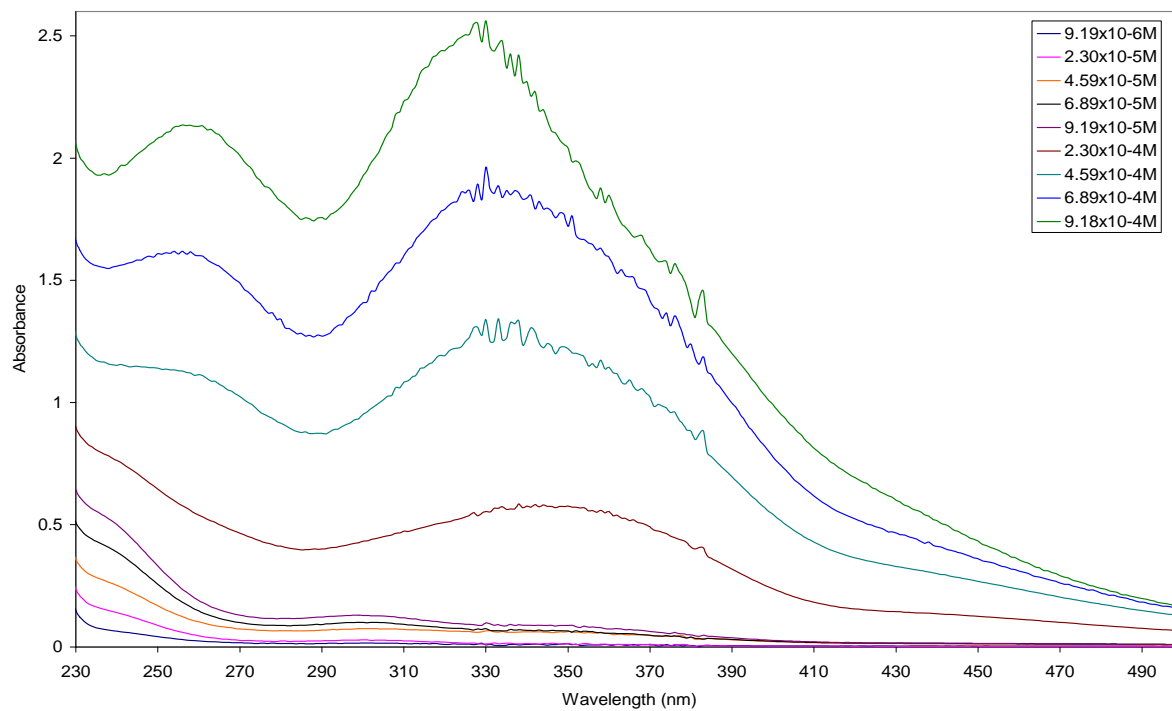


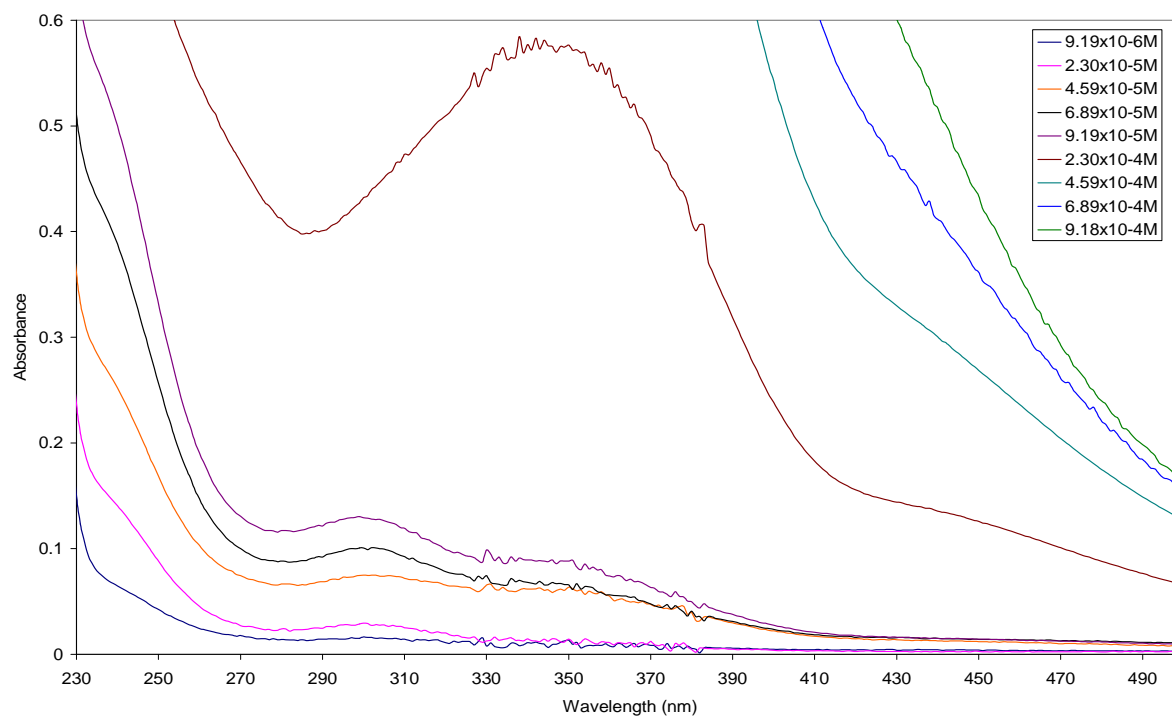
**Figure 4.2: Potentiometric titration curves for the titration of an acidic 0.00193M iron(II) solution with a) 0.00137M osmium tetroxide in distilled water; and b) 0.00116M osmium tetroxide in 2M hydroxide.**

### 4.3.3 Molar extinction coefficients

Figure 4.3 (a) and (b) show the UV-VIS spectra of osmium tetroxide solutions of varying concentration in a 2M sodium hydroxide matrix. The concentrations of the solutions are widespread and the two most concentrated solutions were read in 1mm cuvettes. Their absorbances were then corrected to correspond to the other solutions, which were read in 1cm cuvettes. The least concentrated solutions are shown in Figure 4.3 (b) on a smaller scale y-axis, since they are not clearly visible in Figure 4.4 (a).



(a)



(b)

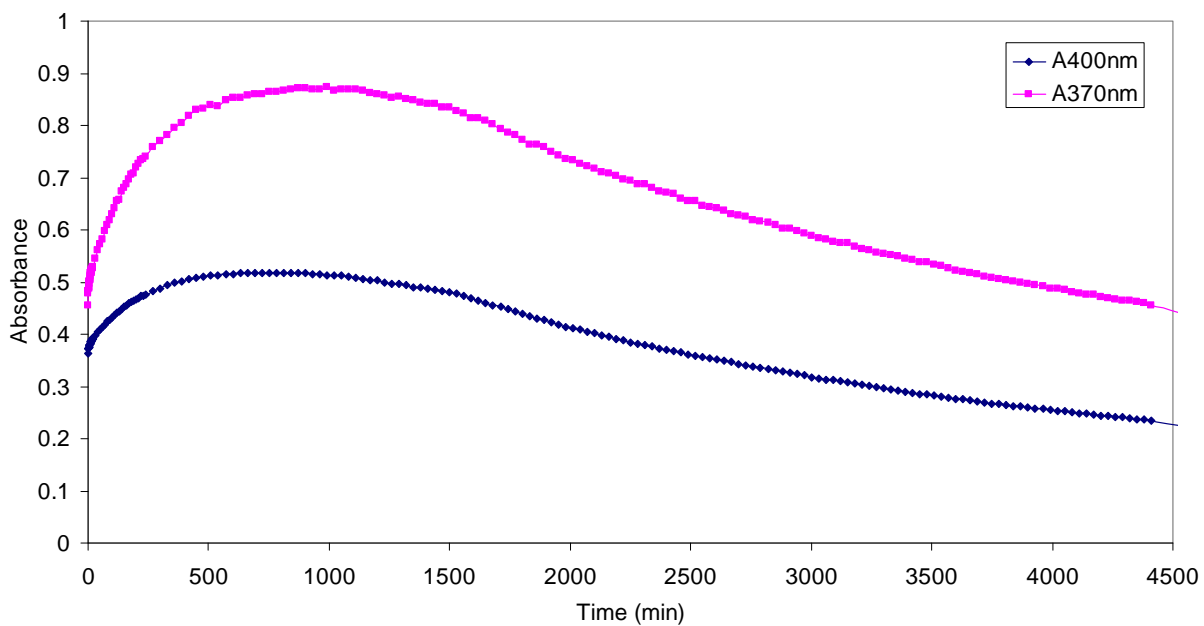
**Figure 4.3: The UV-VIS spectra of osmium tetroxide solutions of varying concentration in 2M hydroxide. (a) y-axis = 0 to 2.6 (b) y-axis = 0 to 0.6**

It is clear from the above figures that the osmium spectrum changes as a function of its concentration. It will be shown later that these spectra are the same as those observed during the reduction of osmium(VIII) by alcohols, aldehydes and ketones. Therefore, the osmium(VIII) is undergoing reduction as a function of the osmium concentration. The rate dependence on the osmium concentration will be discussed in more detail in Chapter 8.3.1.

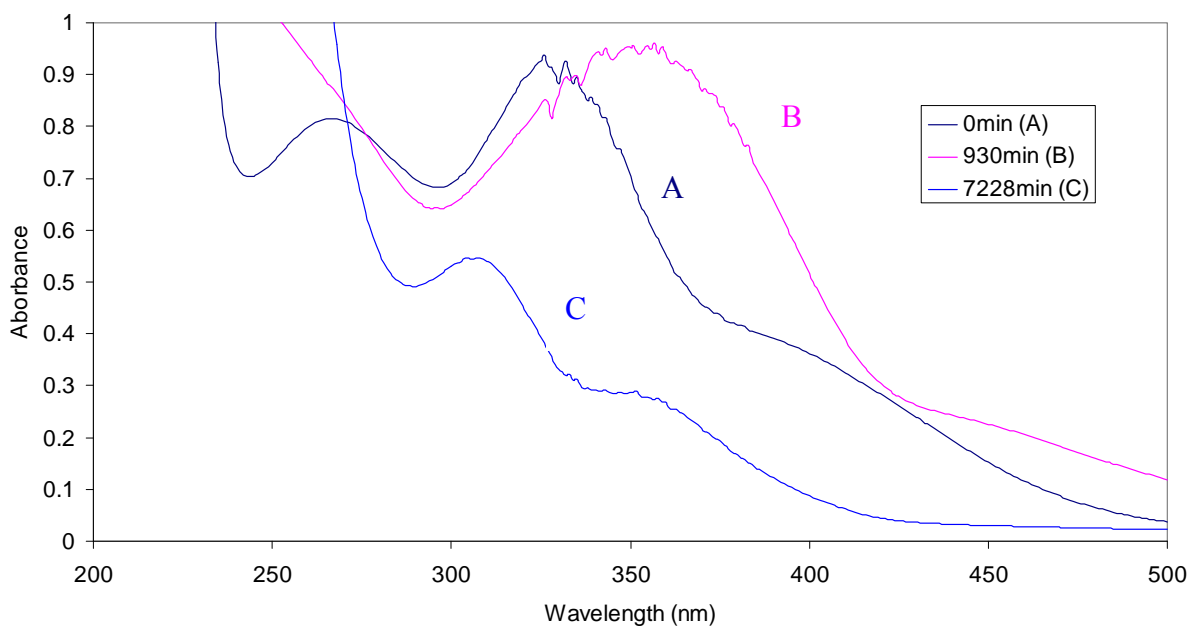
The molar extinction coefficient for osmium tetroxide in 2M hydroxide was calculated at 370nm (the wavelength most commonly used in this study) by using a single solution – the most concentrated osmium tetroxide solution. The molar extinction coefficient thus calculated using Beer's Law ( $A = \epsilon c l$ ), was  $1772 \text{ L}\cdot\text{mol}^{-1}\cdot\text{cm}^{-1}$ .

#### **4.3.4 Stability of osmium(VIII) in hydroxide medium**

Figure 4.4 (a) shows the progress curves of the reaction of osmium tetroxide in hydroxide medium. It is clear to see that there is a reaction taking place and the shape of the progress curve is similar to that for the reduction of osmium(VIII) by ethanol that was seen in the previous chapter. There is an initial increase in absorbance, followed by a slow decrease. Again, a minimum of a two-step process and a minimum of three absorbing osmium species are observed. Figure 4.4 (b) shows some of the spectra in isolation for clearer viewing. The initial spectrum of the osmium tetroxide in 2M hydroxide is shown at time equal to zero minutes (species A). The second spectrum, at 930 minutes (15.5 hours), represents the turning point in the progress curve and would correspond to species B as discussed in the previous chapter. The final spectrum depicts species C at 7228 minutes (or 120 hours). Comparisons between the products of the various reactions will be made in the following chapter, where this will be discussed in more detail.



(a)



(b)

**Figure 4.4:** (a) The progress curves of a  $4.93 \times 10^{-4} \text{ M}$  osmium tetroxide solution in 2M hydroxide over time.

(b) Selected spectra (corresponding to species A, B and C) taken at different times during the reaction of  $4.93 \times 10^{-4} \text{ M}$  osmium tetroxide solution with 2M hydroxide.

From Figures 4.4 (a) and (b) it is evident that the osmium(VIII) reacts with the hydroxide medium, albeit very slowly. The absorbing species that are observed in this reaction are identical to the absorbing species observed in the reduction of osmium(VIII) by ethanol. The assumption is, therefore, that the reduction of the osmium(VIII) is proceeding via the same absorbing osmium species, whether the reducing agent is ethanol or water.

The question to answer here is whether the reaction of the osmium tetroxide with the hydroxide is fast enough to affect the validity of the following experiments into the rate and stoichiometry of the alcohol–osmium(VIII) reaction and the ketone–osmium(VIII) reaction.

Figure 4.5 seeks to answer that question. The “blank”, or reaction of osmium tetroxide with hydroxide, is superimposed on the progress curves of the reaction of osmium tetroxide with ethanol in 2M hydroxide from the previous chapter. During the time period of the experiment (20 minutes) there is a small, but perceptible, increase in the absorbance of the blank. In terms of the kinetics of the experiments, the contribution of the blank is negligible since the rate of the ethanol reaction is orders of magnitude greater than that without ethanol. Comparisons of greater accuracy can be drawn in later chapters once the rate constants of the various reactions have been established. However, in determining stoichiometry, caution must be employed since, while waiting for the alcohol–osmium(VIII) equilibrium to be established, there may be a contribution by the hydroxide–osmium(VIII) reaction. This must be borne in mind in later chapters dealing with stoichiometry.

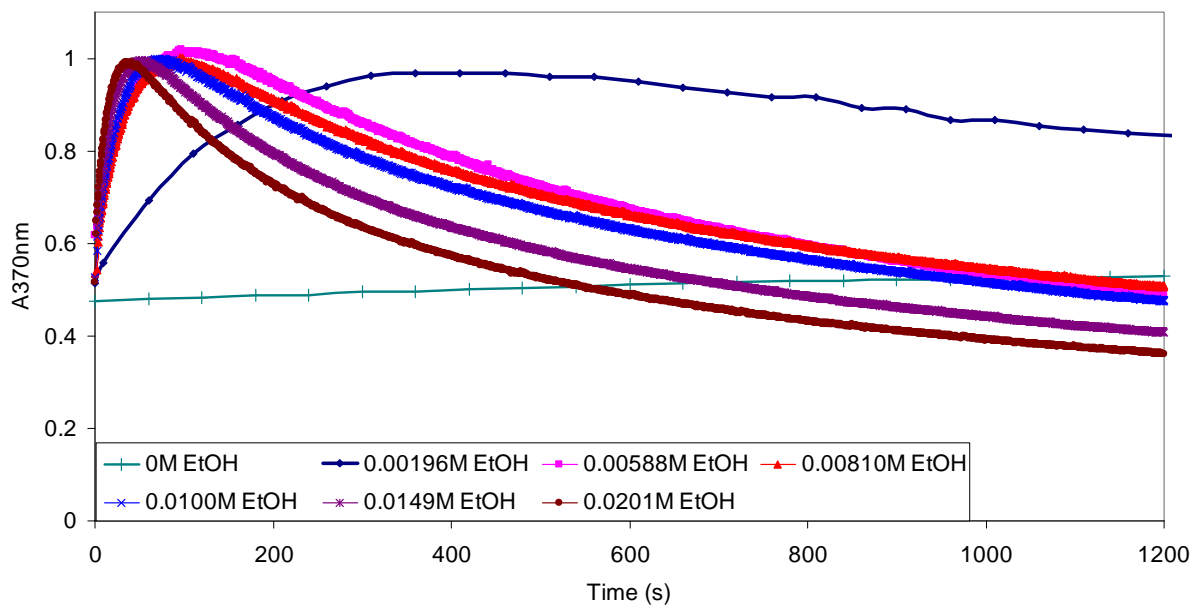
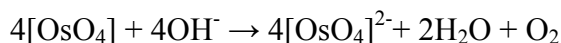
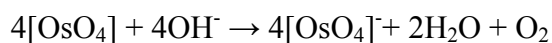


**Figure 4.5:** The progress curves of the rate of change of absorbance at 370nm at varying ethanol concentrations.  $[\text{OsO}_4] = 4.32 \times 10^{-4}\text{M}$ ;  $[\text{NaOH}] = 2\text{M}$ . Reaction with 0M ethanol;  $[\text{OsO}_4] = 4.93 \times 10^{-4}\text{M}$ ;  $[\text{NaOH}] = 2\text{M}$ .

## 4.4 SUMMARY

1. The ratios of the initial osmium(VIII) reacting species ( $[\text{OsO}_4]$ ,  $[\text{OsO}_4(\text{OH})]^-$  and  $[\text{OsO}_4(\text{OH})_2]^{2-}$ ) were determined at the various pH's that were used in this study.
2. The initial reacting organic species are as follows:
  - 2.1. Alcohols: A mixture of the alcohol and alkoxide ion determined according to the  $\text{pK}_a$  at various pH's.
  - 2.2. Ketones: A mixture of ketone, 1,1 diol, enolate, enol and aldol.
3. It was found that the oxidation state of the initial osmium reacting species in distilled water and hydroxide medium was +8.
4. The osmium(VIII) in hydroxide medium was reduced as a function of osmium concentration. The more concentrated the osmium, the more stable it was in its +8 state. The molar extinction coefficient of the osmium(VIII) in 2M hydroxide was determined as  $1772 \text{ L}\cdot\text{mol}^{-1}\cdot\text{cm}^{-1}$ .
5. The osmium(VIII) undergoes a two-step reaction in basic medium analogous to that with ethanol, only on a much larger time scale. Therefore, contrary to accepted belief<sup>(42)</sup>, it may be speculated at this stage that osmium(VIII) undergoes a reaction similar to that of ruthenium tetroxide in basic medium that was quoted in the introduction to this chapter, namely:



The basic osmium(VIII), (VII) and (VI) species are written in a simplified version at this stage.

6. It was determined that the osmium(VIII)–hydroxide reaction would not interfere with the kinetic studies, but that caution should be employed when conducting equilibrium studies.

## CHAPTER 5

# DETERMINING THE PRODUCTS

---

---

### 5.1 INTRODUCTION

---

---

In this chapter the products of the osmium(VIII)–alcohol and osmium(VIII)–ketone reactions will be discussed. It was established in Chapters 3 and 4 that the reaction occurs in two steps and that these steps can be followed by UV-VIS spectrophotometry. This chapter will show that this holds true for all the various alcohol and ketone (and miscellaneous other) reactants. It will also be shown that, not only is the two-step mechanism followed throughout the various reactions, but that the absorbing osmium products of the two steps (what have been described as species B and species C in previous chapters), are the same no matter what reductant is used.

Organic products determined for alcohols have been variously identified in the literature as propionic acid for 1-propanol and oxalic acid and acetic acid for 2-propanol by paper chromatography <sup>(2)</sup>; aldehydes for primary alcohols by infra red spectra <sup>(10)</sup>; and keto acids for  $\alpha$ -hydroxy acids by spot tests <sup>(14)</sup>. The products of the reaction of acetone with osmium tetroxide in basic medium have been identified as oxalic acid and acetic acid, seemingly by inference of the same reaction with alkaline permanganate <sup>(5)</sup>. Mandelate ( $\text{Ph-CH(OH)(CO}_2^-)$ ) gave benzoic acid and  $\text{CO}_2$  by paper chromatography <sup>(3)</sup> and tartrate ( $^-2\text{OC-CH(OH)-CH(OH)-CO}^2^-$ ) and malate ( $^-2\text{OC-CH(OH)-CH}_2\text{-CO}^2^-$ ) gave tartronate ( $^-2\text{OC-CH(OH)-CO}^2^-$ ) and malonate ( $^-2\text{OC-CH}_2\text{-CO}^2^-$ ) by paper chromatography <sup>(4)</sup>. There is, therefore, no appreciable consensus in the literature on the products of oxidation of alcohols and ketones, with some publications reporting the products of the reactions to be aldehydes and ketones, while others report the oxidation continuing through to the carboxylic acid. There is even the report of the oxidation of a carboxylic acid, 2-bromopropionic acid, to oxalic acid as identified by paper chromatography <sup>(6)</sup>. All of the above studies were conducted in aqueous alkaline medium.



When it comes to the osmium product of the reaction, the consensus is that it is an osmium(VI) species, formulated variously as  $[\text{OsO}_2(\text{OH})_4]^{2-}$  (2, 10),  $[\text{OsO}_3]^{(14)}$ ,  $[\text{OsO}_4(\text{OH})_2]^{4-}$  (4) and  $[\text{OsO}_4]^{2-}$  (3, 5).

In no cases has the existence of a stable intermediate been reported.

---

## 5.2 EXPERIMENTAL

---

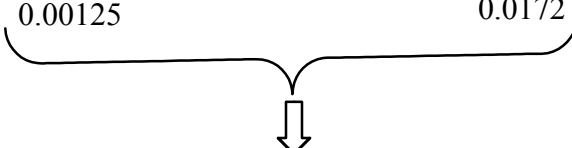
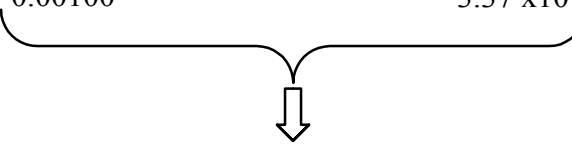
### 5.2.1 Osmium products

#### 5.2.1.1 Determining oxidation state

The oxidation states of the osmium products were determined by iron(II) potentiometric titration. In some instances the titrations were performed as a “by-product” of a mole ratio or kinetic experiment. In the case of mole ratio experiments, volumetric flasks were made up with a constant osmium tetroxide concentration and increasing 1-propanol and 2-propanol concentrations, respectively, in a 2M hydroxide matrix. The solutions were allowed to react for 3 hours at 25°C, which was considered the optimum time during which the osmium tetroxide–propanol reaction would have equilibrated, while the osmium tetroxide–hydroxide reaction would not have proceeded to any appreciable extent. Certain solutions were then selected, based on their position on the mole-ratio plot (see results), to be titrated against an acidic iron(II) solution as described in Chapter 2.

The oxidation state of final (species C) osmium products were determined for experiments using ethanol and methanol as substrate. In the case of ethanol,  $4.40 \times 10^{-4}$ M osmium tetroxide in 2M hydroxide was reacted with 0.004M ethanol. The kinetics of the reaction were followed spectrophotometrically for approximately 150 minutes. The reaction was then judged to have gone to completion. The final solution was then titrated against an acidic iron(II) solution. In the case of methanol, two experiments were run. In the first,  $5.2 \times 10^{-4}$ M osmium tetroxide in 2M hydroxide was reacted with 0.00314M methanol for approximately 3 hours and in the second, the same concentration osmium tetroxide in 2M hydroxide was reacted with 0.00986M methanol for the same time. The final solutions were then titrated against an acidic iron(II) solution.

In two other instances, titrations were performed in purpose-designed experiments to determine the oxidation state of the osmium products of alcohol and ketone reactions. The osmium tetroxide was reacted with specific concentrations of ethanol or acetophenone, as calculated from previous equilibria studies, to produce species B and species C, respectively. The ethanol solutions were allowed to react overnight in 0.1M hydroxide matrices. The hydroxide concentration was kept purposely low in order not to promote reduction of the osmium(VIII) by hydroxide. The acetophenone solutions were mixed in a 2M hydroxide matrix, but titrated immediately since the rate of this reaction is extremely fast in 2M hydroxide and equilibrates within minutes. The solutions were titrated against an acidic iron(II) solution as described previously.

<b>[OsO<sub>4</sub>]</b>	<b>reacted with</b>	<b>[ethanol]</b>	<b>Mol Os / Mol Ethanol</b>
0.00120		3.43x10 <sup>-4</sup>	0.25
0.00139		0.00172	1.08
0.00125		0.0172	12
			
Titrated against 0.00193M Fe(II) solution			
<b>[OsO<sub>4</sub>]</b>	<b>reacted with</b>	<b>[acetophenone]</b>	<b>Mol Os / Mol Acetophenone</b>
0.00105		1.09 x10 <sup>-4</sup>	0.10
0.00100		3.37 x10 <sup>-4</sup>	0.32
			
Titrated against 0.00197M Fe(II) solution			

### 5.2.1.2 Comparing the spectra for “species B” and “species C” for different reducing agents

Spectra for both species were selected from kinetic data for all the various alcohols, ketones and other miscellaneous reactants. The spectra were selected by first viewing a progress curve of the reaction at a particular wavelength (370nm). The spectrum at the progress curve maximum was selected as representative of “species B” for that reaction. The final spectrum was chosen as the spectrum representative of “species C” for that reaction. In some cases, the reaction was allowed to run for longer than the usual 20

minute reaction time since it had not yet run to completion in that time and “species C” was not yet fully formed.

#### **5.2.1.3 Osmium(VIII) – osmium(VI) titration**

A surprising discovery was made when a rapid equilibrium between osmium(VIII) and osmium(VI) was observed when adding approximately equal concentrations of potassium osmate to osmium tetroxide in 2M hydroxide. The course of the reaction was followed by UV-VIS spectrophotometry. The reaction equilibrated within 10 seconds and was stable over at least 40 minutes.

Thereafter, a titration was performed during which 2.5ml of a 0.00156M osmium tetroxide solution, 7.5ml distilled water and 5ml of 6M sodium hydroxide were placed in a stirred reaction vessel. This was titrated with a 0.00110M potassium osmate solution made up in 2M sodium hydroxide. The UV-VIS spectrum was read from 500 to 200nm after each addition of potassium osmate. Other titrations were performed with slightly differing concentrations.

#### **5.2.1.4 Determining a molar extinction coefficient for species B**

A known concentration of osmium tetroxide was mixed with hydroxide to make up a 2M hydroxide matrix. In one instance the reaction was started upon addition of the hydroxide. No other reducing agent was used. In the other reactions, a known concentration of alcohol or ketone was added. The reaction was then followed spectrophotometrically, scanning across the range 500nm to 200nm, over time.

Thereafter, two wavelengths were selected – 370nm and 250nm. The absorbances at both of these wavelengths were plotted versus each other as the reaction progressed. This resulted in two straight lines and the absorbance at the intercept of these lines was determined. One of the straight lines represents the first step of the reaction and the other line represents the second step in the reaction. In other words, the first line represents the formation of species B and the second line represents its depletion. At the intercept of the two lines, there should be only species B present and, since the concentration and cuvette pathlength is known, the molar extinction coefficient of B can be determined using Beer’s Law.

### 5.2.2 Organic products

The organic products of the reaction were determined by  $C^{13}$ NMR. In order to detect the organic products by NMR it was necessary to concentrate them in solution. This was done by establishing an experimental set-up as depicted in Figure 5.1.

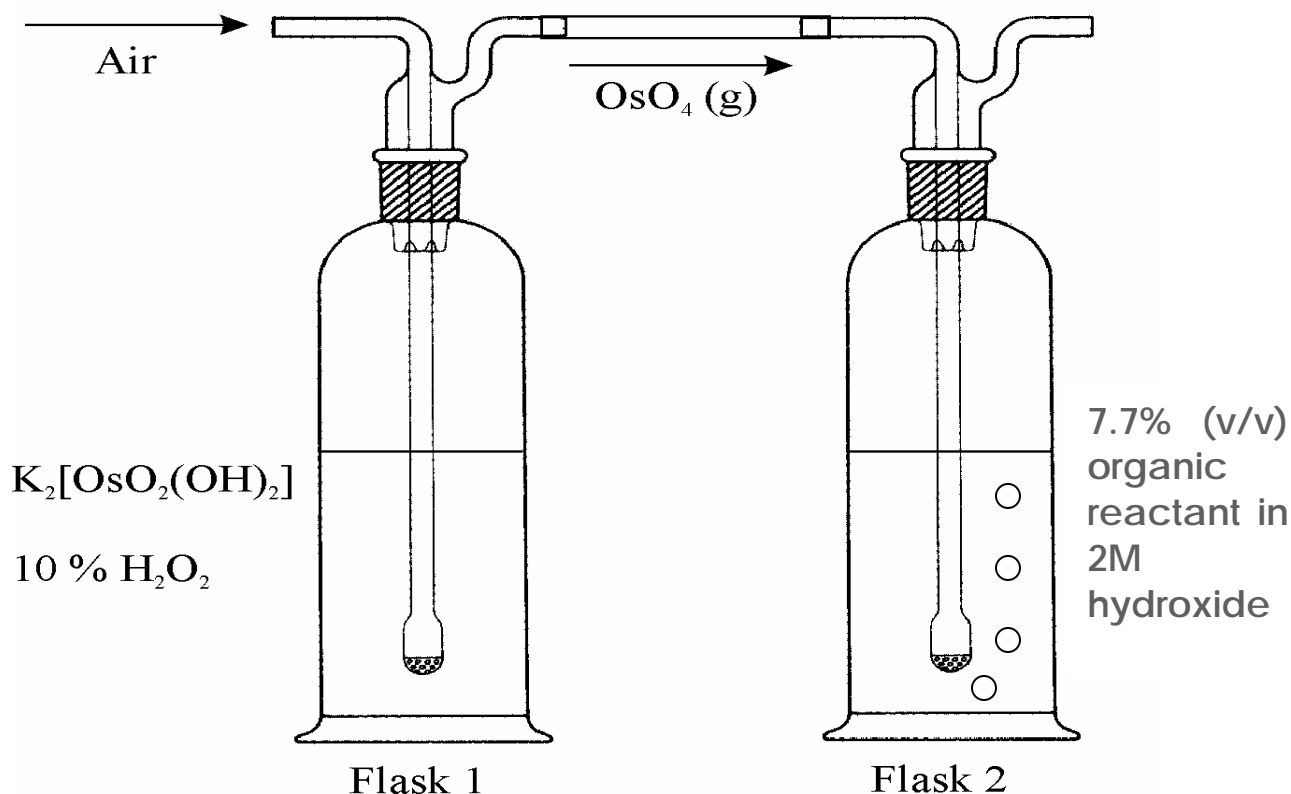


**Figure 5.1: Experimental set-up for the preparation of organic products for NMR analysis**

A source of osmium, potassium osmate, was put into flask 1 along with the oxidant, a 10% (v/v) of a 30% hydrogen peroxide solution in 50% (v/v) phosphoric acid. This was connected to the second flask in which was 2.5ml of the reductant in 30ml 2M sodium hydroxide. Air was bubbled through, which forced the osmium tetroxide produced in flask one, through the solution in flask two. This was allowed to run for between 12 and 24 hours in order to accumulate a large enough concentration of osmium tetroxide to generate enough oxidised organic product to be visible on NMR.

NMR spectra were gathered as described in Chapter 2.1.3.

## 5.3 RESULTS AND DISCUSSION

### 5.3.1 Osmium products

#### 5.3.1.1 Determining oxidation state

Figures 5.2 and 5.3 below show the mole ratio plots for the reactions of osmium tetroxide in 2M hydroxide with 1-propanol and 2-propanol, respectively. The solutions were labelled *a* to *s* and those depicted on the figures below were the ones titrated against an acidic iron(II) solution to determine their oxidation state. The results of these titrations are given in Table 5.1 below.

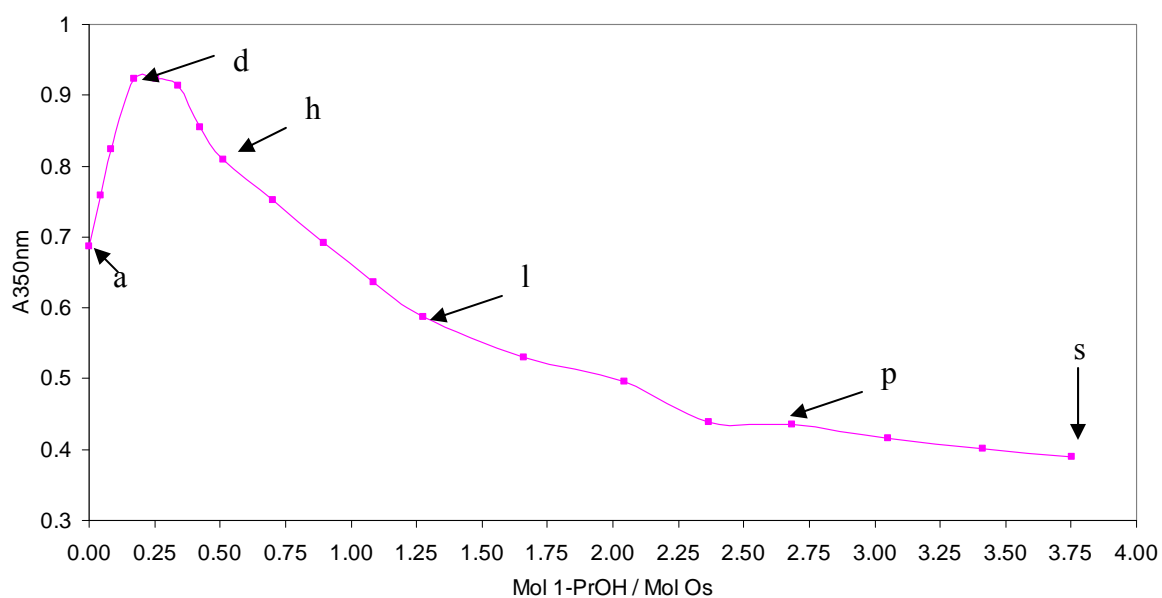


**Figure 5.2:** Mole ratio plot for the reaction of  $4.07 \times 10^{-4}$  M osmium tetroxide with increasing concentrations of 1-propanol in 2M hydroxide. Solutions were reacted for 3 hours at 25°C.

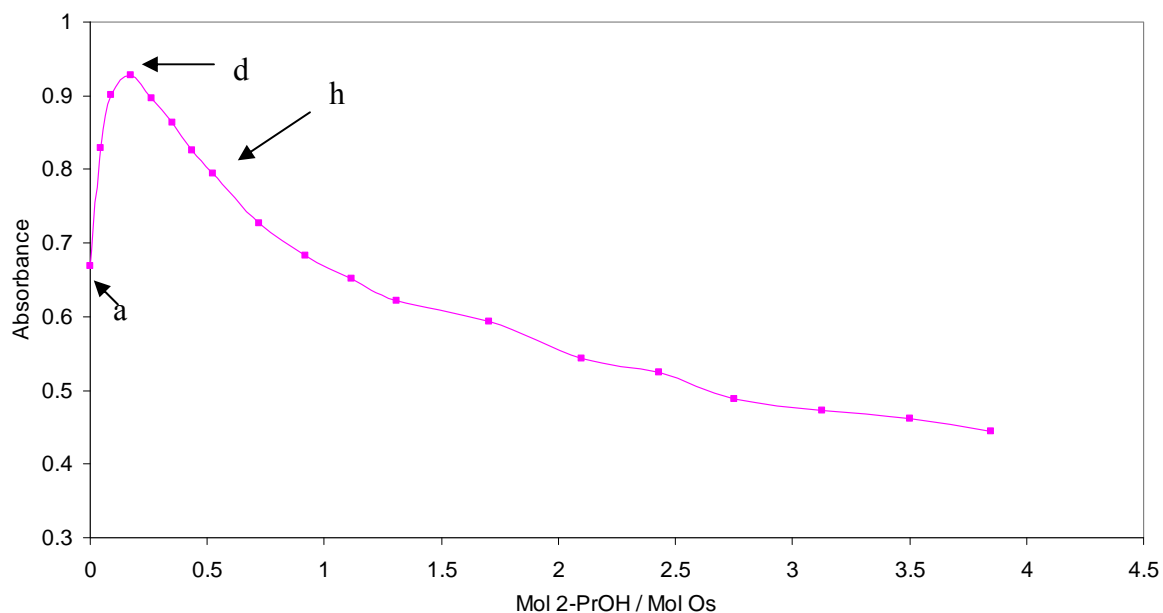


**Figure 5.3:** Mole ratio plot for the reaction of  $3.97 \times 10^{-4} \text{M}$  osmium tetroxide with increasing concentrations of 2-propanol in 2M hydroxide. Solutions were reacted for 3 hours at  $25^\circ\text{C}$ .

**Table 5.1:** Number of equivalents Fe(II) ( $n$ ) required to reduce osmium solutions (labelled in Figures 5.2 and 5.3) to osmium(IV) and the starting oxidation state that this implies (see discussion below).

Solution #	1-Propanol		2-Propanol	
	$n$	Osmium <sup>+x</sup>	$n$	Osmium <sup>+x</sup>
a	3.5	~ +8	3.5	~ +8
d	2.5	~ +7	2.6	~ +7
h	2.3	~ +6	2.2	~ +6
l	2.2	~ +6	-	-
p	2.0	+6	-	-
s	2.0	+6	-	-

It is evident from the above table that the values for  $n$  of solutions *a* to *l* are somewhat smaller than expected. What this implies is that the osmium is in a lower oxidation state than expected and is in a somewhat lower oxidation state than that given for it in columns 3 and 5. However, it must be borne in mind that there was some reduction by the hydroxide in these solutions. In determining the reactants in the previous chapter, it was

established that the initial oxidation state of the osmium is +8. The current experiment shows the oxidation state to be slightly less than that, which simply proves the contention that some reduction took place via the hydroxide reaction. However, it is useful to note that the difference between the iron(II) equivalents of solutions *a* and *d* (which correspond to species A and species B as shown in Figures 5.2 and 5.3) is exactly one. Therefore, the osmium species is undergoing a one electron reduction from species B to species C. The reaction in solution *s*, which has a four times excess of 1-propanol and has proceeded to completion, expresses a perfect two electron reduction – from osmium(VI) to osmium(IV). The effect of hydroxide is now not noticed because the reaction has proceeded to equilibrium. Therefore, the final oxidation state of the osmium can be said, with relative certainty, to be the +6 oxidation state. However, this will be re-emphasised in the following experiments.

The oxidation state of the final product of the two-step reaction, species C, was determined after the osmium(VIII) had been reacted with ethanol and methanol. The kinetic experiment was allowed to run to completion and the oxidation state of the final osmium products determined by iron(II) titration. Table 5.2 shows the results of these experiments.

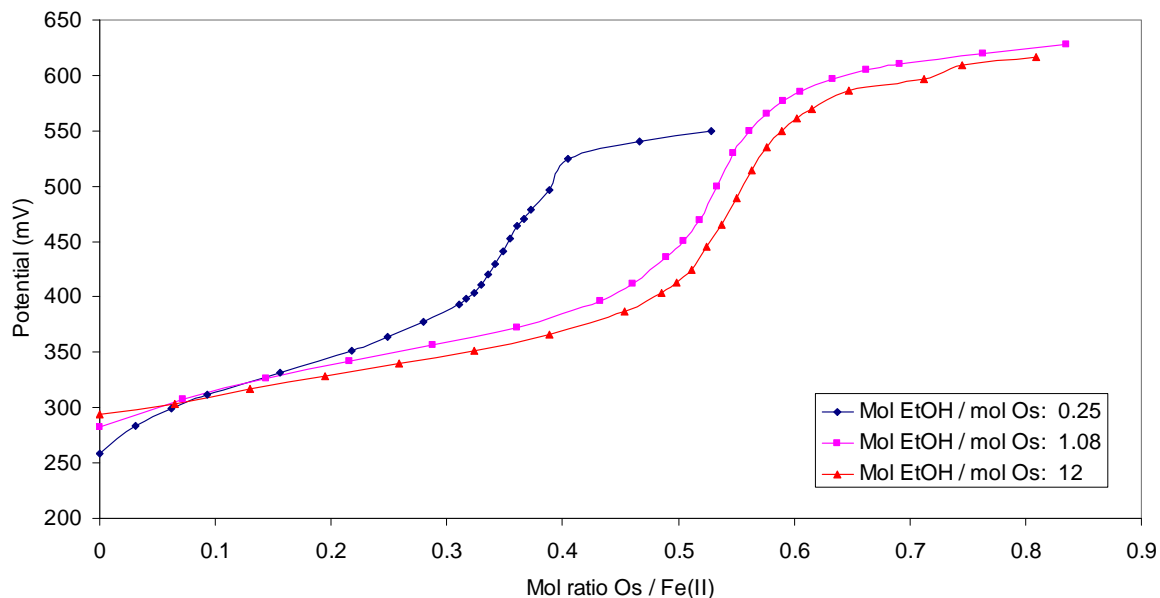
**Table 5.2: Number of equivalents Fe(II) (*n*) required to reduce osmium solutions to osmium(IV) and the starting oxidation state that this implies**

Ethanol		Methanol	
<i>n</i>	Osmium <sup>x+</sup>	<i>n</i>	Osmium <sup>x+</sup>
2.25	+6	2.00	+6
-	-	2.03	+6

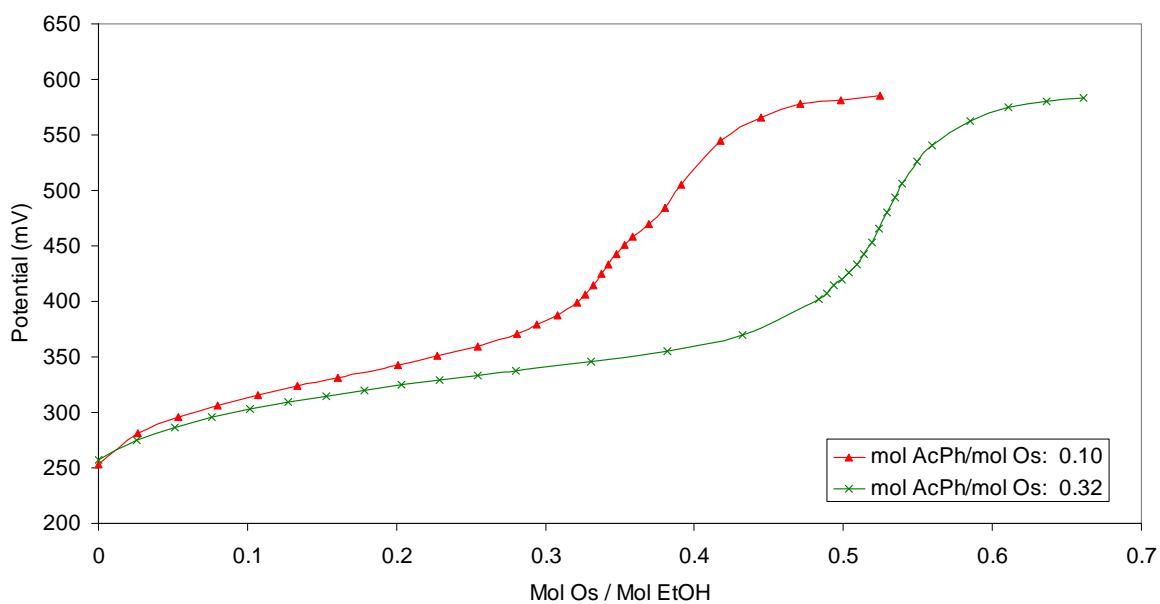
As is evident from Table 5.2, the final oxidation state when the reaction is at equilibrium can confidently be said to be osmium(VI).

In the following experiments, the osmium(VIII) was reacted in a pre-determined mole ratio with ethanol or acetophenone (being representative of the alcohols and ketones, respectively) until equilibrium was reached. Figures 5.4 (a) and (b) show the potentiometric titrations of these equilibrated solutions with an acidic iron(II) solution and

Table 5.3 gives the calculated equivalents of iron(II) required to reduce the osmium to osmium(IV).



(a)



(b)

**Figure 5.4: Potentiometric titration curves for the reaction of an acidic iron(II) solution of known concentration with an osmium solution obtained in the following manner: (a) Osmium tetroxide and ethanol of known concentrations reacted overnight in 0.1M hydroxide (b) Osmium tetroxide and acetophenone of known concentrations reacted for 10 minutes in 2M hydroxide**



**Table 5.3: Number of equivalents Fe(II) ( $n$ ) required to reduce osmium solutions to osmium(IV) and the starting oxidation state that this implies**

Osmium reacted first with Ethanol			Osmium reacted first with Acetophenone		
Mol ratio ethanol:osmium in original solution	$n$ for Fe(II) titration	Final osmium <sup>x+</sup> in original solution	Mol ratio acetophenone: osmium in original solution	$n$ for Fe(II) titration	Final osmium <sup>x+</sup> in original solution
0.25	2.91	+7	0.10	2.98	+7
1.08	1.83	+6	0.32	1.90	+6
12	1.80	+6	-	-	-

It is evident from the data in Table 5.3 that the alcohol or ketone reduction of osmium tetroxide can be stopped at a particular point in the reaction by adding just sufficient alcohol or ketone. This is shown by the good correlation of  $n$  values to particular oxidation states. UV-VIS spectra were read on small volumes of the ethanol/osmium and the acetophenone/osmium solutions while Fe(II) titrations were performed with the remainder of the solutions. This was in order to check that the spectrum of the solution resembled either a species B or species C spectrum and to check that there was no continuing reaction occurring – that the alcohol/osmium and ketone/osmium reaction was at equilibrium during the time scale of the experiment. The fact that there was a continuing hydroxide/osmium reaction is not in dispute, but the experiments were designed in such a way that that reaction played no part in the reaction of interest. It was for that reason that the hydroxide concentration was kept low in the ethanol reactions and that the acetophenone reactions were mixed freshly and titrated immediately. It was, therefore, found that the spectra of the ethanol/osmium and the acetophenone/osmium solutions did not change during the time scale of this experiment.

It will also become evident in the following chapter that the reacting mole ratios of alcohol to osmium and ketone to osmium were chosen for specific reasons. The ratio of 0.25 for ethanol and 0.10 for acetophenone are the specific ratios required to bring about the completion of step one of the two step reaction. This means that at these mole ratios, the osmium species in solution is the so-called “species B”. Therefore, we see that the number of equivalents of iron(II) required to reduce species B to osmium(IV), is approximately three. This implies that, either species B is in oxidation state +7, or that there is an equal

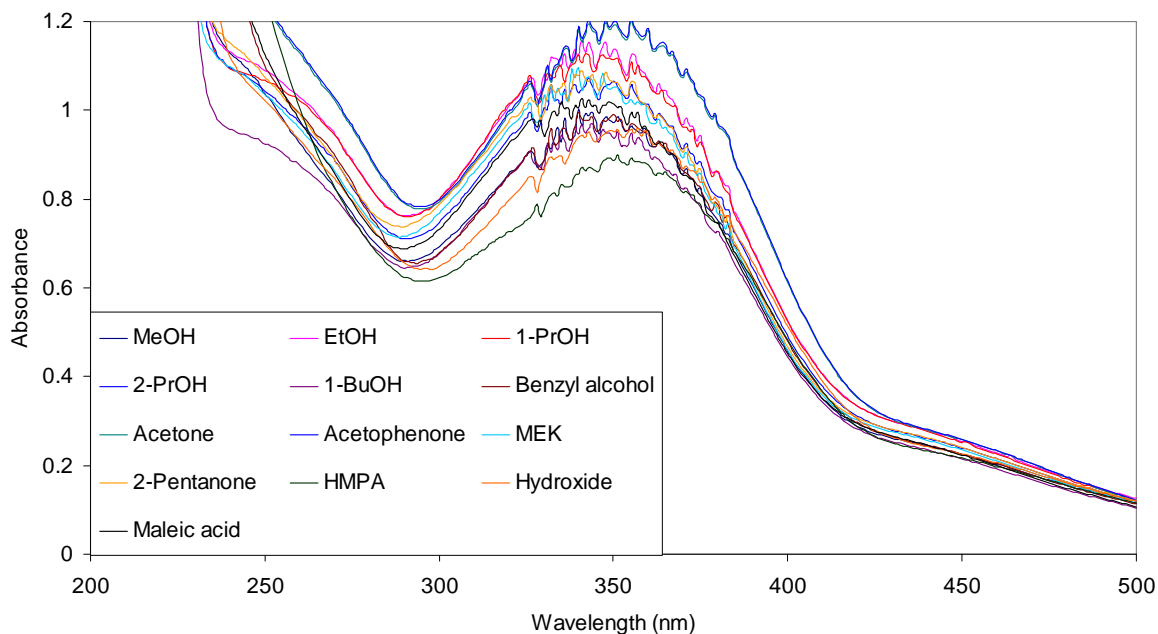
mix of +6 and +8 oxidation states in solution. Since absorbance is additive, the latter case would result in a spectrum of species B that is an addition spectrum of osmium(VIII) and osmium(VI) in 2M hydroxide medium. This is quite simple to check and is investigated in more detail in Section 5.3.1.3.

Mole ratios of 1.08 and 0.32 for the alcohols and ketones, respectively, were sufficient to bring about the completion of step two of the two-step reaction. At these mole ratios the oxidation state of the osmium species is +6, which confirms the data from Tables 5.1 and 5.2. The oxidation state of the final osmium species, once the reaction has run to equilibrium in an excess of reductant, is osmium(VI). The vast excess of ethanol, represented by a mole ratio of 12, was simply a check to see that there was not some further reaction occurring under a vast excess of reductant. As can be seen, this is not the case and the oxidation state of the osmium species in solution remains +6.

### **5.3.1.2 Comparing the spectra for “species B” and “species C” for different reducing agents**

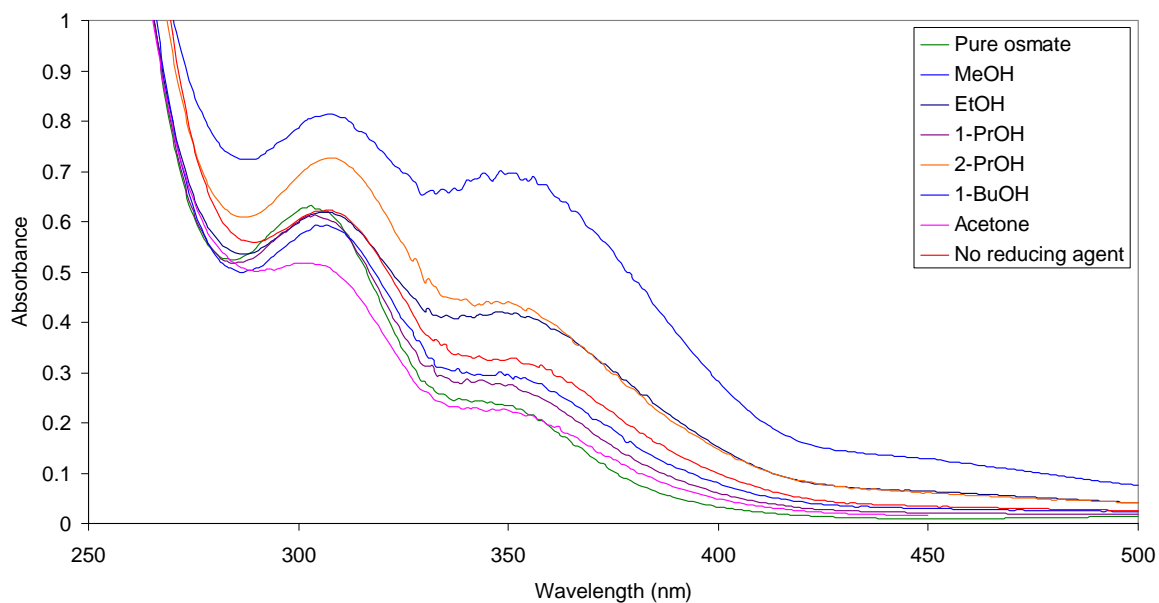
The spectra were compared with a view to establishing the similarities or differences between the spectra when different reducing agents were used. This was especially important for species B, since it was initially thought that the first step in the reaction may have been the formation of an osmium-alcohol/ketone complex. If this were the case, differences in the UV-VIS spectra of each different complex would be expected.

Figure 5.5 shows the spectra of the reactions between osmium tetroxide and the different alcohols, ketones and other reductants in 2M hydroxide, isolated at the point nearest to that where step one of the two-step reaction is over. That is, at the maximum of the kinetic progress curve. It is evident from Figure 5.5 that all the spectra are very similar. Allowing for the fact that it was not always possible to pinpoint a spectrum at the specific point where step one was over, the remarkable similarities in the spectra allow the tentative conclusion at this point that species B is the same for all the different reductants and that the visible first step of the reaction is not the formation of an osmium-substrate complex. This is not to say that such a complex does not occur as a transient intermediate, but it is not the step that is followed visibly using UV-VIS spectrophotometry. Section 5.3.1.3 explores the identity of species B in more detail.



**Figure 5.5:** The UV-VIS spectra of “species B” as formed during the reaction of osmium tetroxide with selected alcohols, ketones, hexamethylphosphoramide, maleic acid or simply in hydroxide. The spectra were selected to conform as closely as possible to the maxima on a kinetic progress curve.

Figure 5.6 shows the final spectra, after equilibration, for the reaction of osmium tetroxide with an excess of various reducing agents. All of the osmium(VIII) has been converted to the final product, species C. Figure 5.6 compares these spectra with the spectrum of potassium osmate ( $K_2[OsO_2(OH)_4]$ ), made as described in Chapter 2, and dissolved in 2M hydroxide. What is clear from some of the spectra, such as that for the reaction with methanol, is that the reaction has not gone to completion and the final osmium(VI) spectrum has not yet been achieved. However, in general, it is clear to see the similarities between the species C spectra and that for potassium osmate.



**Figure 5.6: The UV-VIS spectra of pure potassium osmate in 2M hydroxide compared to the spectra of osmium tetroxide reacted with an excess of selected alcohols or ketones (or just in hydroxide) until final equilibrium was reached.**

### 5.3.1.3 Osmium(VIII) – osmium(VI) titration

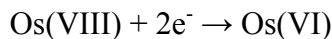
It had thus far been established that Species B, the product of the first step in the reduction of osmium(VIII) by alcohols and ketones,

- (a) Required three equivalents of Fe(II) to reduce it, which suggested a +7 oxidation state, but could as easily be argued to be equal amounts of osmium(VIII) and osmium(VI) in solution;
- (b) Was the same irrespective of what reducing agent was used – therefore, was not an osmium-substrate complex; and
- (c) Was a fairly stable species, whose UV-VIS spectrum did not change over approximately one hour, once equilibrium had been established.

It was therefore decided to investigate the osmium(VIII) – osmium(VI) relationship in more detail with a view to gaining further insight into the identity of species B. The existence of an osmium(VII) oxidation state was not particularly favoured, since it is considered “rare” in the literature<sup>(16)</sup>. Having said that, the existence of ruthenium(VII) in hydroxide solutions of ruthenium tetroxide has already been mentioned<sup>(42)</sup> and the grey-green complex  $(\text{Ph}_4\text{As})[\text{OsO}_4]$  has been reported<sup>(16)</sup>. Cyclic voltammetry studies on this

complex in  $\text{CH}_2\text{Cl}_2$  show a reversible one electron process for the  $[\text{OsO}_4]/[\text{OsO}_4]^-$  couple ( $E_0 = 0.1\text{V}$  versus standard calomel electrode).

However, the two electron process of



was considered more favourable, especially since this would have required the participation of one molecule of osmium(VIII) for every one molecule of alcohol. This would have resulted in the production of osmium(VI) and it was this osmium(VI)-osmium(VIII) interaction that was investigated in more detail. The results of an osmium(VI) titration of osmium(VIII) in 2M hydroxide is shown in Figure 5.7 and 5.8.

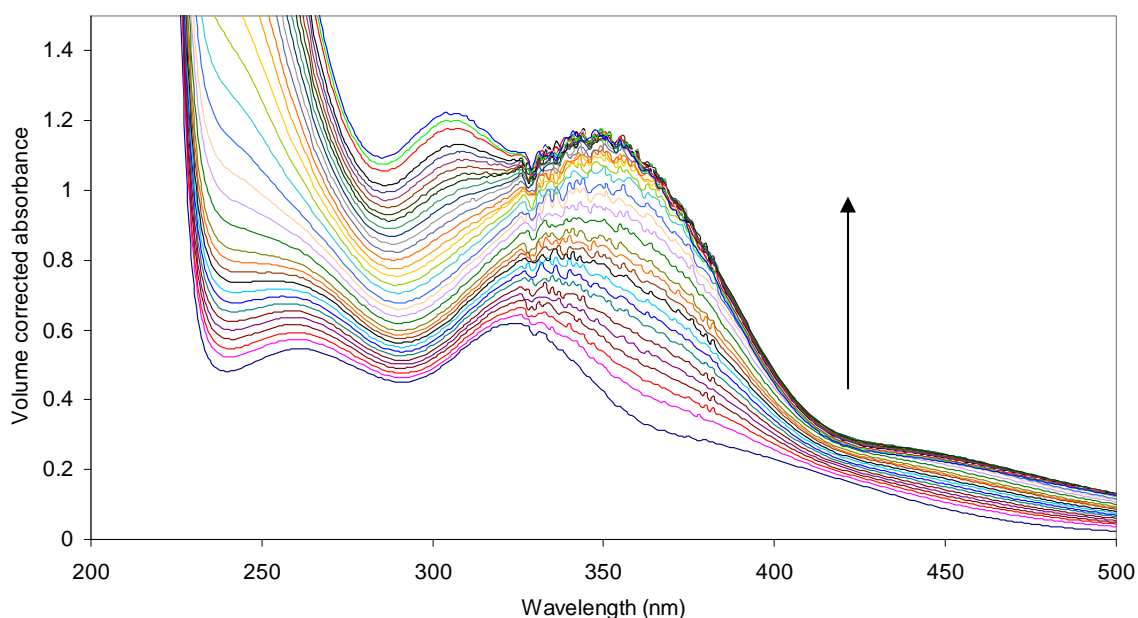


**Figure 5.7:** The volume corrected spectra of the titration of 2.5ml of a 0.00151M osmium tetroxide solution with a 0.00111M osmate solution in 2M hydroxide matrix. The arrow indicates the direction of the absorbance change with an increase in the volume of osmium(VI).

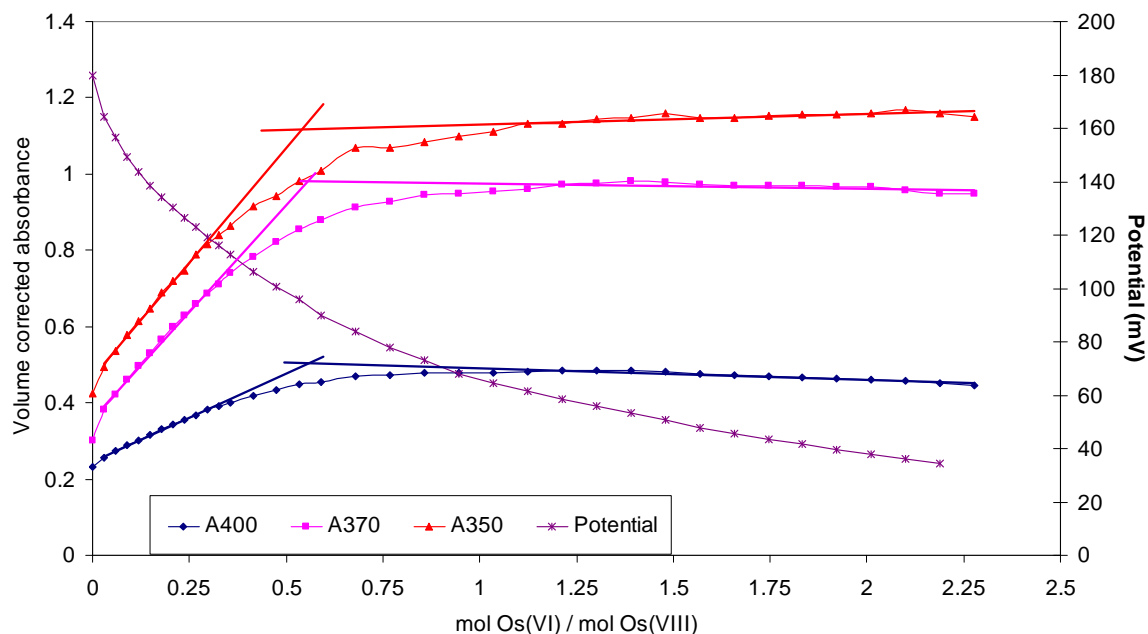
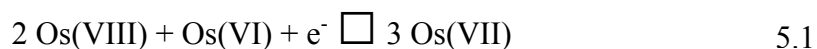


**Figure 5.8:** The mole ratio plot of the same titration (as Figure 5.7) at selected wavelengths with intersecting straight lines drawn through the linear portions of the curves. Also shown is the potential during the titration.

A calculation and averaging of the three intercepts of the straight lines from Figure 5.8 gives a mole ratio value at the endpoint of the titration of 0.55. This corresponds to the reaction of two osmium(VIII) with one osmium(VI). This was, of course, a wholly unexpected result, since it was expected that the two osmium species would react, if at all, in a one-to-one ratio. However, it was confirmed by subsequent titrations. Also raised was the issue of the reliability of concentration determination. However, the thiourea method has been extensively investigated as a method of osmium concentration determination<sup>(31)</sup> and has proved effective and reliable in all previous experiments. It has been used to determine osmium concentration in a wealth of titrations where not only concentration, but oxidation state, is of vital importance. In all cases coherent data were obtained. Of course, the thiourea method cannot determine oxidation state, but that issue has been covered in Chapter 4.3.2 where it was confirmed that the osmium used in these experiments (both in distilled water and 2M hydroxide medium) was in oxidation state +8. It was, therefore, necessary to accept the validity of these experiments and to incorporate the results into the final analysis of the overall reaction.

To account for the stoichiometry of the osmium(VIII) – osmium(VI) reaction, either of the following two equations could apply:



or



Subsequent investigations into the stoichiometry of the reactions at equilibrium would rule out Equation 5.1 and kinetic experiments would confirm these results. Mechanistically, two osmium(VIII) molecules coming together with one ethanol molecule and exchanging two electrons to generate two osmium(VII) species is an unlikely event.

It was necessary to rule out the possibility that the absorbance spectrum produced by the titration of osmium(VIII) with osmium(VI) was not simply a mixture of the two species' absorbance spectra. Since absorbance is additive, the simple addition of an osmium(VI) absorbance spectrum to an osmium(VIII) absorbance spectrum would produce the additive absorbance spectrum that can be compared to the experimental spectrum. It is evident from Figure 5.9 that the additive spectrum of osmium(VIII) and osmium(VI) (in red) does not produce the spectrum that we see during the titration. The spectrum, taken at the endpoint of the titration, is shown in blue in Figure 5.9, labelled “real Os(VIII) + Os(VI) spectrum”. For the sake of comparison, the species B absorbance curve for the reaction of 2-pentanone with osmium(VIII) is shown in purple. It is clear to see that they are identical. Therefore, whatever osmium species is being produced during the titration of osmium(VIII) and osmium(VI) is the same osmium species being produced during the reduction of osmium(VIII) by *all* the various reductants – that is, the elusive species B.

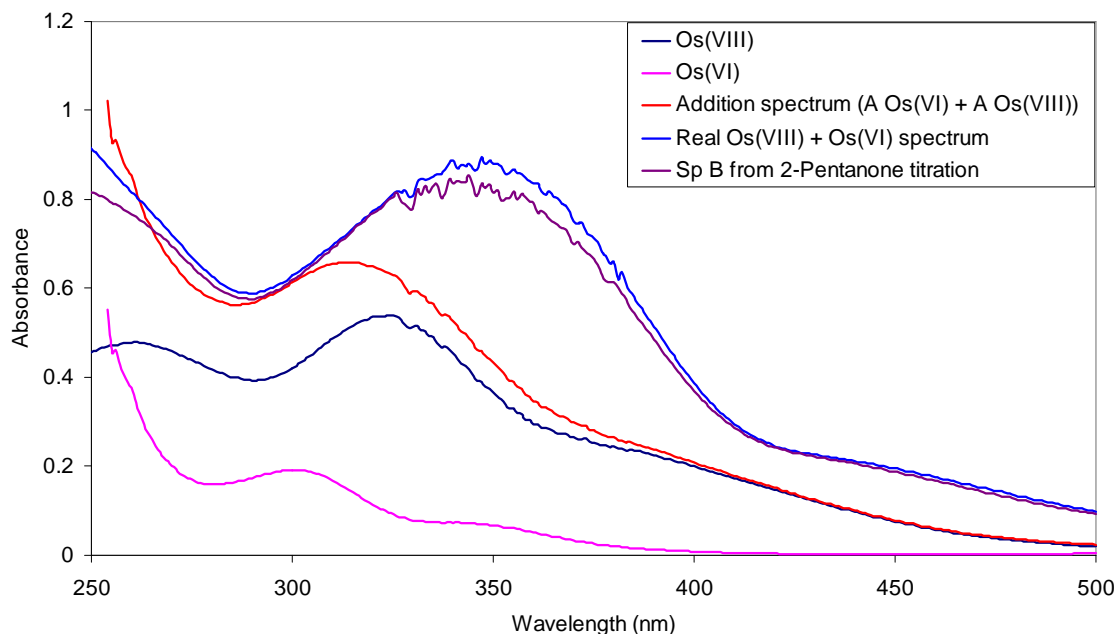


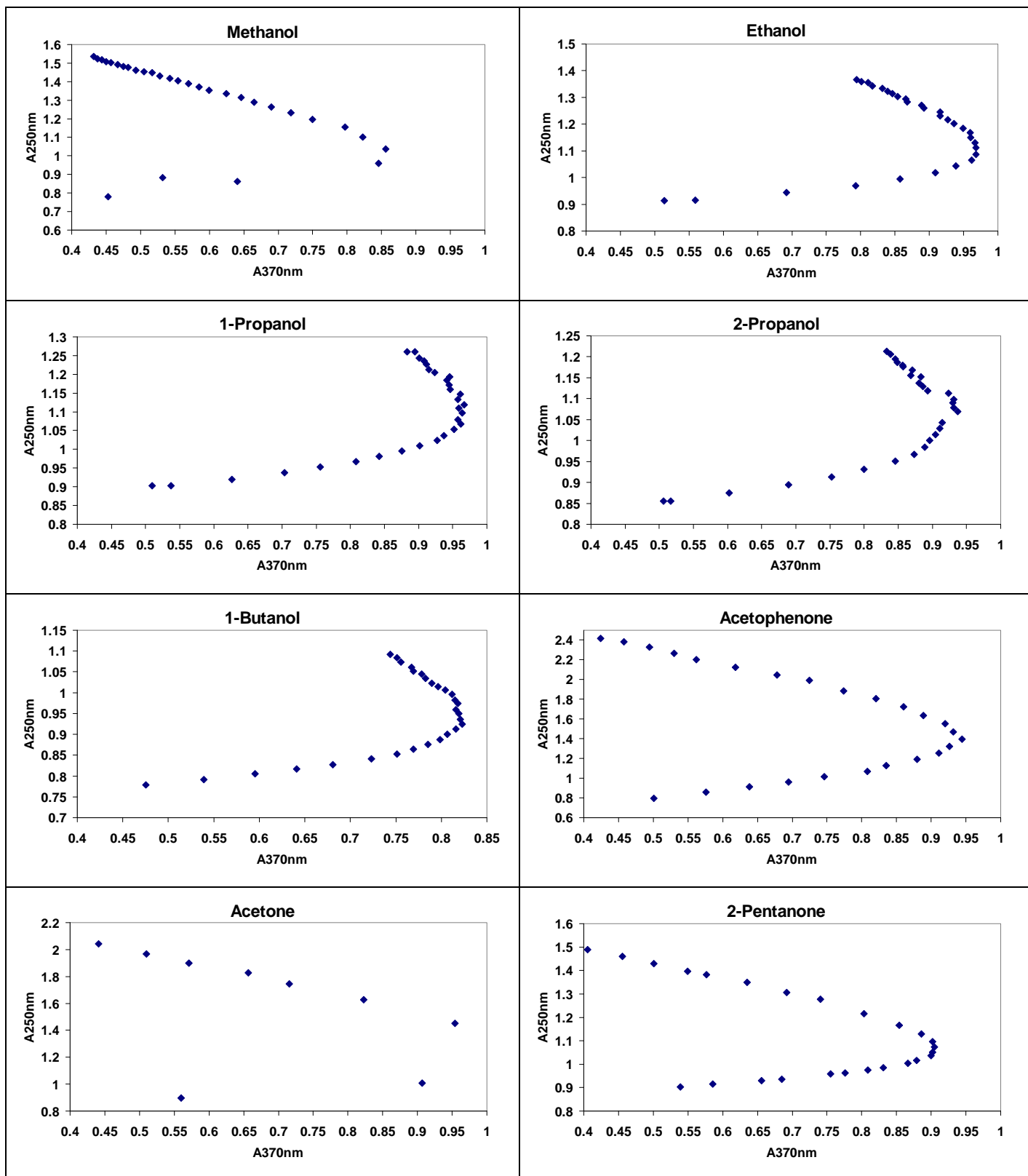
**Figure 5.9:** The UV-VIS spectra of  $1.77 \times 10^{-4} \text{M}$  osmium tetroxide in 2M hydroxide;  $1.61 \times 10^{-4} \text{M}$  potassium osmate in 2M hydroxide; the calculated absorbance spectrum of the osmium tetroxide plus the potassium osmate; the actual absorbance spectrum at the endpoint of the reaction of  $1.77 \times 10^{-4} \text{M}$  osmium tetroxide with  $1.61 \times 10^{-4} \text{M}$  potassium osmate in 2M hydroxide; and a sample of the absorbance spectrum for species B, from a 2-pentanone titration.

One more point should be addressed on this issue before moving on. Section 5.3.1.1 determined that the oxidation state of species B is +7. In view of the latest findings in this section it is apparent that that is not so. However, the combined oxidation state of an  $\text{Os(VIII)}_2\text{Os(VI)}$  complex would be +7.3. That value is not so different from the results obtained, nor were those results so sensitive, as to negate the findings made in Section 5.3.1.1.

#### 5.3.1.4 Determining a molar extinction coefficient for species B

Figure 5.10 shows plots of the absorbance at 370nm versus absorbance at 250nm for the kinetic reactions described in Section 5.2.1.3. Table 5.4 gives the absorbance at the intercepts of these plots and the molar extinction coefficients calculated from these absorbances.





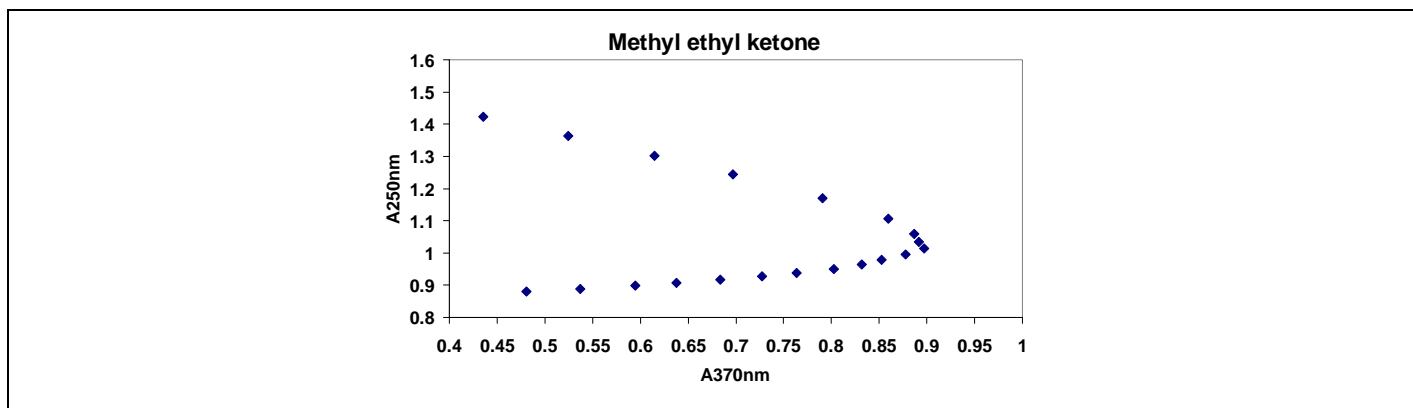


**Figure 5.10:** Absorbance at 370nm versus absorbance at 250nm taken from the spectra of the reactions of osmium tetroxide with various alcohols, ketones and hydroxide over time.

**Table 5.4:** Molar extinction coefficient ( $\epsilon$ ) at 370nm of species B as calculated from the plots in Figure 5.3.

Substrate	$\frac{1}{3} [\text{OsO}_4]_0$ ( $\times 10^{-4}$ mol/l)	A370nm (from intercept of A <sub>370</sub> vs A <sub>250</sub> )	$\epsilon_{370}$ of species B ( $\text{L}\cdot\text{mol}^{-1}\cdot\text{cm}^{-1}$ )
Methanol	1.27	0.945	7441
Ethanol	1.44	1.078	7486
1-Propanol	1.44	1.038	7208
2-Propanol	1.44	0.987	6854
1-Butanol	1.27	0.881	6937
Acetophenone	1.47	1.098	7469
MEK	1.41	1.023	7255
2-Pentanone	1.38	1.051	7616

In order to understand the calculations in Table 5.4 it is necessary to take a step ahead to information that was not available at the time of executing these experiments. According to Beer's law, in order to determine the molar extinction coefficient of species B, the concentration of the complex must be known. At this stage, it must be sufficient to know that the concentration used for species B was one third that of the initial osmium tetroxide concentration ( $[\text{OsO}_4]_0$ ). This will be fully explained once a reaction scheme has been settled on in Chapter 6.3.2.

From Table 5.4 a molar extinction coefficient of  $7283 \text{ L}\cdot\text{mol}^{-1}\cdot\text{cm}^{-1}$  emerges as the average. Relative percentage deviation from this mean value remains under 6% and is closer to 2% for most of the reactions. Therefore, it seems that the identity of species B remains the same, irrespective of which reducing agent is used.

### 5.3.2 Organic products

The  $\text{C}^{13}$  NMR spectra of solutions prepared as described in Section 5.2.2 are shown in Figures 5.11 to 5.20. Accompanying each spectrum is a table showing the major peaks and the identity of those peaks. Peaks were identified by running NMR spectra of the pure compounds of reactants and suspected products in 2M sodium hydroxide.

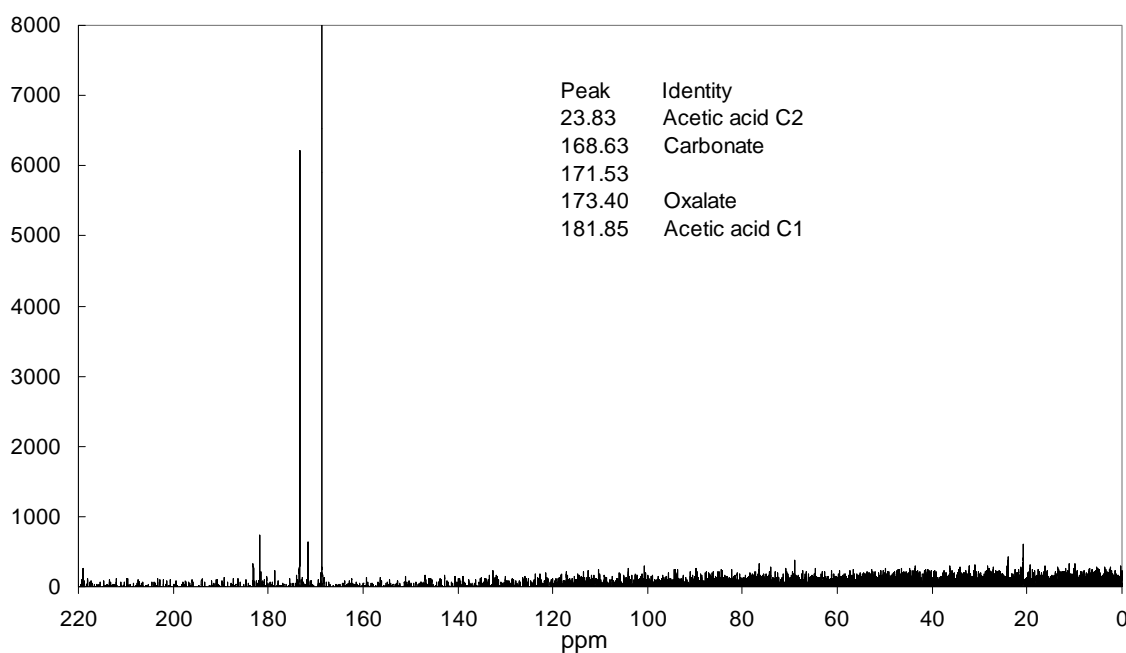


**Figure 5.11:** The  $\text{C}^{13}$  NMR spectrum of the final solution after reaction of osmium tetroxide with ACETONE in 2M hydroxide.

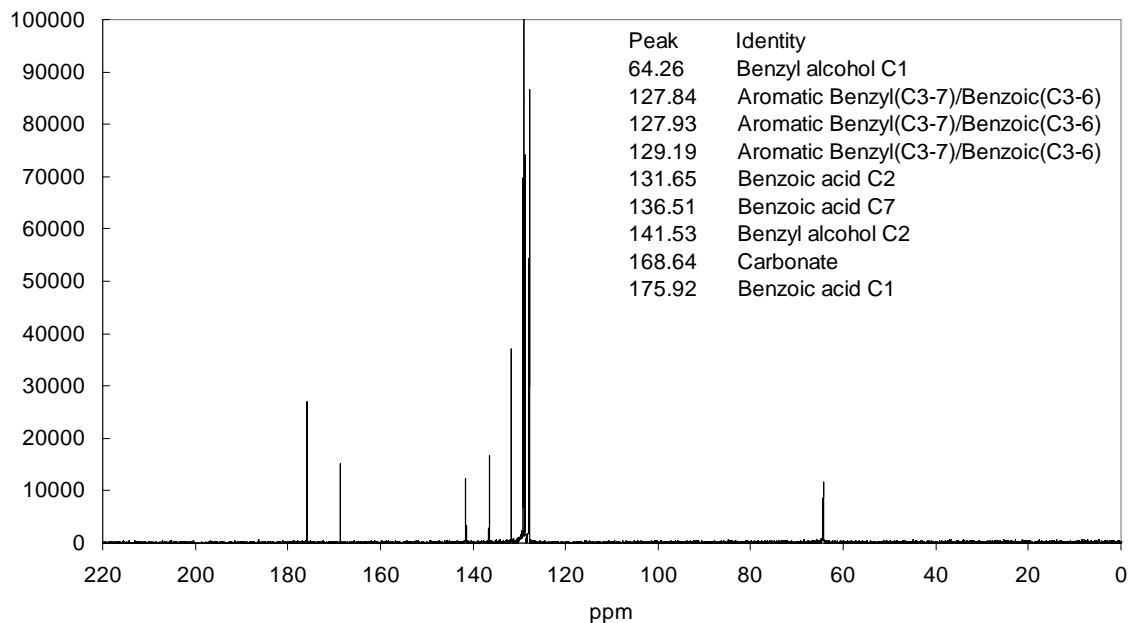


**Figure 5.12:** The  $C^{13}$  NMR spectrum of the final solution after reaction of osmium tetroxide with BENZYL ALCOHOL in 2M hydroxide.

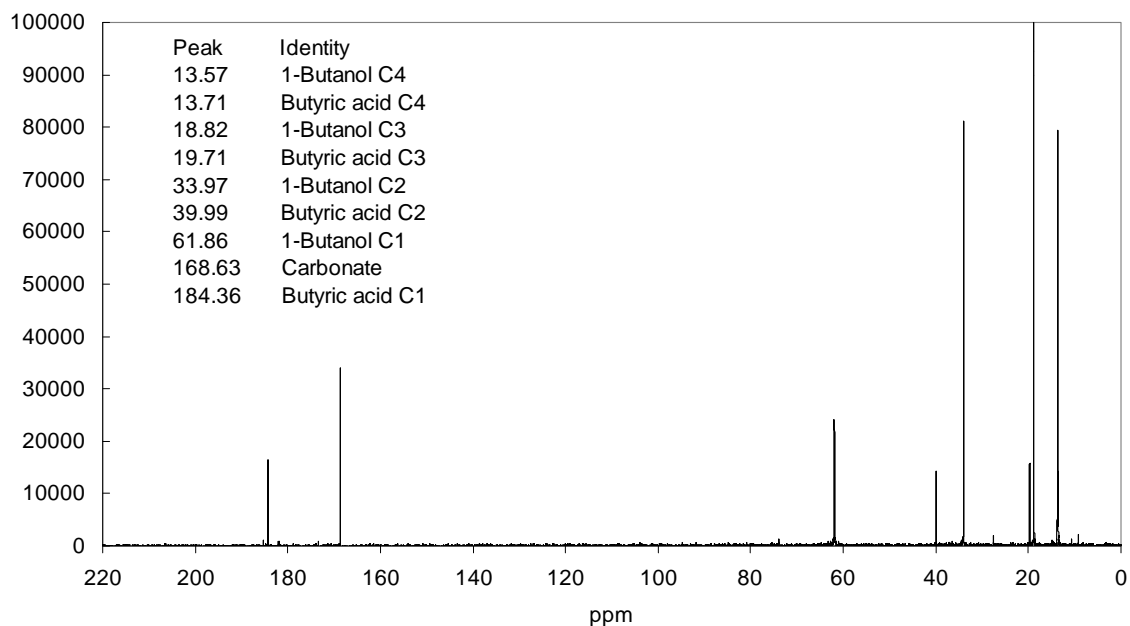


**Figure 5.13:** The  $C^{13}$  NMR spectrum of the final solution after reaction of osmium tetroxide with 1-BUTANOL in 2M hydroxide.

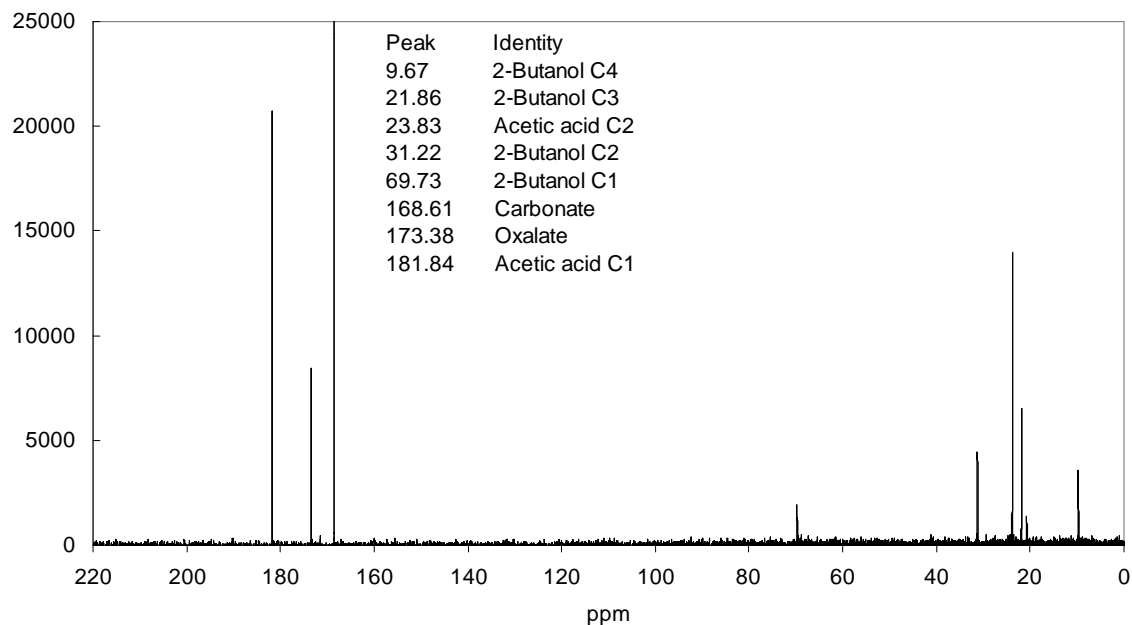


**Figure 5.14:** The  $C^{13}$  NMR spectrum of the final solution after reaction of osmium tetroxide with 2-BUTANOL in 2M hydroxide.

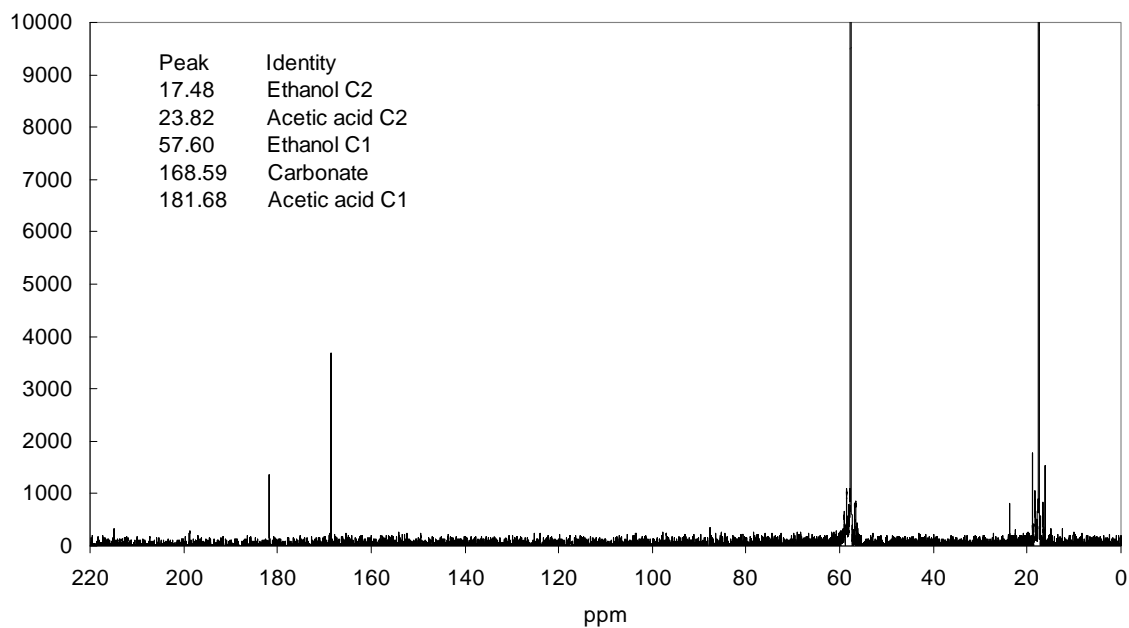


**Figure 5.15:** The  $C^{13}$  NMR spectrum of the final solution after reaction of osmium tetroxide with ETHANOL in 2M hydroxide.

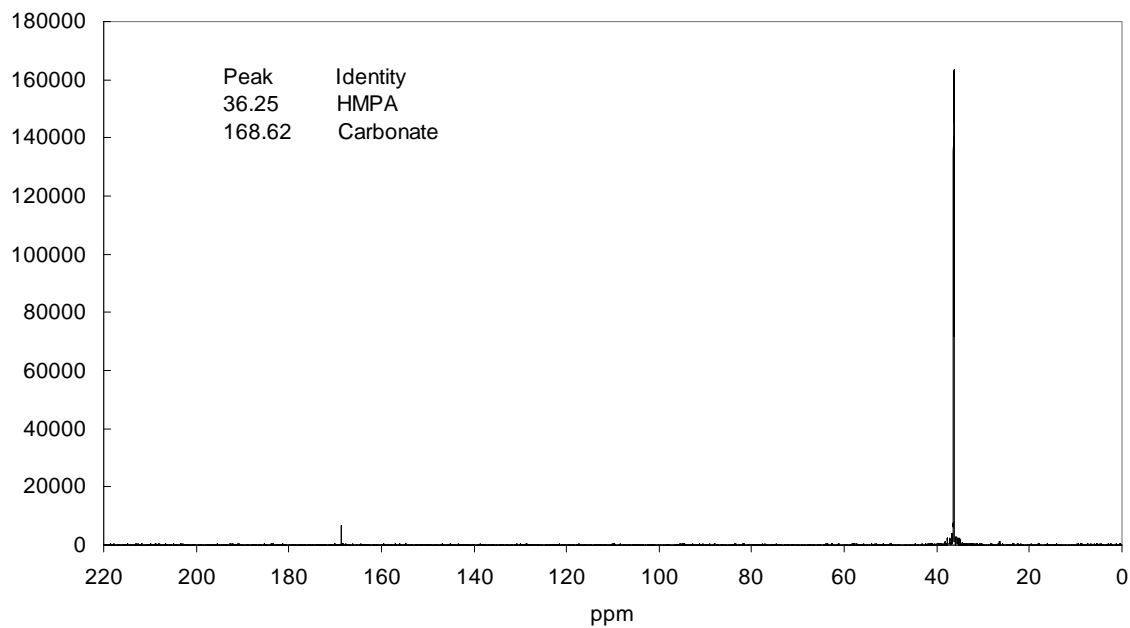


**Figure 5.16:** The  $C^{13}$  NMR spectrum of the final solution after reaction of osmium tetroxide with HEXAMETHYLPHOSPHORAMIDE in 2M hydroxide.

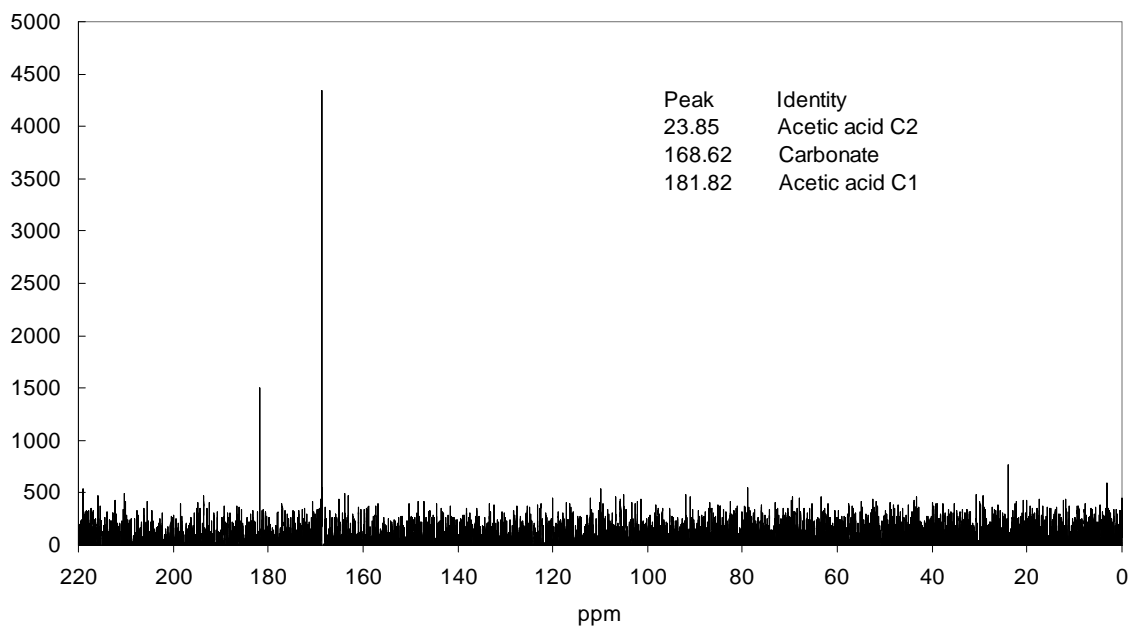


**Figure 5.17:** The  $C^{13}$  NMR spectrum of the final solution after reaction of osmium tetroxide with METHYL ETHYL KETONE in 2M hydroxide.

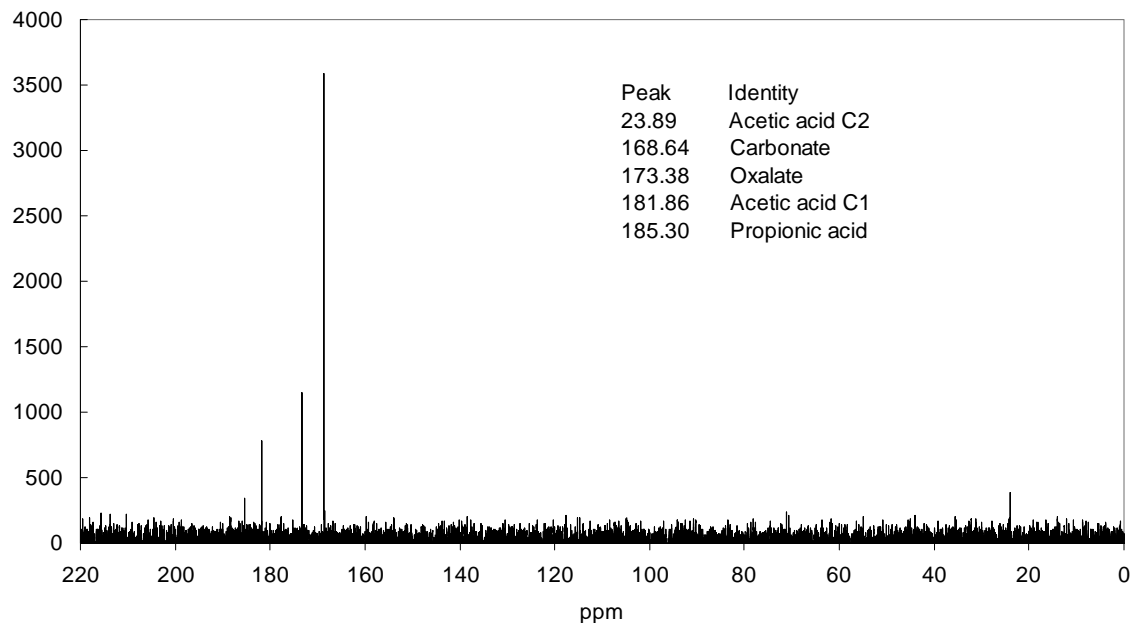


**Figure 5.18: The  $C^{13}$  NMR spectrum of the final solution after reaction of osmium tetroxide with 2-PENTANONE in 2M hydroxide.**

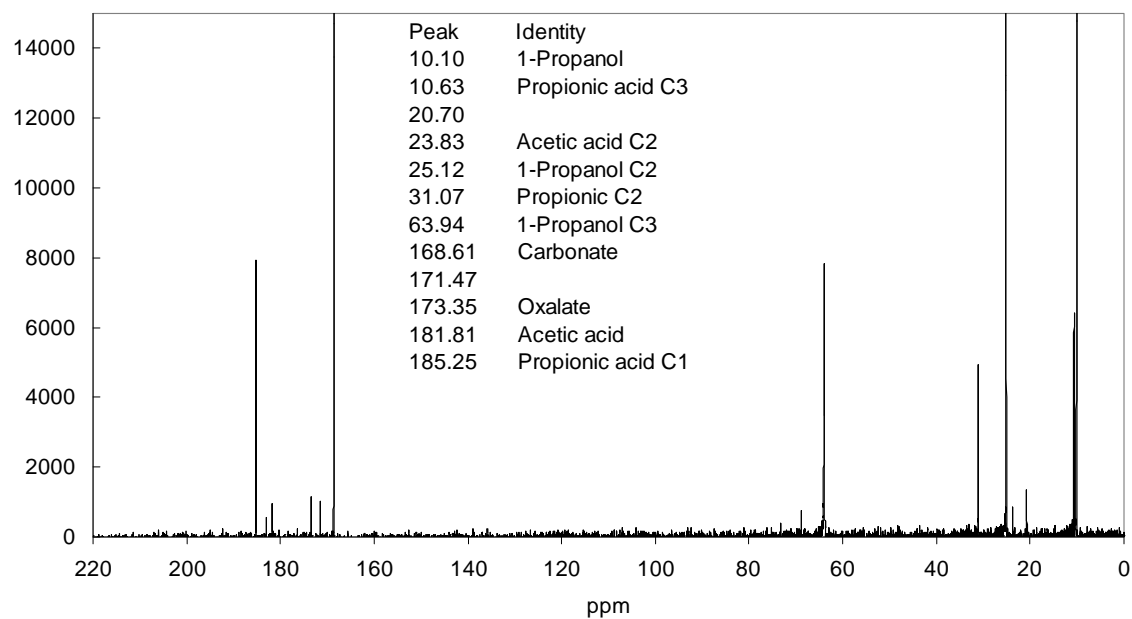


**Figure 5.19: The  $C^{13}$  NMR spectrum of the final solution after reaction of osmium tetroxide with 1-PROPANOL in 2M hydroxide.**

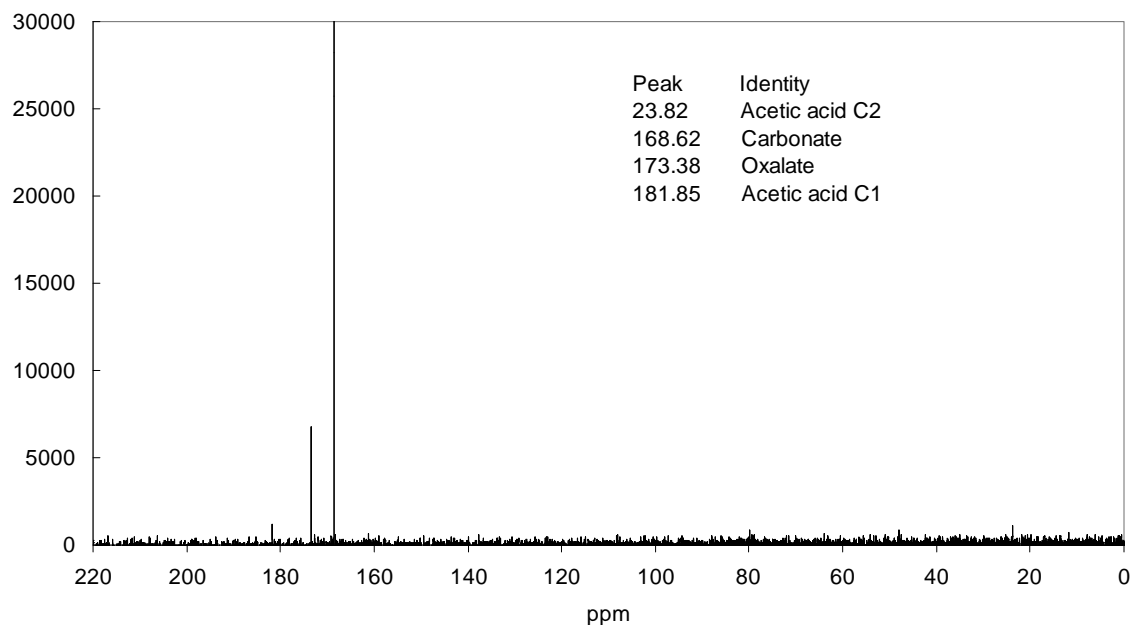


**Figure 5.20: The  $C^{13}$  NMR spectrum of the final solution after reaction of osmium tetroxide with 2-PROPANOL in 2M hydroxide.**

In some cases during the reaction of the osmium(VIII) with the reductant, the reductant was entirely depleted. In other cases there was still some reducing agent left at the end of the reaction. These reactions were in no way meant to be quantitative and  $C^{13}$  NMR do not integrate well, even if that was the intention. However, it is still entirely possible to elucidate the major products of the reaction. These are set out in Table 5.5 for ease of reference.



**Table 5.5: The organic products of the reaction osmium tetroxide with a reducing agent in 2M hydroxide as elucidated by NMR spectroscopy**

<b>Alcohols</b>		
<b>Reactant</b>	<b>Major Products</b>	<b>Minor Products</b>
Ethanol	Acetic acid	-
1-Propanol	Propionic acid	Oxalic acid, acetic acid, CO <sub>2</sub>
2-Propanol	Oxalic acid, CO <sub>2</sub>	Acetic acid
1-Butanol	Butyric acid	-
2-Butanol	Oxalic acid, acetic acid	-
Benzyl alcohol	Benzoic acid	-
<b>Ketones and other</b>		
<b>Reactant</b>	<b>Major Products</b>	<b>Minor Products</b>
Acetone	Oxalic acid, CO <sub>2</sub>	Acetic acid
Methyl Ethyl Ketone	Acetic acid, CO <sub>2</sub>	-
2-Pentanone	Acetic acid, oxalic acid, propionic acid, CO <sub>2</sub>	-
Hexamethylphosphoramide	Hexamethylphosphoramide	-

The evolution of carbon dioxide is difficult to assign in the above reactions. Because of the design of the experimental conditions, it is impossible to exclude carbon dioxide from the atmosphere from accumulating in the basic solutions. However, with a knowledge of the other major products, it is possible to infer when carbon dioxide would be a product of the reaction. In some cases, the organic reactant breaks up during the oxidation. There is then production of carbon dioxide, as well as longer chain carbon product/s.

What should be clearly stated here is the fact that primary alcohols are oxidised to their respective carboxylic acids, while secondary alcohols and ketones are cleaved at the carbon attached to the oxygen and oxidised to smaller carboxylic acids and carbon dioxide. Only the major products are of interest here. A good qualitative observation of the above experiments is that when primary alcohols are allowed to react for extended periods of time (i.e. days), one begins to see small amounts of minor products. However, in many

cases there were no minor products and these were the reactions in which the NMR spectra were read within about 24 hours of beginning the experiment.

Tertiary alcohols, such as tertiary butanol, are not oxidised, but remain unchanged during approximately 48 hours in contact with osmium tetroxide in a 2M hydroxide medium. This is true also for hexamethylphosphoramide (HMPA).

The following redox half-reactions are given for all the various alcohols and ketones from Table 5.5, using the major organic products determined by NMR.

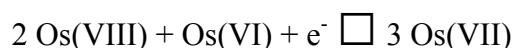
**Table 5.6: Organic half-reactions using the known major products of the reactants**

<b>Ethanol</b>	$\text{CH}_3\text{CH}_2\text{OH} + 4\text{OH}^- \rightarrow \text{CH}_3\text{COOH} + 3\text{H}_2\text{O} + 4\text{e}^-$
<b>1-Propanol</b>	$\text{CH}_3(\text{CH}_2)_2\text{OH} + 4\text{OH}^- \rightarrow \text{CH}_3\text{CH}_2\text{COOH} + 3\text{H}_2\text{O} + 4\text{e}^-$
<b>2-Propanol</b>	$\text{CH}_3\text{CH}(\text{OH})\text{CH}_3 + 16\text{OH}^- \rightarrow \text{C}_2\text{O}_4\text{H}_2 + \text{CO}_2 + 11\text{H}_2\text{O} + 16\text{e}^-$
<b>1-Butanol</b>	$\text{CH}_3(\text{CH}_2)_3\text{OH} + 4\text{OH}^- \rightarrow \text{CH}_3(\text{CH}_2)_2\text{COOH} + 3\text{H}_2\text{O} + 4\text{e}^-$
<b>2-Butanol</b>	$\text{CH}_3\text{CH}(\text{OH})\text{CH}_2\text{CH}_3 + 14\text{OH}^- \rightarrow \text{C}_2\text{O}_4\text{H}_2 + \text{CH}_3\text{COOH} + 9\text{H}_2\text{O} + 14\text{e}^-$
<b>Benzyl alcohol</b>	$\text{Ph-CH}_2\text{OH} + 4\text{OH}^- \rightarrow \text{Ph-COOH} + 3\text{H}_2\text{O} + 4\text{e}^-$
<b>Acetone</b>	$\text{CH}_3\text{C}(\text{O})\text{CH}_3 + 14\text{OH}^- \rightarrow \text{C}_2\text{O}_4\text{H}_2 + \text{CO}_2 + 9\text{H}_2\text{O} + 14\text{e}^-$
<b>Methyl ethyl ketone</b>	$\text{CH}_3\text{C}(\text{O})\text{CH}_2\text{CH}_3 + 14\text{OH}^- \rightarrow \text{CH}_3\text{COOH} + 2\text{CO}_2 + 9\text{H}_2\text{O} + 14\text{e}^-$
<b>2-Pentanone</b>	$2\text{CH}_3\text{C}(\text{O})(\text{CH}_2)_2\text{CH}_3 + 24\text{OH}^- \rightarrow 2\text{CH}_3\text{COOH} + \text{C}_2\text{O}_4\text{H}_2 + \text{CH}_3\text{CH}_2\text{COOH} + \text{CO}_2 + 14\text{H}_2\text{O} + 24\text{e}^-$

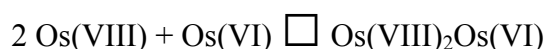
## 5.4 SUMMARY

### Species B

1. Approximately three equivalents of iron(II) were required to reduce species B to osmium(IV).
2. The above held true irrespective of whether species B was produced by the reaction of osmium tetroxide with an alcohol or a ketone.
3. The absorbance spectrum of species B is not an additive osmium(VIII)–osmium(VI) absorbance spectrum.
4. Therefore, species B *appears* to be a +7 oxidation state species.
5. The absorbance spectrum for species B was the same no matter what reducing agent was used. Therefore, species B is not an osmium-substrate complex.
6. An osmium(VIII)-osmium(VI) titration produced species B in a 2:1 ratio of reactants. This implied one of the following two equations:



or



7. The molar extinction coefficient of species B at 370nm was calculated as 7283 L.mol<sup>-1</sup>.cm<sup>-1</sup> by an A<sub>x</sub> versus A<sub>y</sub> plot and, again, shown to be constant no matter what reducing agent was used. Species B was assumed to be Os(VIII)<sub>2</sub>Os(VI).

### Species C

8. The oxidation state of species C was determined as +6 irrespective of whether an alcohol or ketone was used to produce species C.
9. The absorbance spectrum for species C was the same no matter what reducing agent was used.
10. The absorbance spectrum of species C was the same as that of a solution of potassium osmate in a 2M hydroxide matrix.
11. Therefore, it is concluded that species C is [OsO<sub>2</sub>(OH)<sub>4</sub>]<sup>2-</sup>.

### Organic products

12. Primary alcohols were oxidised to their corresponding carboxylic acid.

13. Secondary alcohols were cleaved at the carbon attached to the oxygen into smaller carboxylic acids and carbon dioxide.
14. Ketones were cleaved at the carbonyl carbon into smaller carboxylic acids and carbon dioxide.

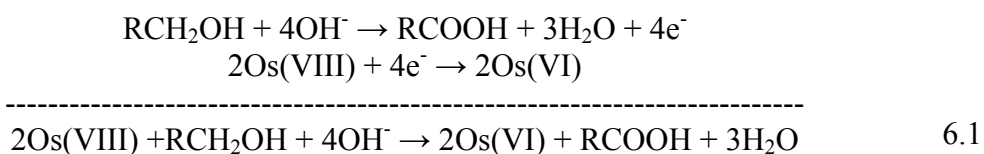
## CHAPTER 6

# EQUILIBRIUM STOICHIOMETRY

### 6.1 INTRODUCTION

The equilibrium stoichiometry of the reported alcohol – osmium(VIII) reactions have all centred on a one-to-one reaction mechanism. The osmium(VIII) forms a one-to-one complex with the alcohol in a transient intermediate and then breaks down to osmium(VI) and the aldehyde or ketone in a rate-limiting step <sup>(2)</sup>. The authors of *10*, *13* and *14* state specifically that equilibrium studies reveal that one mole of osmium(VIII) was used for every one mole of alcohol and two mole osmium(VIII) for every one mole of diol.

However, the same authors <sup>(5)</sup> found that the stoichiometry for the reaction of osmium(VIII) with the ketones acetone and methyl ethyl ketone, were also one-to-one. If ketones are the products of the alcohol oxidation, but the ketones also react in a one-to-one ratio with the osmium(VIII), then surely the stoichiometry for the alcohol reactions must be at fault. Since most authors report that the organic products of the reaction are carboxylic acids and it is agreed that the osmium product is osmium(VI), then it is apparent from Equation 6.1 that the osmium(VIII) and alcohols cannot react on a one-to-one basis.



---

---

## 6.2 EXPERIMENTAL

---

---

### 6.2.1 Alcohols

For each of the alcohols methanol, ethanol, 1-propanol, 2-propanol, 1-butanol, 2-butanol and benzyl alcohol, a series of solutions in a 2M hydroxide matrix were prepared. The osmium concentration in each volumetric flask was kept constant, while the concentration of the alcohol was increased.

The solutions were allowed to equilibrate for three hours. Previous observations showed that this was the optimum time during which the osmium(VIII) – alcohol equilibrium could be reached without the osmium(VIII) – hydroxide reaction interfering too much.

Two different equilibrium reaction models were simulated using the computer programmes SPC-V-MR and the commercially available Dynafit, discussed in Chapter 2.

### 6.2.2 Ketones

It was observed that the rate of the osmium(VIII) – ketone reaction was extremely fast. The reaction rate increased even more at high hydroxide concentration. Thus, in a 2M hydroxide medium, the reaction was fast enough to titrate the osmium(VIII) with the various ketones. Ketones used in the reactions were acetone, acetophenone, methyl ethyl ketone and 2-pentanone.

The titration procedure used: 10ml osmium tetroxide in distilled water plus 25ml 2.8M sodium hydroxide in a beaker stirred with a magnetic follower to bring the total hydroxide concentration to 2M. A platinum electrode was used to follow the potential and the solution was titrated against a known concentration ketone dissolved in 2M hydroxide.

Mole ratios of reacting ketone to osmium(VIII) were determined from the mole ratio plots since the modelling programmes could not handle the large stoichiometries involved, as will become apparent in the following section.

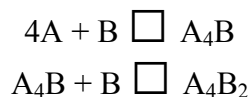
## 6.3 RESULTS

The results were approached from two entirely different perspectives, neither of which were entirely satisfactory. Both are presented here as they form part of the journey towards an acceptable explanation for this reaction mechanism. They will be termed equilibrium reaction models 1 and 2.

### 6.3.1 Equilibrium Reaction Model 1

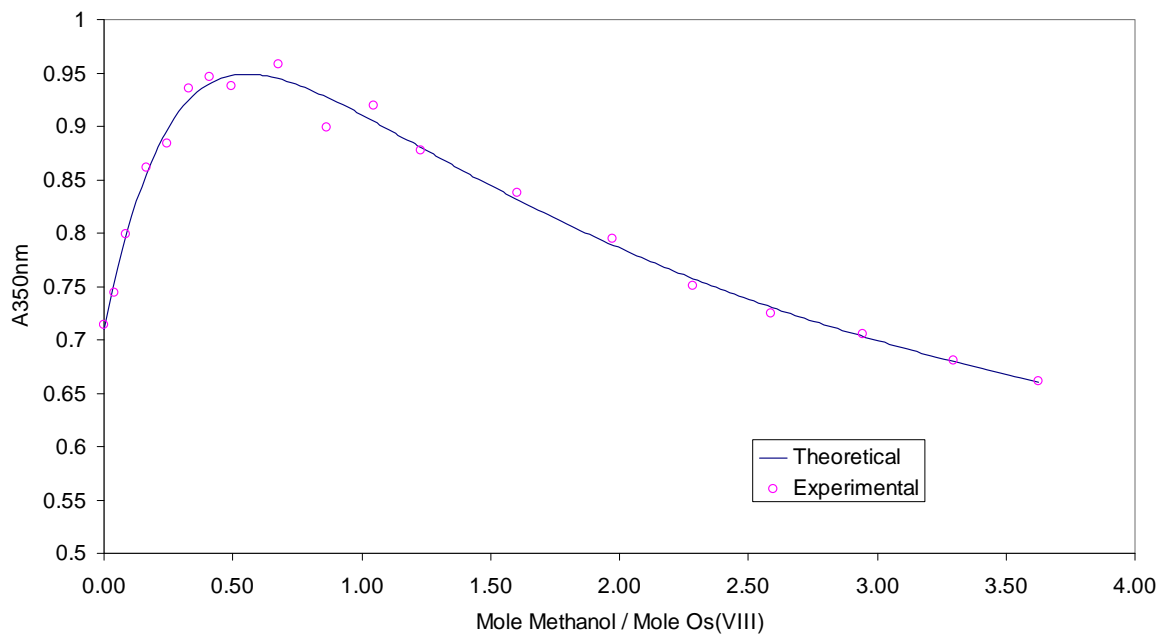
#### 6.3.1.1 Alcohols

Figures 6.1 to 6.4 that follow, show the theoretical computer-generated curve for the model

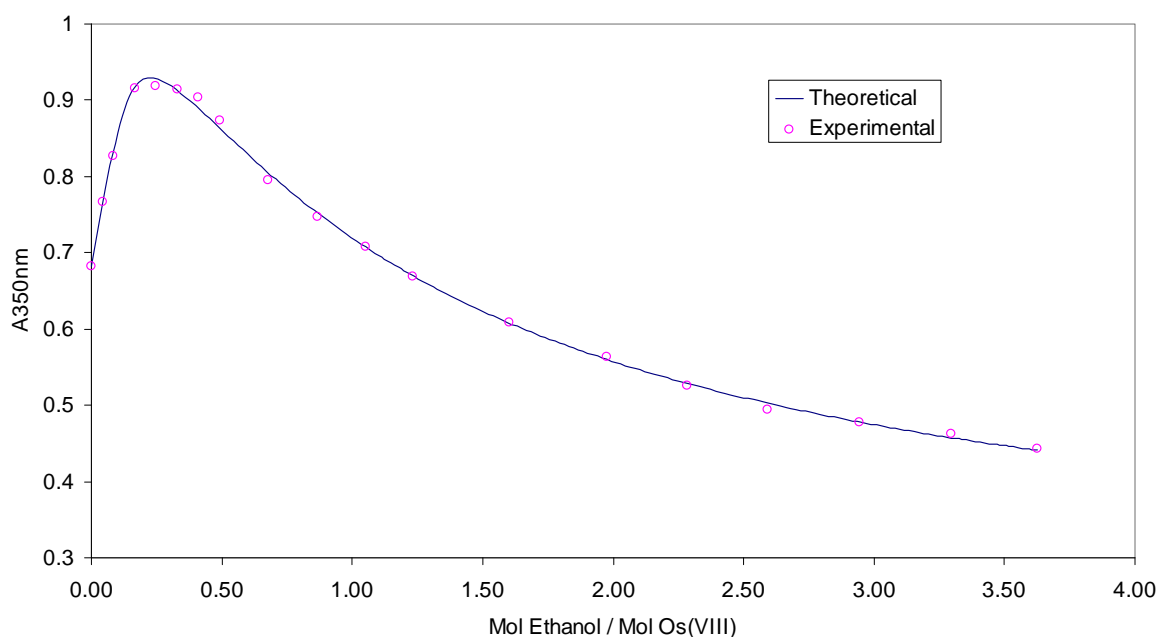


overlayed on the experimental data points. This simulates the stoichiometry of four mole osmium(VIII) reacting with one mole alcohol in the first step of the reaction. In the second step, another mole of alcohol reacts with the product of the first step. Various other models were attempted such as a three-to-one and two-to-one osmium-to-ethanol ratio, but this model gave the best fit.

Figure 6.5 shows an example of the UV-VIS spectra that were generated for each different mole ratio solution – for benzyl alcohol, in this case. This shows that the shapes of the spectra during the equilibrium reaction in stoichiometrically limiting quantities of reducing agent are identical to the shapes of the spectra during the kinetic reaction in an excess of reducing agent. This simply proves that the kinetic reaction can be halted at any point during its progression by using a limiting quantity of alcohol.



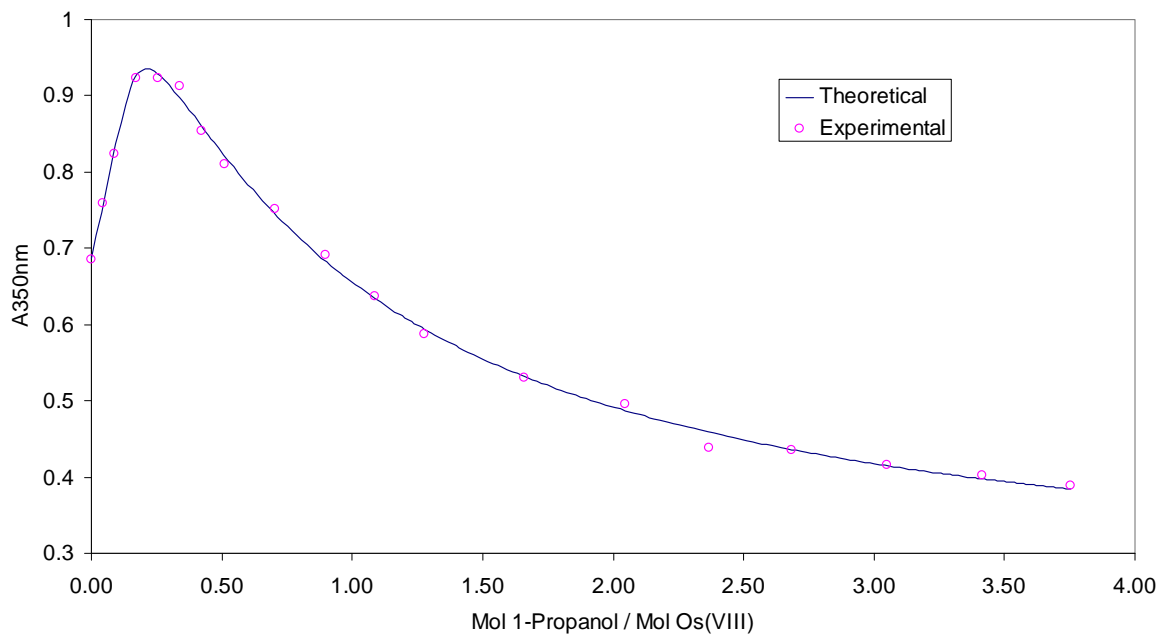
(a)



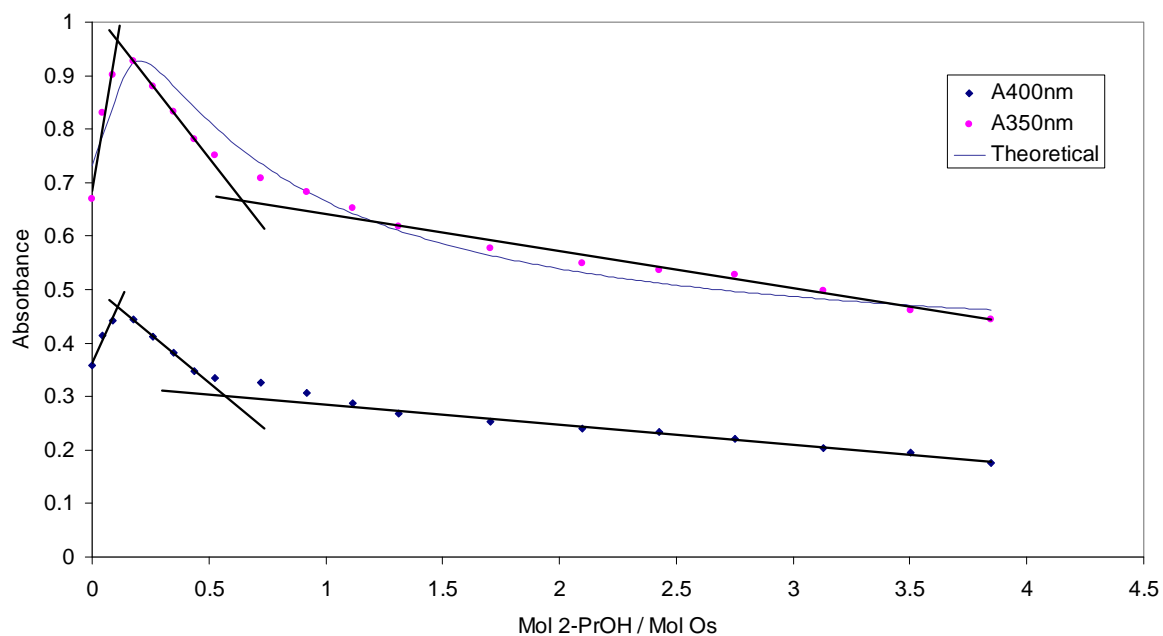
(b)

**Figure 6.1: Mole ratio plot of  $4.05 \times 10^{-4}$  M osmium tetroxide with increasing concentrations; (a) methanol; and (b) ethanol; in 2M hydroxide medium**



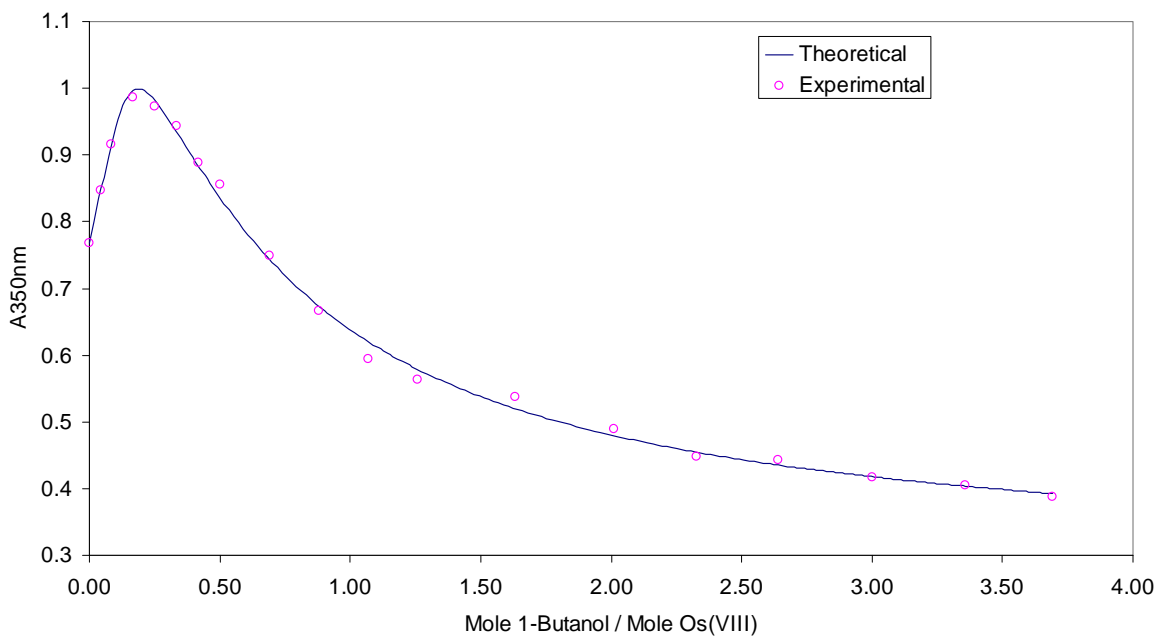


(a)

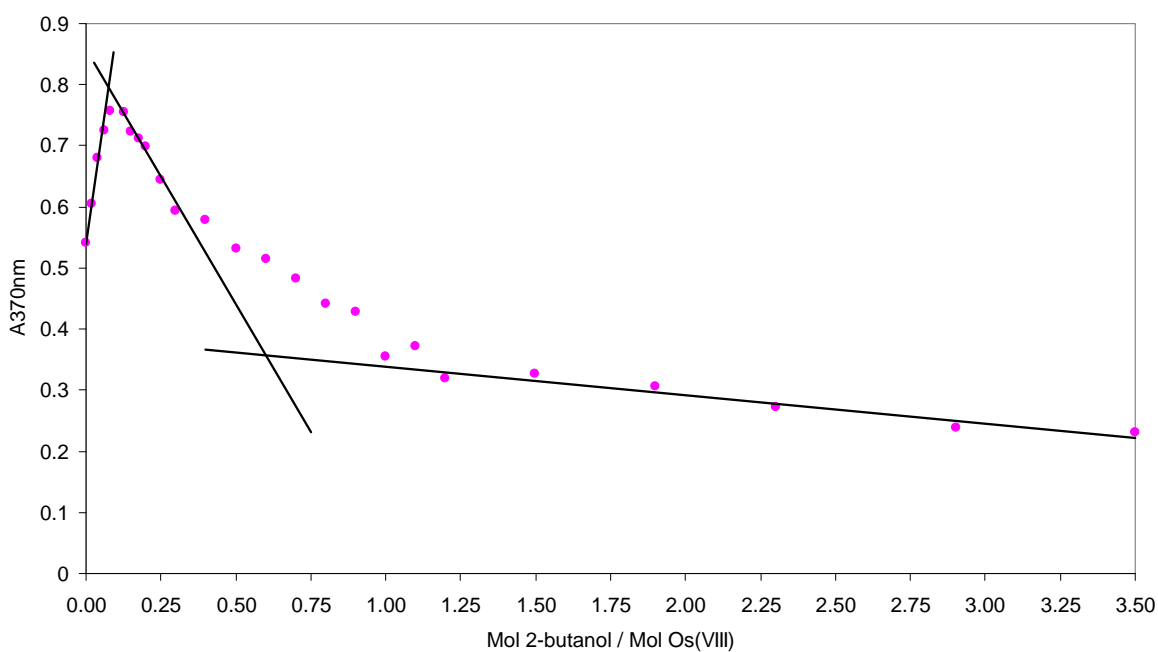


(b)

Figure 6.2: Mole ratio plot of (a)  $4.07 \times 10^{-4} \text{M}$  osmium tetroxide with increasing concentrations 1-propanol; and (b)  $3.97 \times 10^{-4} \text{M}$  osmium tetroxide with increasing concentrations 2-propanol; in 2M hydroxide medium.



(a)



(b)

**Figure 6.3: Mole ratio plot of (a)  $4.14 \times 10^{-4}$  M osmium tetroxide with increasing concentrations 1-butanol; and (b)  $4.28 \times 10^{-4}$  M osmium tetroxide with increasing concentrations 2-butanol; in 2M hydroxide medium**

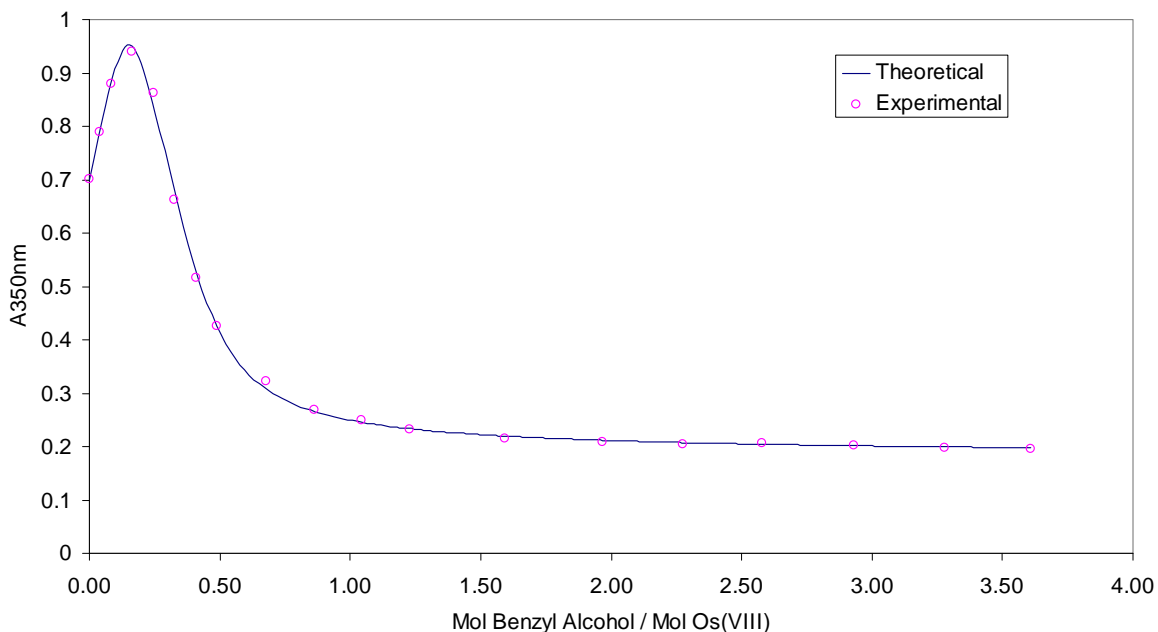


**Figure 6.4: Mole ratio plot of  $4.07 \times 10^{-4} \text{M}$  osmium tetroxide with increasing concentrations benzyl alcohol in 2M hydroxide medium.**

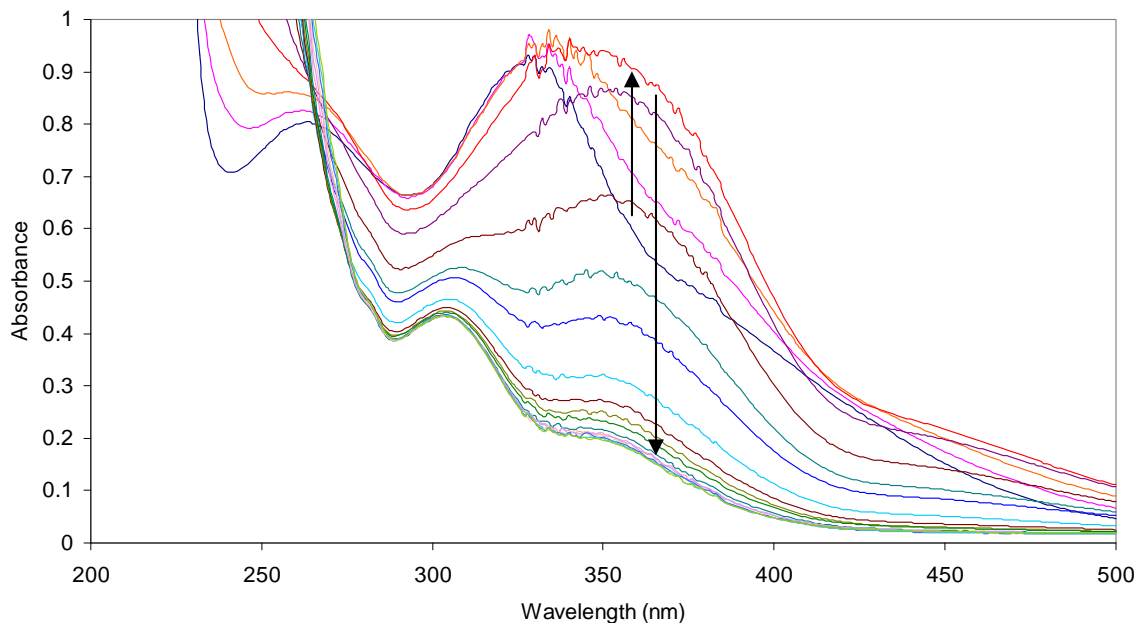
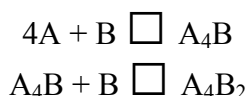


**Figure 6.5: The complete spectrum (500nm to 200nm) of each solution given by the mole ratios at each point in Figure 6.4. The direction of increasing benzyl alcohol concentration is given by, firstly, the upward arrow and, secondly, the downward arrow.**

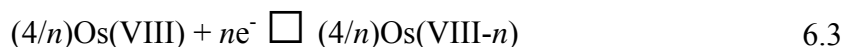
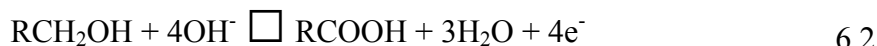
In this discussion it is necessary to separate the discussion between primary alcohols and secondary alcohols.

### Primary alcohols

It is apparent from plots 6.1 to 6.4 that (for primary alcohols) a good fit is obtained for the model



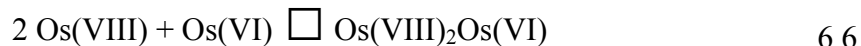
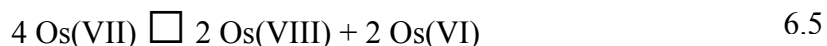
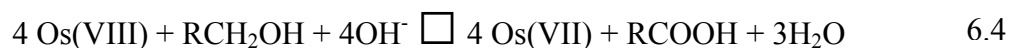
This model was attempted since it is the most basic and obvious answer to the stoichiometric question posed – in what ratio does the osmium(VIII) react with the alcohol? The products of the primary alcohols were found in Chapter 5 to be their corresponding carboxylic acids. This is a four electron process. This leaves only one variable to solve in balancing the other redox half-reactions – the number of electrons attributed to the osmium half-reaction (osmium and alcohol concentrations and volumes are accounted for).



In order for the experimentally determined stoichiometry to hold true for the first step,  $n$  must equal one. That is, the osmium half-reaction is a one-electron reduction to osmium(VII). This fits with the previously determined oxidation state of species B by iron(II) titration.

However, this holds some challenges in explaining the stoichiometry of the second step. Clearly, the reduction of osmium(VII) to osmium(VI) is a one-electron process and would result in the identical stoichiometry of the first step – that is, four moles osmium per mole of alcohol. In order for the stoichiometry of the second step to be satisfied, the osmium must undergo a four-electron reduction. At this point, the osmium(VIII)-osmium(VI) interaction from the previous chapter is reintroduced. There it was shown that osmium(VIII) interacts with osmium(VI) in a two to one ratio, either producing  $Os(VIII)_2Os(VI)$  or three  $Os(VII)$  molecules.

These results were therefore introduced into the equilibrium equations and the following fit to the experimental data obtained:



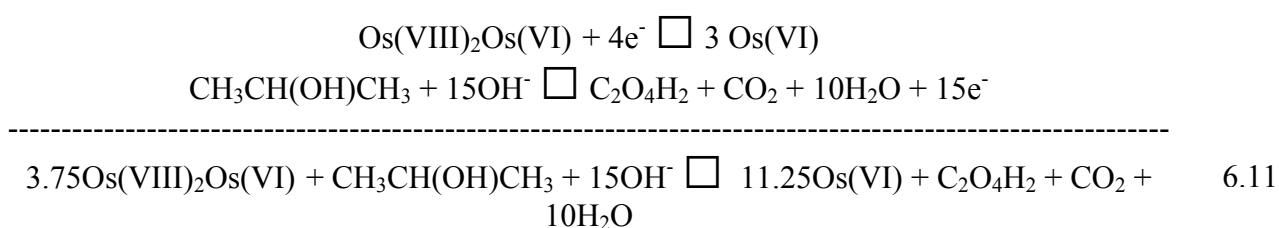
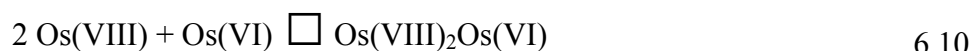
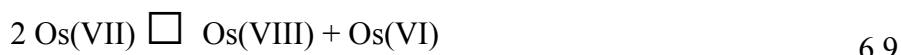
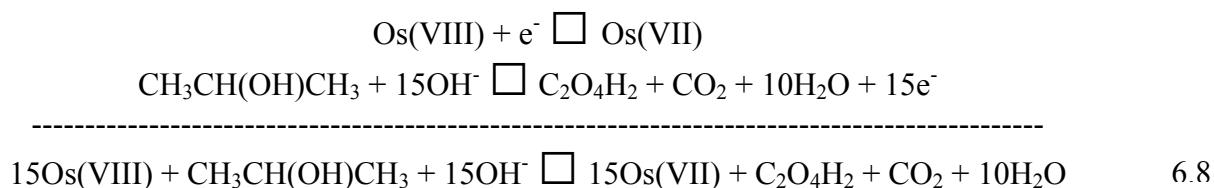
### Reaction scheme 1

The osmium(VII) produced in the first step disproportionates to osmium(VI) and osmium(VIII). An osmium(VIII)-(VI) trimer is formed and the alcohol then reacts preferentially with the trimer. This may occur through an energetically favourable multidentate intermediate. This reaction scheme accounts for the observed 4:1 ratio observed in the first step of Reaction model 1 (Equation 6.4) as well as the observed ratio of one mole of the product of step one reacting with one mole of alcohol (Equation 6.7). The two intervening steps (Equations 6.5 and 6.6) are required to account for the stoichiometry observed in Reaction model 1.

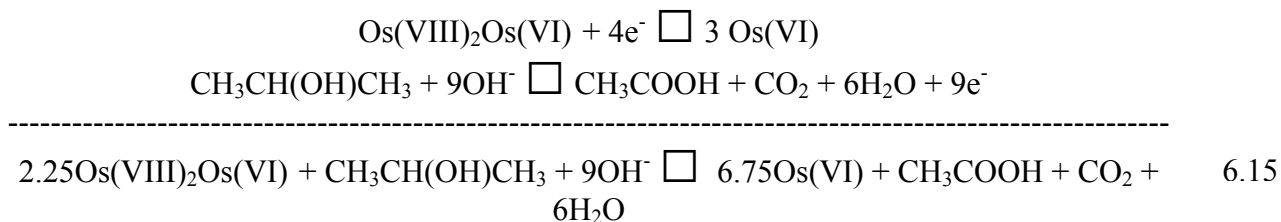
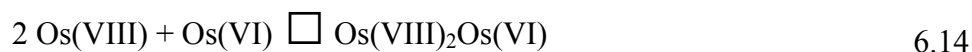
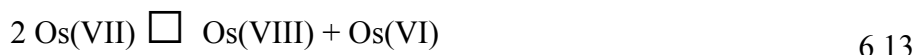
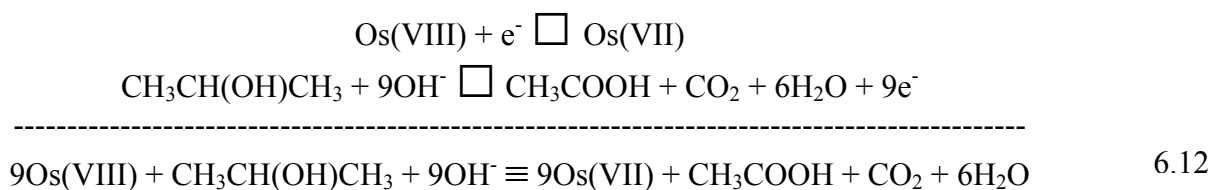
### Secondary alcohols

In the case of both 2-propanol (Figure 6.2 (b)) and 2-butanol (Figure 6.3(b)) the theoretical model does not fit the experimental data points very well and the reacting mole ratios have been determined by least squares analysis of the linear portions of the graph. This returns mole ratios at the intersecting portions of the straight lines as 0.11 and 0.61 for 2-propanol and 0.12 and 0.54 for 2-butanol, respectively. This implies that 10 mole osmium(VIII) reacts with 1 mole secondary alcohol in the first step of the reaction. Two moles of osmium then reacts with one mole of secondary alcohol in the second step of the reaction. This may seem to be an inordinately large ratio, but a clue was given in the preceding chapter, where the major organic products of the osmium(VIII)–2-propanol reaction were found to be oxalic acid and carbon dioxide, with some acetic acid. The products of the 2-butanol reaction were oxalic acid and acetic acid.

Reaction scheme 2 and 3 give the series of balanced equations that give the best fit to the 2-propanol experimental data in terms of Reaction scheme 1, assuming that the organic products are oxalic acid and carbon dioxide (Reaction scheme 2) or acetic acid and carbon dioxide (Reaction scheme 3).



**Reaction scheme 2: 2-propanol**



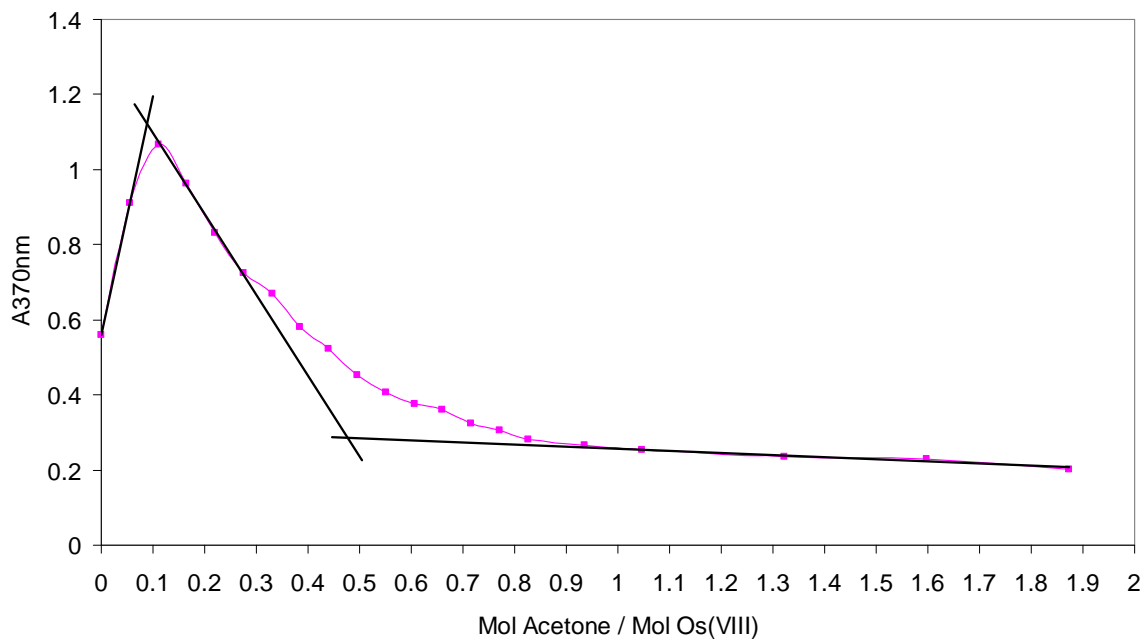
**Reaction scheme 3**

Overall, Reaction scheme 2 gives a better fit to the experimental data than Reaction scheme 1. The first step shows a mole ratio of osmium to alcohol of nine to one – close to the experimental value of ten to one. The second step theoretically predicts an osmium to alcohol mole ratio of 2.25 to one. It was found experimentally to be two to one. In reality, the reaction scheme is probably a mixture of Reaction schemes one and two. It is not necessary to go into the same complexities for the 2-butanol reaction. The equilibrium reaction model 1 will be amply demonstrated in the section on ketones to follow.

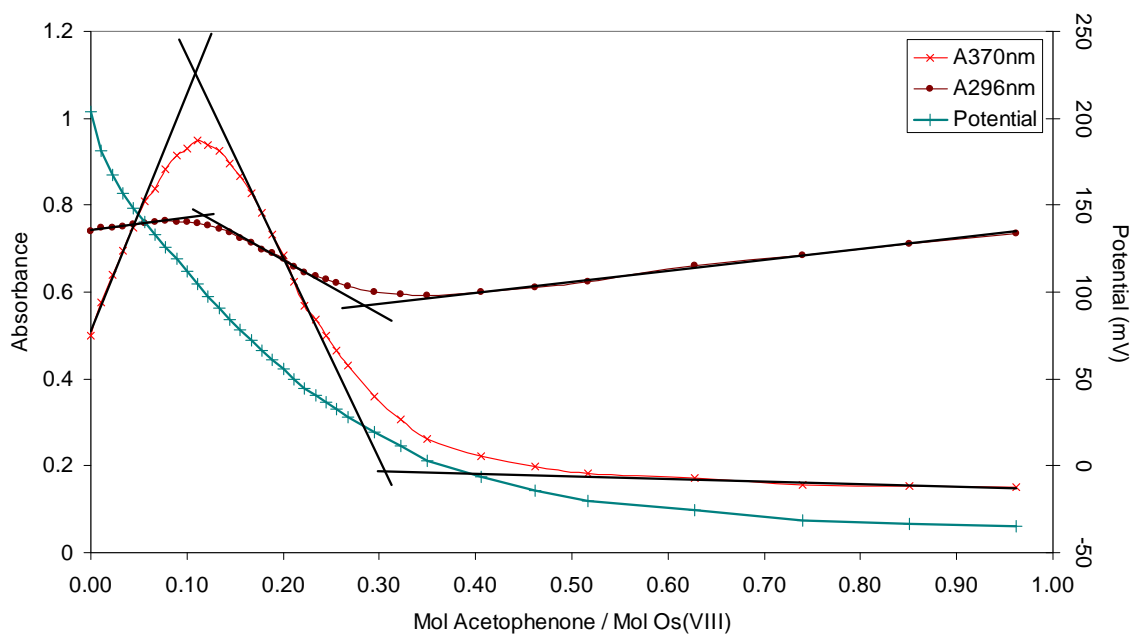
### **6.3.1.2 Ketones**

Figures 6.6 and 6.7 show the spectrophotometric titration curves for the titrations of osmium tetroxide with ketones in 2M hydroxide matrix. The ratio of the reacted ketone to osmium(VIII) has been determined at each endpoint by least squares analysis of the linear portions of the graphs and is given in Table 6.1. In some cases only absorbance at 370nm is used to determine endpoints (Figure 6.7), while in others a number of different wavelengths are averaged. The change in potential during the titration is also shown in some cases.

The complete spectrum after each addition of reducing agent is shown in Figure 6.8 for the titration of osmium(VIII) with acetophenone. The final endpoint of the titration can be seen as the peak at 295nm, which is due to an excess of acetophenone.



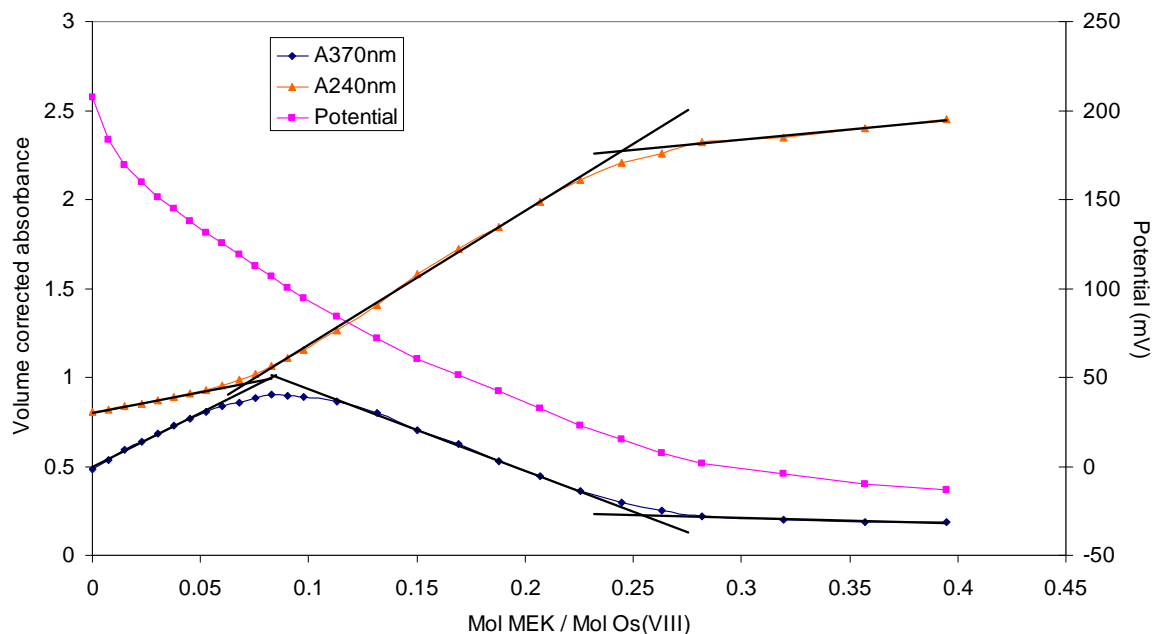
(a)



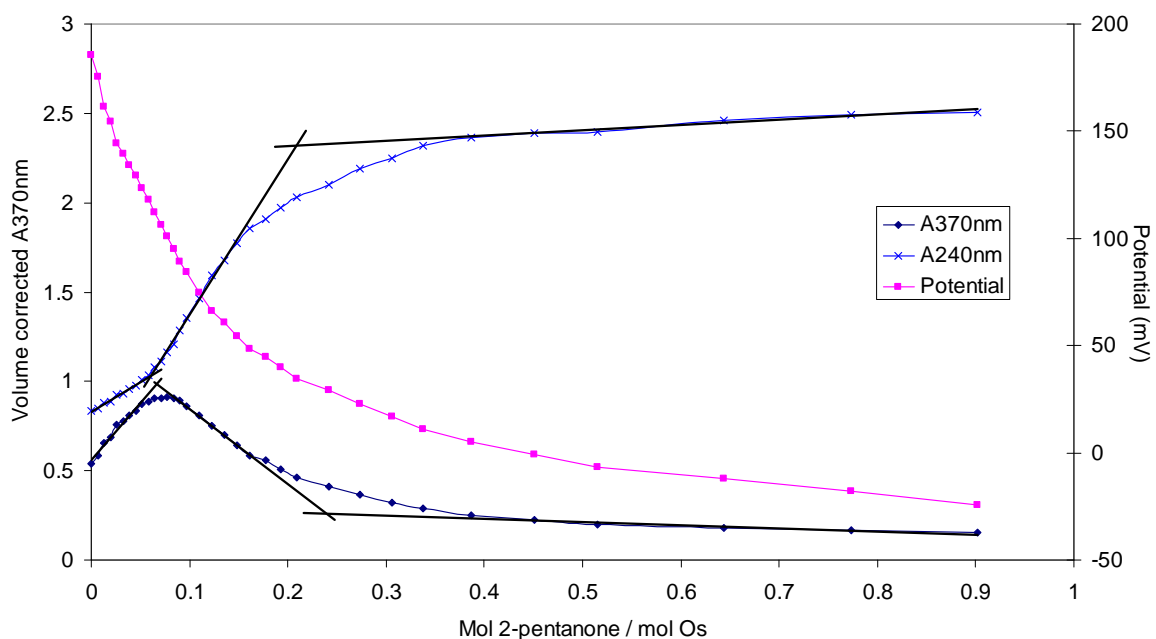
(b)

**Figure 6.6:** The spectrophotometric titration of (a) 10ml of 0.00173M osmium tetroxide in 2M hydroxide with 0.00950M ACETONE in 2M hydroxide; and (b) 10ml of 0.00154M osmium tetroxide in 2M hydroxide with 0.00856M ACETOPHENONE in 2M hydroxide.





(a)



(b)

**Figure 6.7:** The spectrophotometric titration of (a) 10ml of 0.00149M osmium tetroxide in 2M hydroxide with 0.00558M METHYL ETHYL KETONE in 2M hydroxide; and (b) 10ml of 0.00145M osmium tetroxide in 2M hydroxide with 0.00468M 2-PENTANONE in 2M hydroxide.

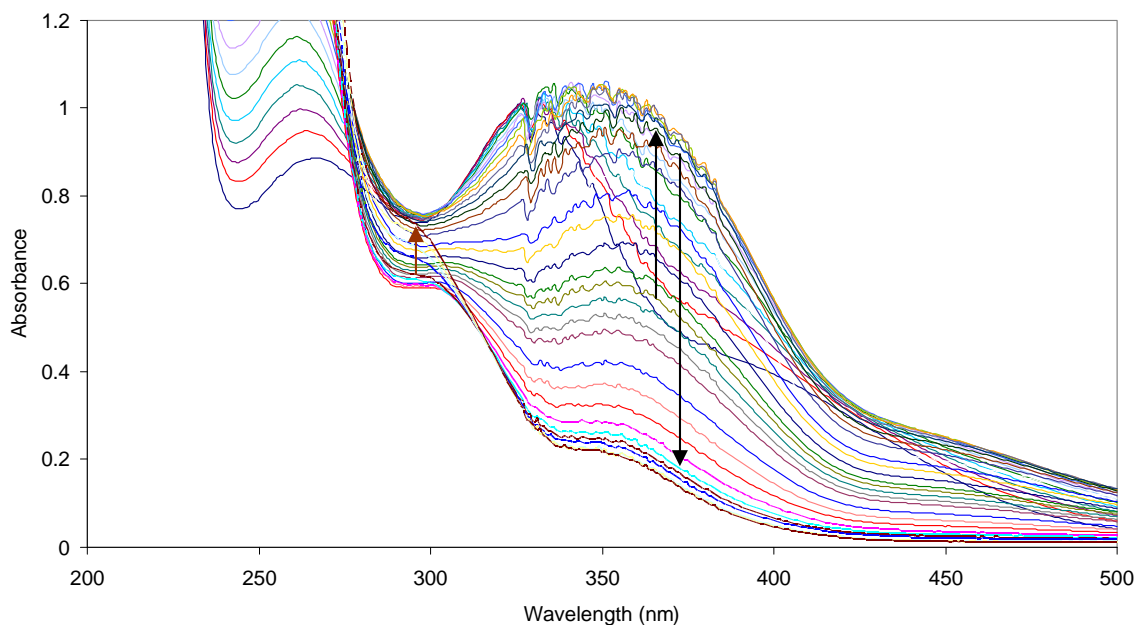


**Figure 6.8:** The complete spectrum (500nm to 200nm) after each addition of acetophenone. The direction of increasing acetophenone concentration is given by, firstly, the upward arrow and, secondly, the downward arrow. The brown arrow at 295nm indicates the increase in absorbance of acetophenone after the final endpoint of the titration.

**Table 6.1:** The mole ratios are given at the endpoints of the reactions as determined by least squares analysis of the linear portions of the graphs depicted in Figures 6.5 and 6.6. Also given are the ratios of ketones to osmium(VIII) that these endpoints imply.

	Endpoint 1		Endpoint 2	
	Mole ratio	Ketone:Os(VIII)	Mole ratio	Ketone:Os(VIII)
Acetone	0.089	1:11	0.48	2:5
Acetophenone	0.11	1:10	0.31	1:5
Methyl Ethyl Ketone	0.072	1:14	0.25	1:5
2-Pentanone	0.064	1:16	0.23	1:5

It is necessary at the outset to make clear that the number of reacting electrons for each ketone is only a guide. At this stage it is not possible to say exactly what the products of the ketone reactions are and in what proportions they are produced, since their oxidation is a complex process. This is clear from Table 6.2, which gives the half reactions for each of the ketones. The products are given according to the NMR findings here and the products reported in the literature. These organic half reactions are the ones used in the following reaction schemes as they approximate, as closely as possible, the organic oxidations that are believed to occur.

**Table 6.2: Half reactions for the oxidation of ketones**

<b>Acetone</b>	$\text{CH}_3\text{C}(\text{O})\text{CH}_3 + 14\text{OH}^- \rightarrow \text{C}_2\text{O}_4\text{H}_2 + \text{CO}_2 + 9\text{H}_2\text{O} + 14\text{e}^-$
<b>Acetophenone</b>	$\text{Ph-C}(\text{O})\text{CH}_3 + 8\text{OH}^- \rightarrow \text{Ph-COOH} + \text{CO}_2 + 5\text{H}_2\text{O} + 8\text{e}^-$
<b>Methyl ethyl ketone</b>	$\text{CH}_3\text{C}(\text{O})\text{CH}_2\text{CH}_3 + 14\text{OH}^- \rightarrow \text{CH}_3\text{COOH} + 2\text{CO}_2 + 9\text{H}_2\text{O} + 14\text{e}^-$
<b>2-Pentanone</b>	$\text{CH}_3\text{C}(\text{O})(\text{CH}_2)_2\text{CH}_3 + 18\text{OH}^- \rightarrow \text{CH}_3\text{COOH} + \text{C}_2\text{O}_4\text{H}_2 + \text{CO}_2 + 11\text{H}_2\text{O} + 18\text{e}^-$

Each ketone was analysed separately and a reaction scheme fitted to each to attempt to explain the mole ratios obtained at the endpoints of the two steps in Table 6.1. Naturally, a coherent reaction scheme that was consistent across the whole spectrum of experimental results was necessary, too. This resulted in a less than perfect correlation to the endpoint mole ratios in some cases, notably that of step two in the acetophenone reaction.

In all cases, it is indisputable that the first step is a one-electron reduction. The resulting stoichiometry was very close, if not perfect, to that predicted in Table 6.1. Once again, small allowances must be made for the fact that the exact organic products and their ratios are not known.

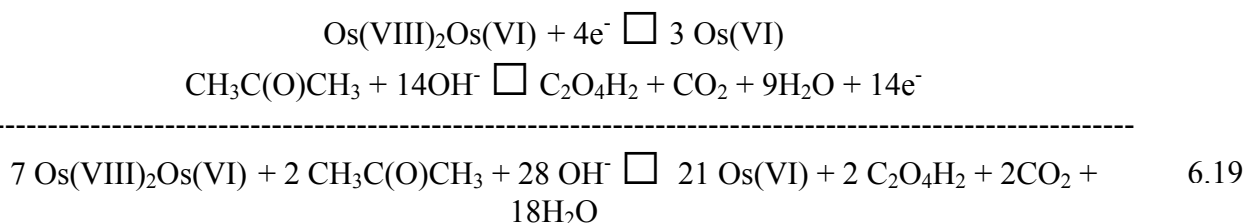
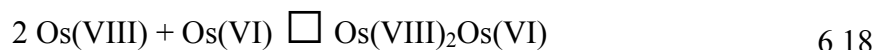
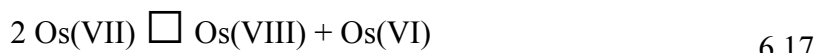
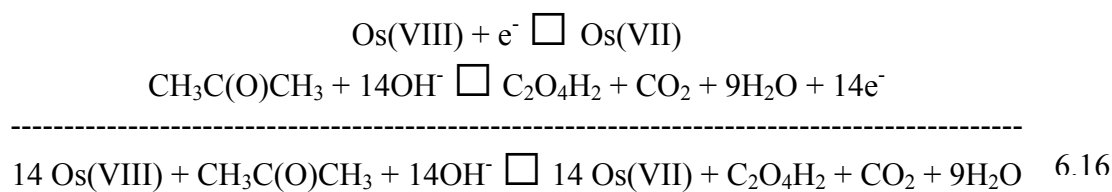
The second step of the reaction was, as for the alcohol reactions, taken as a four electron reduction of the  $\text{Os}(\text{VIII})_2\text{Os}(\text{VI})$  complex. The complex was, once again formed in the same way – due to a disproportionation of the osmium(VII) produced in the first step to osmium(VIII) and osmium(VI). The osmium(VIII) reacted with the osmium(VI) in a two-to-one ratio.

In the case of acetone, two reaction schemes are given – Reaction scheme 4 and 5. These show the differences in stoichiometry if an alternative organic product is given. Reaction scheme 4 gives the organic products as oxalic acid and carbon dioxide, whereas Reaction scheme 5 gives the products as acetic acid and carbon dioxide. This results in the mole ratios, for step two, of seven osmium to two acetone and four osmium to two acetone, respectively. Since the experimental prediction given in Table 6.1 is five osmium to two acetone, the true organic products are likely a mix of acetic acid, oxalic acid and carbon dioxide.

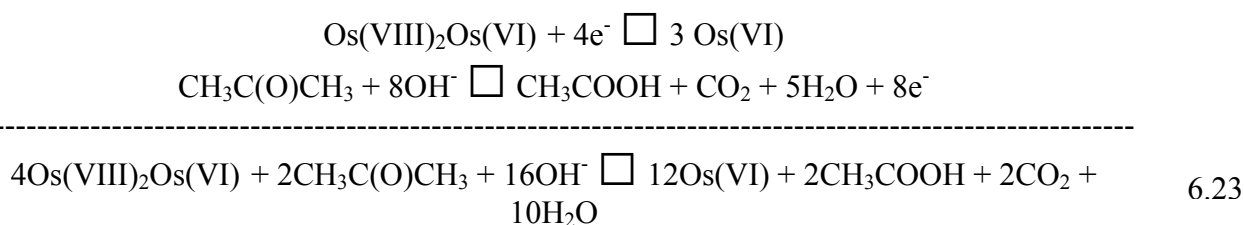
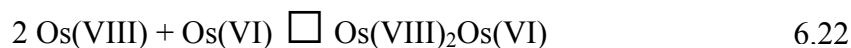
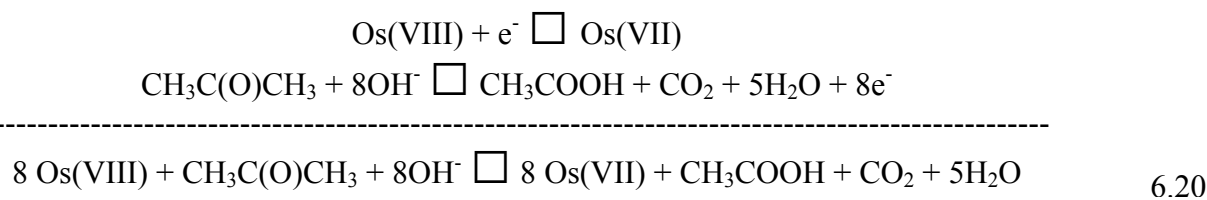
Likewise, reactions schemes are given for acetophenone (Reaction scheme 6), methyl ethyl ketone (Reaction scheme 7) and 2-pentanone (Reaction scheme 8). The second step in the acetophenone reaction shows that the mole ratio predicted from experimental data (five osmium to one acetophenone) differs from the postulated reaction mechanism, which shows two moles of osmium reacting with one of acetophenone. Alternative reaction products may, once again offer an explanation although none can, at this stage, be put forward that would offer many more electrons per half reaction.

Reaction scheme 7, for methyl ethyl ketone comes closer to the experimental values by predicting 3.5 mole osmium per methyl ethyl ketone consumed in step two, as opposed to the five mole osmium to one mole methyl ethyl ketone determined experimentally.

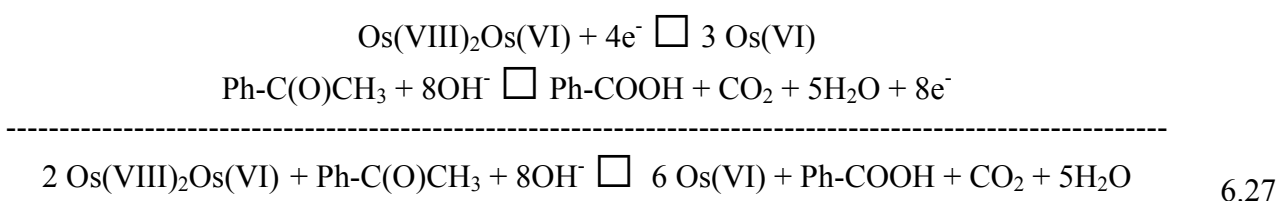
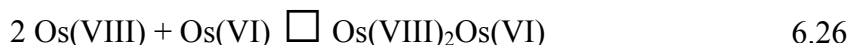
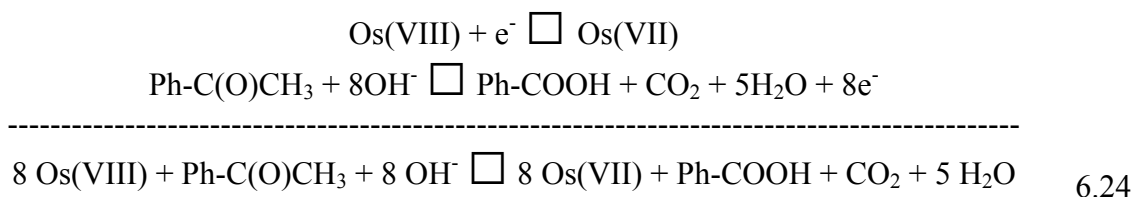
2-Pentanone, in Reaction scheme 8, conforms most closely yet with a theoretically predicted 4.5 mole osmium per 2-pentanone. Experimentally, step two of this reaction consumed 5 moles of osmium per mole of 2-pentanone.



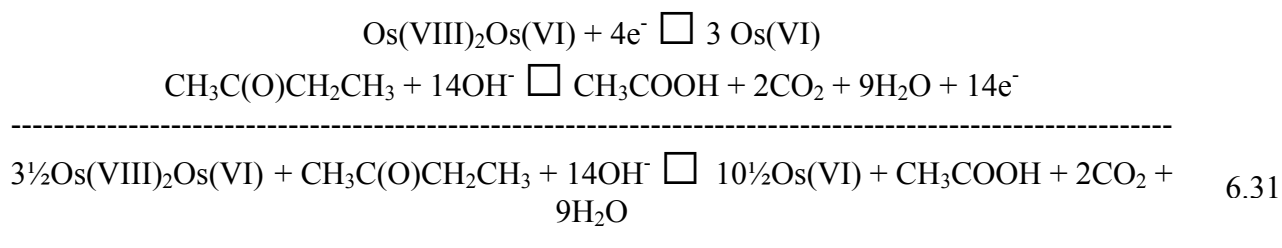
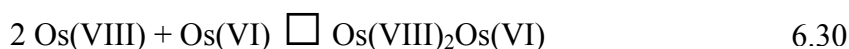
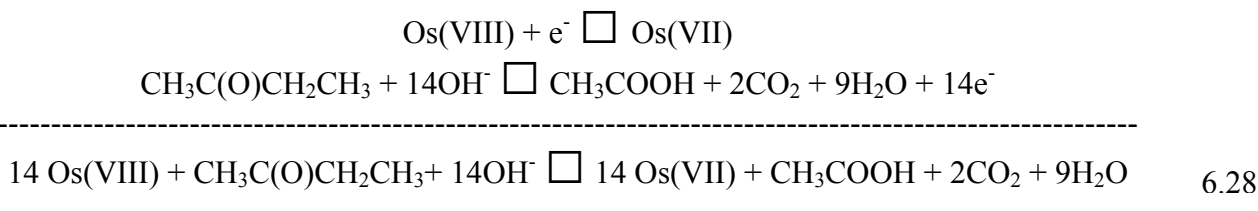
**Reaction scheme 4 – acetone**



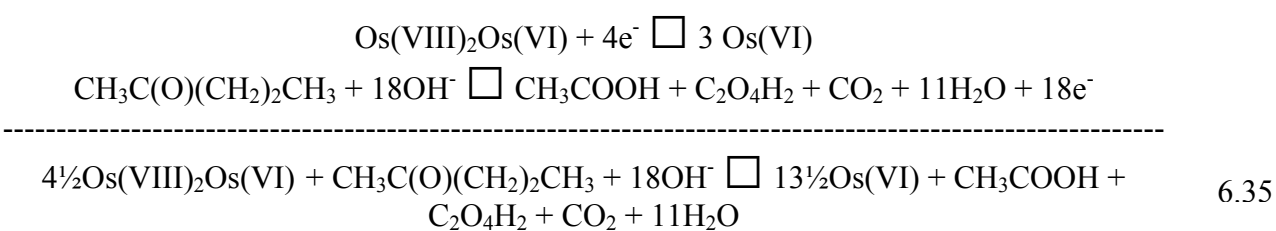
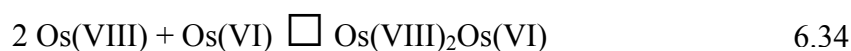
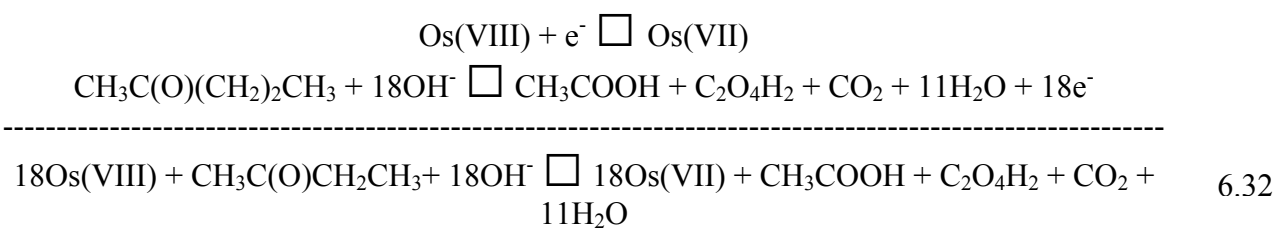
**Reaction scheme 5: acetone**



**Reaction scheme 6: acetophenone**



**Reaction scheme 7: methyl ethyl ketone**



### Reaction scheme 8: 2-pentanone

It was found that the theoretical reaction schemes for the ketones did not conform to the experimental results as well as those for the primary alcohols. However, an explanation was put forward concerning the complexity of the ketone oxidation, which sought to explain this shortcoming.

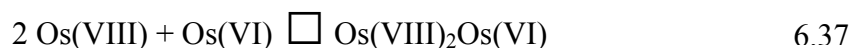
## 6.3.2 Equilibrium Reaction Model 2

### 6.3.2.1 Primary alcohols

An entirely different approach was used in this analysis of the data. The model is much less complex than Reaction Model 1 and more appealing in its simplicity.

From the outset it was felt that the likelihood of an elementary step between one molecule of osmium and one molecule of alcohol was far more probable than two molecules of osmium coming together to exchange two electrons with just one alcohol molecule. The latter scenario is depicted in Reaction Model 1 and is difficult to explain mechanistically. The former scenario, in the case of primary alcohols, would result in one molecule of osmium(VIII) reacting with one molecule of alcohol to form osmium(VI) and the

corresponding aldehyde. Before equilibrium is reached the aldehyde may once again react with an osmium(VIII) in a fast step to produce more osmium(VI) and the corresponding carboxylic acid. Bringing the Os(VIII)<sub>2</sub>Os(VI) complex into the reaction model, results in the scheme depicted below in Reaction scheme 9.



### Reaction scheme 9

This scheme has parallels with the reaction scheme put forward in Section 6.3.1 in that four moles of osmium(VIII) react with one mole of alcohol in the first step of the reaction, albeit indirectly. The scheme was modelled using the Dynafit modelling software<sup>(43)</sup> and the reaction model:



Figures 6.9 to 6.13 show the extent of the fit of the theoretical model to the experimental data points. The fit was very good for the primary alcohols. The molar extinction coefficients for all three absorbing species, Os(VIII), Os(VI) and Os(VIII)<sub>2</sub>Os(VI), were kept constant. The conditional equilibrium constants\*,  $K_1$  and  $K_2$  are given separately for each figure.

---

\* The equilibrium constants are conditional on pH, as will be seen in Chapter 8.



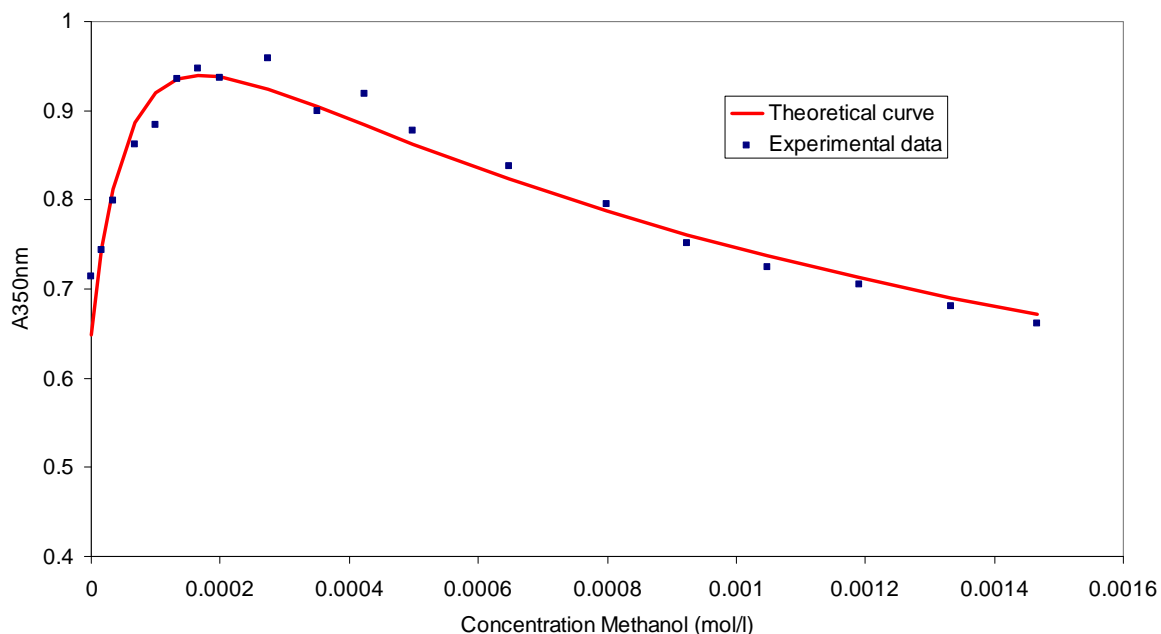


**Figure 6.9:** Theoretical and experimental curves for the reaction of increasing concentrations methanol with  $4.05 \times 10^{-4} \text{M}$  osmium tetroxide in 2M hydroxide, at equilibrium.

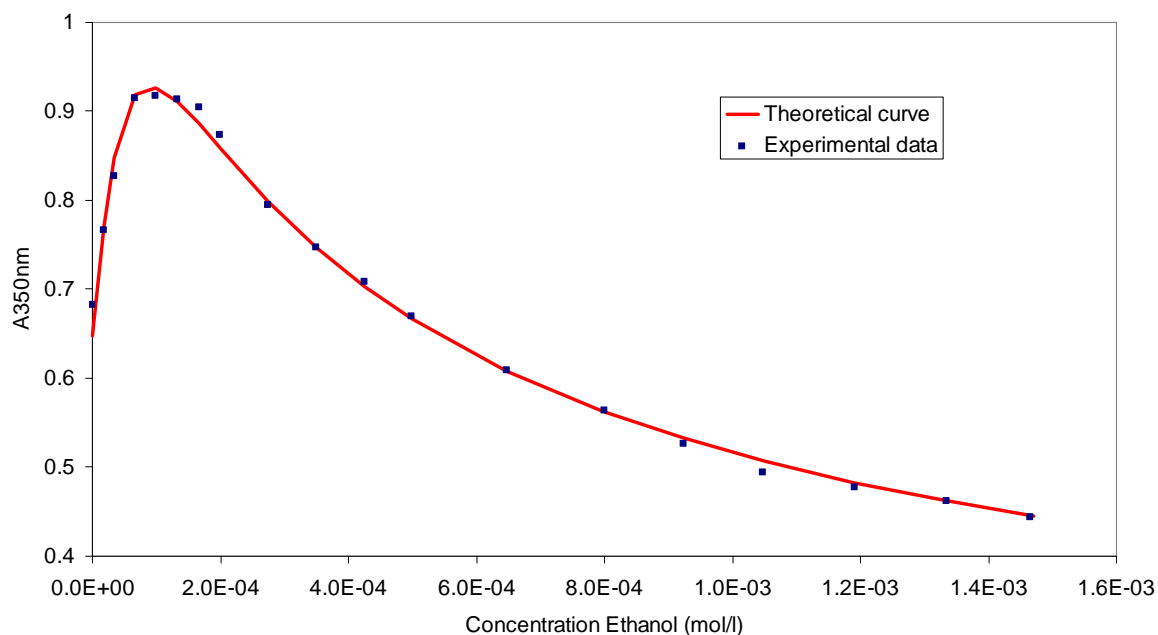


**Figure 6.10:** Theoretical and experimental curves for the reaction of increasing concentrations ethanol with  $4.05 \times 10^{-4} \text{M}$  osmium tetroxide in 2M hydroxide, at equilibrium.

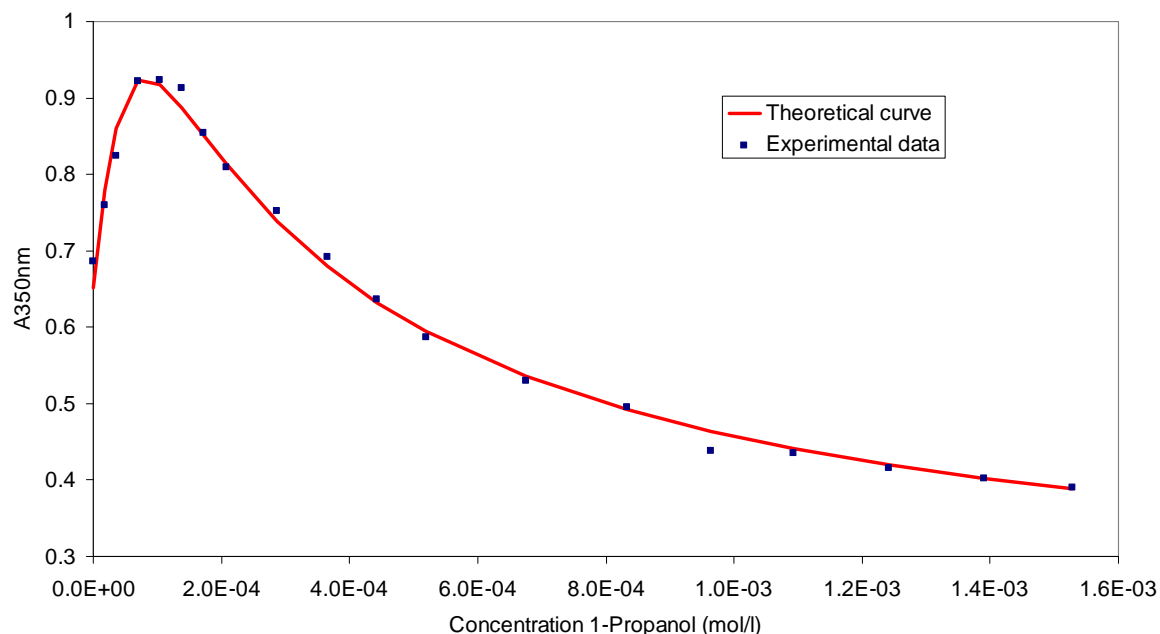


**Figure 6.11: Theoretical and experimental curves for the reaction of increasing concentrations 1-propanol with  $4.07 \times 10^{-4}$  M osmium tetroxide in 2M hydroxide, at equilibrium.**

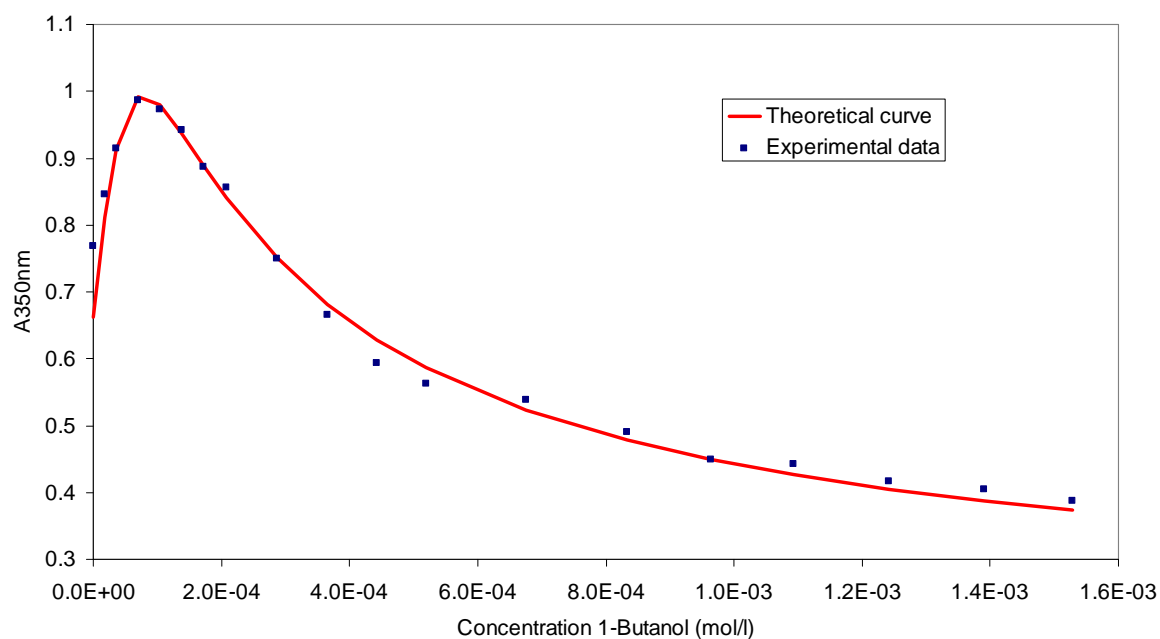


**Figure 6.12: Theoretical and experimental curves for the reaction of increasing concentrations 1-butanol with  $4.14 \times 10^{-4}$  M osmium tetroxide in 2M hydroxide, at equilibrium.**

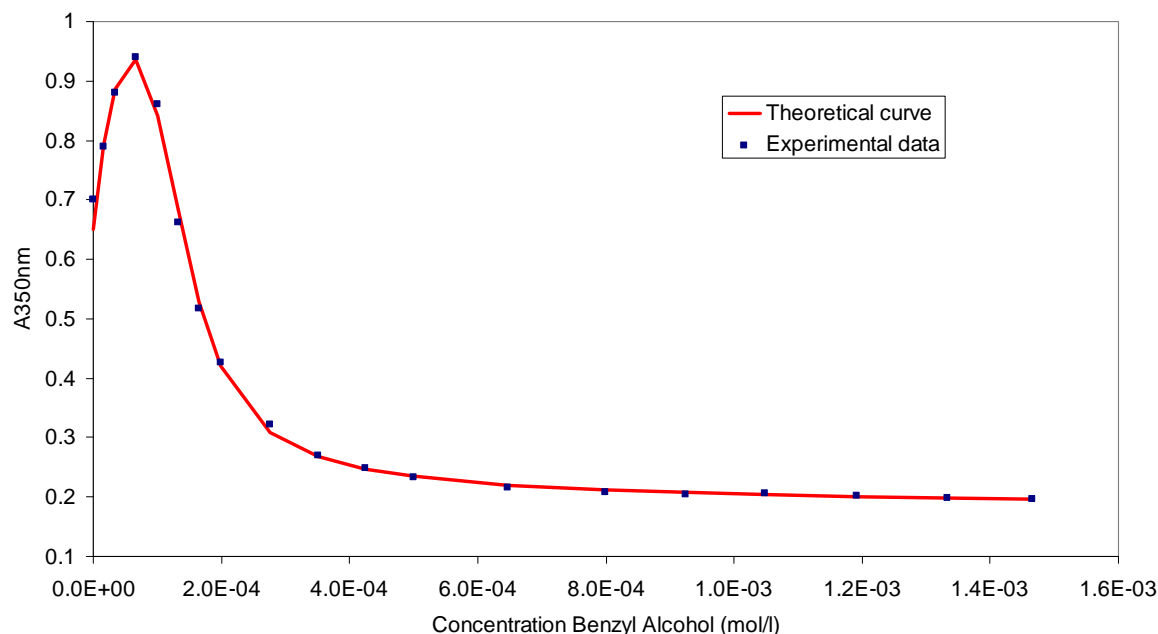


**Figure 6.13:** Theoretical and experimental curves for the reaction of increasing concentrations benzyl alcohol with  $4.07 \times 10^{-4}$  M osmium tetroxide in 2M hydroxide, at equilibrium.

**Table 6.3:** Conditional equilibrium constants,  $K_1$  and  $K_2$ , for Reaction Scheme 9.

	$K_1$ ( $M^{-2} \times 10^7$ )	$K_2$ ( $M^{-2} \times 10^6$ )
<b>Methanol</b>	0.554	10.3
<b>Ethanol</b>	1.89	9.72
<b>1-Propanol</b>	2.68	9.39
<b>1-Butanol</b>	3.83	11.4
<b>Benzyl alcohol</b>	80.6	9.99
<b>Ave <math>K_2</math></b>	-	10.16

Clearly, this model produced good fits and coherent parameters for the primary alcohols. The first equilibrium constant,  $K_1$ , increases as the size of the alcohol increases, which is in line with the qualitative observation that the rate of the reaction increases with an increase in size of the alcohol.  $K_1$  is extremely large for benzyl alcohol, which is also confirmed by the qualitative observation of an extremely fast rate for the benzyl alcohol reaction.  $K_2$ , on the other hand, although not restricted during the simulation in any way, is approximately constant for the primary alcohols. This lends consistency to the model, since  $K_2$  is describing the same equilibrium in each case.

### 6.3.2.2 Secondary alcohols and ketones

Figures 6.14 and 6.15 simulate Equilibrium reaction model 2 for the secondary alcohols. It is clear that the fit is not as good as for the primary alcohols. It is shown in Section 6.3.1 that, since the products of the secondary alcohol and ketone reactions were more oxidised than their corresponding carboxylic acid, the stoichiometry was correspondingly greater than for the primary alcohols. Unfortunately it is not possible to attempt models with stoichiometry greater than  $3A + B$ , since the very large constants that this generates causes the Dynafit modelling software to crash. However, seen from the point of view of the mole ratio plots in Figures 6.2(b), 6.3(b), 6.6 and 6.7, it is clear that one mole of secondary alcohol or one mole of ketone has more oxidising power than one mole of primary alcohol. Therefore, a similar equilibrium reaction model should be able to be applied to secondary alcohols and ketones as Reaction scheme 9, albeit with a greater ratio of osmium(VIII) to secondary alcohol or ketone. It is trivial to attempt a serious accounting of the stoichiometry of the secondary alcohols and ketones. Their oxidation products are complex and varied, which obviously affects their stoichiometry. However, the mole ratio plots inform us that the first step of the two-step reaction is completed after between ten and sixteen moles of osmium have reacted with one mole of secondary alcohol or ketone. The number of moles of osmium can be rounded off to twelve (since this number balances the equations) and a generic reaction model for the secondary alcohols and the ketones is put forward:



Therefore, a total of twelve moles of osmium have been consumed for the consumption of every one mole of secondary alcohol or ketone.

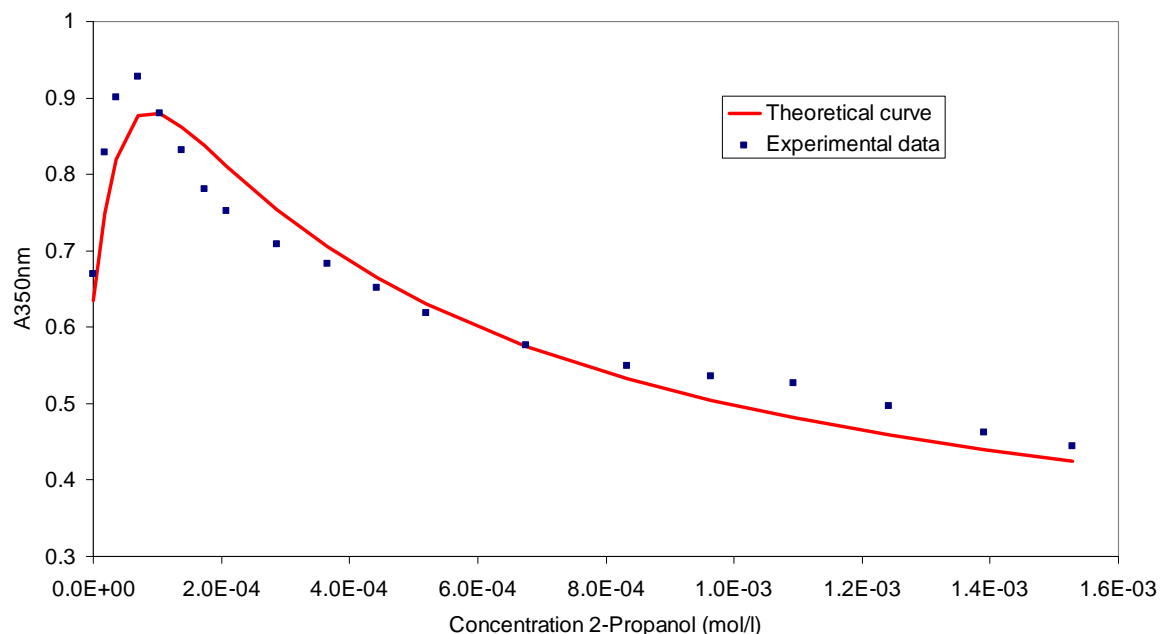


**Figure 6.14:** Theoretical and experimental curves for the reaction of increasing concentrations 2-propanol with  $3.97 \times 10^{-4} \text{M}$  osmium tetroxide in 2M hydroxide, at equilibrium.

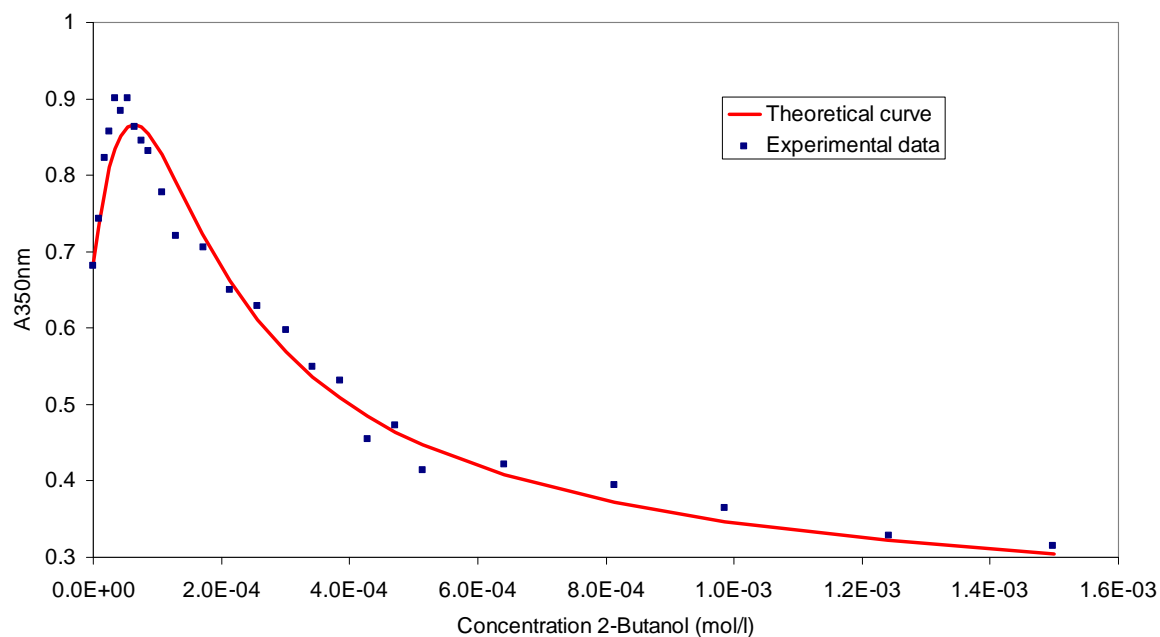


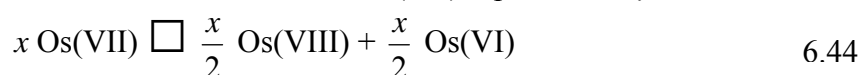
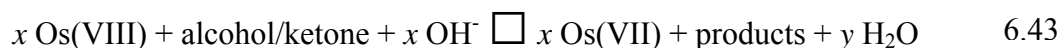
**Figure 6.15:** Theoretical and experimental curves for the reaction of increasing concentrations 2-butanol with  $4.28 \times 10^{-4} \text{M}$  osmium tetroxide in 2M hydroxide, at equilibrium.

An alternative explanation has now been put forward as Equilibrium Reaction Model 2. It has proved coherent and simple and altogether more appealing than Equilibrium Reaction Model 1, which was clumsy and inelegant. Unfortunately, it is not possible to follow through with a simulation for the secondary alcohols and ketones, but these will be pursued in the following chapter on kinetic modelling where it is possible to simplify the reactions to their rate-limiting steps. The following section will provide a summary and comparison, giving a clearer perspective of the two models.

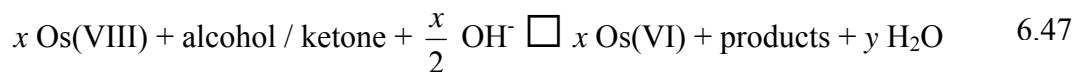
However, before moving on it is necessary to return briefly to Chapter 5.3.1.4. In that section, the molar extinction coefficient at 370nm for “species B” was calculated as  $7283 \text{ L}\cdot\text{mol}^{-1}\cdot\text{cm}^{-1}$ . Now that a reaction model has been settled on, it will become clear how that value was calculated. Table 6.3 shows that the equilibrium constant,  $K_2$ , for complex formation is large. Therefore, the equilibrium for complex formation will lie far to the right. This means that osmium(VI) produced by the osmium(VIII)-alcohol reaction, will be immediately incorporated into the  $\text{Os(VIII)}_2\text{Os(VI)}$  complex. When the concentration of the  $\text{Os(VIII)}_2\text{Os(VI)}$  complex is highest, all of the available osmium will be incorporated into the complex, because of its large equilibrium constant. Thus, two thirds of all available osmium will be incorporated into the complex as osmium(VIII) and the remaining one third will be incorporated into the complex as osmium(VI). Thus, the highest concentration of the complex will be one third of the initial osmium(VIII) concentration. This is the concentration used to calculate the molar extinction coefficient of “species B” – the  $\text{Os(VIII)}_2\text{Os(VI)}$  complex. This value proved remarkably similar to the molar extinction coefficient generated by the kinetic modelling software in Chapter 8.

## 6.4 SUMMARY

1. Primary alcohols: one mole alcohol reacts with four mole osmium in the first step of the reaction.
2. Secondary alcohols and ketones: one mole alcohol or ketone reacts with between ten and sixteen mole osmium in the first step of the reaction.
3. The discrepancies were attributed to the more oxidised products of the secondary alcohols and ketones – each mole of secondary alcohol or ketone has more “oxidising power” than a mole of primary alcohol.
4. **Equilibrium Reaction Model 1** postulated:
  - 4.1. An **osmium(VII) intermediate**;
  - 4.2. **Disproportionation** of the osmium(VII) to osmium(VI) and osmium(VIII);
  - 4.3. **Complexation** between osmium(VIII) and osmium(VI) to form  $\text{Os(VIII)}_2\text{Os(VI)}$ ;
  - 4.4. Reaction between the complex and alcohol or ketone to form **osmium(VI)**.



5. **Equilibrium Reaction Model 2** postulated:
  - 5.1. Reduction of osmium(VIII) to **osmium(VI)** (**not** osmium(VII));
  - 5.2. **Complexation** between osmium(VIII) and osmium(VI) to form  $\text{Os(VIII)}_2\text{Os(VI)}$ .



6. **Favourable characteristics of Equilibrium Reaction Model 2:**
  - 6.1. Simplicity;
  - 6.2. Production of osmium(VI) – which results in the reaction of **one mole** osmium(VIII) with **one mole** alcohol/ketone in the slow step.

6.3. Only **three absorbing species** – osmium(VIII), osmium(VI) and the complex – whereas model 1 has four absorbing species – osmium(VIII), osmium(VI), osmium(VII) and the complex. This does not necessarily negate model 1, but further complicates matters.



## CHAPTER 7

### FITTING THE KINETIC REACTION MODEL

#### 7.1 INTRODUCTION

Since kinetic data plays a large part in this study it is fitting to take a brief look at the theory that underlies much of the results. The osmium-alcohol reaction may be represented as follows:



The rate of the reaction can therefore be written as:

$$\text{Rate} = - \frac{d[\text{Os(VIII)}]}{dt} = - \frac{d[\text{RCH}_2\text{OH}]}{dt} = - \frac{d[\text{OH}^-]}{dt} = k [\text{Os(VIII)}]^x [\text{alcohol}]^y \quad 7.2$$

By maintaining the alcohol concentration in large excess, they can be incorporated into the rate constant. Equation 7.2 then becomes:

$$\text{Rate} = - \frac{d[\text{Os(VIII)}]}{dt} = k_{\text{obs}} [\text{Os(VIII)}]^x \quad 7.3$$

When  $x = 1$  the reaction is first order in Os(VIII) and can be written as follows:

$$- \frac{d[\text{Os(VIII)}]}{[\text{Os(VIII)}]} = k_{\text{obs}} dt \quad 7.4$$

This equation can be integrated between time = 0 and a later time = t, using the Os(VIII) concentration at time = 0 and time = t.

$$\int_{[\text{Os(VIII)}]_0}^{[\text{Os(VIII)}]} \frac{d[\text{Os(VIII)}]}{[\text{Os(VIII)}]} = k \int_0^t dt \quad 7.5$$

Which, upon integration, gives:

$$\ln [\text{Os(VIII)}] = kt - \ln [\text{Os(VIII)}]_0 \quad 7.6$$

In the same manner, one can derive linear equations for zero (Equation 7.7) and second order (Equation 7.8) reactions:

$$[\text{Os(VIII)}] = [\text{Os(VIII)}]_0 - kt \quad 7.7$$

$$\frac{1}{[\text{Os(VIII)}]} - \frac{1}{[\text{Os(VIII)}]_0} = kt \quad 7.8$$

A straightforward single-step reaction could have been plotted in terms of Equations 7.6, 7.7 and 7.8. However, the complexities of the alcohol–osmium and ketone–osmium reactions called for the utilisation of kinetic modelling software. Simply the fact that there were two reactions occurring meant that the equations could not be plotted in terms of two variables since, if the reactions overlapped, there could be three or more absorbing species contributing to the absorbance in varying degrees at any one time. Therefore, the Dynafit kinetic modelling software <sup>(43)</sup> made it possible to fit more complex reaction models to the experimental data.

This chapter describes the challenges in finding a reaction model that fits the experimental data to within acceptable parameters. It is necessary, in this regard, to put forward a large number of different reaction models, show the theoretical fit to the experimental data and explain why the model is acceptable or not. Finally, a reaction model is chosen to be representative of the experimental data, and reasons are put forward for the choice. It is necessary to show the process of elimination that went into the choice of the final reaction model in order that the reader might draw their own conclusions as to the aptness of this choice.

It is important to bear in mind that these are kinetic models and that, as such, they give information on the rate-limiting steps of the reaction. Therefore, models that may have been represented by equations with large osmium-to-alcohol or osmium-to-ketone ratios in the previous chapter can now be simplified to their elementary steps. It is important to emphasise that a rate study will give information about steps up to and including the slowest step and the rate law will be determined by that step.

---

---

## 7.2 EXPERIMENTAL

---

---

The kinetic data presented in the following section was obtained by reacting a known concentration of alcohol or ketone dissolved in 2M sodium hydroxide, with a known concentration of osmium(VIII) in 2M hydroxide, and the reaction followed spectrophotometrically over time. Therefore, using the ethanol-osmium(VIII) reaction as a representative reaction:

A stock 0.00151M osmium tetroxide solution in water was prepared as described in Chapter 2 and standardised by the thiourea method. A stock ethanol solution of 0.1715M was prepared in 2M hydroxide. Six consecutive kinetic reactions were executed with increasing concentrations of ethanol. Consecutive ethanol concentrations were: 0.00196M, 0.00588M, 0.00810M, 0.0100M, 0.0149M and 0.0201M. Each reaction was prepared *in situ* in a 1cm quartz cuvette with magnetic follower. Reactions were carried out at 25°C. The reactants were kept in a water bath at 25°C and the cuvette was enclosed in a constant temperature sleeve at 25°C. Measured volumes of 6M sodium hydroxide were added such that the final hydroxide concentration was 2M. Measured quantities of osmium tetroxide were then added such that the final osmium tetroxide concentration was  $4.32 \times 10^{-4}$ M. Measured volumes of water were added to bring the volume to a constant final value. Then an initial reading was taken on the spectrophotometer, either at a fixed wavelength of 370nm or by scanning across the range of 500 to 200nm\*. The reaction was started at time = zero minutes by adding a measured volume of the stock ethanol solution and the progress of the reaction followed as described. The reaction was allowed to run for 20 minutes after which it was stopped and the experimental data fitted to one of the theoretical models shown in Section 7.3.

The same general format was followed for all the kinetic reactions. The kinetic reactions of ethanol with osmium(VIII) and methyl ethyl ketone (MEK) with osmium(VIII) are taken as

---

\* In general, the slowest reaction – that is, the one with the lowest alcohol or ketone concentration – was followed by scanning 500 to 200nm at one cycle per 50 seconds and a rate of 960nm per minute. Thereafter, the rest of the reactions were followed at a fixed wavelength of 370nm with a reading taken every half a second.

representative of the alcohols and ketones, respectively. The theoretical models are fitted to these reactions. The best-fit model is then applied to all the other kinetic data.

Consecutive methyl ethyl ketone concentrations were:  $8.0 \times 10^{-5} \text{M}$ ,  $1.6 \times 10^{-4} \text{M}$ ,  $2.4 \times 10^{-4} \text{M}$ ,  $3.5 \times 10^{-4} \text{M}$ ,  $4.0 \times 10^{-4} \text{M}$  and  $4.8 \times 10^{-4} \text{M}$ . Osmium tetroxide concentration was  $3.76 \times 10^{-4} \text{M}$  and the hydroxide concentration was 0.1M. The low hydroxide and MEK concentrations were chosen in order to keep the rate of the reaction slow enough that it could be followed on the time scale of the experiments, i.e. 20 minutes. It should be remembered that the equilibrium ratio of ketone to osmium(VIII) was between ten and sixteen. However, the rate limiting steps have a ratio of one-to-one and the rate modelling software does not recognise that there is sufficient MEK present to complete the reactions (which there is, since the reactions run to completion). For this reason the MEK concentration was multiplied by ten in order to model their reactions. This will be taken into account when reporting rate constants.

---

---

## 7.3 RESULTS

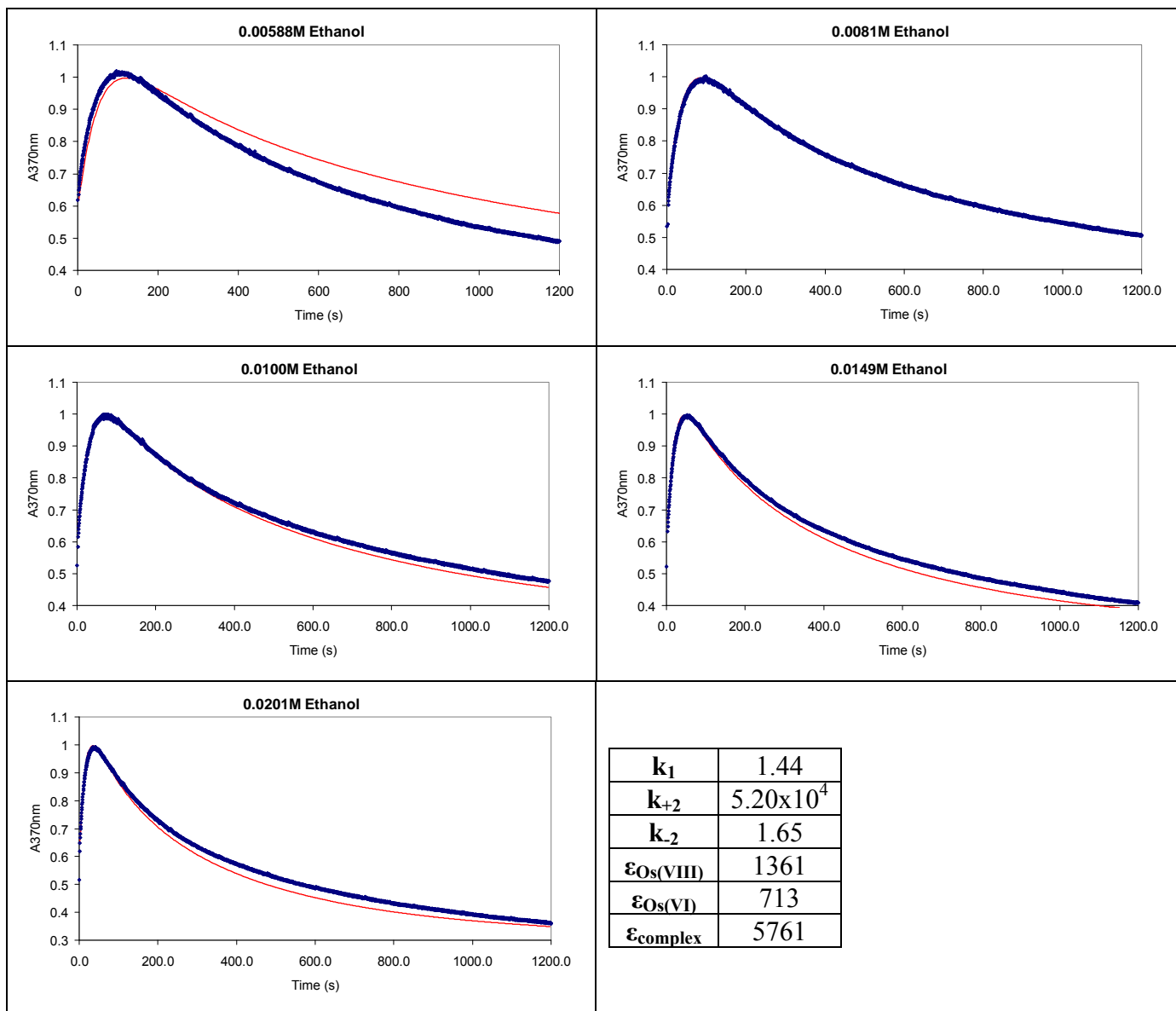
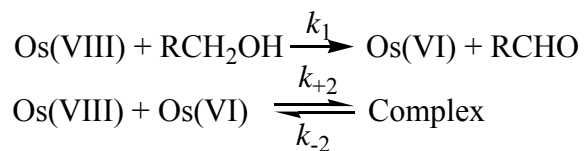
---

---

Models 1.1 to 1.10 below show the theoretical fit of the various models that were attempted. The best fit for each model at each concentration returned a set of molar extinction coefficients and rate constants. These parameters are, by definition, constant across the range of alcohol or ketone concentrations. However, because of experimental error or because the theoretical model was not appropriate to the experimental data, the parameters varied from one ethanol or MEK concentration to another. Therefore, in most cases, the best-fit parameters were averaged over the whole concentration range and the theoretical curve given by these average parameters was superimposed on the experimental data. All the ethanol data was treated in this way. However, in some cases using the MEK data, the fit of the model was so poor that it was not considered worth determining the average theoretical curve. Therefore, for Models 2.3, 2.4, 2.5 and 2.10, the parameters generated for each separate concentration are given. A short explanatory comment is attached to each model.

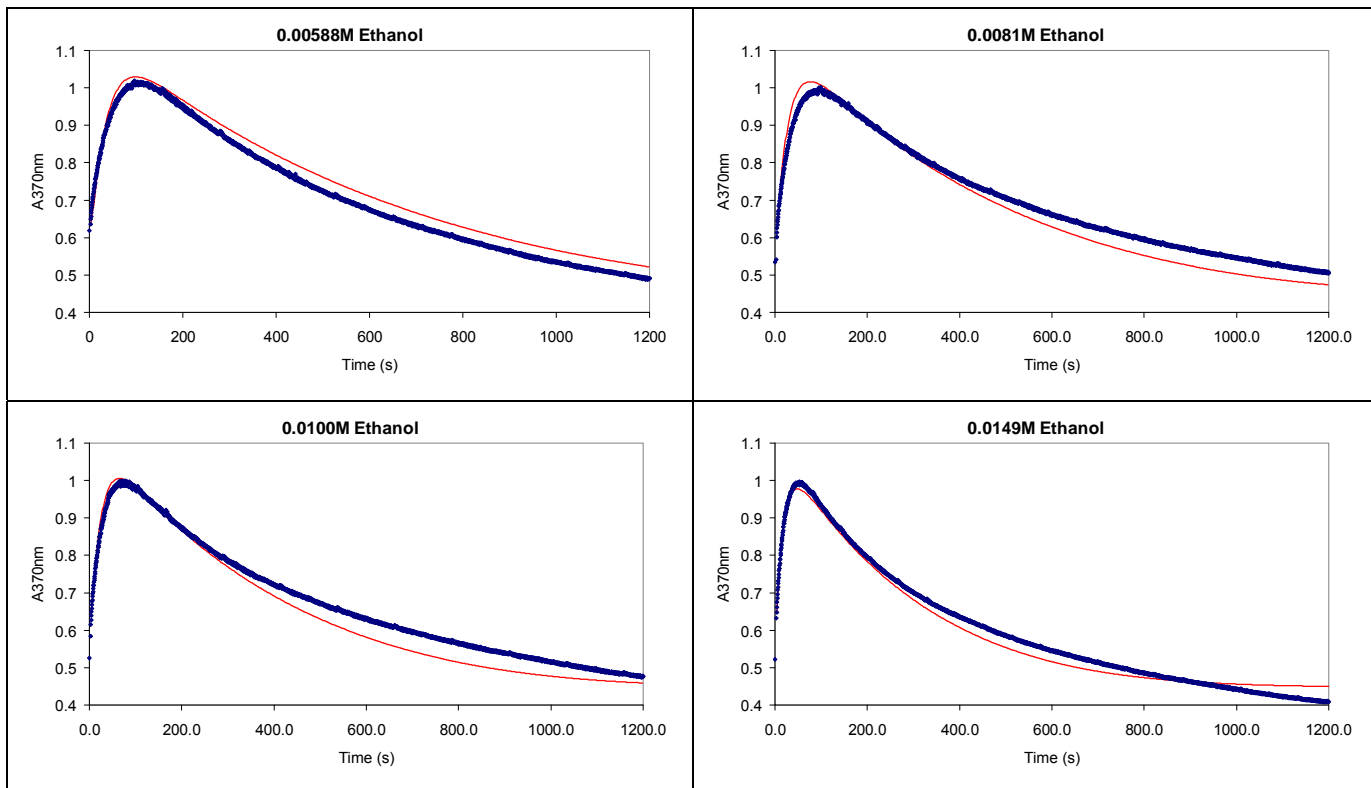
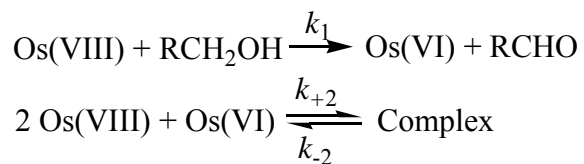
### 7.3.1 ALCOHOL MODELS

#### Model 1.1:



**Comments:** The fit is not bad and the constants are fairly good, but the complex formation is 1:1 instead of the experimentally determined ratio of 2:1.

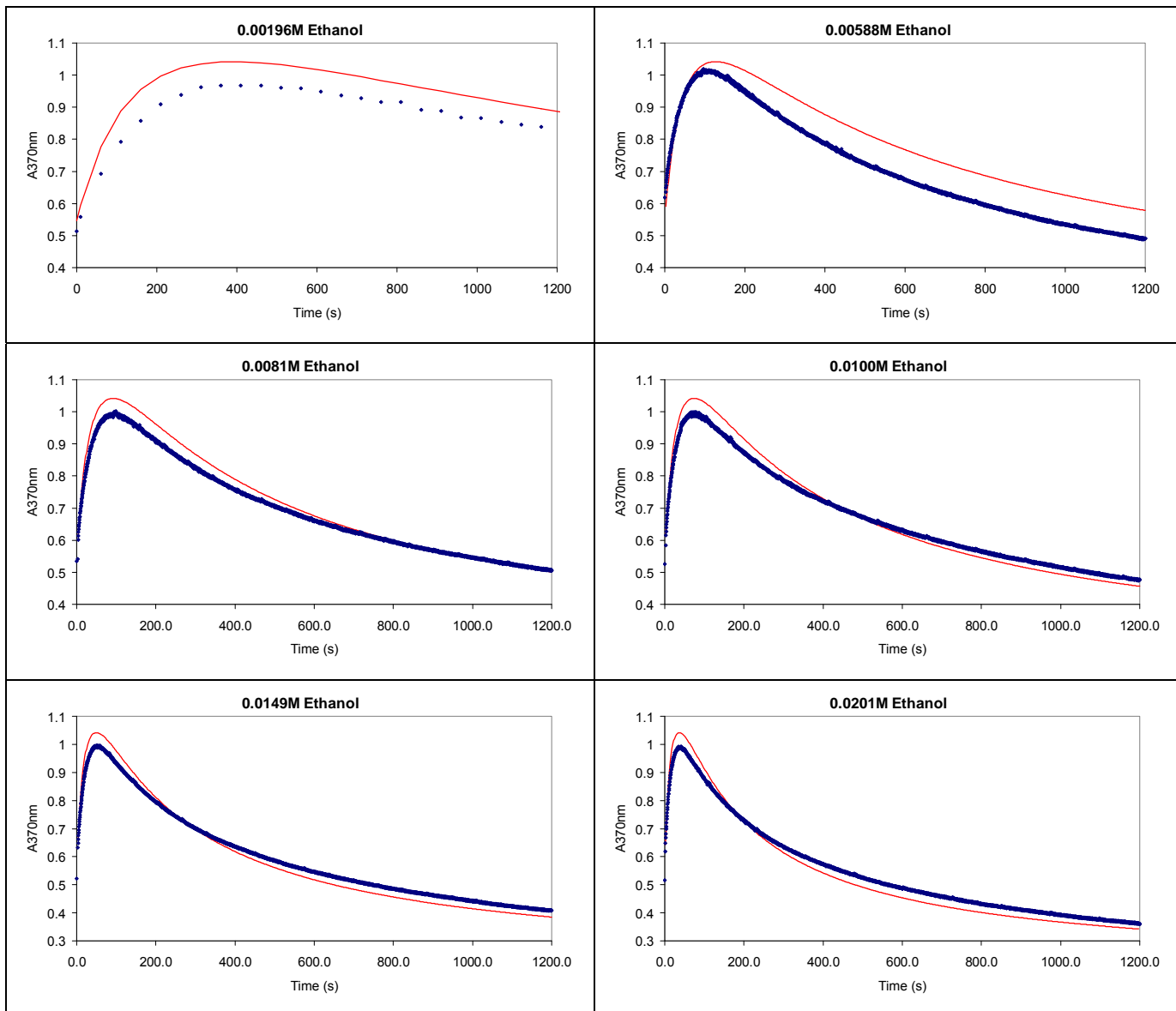
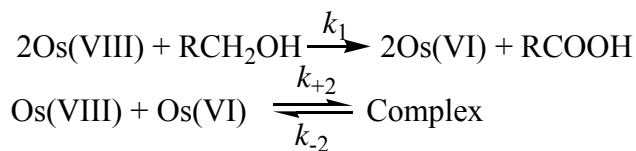
**Model 1.2:**



$k_1$	1.42
$k_{+2}$	$1.07 \times 10^6$
$k_{-2}$	0.00589
$\epsilon_{\text{Os(VIII)}}$	1444
$\epsilon_{\text{Os(VI)}}$	1034
$\epsilon_{\text{complex}}$	9122

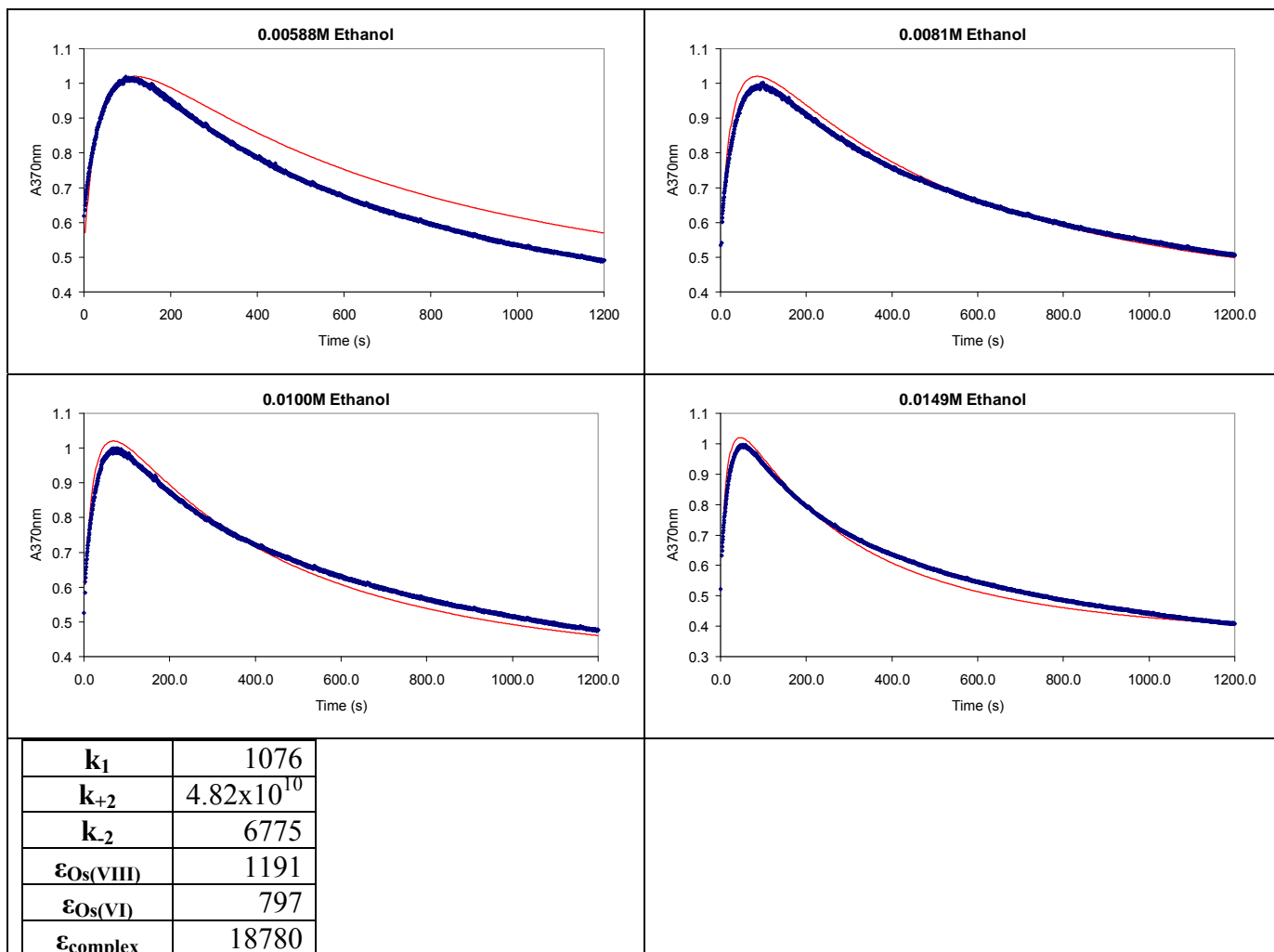
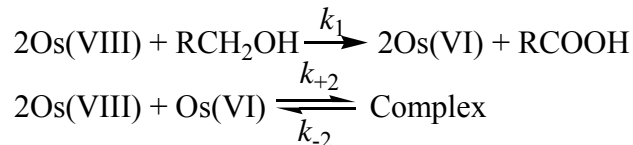
**Comments:** This is the model that was assigned in the previous chapter as the best fit to the equilibrium data. It is not a perfect fit, but is not too bad.

**Model 1.3:**



$k_1$	1369
$k_{+2}$	$1.99 \times 10^6$
$k_{-2}$	2829
$\epsilon_{\text{Os(VIII)}}$	1263
$\epsilon_{\text{Os(VI)}}$	451
$\epsilon_{\text{complex}}$	27583

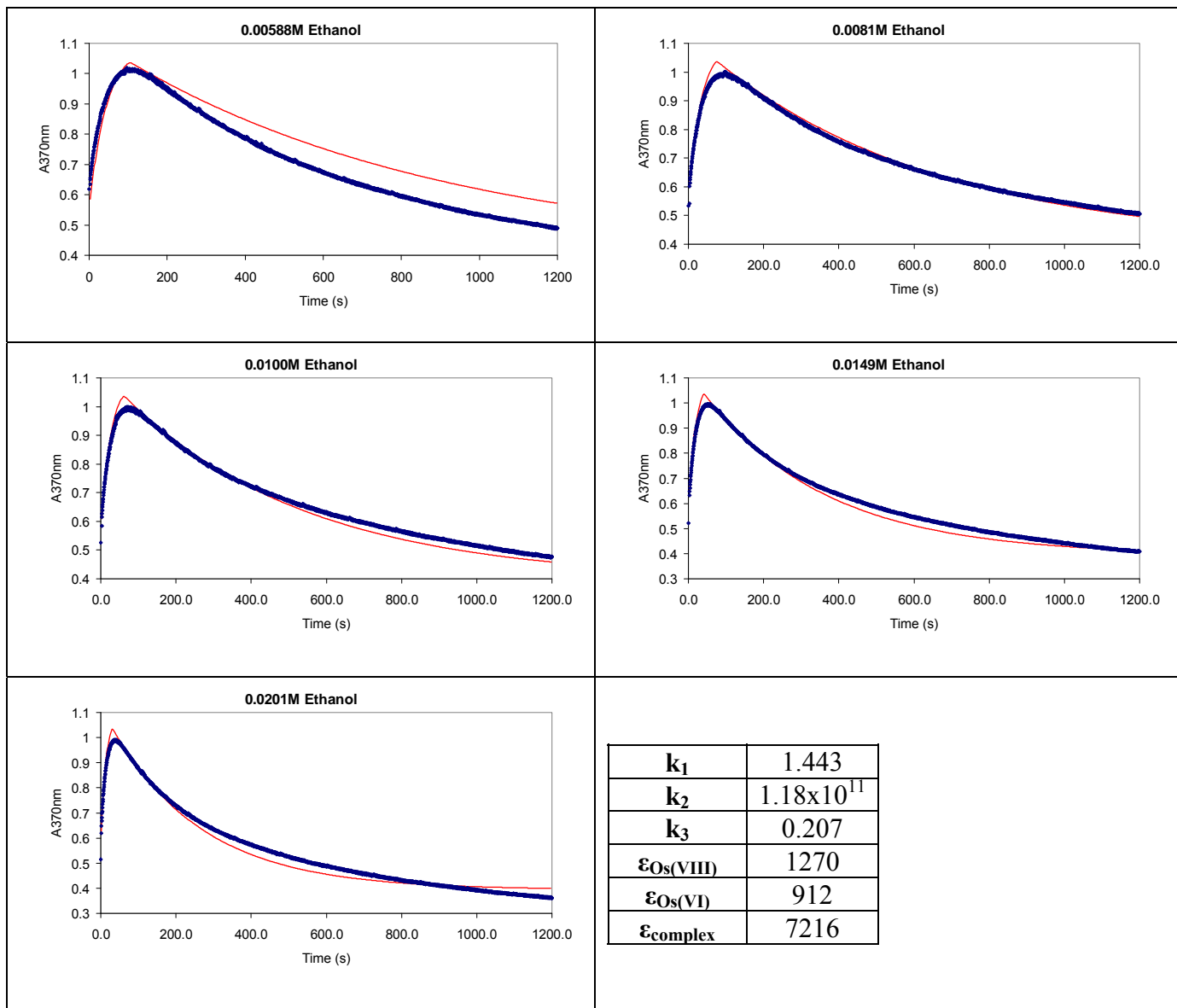
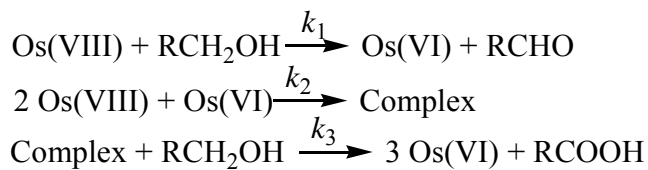
**Comments:** Once again attempting various combinations in the hope of a perfect fit. Not a very good fit in this case and mechanistically unlikely in that two molecules of osmium(VIII) come together with one molecule of ethanol.

**Model 1.4:**

**Comments:** Another combination permutation. Not a bad fit. Very similar to Model 1.1, although 1.1 gave a somewhat better fit. The rate model gives information up to and including the slowest step. Therefore, if the aldehyde  $\rightarrow$  carboxylic acid step is slowest, then this reaction is valid. However, this is not the empirical observation – the reaction of osmium(VIII) with aldehydes and ketones is much faster than the reaction with osmium(VIII) and alcohols. This argument holds true for any elementary step that sees alcohols being reduced to carboxylic acids, i.e. Model 1.3.

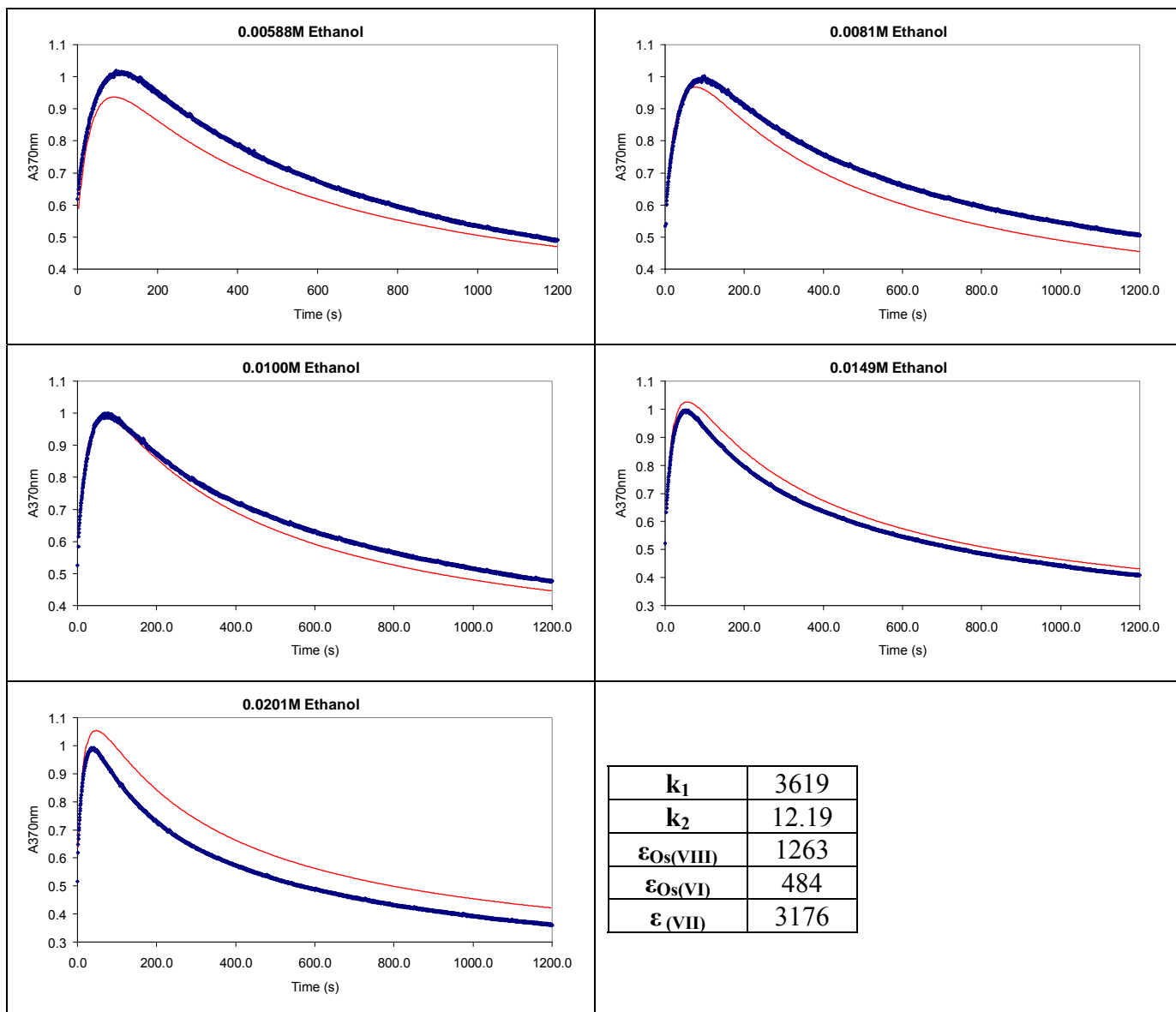
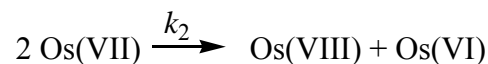
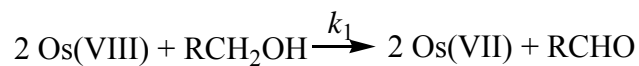


**Model 1.5:**



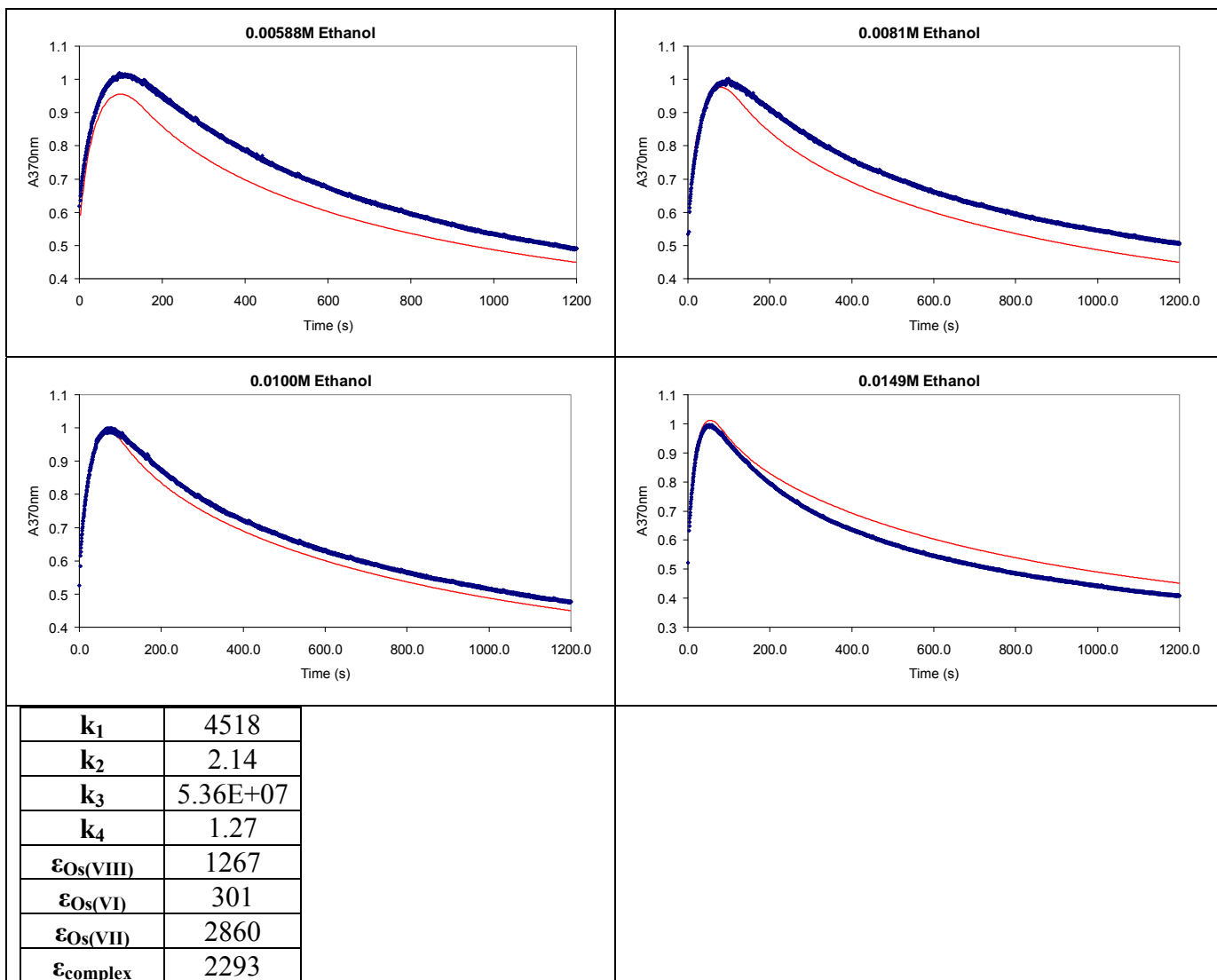
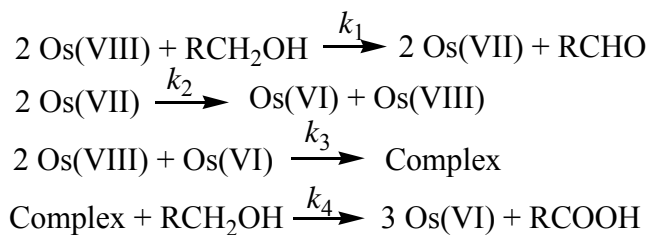
**Comments:** This is an extension of Model 1.2. After the complex is formed, it goes on to react with another mole of alcohol. The shape at the apex of the curve does not fit with the empirical data. The complex is being depleted too fast.

**Model 1.6:**



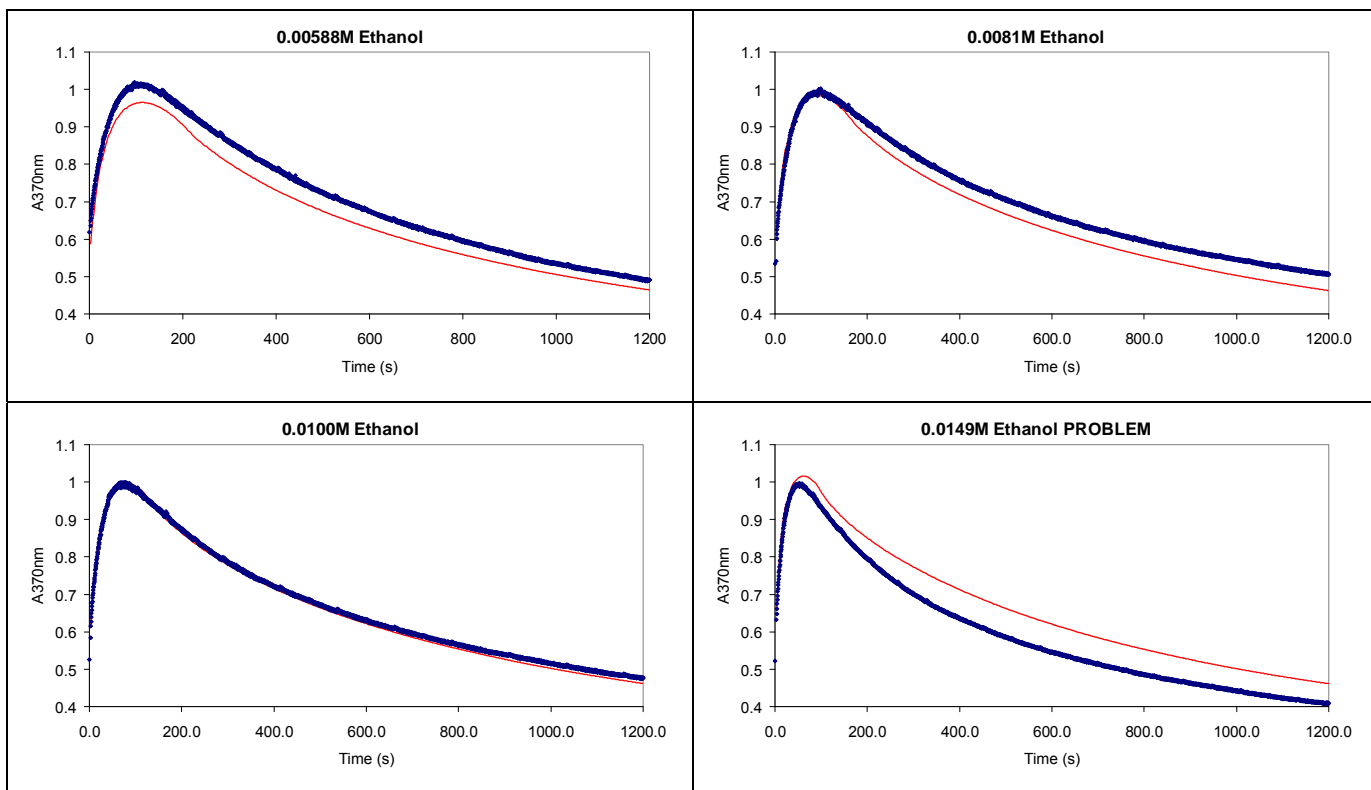
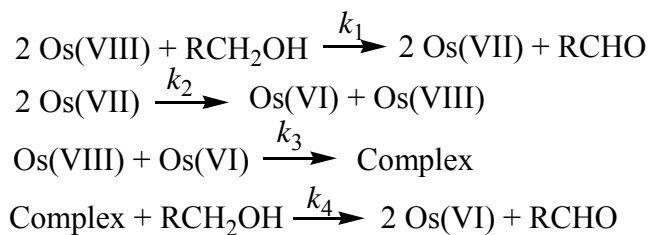
**Comments:** This model is very similar to Model 1.2 except that the osmium(VIII) is reduced to osmium(VII) in this case and not osmium(VI) as in Model 1.2. This results in an elementary step in which two mole of osmium(VIII) exchange one electron with one mole of alcohol – difficult to explain mechanistically. This argument will hold true for any model in which osmium(VIII) is reduced to osmium(VII) in an elementary step.

**Model 1.7:**



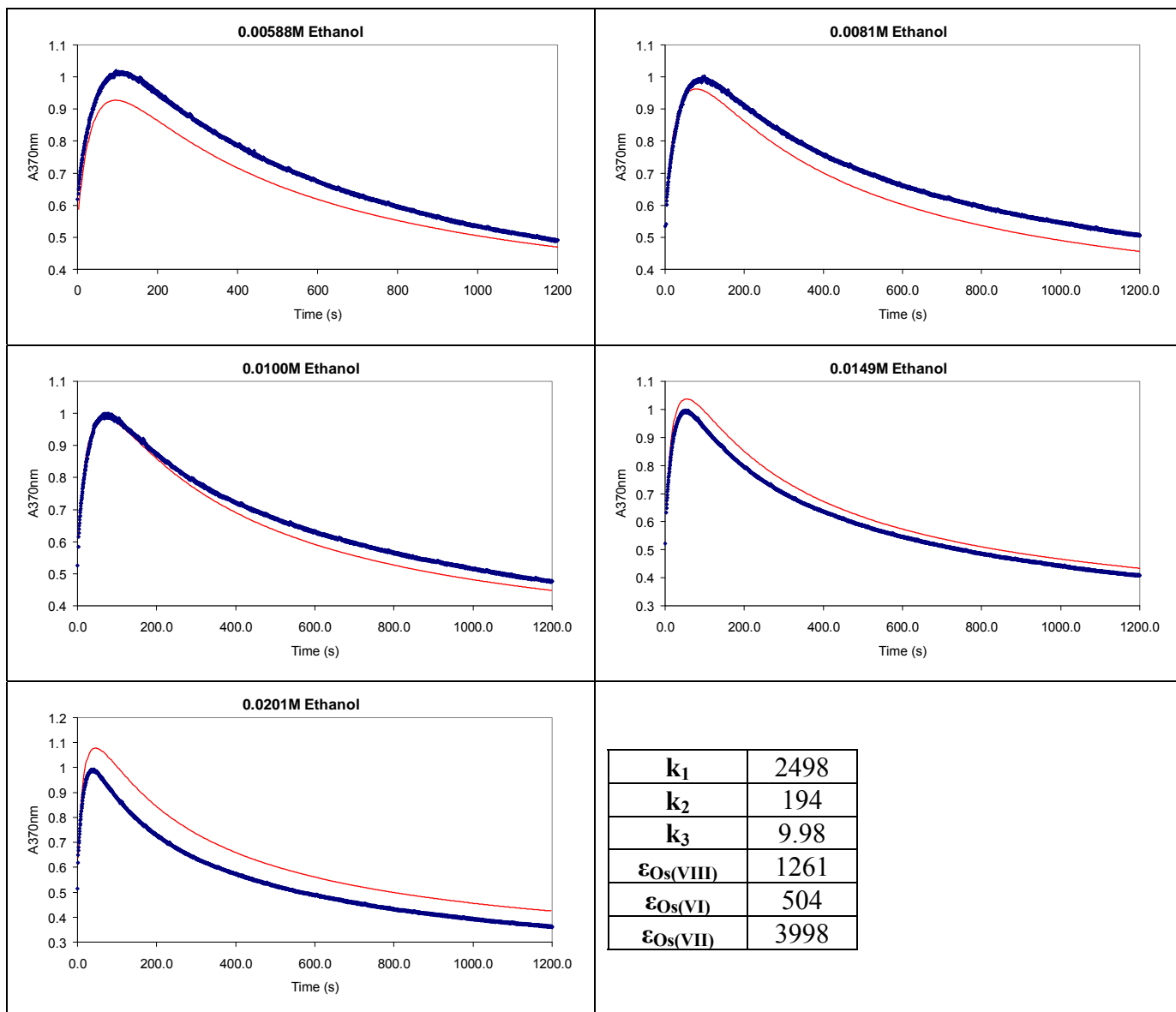
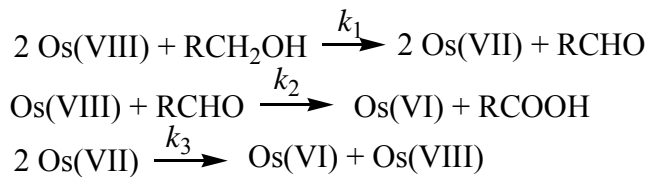
**Comments:** This is the same model that was assigned in the previous chapter as a fit to the equilibrium data. It was relegated to second place in that case due to reasons explained in Chapter 6. In this case, the fit is not particularly good.

**Model 1.8:**

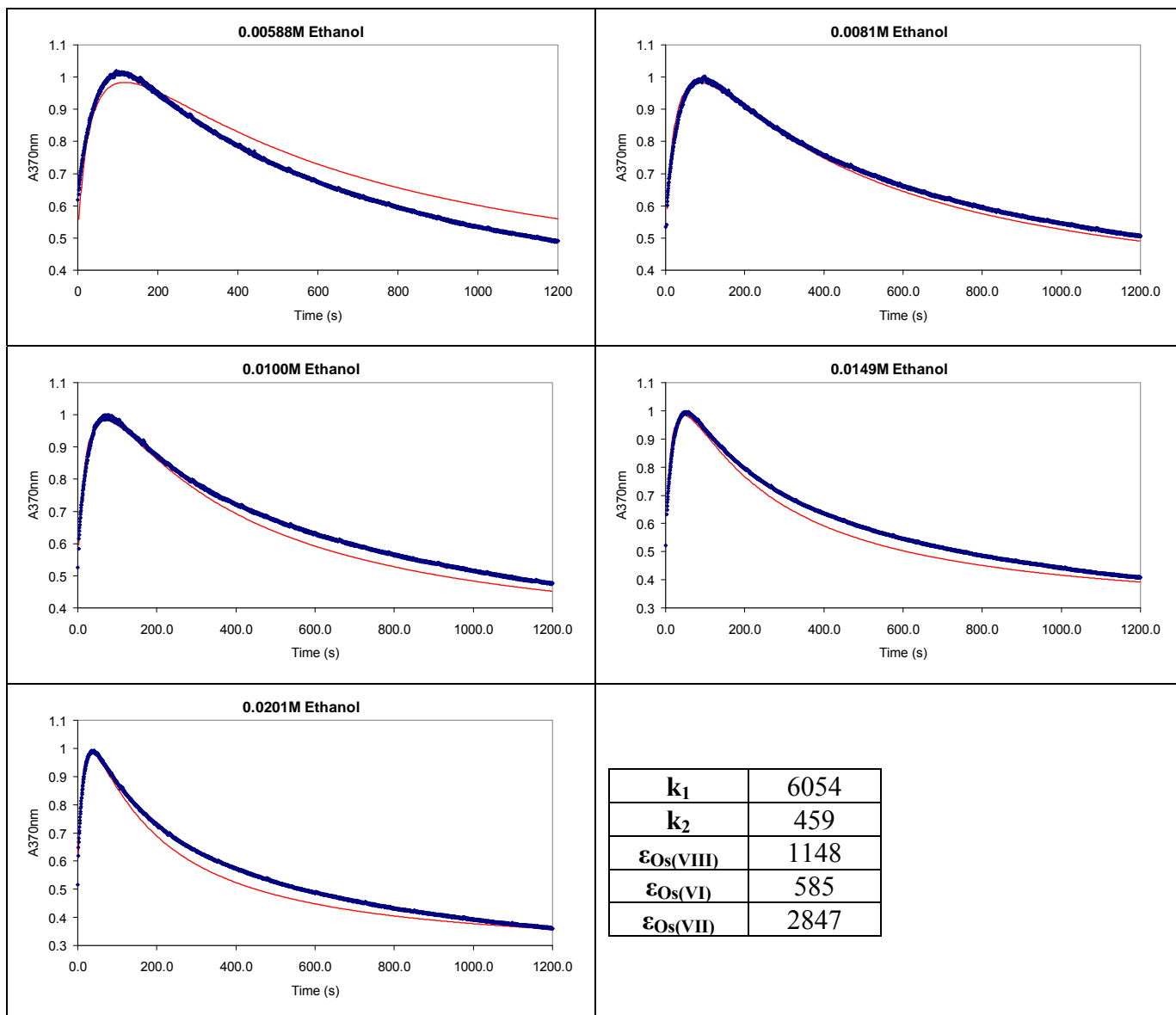
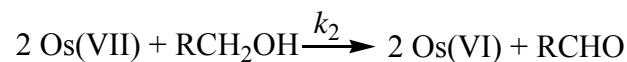
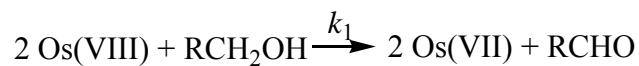


$k_1$	5518
$k_2$	1.92
$k_3$	$3.94 \times 10^7$
$k_4$	1.41
$\epsilon_{\text{Os(VIII)}}$	1241
$\epsilon_{\text{Os(VI)}}$	278
$\epsilon_{\text{Os(VII)}}$	2752
$\epsilon_{\text{complex}}$	1224

**Comments:** This model is the same as Model 1.7, except that the osmium(VIII)-(VI) complex is 1:1, which is not empirically valid. The fit is not particularly good.

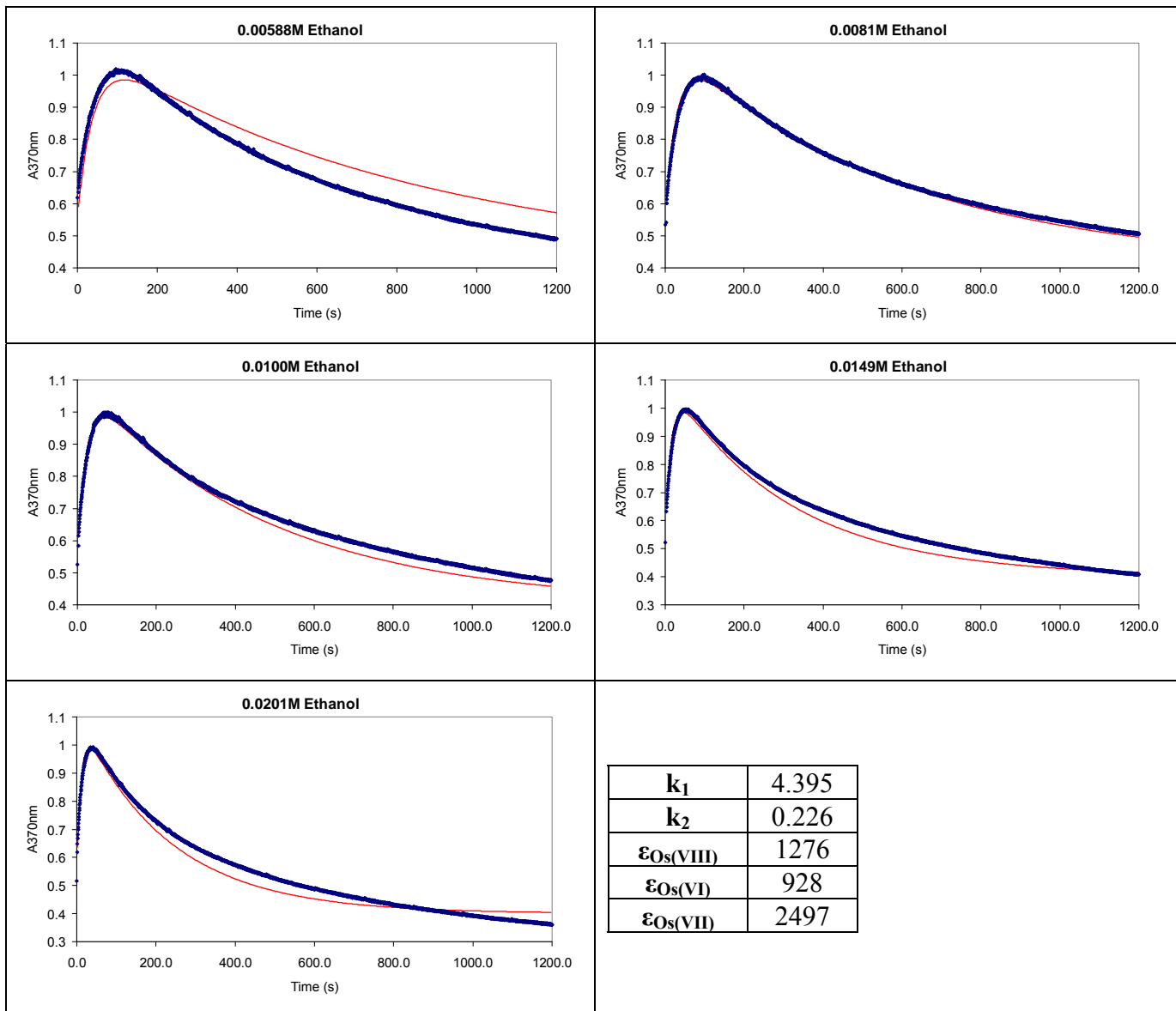
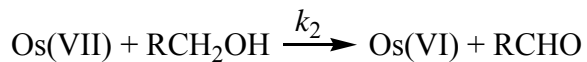
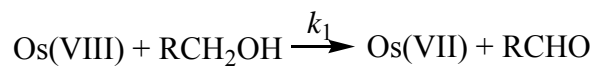
**Model 1.9:**

**Comments:** Since none of the models attempted so far had produced a perfect fit, this one gets a little imaginative. Initially, the osmium(VIII) is reduced to osmium(VII). In the second step, the aldehyde produced in the first step reacts preferentially with the osmium(VIII) to produce osmium(VI). The osmium(VII) produced in the first step disproportionates to osmium(VIII) and osmium(VI). It explains the stoichiometry of the reactions but is highly imaginative, and not a very good fit.

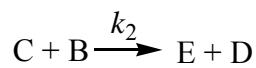
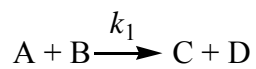
**Model 1.10:**

**Comments:** Since none of the models was a perfect fit, this model and the following Model 1.11 were attempted as a “generic” fit. They do not explain the stoichiometry of the reactions satisfactorily, but it was thought that the rate constants could be used as an empirical comparative tool in Chapter 8, where consistency is vital to the comparative studies. The fit and the molar extinction coefficients are good.

**Model 1.11:**



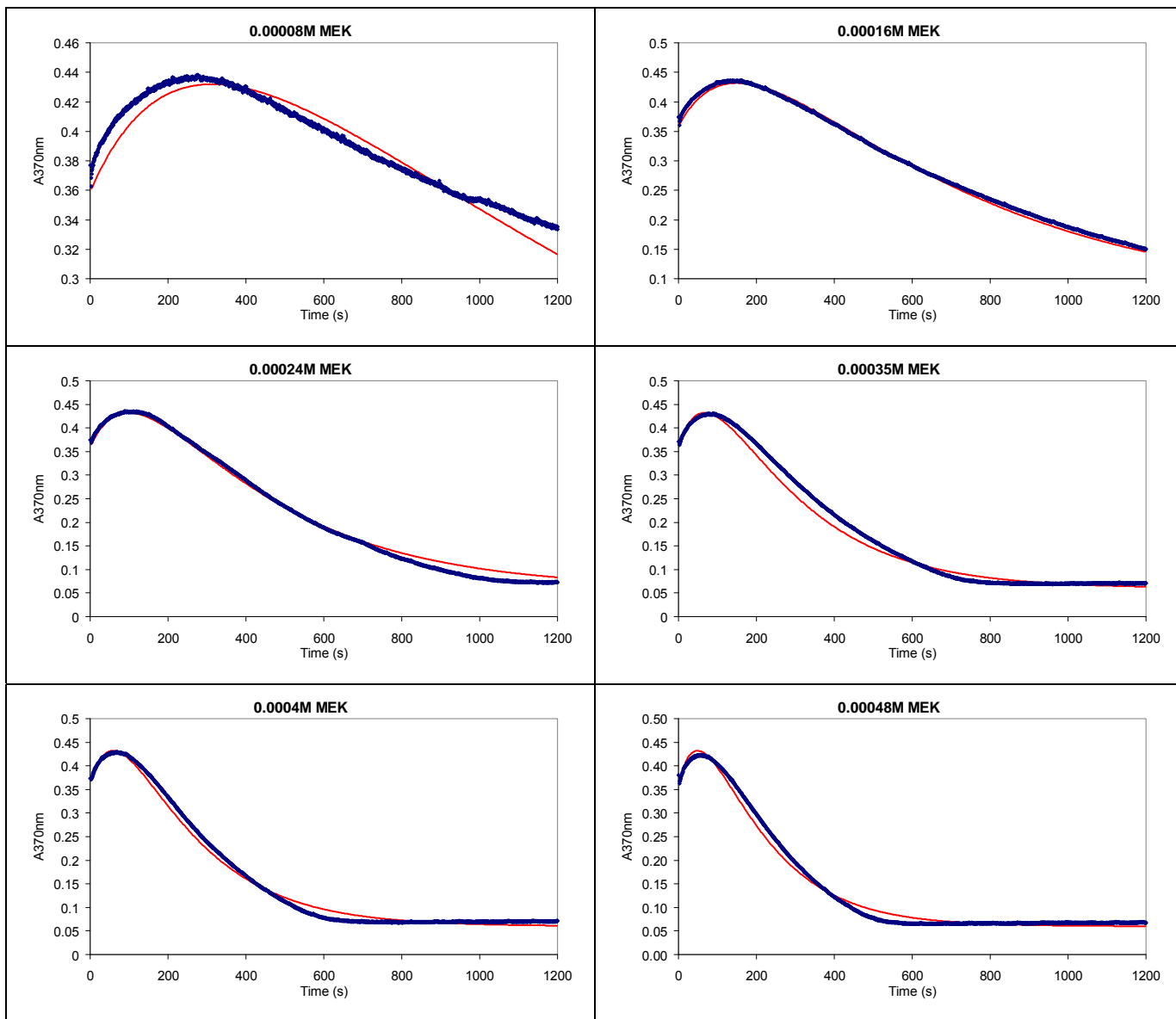
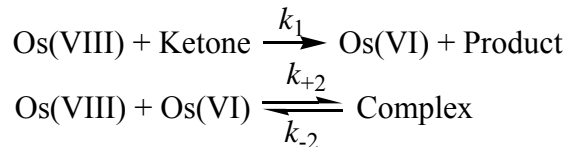
**Comments:** The stoichiometry of this model is unbalanced and a more correct manner of putting forward the model would be as:



The fit and the molar extinction coefficients are fairly good.

### 7.3.2 KETONE MODELS

#### Model 2.1:

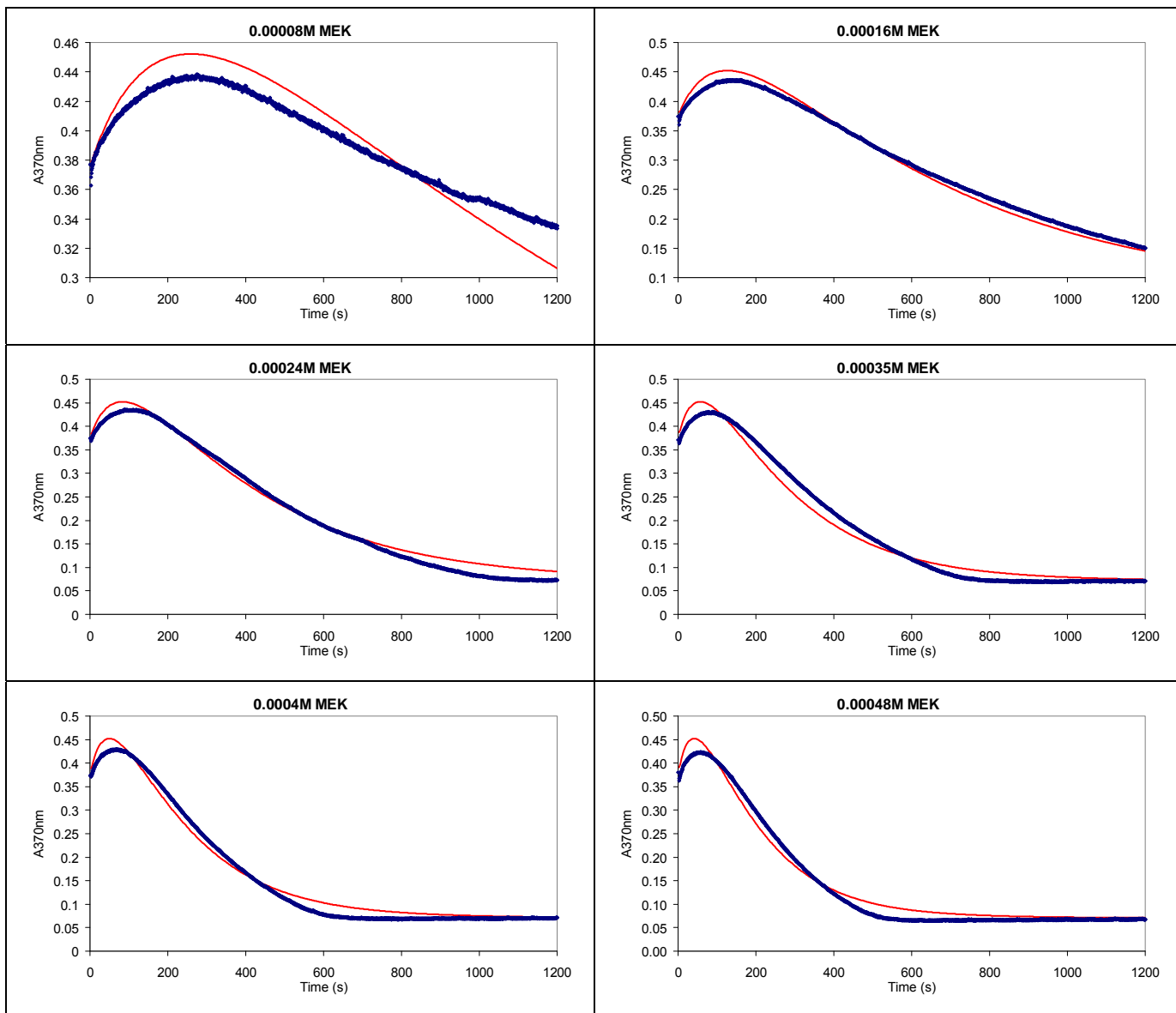
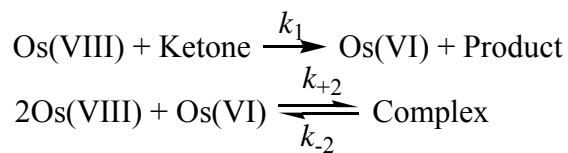


$k_1$	16.15
$k_{+2}$	$2.75 \times 10^5$
$k_{-2}$	965
$\epsilon_{\text{Os(VIII)}}$	955
$\epsilon_{\text{Os(VI)}}$	159
$\epsilon_{\text{complex}}$	$2.24 \times 10^4$

**Comments:** This is the equivalent of Model 1.1. The fit is good but the 1:1 complex is not empirically correct.



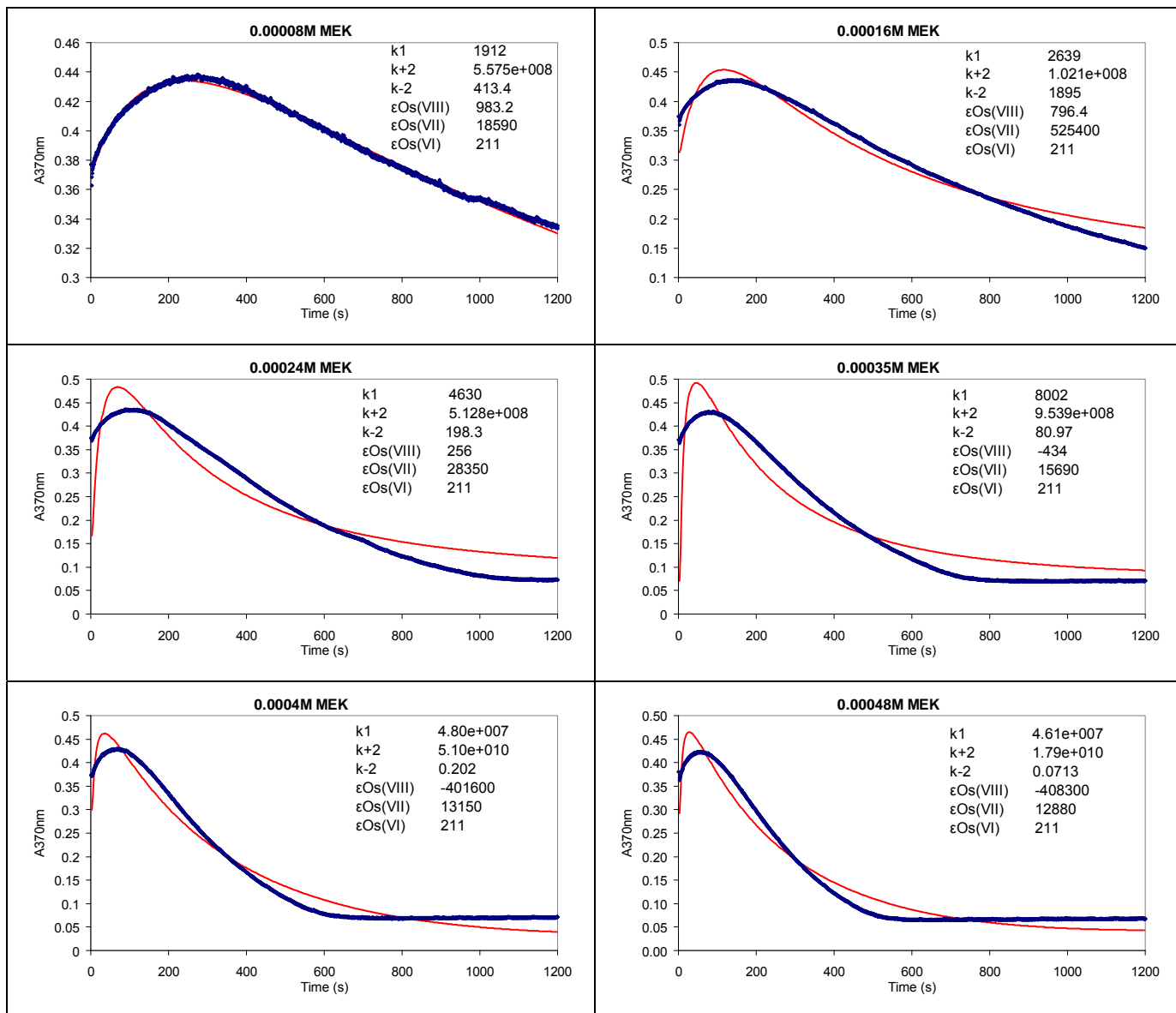
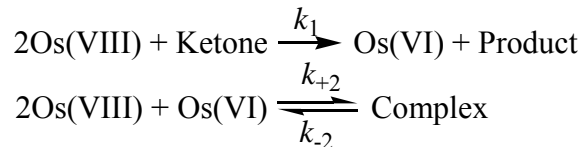
**Model 2.2:**



$k_1$	12.35
$k_{+2}$	$1.20 \times 10^8$
$k_{-2}$	47.9
$\epsilon_{\text{Os(VIII)}}$	1000
$\epsilon_{\text{Os(VI)}}$	188
$\epsilon_{\text{complex}}$	$1.36 \times 10^4$

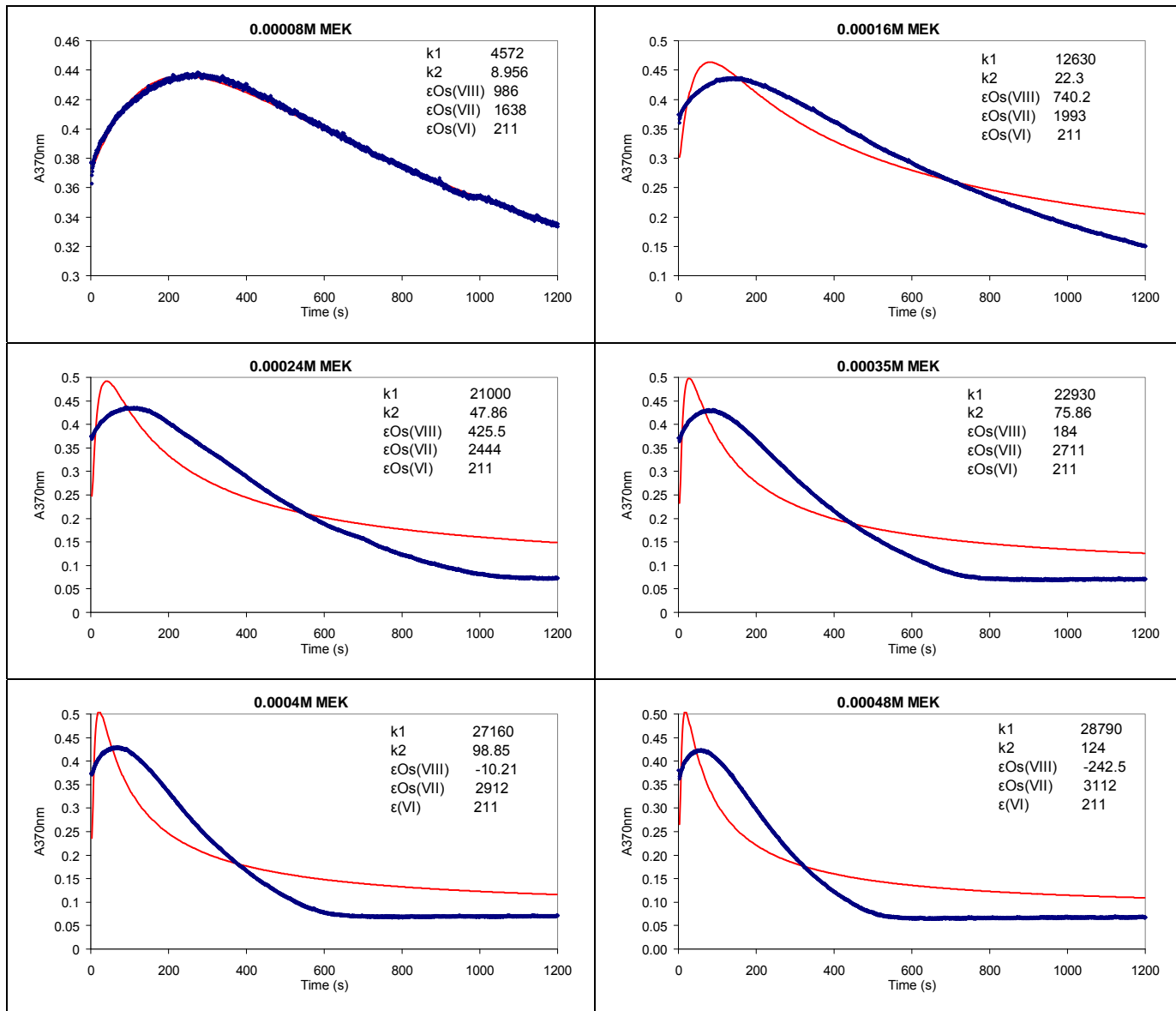
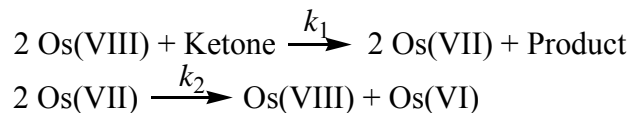
**Comments:** This model is equivalent to Model 1.2 and to the Equilibrium Reaction Model 2. The fit is quite good, except at lower MEK concentration.

**Model 2.3:**



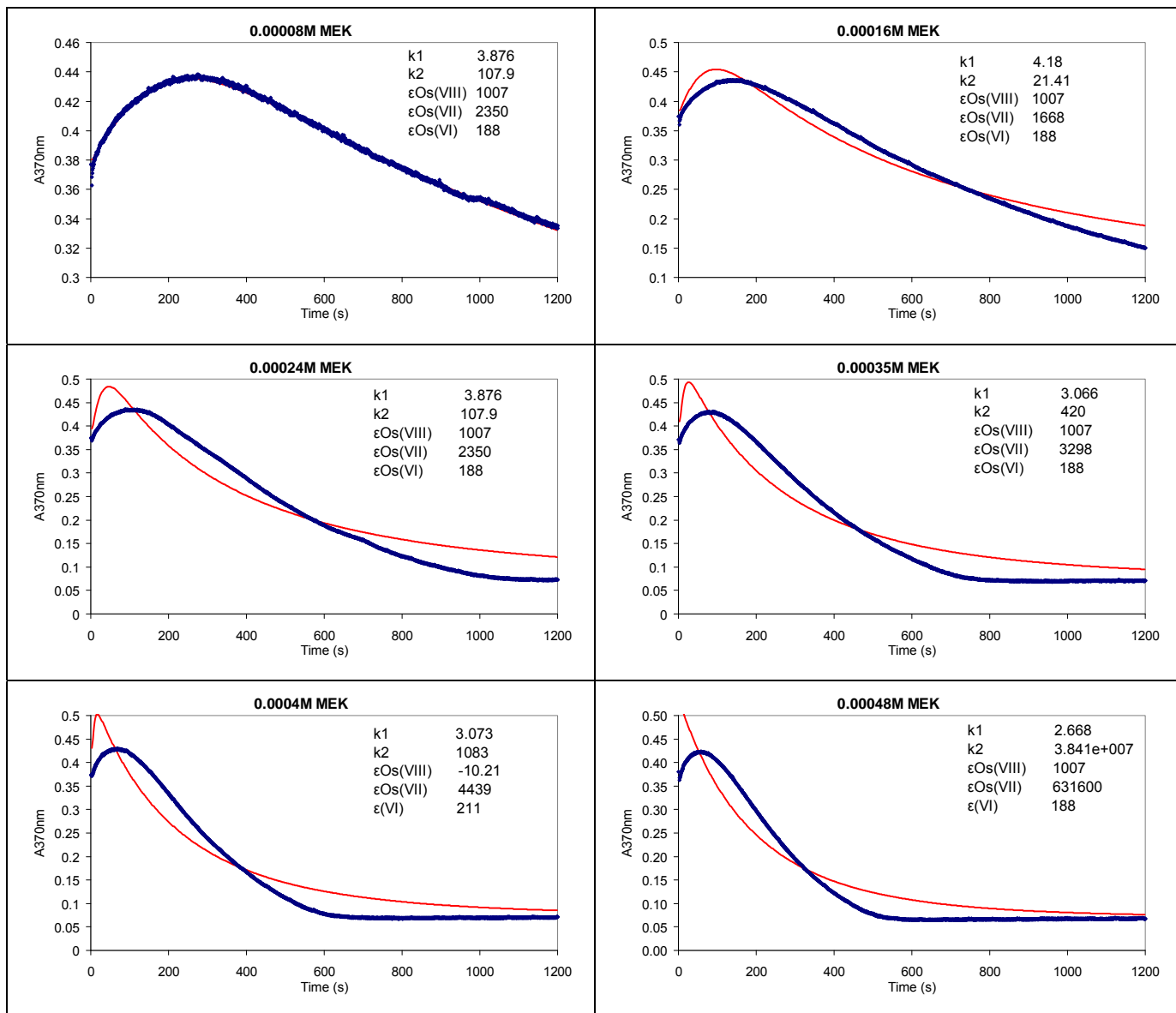
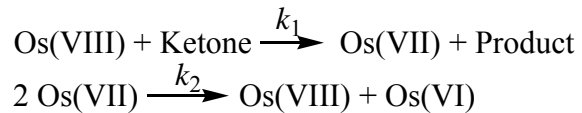
**Comments:** The two mole osmium(VIII) to one mole ketone model does not fit the experimental data very well at all. This is a trend that will be repeated in all osmium-ketone rate models.

**Model 2.4:**



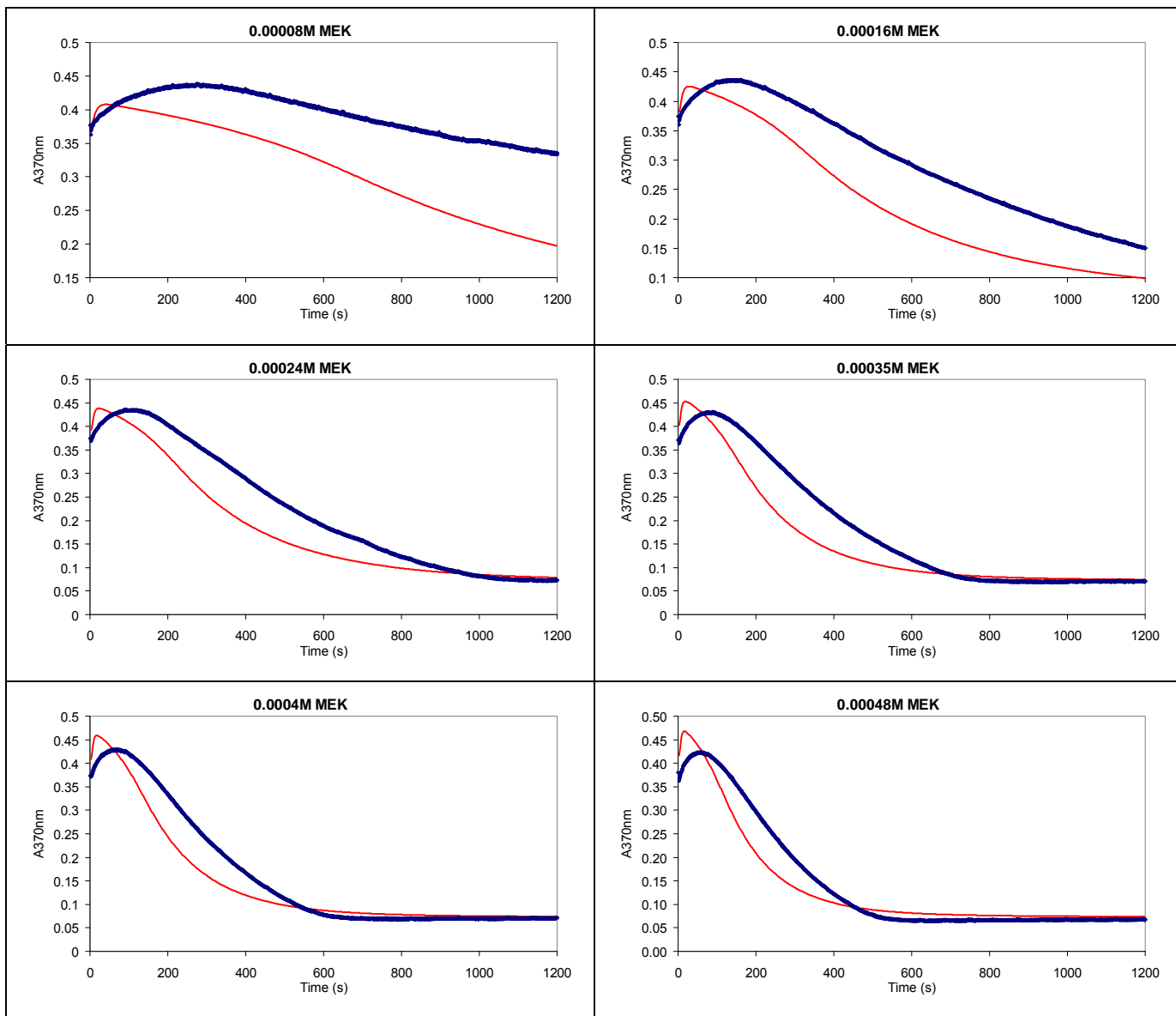
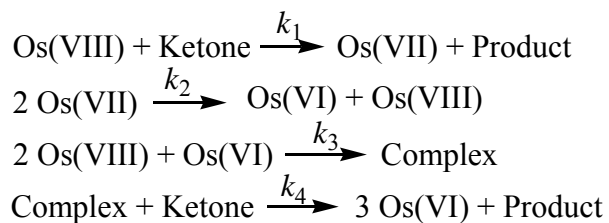
**Comments:** A very poor fit for the osmium(VIII):ketone, 2:1 ratio once again.

**Model 2.5:**



**Comments:** This model is the equivalent of Model 1.6 and is a very poor fit.

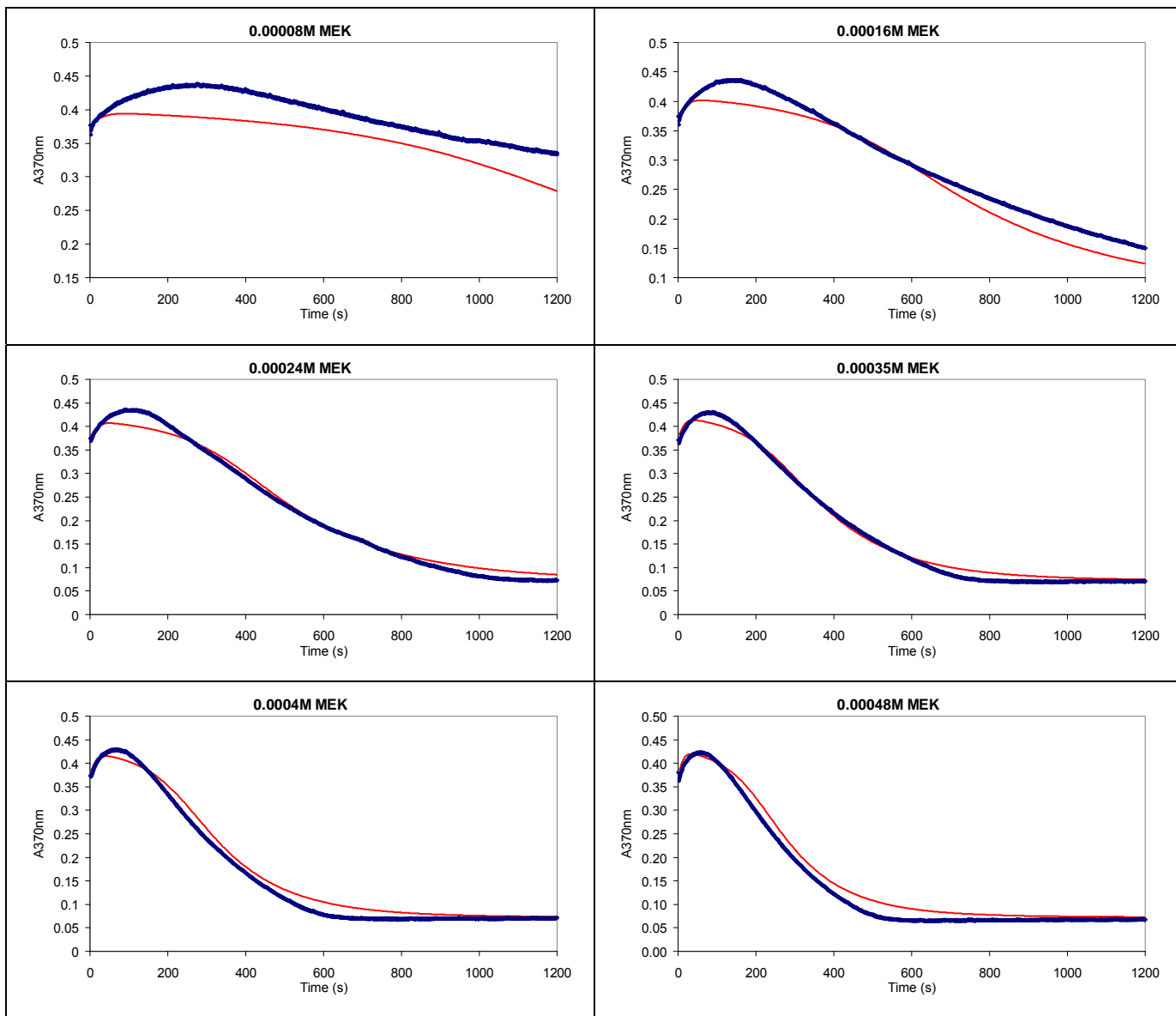
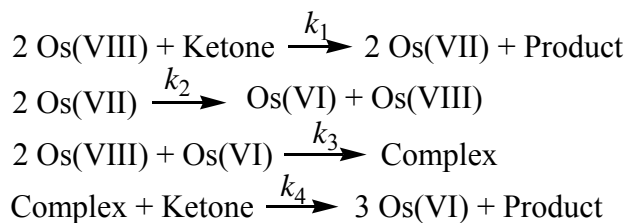
**Model 2.6:**



$k_1$	8.58
$k_2$	6475
$k_3$	$3.67 \times 10^6$
$k_4$	18.6
$\epsilon_{\text{Os(VIII)}}$	970
$\epsilon_{\text{Os(VII)}}$	11318
$\epsilon_{\text{Os(VI)}}$	188
$\epsilon_{\text{complex}}$	2438

**Comments:** This model is the equivalent of Model 1.7 and of the Equilibrium Reaction Model 1, which was not the favoured equilibrium model. The poorness of this fit shows that it would be wise to discard this model altogether.

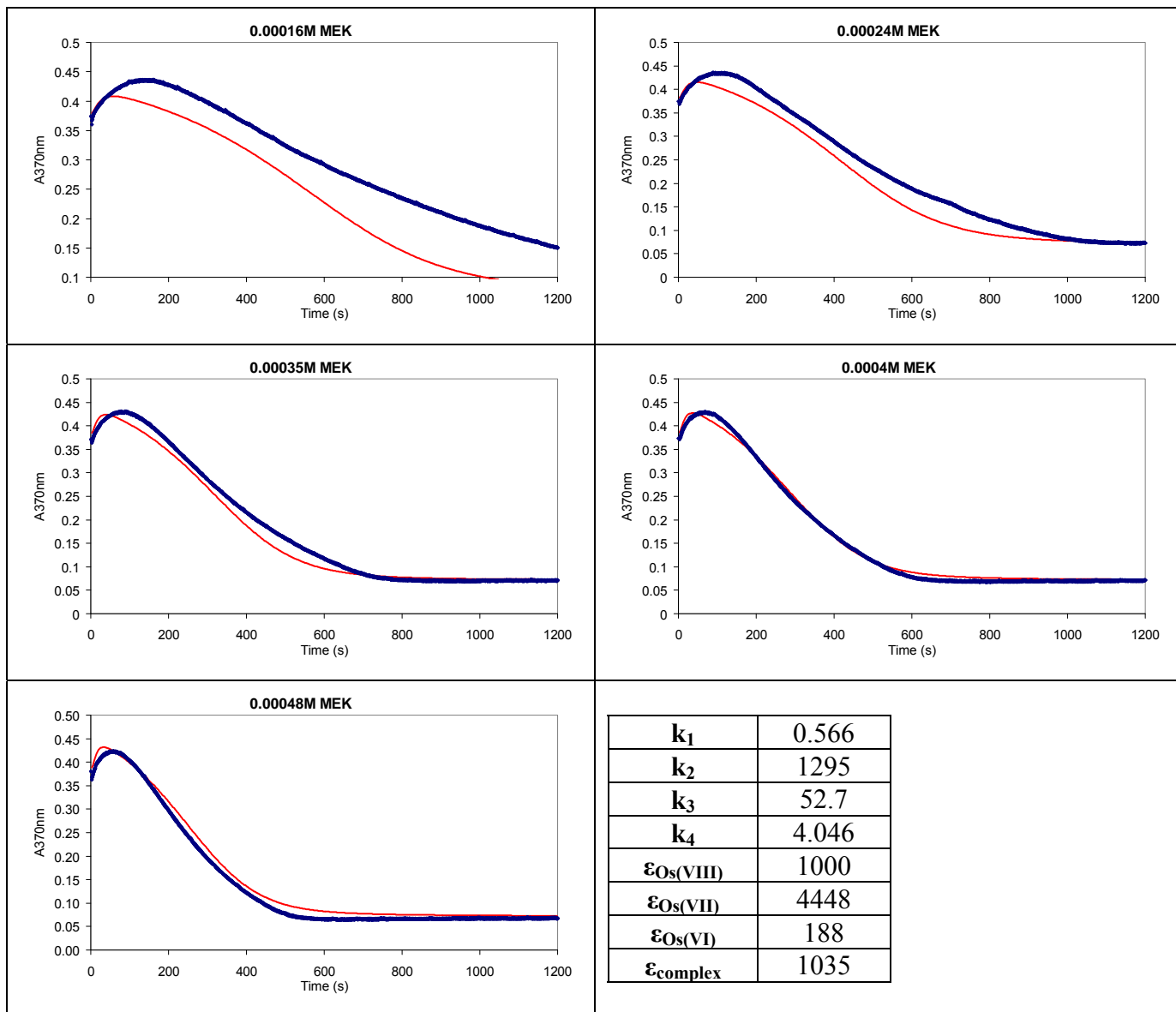
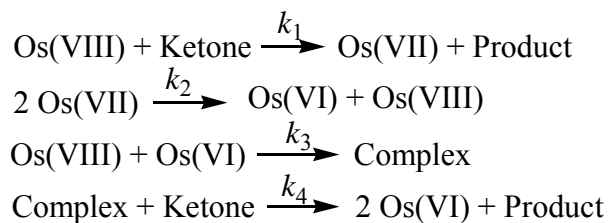
**Model 2.7:**



$k_1$	2561
$k_2$	5299
$k_3$	$1.14 \times 10^6$
$k_4$	1822
$\epsilon_{\text{Os(VIII)}}$	1000
$\epsilon_{\text{Os(VII)}}$	9482
$\epsilon_{\text{Os(VI)}}$	188
$\epsilon_{\text{complex}}$	2384

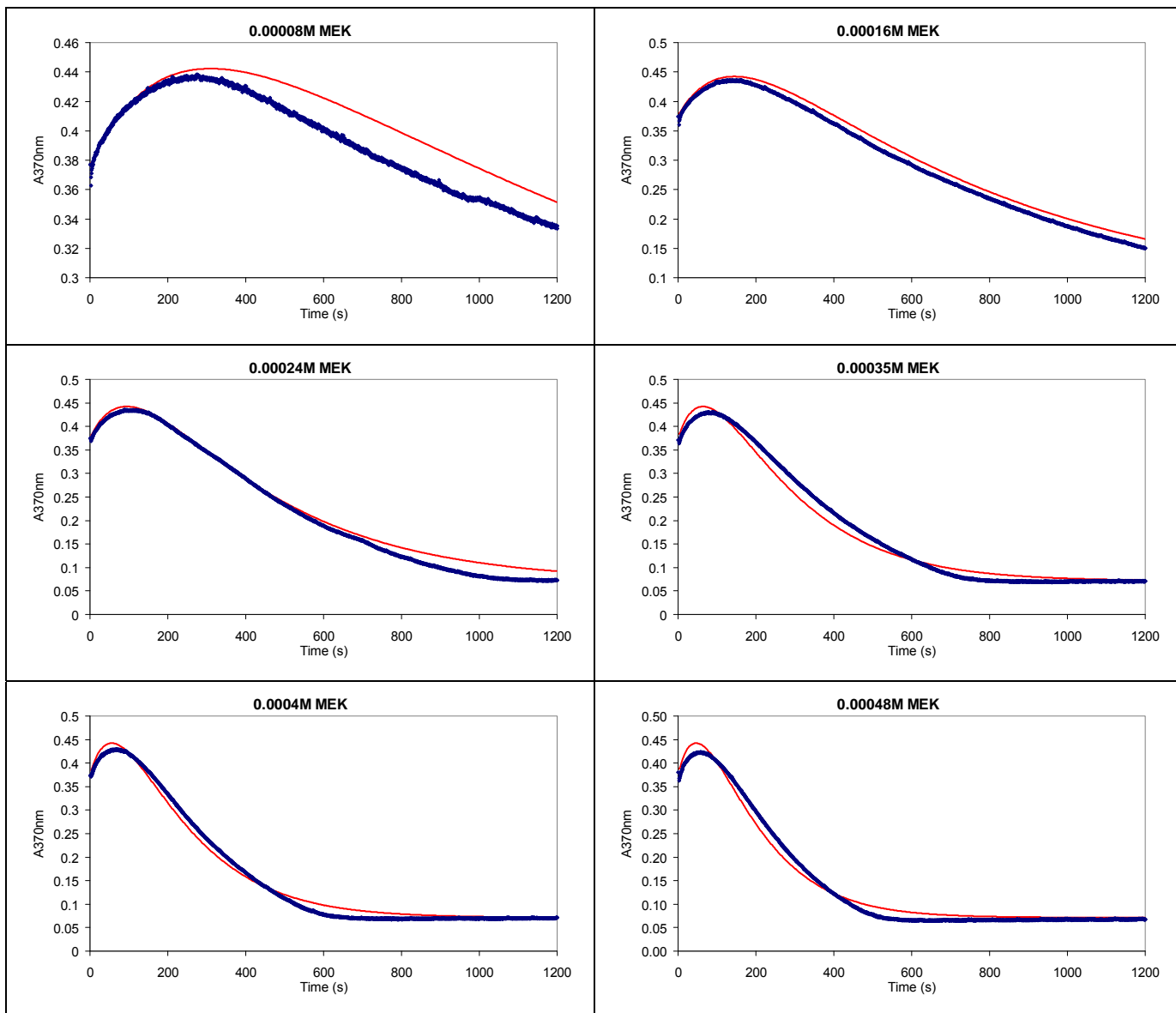
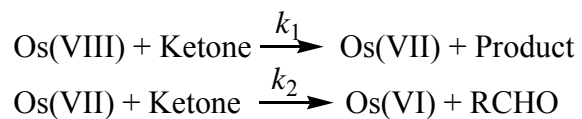
**Comments:** This is the same model as the previous one, just with a different osmium(VIII)-to-ketone ratio. The fit is slightly better than the previous model, but the complex shape of the theoretical curve shows that this model is not the best fit to the experimental data.

**Model 2.8:**



**Comments:** Once again, a fairly good fit at high MEK concentrations, but the complex shape of the theoretical curve denotes a poor depiction of the real reaction.

**Model 2.9:**

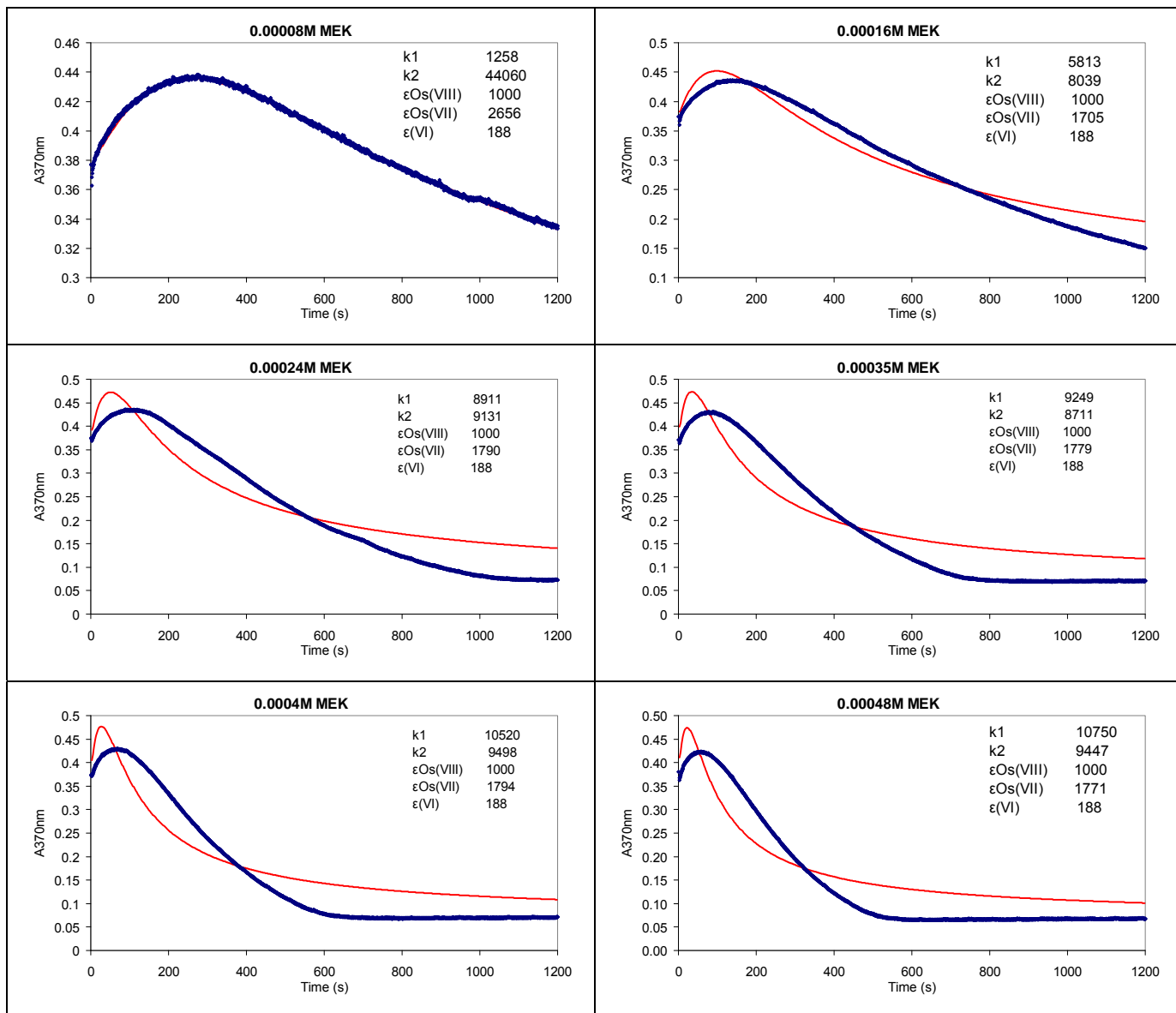
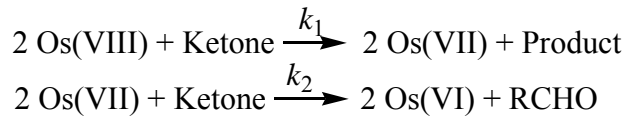


$k_1$	2.32
$k_2$	2.30
$\epsilon_{\text{Os(VIII)}}$	1000
$\epsilon_{\text{Os(VII)}}$	1819
$\epsilon_{\text{Os(VI)}}$	190

**Comments:** This model is the equivalent of Model 1.10 and is not intended to explain the stoichiometry of the reaction but is intended as an empirical model to establish rate constants for comparative studies. The fit and molar extinction coefficients are good.



**Model 2.10:**



**Comments:** The second “generic” model does not fit the experimental data well at all.

### 7.3.3 DISCUSSION

The above models represent the sum of the models fitted using the kinetic modelling software. Some give noticeably poor fits and may be discarded at once. However, it is apparent that none give a perfect fit. It is important to stress that there are two components to the uncertainty inherent in these reactions. The first is the experimental uncertainty inherent in the measuring and mixing of each reaction, itself. The second is the uncertainty inherent in the determination of osmium concentration. This has a twofold component, in itself – the percentage error in the concentration determination method and the error in the percentage of osmium(VIII) to other oxidations states present in the starting solutions. Although these errors should be small, their additive qualities may account for the fact that, once rate constants and molar extinction coefficients have been averaged, the fit of even the best models is not perfect. It may be instructive to show the fit of one of the models before the parameters are averaged to show that, for each reaction, a good fit to the experimental data is possible. Figure 7.1 below, shows the best fit at each ethanol concentration for Model 1.2.

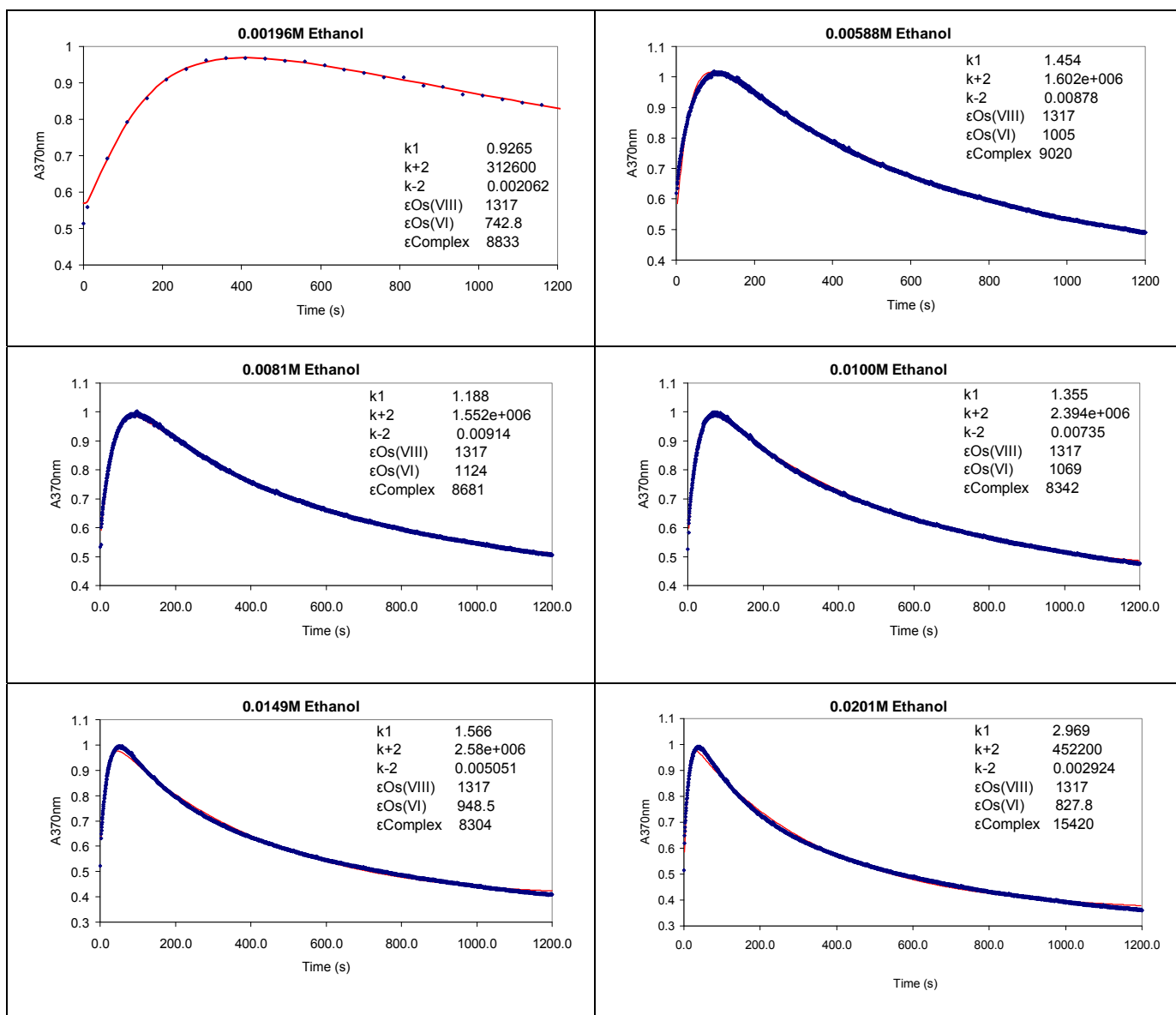
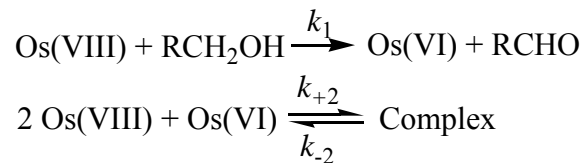


Figure 7.1: The best theoretical fit to the experimental data for the model:



The theoretical curve is given in red and the experimental data points, in blue. Parameters for each reaction are given on the graph.

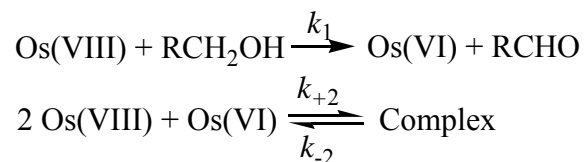
It, therefore, now falls due to make a choice as to the reaction model that will be adopted to complete the comparative study in the following chapter. The comments associated with each reaction model give insight into the selection process and those which gave a poor fit to the experimental data may now be discarded. This means that Models 2.3, 2.4, 2.5, 2.6, 2.7, 2.8 and 2.10 may be discarded.

Also discarded are models in which the stoichiometry does not conform to experimentally determined stoichiometry as in the cases of Models 1.1, 1.3, 1.8 and 2.1. In these cases the stoichiometry of the Os(VIII)-Os(VI) complex was modelled as 1:1 instead of the experimentally determined 2:1. Also discarded are those alcohol models in which the stoichiometry does not reflect an elementary step. That is, those models in which the alcohol is depicted as being reduced to the carboxylic acid. It was an empirical observation, which will be borne out by the rate constants in the following chapter, that the aldehyde/ketone reaction is far faster than the alcohol reaction. This means that the elementary step of the oxidation of the alcohol to the aldehyde or ketone is the rate limiting step. It should, therefore, be assumed to be the elementary step in the reaction up to which point information concerning the rate law can be gathered. This effectively discards Model 1.4, of those not already discarded for other reasons.

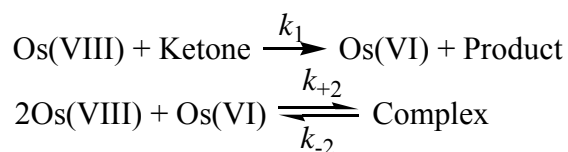
The next decision related to models depicting the reduction of osmium(VIII) to osmium(VII). For the alcohol models, this requires the coming together of two osmium(VIII) molecules with one molecule of alcohol in the elementary step, during which two electrons are exchanged. Mechanistically, this is not favourable and for this reason alcohol models depicting osmium(VII) as an intermediary product were discarded. Stoichiometry is not as clear-cut for the ketone models since the intermediary products are not yet defined. However, it has been shown in Chapter 5 that the osmium products are the same for both alcohol and ketone reactions. Therefore, if osmium(VII) cannot be a product for the alcohol reactions, neither can it be a product for the ketone reactions. For this reason all of the following Models were discarded: 1.6, 1.7, 1.9, 2.4, 2.5, 2.6, 2.7 and 2.8. These include some already covered above, but this justifies their exclusion still further.

Of the models that are left, each will now be treated separately. Model 1.5 is an extension of Model 1.2. The shape at the apex of the curve is a poor fit and shows that the complex is being depleted too fast when an extra step is introduced into the model. Model 1.2, left as it was, is a better fit to the data.

Models 1.10, 1.11 and 2.9 were not excluded when all other models with an osmium(VII) product were discarded above. This is because these models were meant as empirical models for use in comparative studies if no better fit could be found. The stoichiometry generated cannot be explained empirically but the models gave rate constants that could be used comparatively. However, another model gave fits that were as good as those for Models 1.10, 1.11 and 2.9 and had the added benefit of fitting the equilibrium data as well. It was also a model that could be equally applied to the alcohol and ketone reactions. That is, Models 1.2 and 2.2, which are reproduced below.



**Model 1.2**



**Model 2.2**

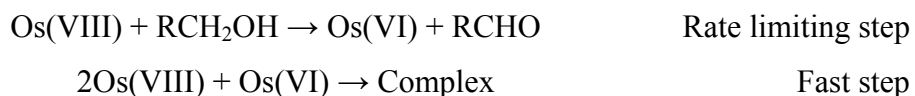
These models, which will be known as the Complexation Reaction Model, are mechanistically reasonable in that one molecule of osmium(VIII) comes together with one molecule of alcohol or ketone to exchange two electrons. The complexation reaction is a side-reaction that is in dynamic equilibrium, whose conditional equilibrium constant,  $K_{\text{eq}}$ , can be calculated from the rate constants,  $k_{+2}$ , and  $k_{-2}$ .<sup>†</sup> The equilibrium constant will be quoted in the following chapters since it is a more easily comparable parameter than forward and reverse rate constants that may vary within a constant set of experimental parameters. The equilibrium reaction will

---

<sup>†</sup>  $K_{\text{eq}} = k_{+2} / k_{-2}$

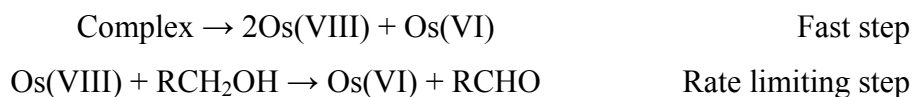
favour the products while the concentration of osmium(VIII) is high. However, as the concentration of osmium(VIII) is depleted, so the equilibrium reaction will begin to favour the reactants. The value of  $K_{eq}$ , however, is high which implies that the concentration of osmium(VIII) attributable to this reaction will always be very low – especially since the osmium(VIII) concentration term in the equilibrium equation is squared. This model, together with models 1.10 and 2.9, was exhaustively tested on other experimental data as well. While the fits are not ideal, they are within the bounds of experimental error as discussed above and the decision was therefore made to adopt the Complexation Reaction Models 1.2 and 2.2 as the models for further comparative studies.

In addition, it is now clear why Models 1.11 and 2.9 also fitted the experimental data. The first step of the reaction given by Model 1.2 is:



Since the kinetic data only gives information up to the rate-limiting step, the first step could just as well be represented by the rate-limiting step above.

Similarly, for the second step in the reaction:



And, therefore, the second step in the reaction can be similarly represented by the same rate-limiting step.

## CHAPTER 8

### A COMPARATIVE RATE STUDY

#### 8.1 INTRODUCTION

By measuring the rates of the reactions while changing various experimental parameters, mechanistic inferences can be made. For example, by varying the nature of the reducing agent, one may change its reaction affinity and therefore make an inference as to the electronic demands of the reaction. Varying the pH of the matrix alters the concentration ratio of the osmium species ( $[\text{OsO}_4(\text{OH})_2]^{2-}$ ,  $[\text{OsO}_4(\text{OH})]^-$  and  $[\text{OsO}_4]$ ), as well as the alcohol/alkoxide ratio. A change in ionic strength may indicate whether the reacting species are charged or neutral. Finally, the effect of temperature variation on the rates of the reactions allows the activation parameters to be calculated.

##### 8.1.1 Varying the osmium concentration

Other studies have assigned first order dependence to the osmium concentration on the basis that the experimental data returned a straight line when subjected to a first order plot ( $\ln [\text{Os(VIII)}]$  versus time). It should be remembered that all these studies found a single-step reaction, but that the first reading was only taken after 5 or 10 minutes had elapsed<sup>(2, 4, 5, 10, 11, 14)</sup>.

An alternative method of determining the order of a reaction with respect to osmium(VIII) is to determine the initial rate of the reaction at various osmium(VIII) concentrations, while holding the alcohol and hydroxide concentrations constant, and plot these versus the initial osmium(VIII) concentrations. The importance of the initial rate of a reaction is that it is a kinetic parameter determined for conditions that are easily specified. The concentrations of the reactants are known from the amounts actually added. If

$$\text{Rate} = k[\text{A}]^x$$

then

$$\text{Rate}_o = k[\text{A}]_o^x$$

and

$$\log \text{rate}_o = \log k + x \log [\text{A}]_o$$

and a plot of  $\log$  (initial concentration) versus  $\log$  (initial rate) will give a straight line with the slope equal to the order of the reaction.

### 8.1.2 Varying the ionic strength

When ions react in solution, their charges result in electrostatic forces that affect the kinetics of the reactions. Due to their ionic charges, changes in solute concentration bring about alterations in activity coefficients, and thus the rate constant, which is dependent on activity coefficients. It can be shown<sup>(44)</sup> that

$$\log k = a + 1.018Z_A Z_B I^{1/2} \quad 8.1$$

where  $Z_A$  and  $Z_B$  are the charges on the reacting species and  $I$  is the ionic strength of the solution.  $a$  is a constant at constant temperature. This is only valid for dilute solutions – less than 0.01M for univalent electrolytes. It is clear that a plot of  $\log k$  versus  $I^{1/2}$  should yield a straight line. However, if the charge on one of the reacting species is zero, then a change in ionic strength should have little or no effect on the rate of the reaction. If A and B are both positive or both negative, the rate should increase linearly with  $I^{1/2}$ . Similarly, if A and B are oppositely charged, then the rate should decrease linearly with  $I^{1/2}$ .

To avoid the effects of a change in ionic strength, experiments are usually carried out using a constant and large excess of an inert salt such as sodium perchlorate. This swamps variations in ionic strength that would otherwise occur due to changes in reactant concentrations and acidity, amongst others. However, during this study, the sodium hydroxide concentration was necessarily high in order for the reaction to proceed. This effectively resulted in the sodium hydroxide acting as the excess salt in these reactions. Even though it participated in the reaction, there was such a large excess that it swamped ionic strength changes. The upshot of this was that investigations into determining charge on the reactants using Equation 8.1 were impossible. A solution that was dilute enough to conform to the requirements of Equation 8.1 was too dilute in sodium hydroxide for any reaction to occur. However, variations in ionic strength were still performed at the lowest hydroxide concentration possible (0.05M). This was done to establish without doubt whether ionic strength variations were interfering in the reaction rates.

### 8.1.3 Varying the pH

Hydroxide concentration, or pH, was another variable parameter. Many of the publications dealing with the catalytic oxidation of alcohols by osmium tetroxide, report an initial increase in the rate of the reaction with increasing hydroxide concentration. They report a first order dependence on hydroxide concentration at low hydroxide concentrations,



becoming zero order at higher hydroxide concentrations. However, the actual hydroxide concentrations used in the experiments varies greatly. Uma *et al* <sup>(10)</sup> and Singh *et al* <sup>(5)</sup> report first order kinetics for hydroxide concentrations in the  $10^{-4}$  mol/l region for primary alcohols <sup>(10)</sup>, acetone and MEK <sup>(5)</sup>, respectively. Others report first order kinetics for hydroxide up to about 0.01 mol/l hydroxide and zero order thereafter, using the organic substrates 2-propanol and 1-propanol <sup>(2)</sup> or tartrate and malate <sup>(4)</sup>. Using mandelate as the substrate, Singh *et al* <sup>(3)</sup> found a first order dependence up to 0.1 mol/l hydroxide and zero order thereafter. The same author found that the rate of the ethanol reaction with osmium tetroxide increased linearly with respect to hydroxide concentration up till about 1.3 mol/l, whereafter the rate started levelling out up till 5.6 mol/l. The only study that used stoichiometric quantities of osmium tetroxide and a range of alcohols, diols and  $\alpha$ -hydroxy acids, concluded that the order of the reactions with respect to hydroxide were fractional <sup>(14)</sup>.

#### 8.1.4 Varying the dielectric constant

The dielectric constant is embodied in Coulomb's law, which states that the force ( $F$ ) between two ions, A and B, in a dilute solution is proportional to the product of the charges on A and B,  $Z_A$  and  $Z_B$ , divided by the square of the distance between them,  $r^2$ . The constant of proportionality is  $e^2/D$ , where  $e$  is one unit of electronic charge and  $D$  is the dielectric constant of the medium.

$$F = \frac{Z_A Z_B e^2}{D r^2} \quad 8.2$$

The effects of solvent polarity on the rate of a reaction can be extremely complex. However, simply put, the more strongly solvated an ion or molecule is in solution, the more difficult it is for desolvation to occur so that an active site is exposed <sup>(44)</sup>. Transition states that produce ions will usually be accelerated by solvents having higher dielectric constants and dipole moments. However, these same solvents will retard the formation of a low charge transition state formed from the coming together of two ions, since desolvation of the ions will be difficult.

However, dipole moment alone is not a good predictor of solvent behaviour towards ions. Nitrobenzene is quite polar, but is a poor solvent for solutions of small ions such as  $\text{Na}^+$  and  $\text{Cl}^-$ . Some solvents solvate anions and cations to different degrees. For example, DMF,  $(\text{CH}_3)_2\text{SO}$  and  $\text{CH}_3\text{CN}$  are polar, but the positive end of these molecules is not as accessible as the negative end. Therefore, they solvate cations better than they solvate anions.

Uma *et al* <sup>(10)</sup> investigated the effect of dielectric constant by carrying out the catalytic oxidation of primary alcohols by osmium tetroxide in varying compositions of tertiary butanol and water mixture. The rates of the reactions decreased with increasing *t*-butanol concentration.

### 8.1.5 Varying the temperature

In order for a complex to be transformed from a species, A, into a different species, B, the molecule must pass through a transition state higher in energy than either the reactants or products. The transition state is deemed to be governed by all the normal thermodynamic properties ( $H$ ,  $G$ ,  $S$ , etc). There will, thus, be an equilibrium between the reactants and the transition state. The temperature dependence of this equilibrium constant is governed by the van't Hoff equation <sup>(45)</sup>.

$$\frac{d \ln K}{dT} = \frac{\Delta H^*}{RT^2} \quad 8.3$$

where  $\Delta H^*$  is the activation enthalpy.

Therefore, an increase in temperature will increase the concentration of the transition state, which will result in an increase in the rate of the reaction. The Arrhenius equation (Equation 8.4) is an empirical expression of this principle. Biological systems and explosive reactions show a different dependence on temperature but are of no concern here.

$$k = A e^{-E_a / RT}, \quad \text{or} \quad \ln k = \ln A - \frac{E_a}{RT} \quad 8.4$$

where  $A$  is the pre-exponential factor,  $E_a$  is the activation energy,  $R$  is the gas constant and  $T$  is the temperature in Kelvin.

The empirical quantity  $E_a$  can be shown to be the minimum energy that reactants must have in order to form products. The pre-exponential factor in Equation 8.4 can be interpreted as the rate at which collisions occur irrespective of their energy<sup>(46)</sup> or, in other words, the extrapolated rate at infinitely high temperatures. Therefore, the product of  $A$  and the exponential factor gives the rate of successful collisions.

The Arrhenius parameters,  $A$  and  $E_a$ , are related to the activation enthalpy,  $\Delta H^*$ , and the activation entropy,  $\Delta S^*$ , by the equations<sup>(9)</sup>:

$$\Delta H^* = E_a - RT \quad \text{and} \quad \Delta S^* = 4.58 (\log A - 13.2) \quad 8.5 \text{ and } 8.6$$

### 8.1.5 Varying the substrate concentration

A look at the published studies<sup>(2, 4, 5, 10, 11, 14)</sup> will show that all have found that the reaction between osmium tetroxide and organic substrate is first order in substrate. This is true even for the case where the rate “constant” at increasing substrate concentrations was not constant, but decreased with increasing ketone concentration. This was justified by the argument that increasing ketone concentration decreased the dielectric constant of the medium, which affected the reaction rate. It was therefore considered justifiable to assign first order dependence to the ketone concentration<sup>(5)</sup>.

### 8.1.6 Varying the substrate

The effect of varying not just the concentration of the substrate, but the substrate itself, on the rate of the reaction may give insight into the mechanism of the reaction. Substituent groups on an organic reagent, which do not themselves take part in the reaction, can be electron withdrawing or electron donating. Electron withdrawing groups enhance the electrophilic strength (acidity) of the reagent, whereas electron donating groups enhance the nucleophilic strength (basicity) of the reagent. In effect, this means that by measuring the rates of reactions, one may assess the electron-perturbing effect of the substituents.

For example, if one were considering a mechanism in which the alcohol was deprotonated in basic solution and it was this alkoxide ion that reacted with the osmium(VIII), then one would expect an increase in the rate of the reaction with increasing acidity of the alcohol. Alkyl groups are positively inductive, which means that they inductively donate electrons.

This destabilises an alkoxide ion, which would be stabilised by a negatively inductive group that would distribute electron-density more evenly in the molecule. Therefore, the acidity of the following alcohols increases in the following manner:



$\text{p}K_{\text{a}}$ :                      18.00                      16.00                      15.54                      5.4

If the mechanism involved the participation of an alkoxide ion, then one would expect that the rate of the reaction would increase similarly using these different substrates.

On the other hand, if the mechanism involved an intermediate that would be stabilised by positive induction, then one would expect an increase in the rate of the reaction with an increase in the number of positively inductive alkyl groups from methanol to ethanol to propanol to butanol and, most of all, for the powerfully inductive benzyl alcohol.

Veerasomaiah *et al* <sup>(14)</sup> put forward a mechanism in which the alcohol complexes with the osmium tetroxide and the osmium tetroxide then abstracts a hydride ion from the  $\alpha$ -carbon in a rate-limiting step. If this were true, the more positively inductive the substituents attached to the  $\alpha$ -carbon, the faster would be the rate of the reaction. Their experimental evidence supported this hypothesis since they found that the rate of the reaction increased in the following order: methanol < chloroethanol < ethanol < *n*-propanol < 2-propanol < isobutanol < *n*-pentanol < *n*-butanol < allyl alcohol < benzyl alcohol.

One may study reactions in a systematic way by choosing a reference reaction and by comparing the rates of closely similar reactions with this reference reaction. Hammet formalised the relationship between the rates of the reference reaction and the sample reaction in the Hammet equation<sup>(44)</sup>:

$$\log \frac{k}{k_0} = \rho\sigma$$

where  $k_0$  is the rate constant of the reference reaction,  $k$  is the rate constant of the sample reaction and  $\rho$  and  $\sigma$  are constants. Hammet's equation relates to the acid dissociation of benzoic acid as the reference reaction versus various substituted benzoic acids. Taft extended the studies to include aliphatic reactions and the Taft equation can be written as:

$$\log \frac{k}{k_0} = \rho^* \sigma^*$$

where  $\sigma^*$  is a constant related to polar substituent effects and  $\rho^*$  is a reaction constant<sup>(44)</sup>.  $\rho^*$  is a measure of the sensitivity of the reaction to electronic perturbation. If  $\rho^*$  is positive then the rate of the reaction will be increased by adding electron-withdrawing substituents. Conversely, if  $\rho^*$  is negative then the rate of the reaction will be increased by electron-donating substituents<sup>(45)</sup>. Veerasomaiah *et al*<sup>(14)</sup> reported a linear Taft plot for the alcohols methanol, ethanol, 1-propanol, 1-butanol, isobutanol and 1-pentanol with a slope,  $\rho^*$ , of -1.91.

---

---

## 8.2 EXPERIMENTAL

---

---

All kinetic experiments were prepared in the same way. Each reaction was prepared *in situ* in a 1cm quartz cuvette with magnetic follower. Reactants were added in the order: hydroxide, distilled water and osmium. This brought the reaction to the desired concentration in hydroxide and osmium(VIII). This initial solution was then read for absorbance at 370nm or a spectrum in the range 500nm to 200nm was recorded. Thereafter, the reducing agent was added at time equals zero seconds. The progress of the reaction was followed, either by scanning the entire spectral range between 500nm and 200nm at 960nm per minute, with a cycle every 50 seconds, or by reading the absorbance at 370nm every 0.5 seconds. Reactions were performed at 25°C unless otherwise stated. This was accomplished by placing all reagent vessels in a water-bath. The water from the water-bath was also circulating through an outer sleeve surrounding the cuvette holder, which kept the cuvette at 25°C. The room temperature was kept as close to 25°C as possible.

The reactions were then modelled using the Dynafit modelling software and Model 1.2 or 2.2 discussed in Chapter 7. MEK concentrations were kept low in order to keep the rate of the reaction slow enough that it could be followed on the time scale of the experiments, i.e. 20 minutes. It should be remembered from Chapter 6, that the equilibrium ratio of ketone to osmium(VIII) was between ten and sixteen. However, the rate limiting steps have a ratio of one-to-one and the rate modelling software does not recognise that there is sufficient MEK present to complete the reactions (as is evidenced by the fact that the reactions run to completion). For this reason the MEK concentration was multiplied by ten in order to model the reactions. The rate constants reported are corrected for this.

It will be observed, in this Chapter, that the best fit graphs of the kinetic simulation to the experimental data are not shown for every experiment due to space constraints. Rather, tables of kinetic parameters generated by the best fits to the experimental data are presented.

All alcohol reactions were conducted in a 2M hydroxide matrix, while all ketone reactions were conducted in a 0.1M hydroxide matrix, unless otherwise stated. These concentrations were chosen to be able to observe the reaction over a reasonable time scale. 0.1M Hydroxide caused the alcohol reactions to be too slow, while in a 2M hydroxide matrix the ketone reactions were too fast to follow.

### **8.2.1 Varying the osmium concentration**

Solutions with varying osmium tetroxide concentrations were allowed to react under the same concentration of ethanol and hydroxide. Specific concentrations and reaction conditions are given in Section 8.3.

### **8.2.2 Varying the ionic strength**

Sodium perchlorate was used as the inert salt to regulate ionic strength. Two separate series of experiments were performed. The first used lower sodium perchlorate concentrations (0.01M to 0.05M) with a constant hydroxide concentration of 0.05M, osmium tetroxide concentration of  $4.23 \times 10^{-4}$ M and ethanol concentration of 0.0095M. The second series of experiments used a larger range of sodium perchlorate concentrations (zero to 1M) with constant hydroxide concentration of 0.1M, osmium tetroxide concentration of 0.00248M and ethanol concentration of 0.01M.

### **8.2.3 Varying the hydroxide concentration**

Two series of experiments were performed – one for alcohols (using ethanol) in varying hydroxide concentrations and one for ketones (using methyl ethyl ketone) in varying hydroxide concentrations. The hydroxide concentrations were varied between  $1 \times 10^{-4}$ M and 3M, while the osmium tetroxide and ethanol or MEK concentration was kept constant. Specific reaction conditions are given in Section 8.3.3.

#### 8.2.4 Varying the dielectric constant

Solutions with the same concentrations of osmium tetroxide, ethanol and sodium hydroxide were allowed to react under conditions of varying tertiary butanol or acetonitrile concentrations. In a separate set of reactions, a constant concentration of osmium tetroxide in 2M hydroxide was reacted with increasing concentrations of hexamethylphosphoramide (HMPA). Specific reaction conditions are given in Section 8.34.

#### 8.2.5 Varying the temperature

Reactions were performed in either a constant temperature room (alcohols) or with a water bath as described previously in a temperature regulated room (ketones). Constant temperature experiments were performed using a variety of substrates (methanol, ethanol, 1-propanol, 2-propanol, 1-butanol, 2-butanol, acetone, methyl ethyl ketone and acetophenone) and a constant concentration of osmium tetroxide. The alcohol reactions were performed in a 2M hydroxide matrix, while the ketone reactions were performed in a 0.1M hydroxide matrix, for the same reasons as explained previously.

#### 8.2.6 Varying the reducing agent

The reducing agents used were all simple alcohols and ketones that, generally, formed a progression by the addition of an extra carbon to the chain each time. They were:

**Alcohols:** methanol, ethanol, 1-propanol, 2-propanol, 1-butanol, 2-butanol, 2-chloroethanol and benzyl alcohol

**Ketones:** acetone, methyl ethyl ketone (MEK), 2-pentanone and acetophenone

Six reactions were performed for each reducing agent at increasing concentrations of reducing agent and at a constant temperature of 25°C. Specific concentrations for each reaction are provided in Section 8.3.

## 8.3 RESULTS

### 8.3.1 Varying the osmium concentration

Figure 8.1 shows the progress curves of the reactions of increasing concentration osmium tetroxide with 0.01M ethanol in a 2M hydroxide medium. The slopes of the tangents to the curves give the initial rates of the reactions and these are reported in Table 8.1. The logarithms of the initial rates are then plotted against the logarithm of the osmium concentrations and these result in straight lines for both steps one and two as shown in Figure 8.2.

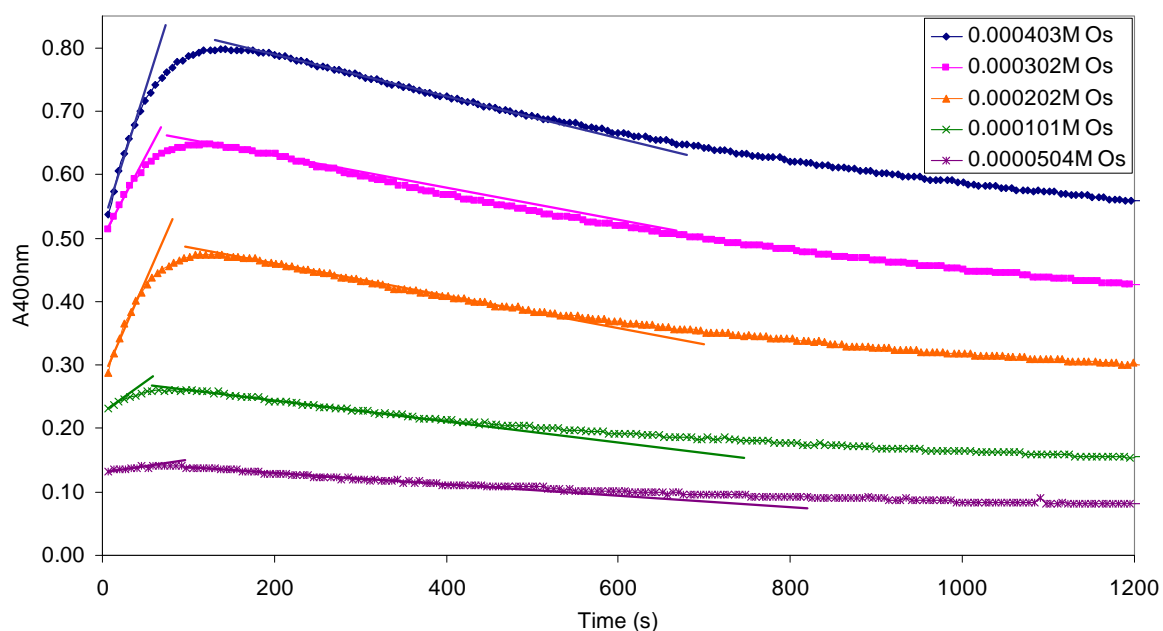
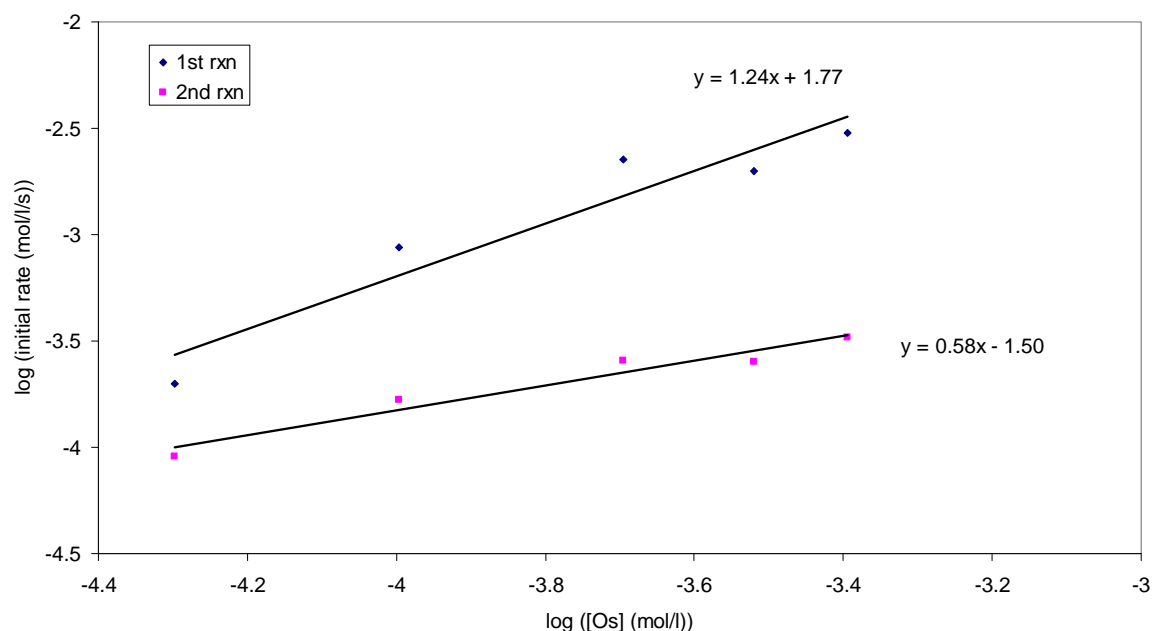


**Figure 8.1: Progress curves of the reaction of varying concentrations of osmium tetroxide with 0.01M ethanol in a 2M hydroxide matrix. The slopes of the tangents to the curves give the initial rate of the first and second steps of the reaction.**



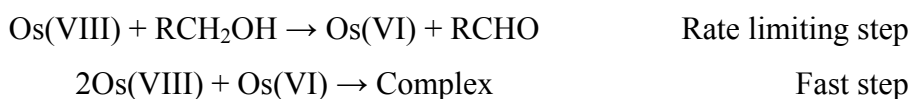
**Table 8.1: The initial rates of the first and second steps of the osmium(VIII)-ethanol reaction taken from the slopes of the tangents to the curves shown in Figure 8.1.**

Initial [Os(VIII)] ( $\times 10^{-4}$ mol/l)	$\frac{dA}{dt}$ - first step	$\frac{dA}{dt}$ - second step
4.03	0.00300	0.000329
3.02	0.00200	0.000253
2.02	0.00227	0.000255
1.01	0.000872	0.000167
0.504	0.000200	0.000091



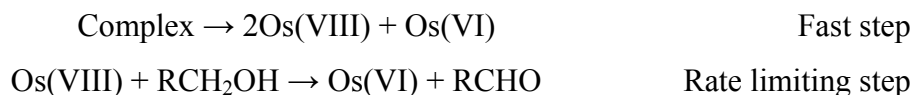
**Figure 8.2: log initial rates of the osmium tetroxide – ethanol reaction for the first and second steps, plotted versus log of the osmium concentrations used.**

Figure 8.2 gives a slope for the first step of the two-step reaction of 1.24. This is close enough to unity to justify the assumption that the first step is first order in osmium concentration. An explanation is required to reconcile this result with the reaction scheme adopted in Chapter 7. The postulated reaction scheme for the first step of the reaction is as follows:



Since the rate law is determined by the slowest step, it is apparent that the rate limiting step shown above is the one which is first order in osmium. Hence, it is reasonable that the experimental data returns such a result.

It difficult to know whether to ascribe any significance to the result obtained for the second step of the reaction. The second step may be represented as follows:



The second step begins when the complex begins giving up osmium(VIII) to be used in the ethanol reaction – this is where we begin to see a decrease in absorbance due to the decay of the osmium complex. If all of the osmium is incorporated into the complex before decay of the complex begins, then it can be argued that the concentration of the complex is a constant ratio of the initial osmium concentration. In this case, the straight line obtained in Figure 8.2 would be valid. However, if the forward and reverse reactions occur simultaneously, then the concentration of the complex will not be a constant ratio of the initial osmium(VIII) concentration. It was already argued in the assigning of a molar extinction coefficient to the complex that, due to the large complexation equilibrium constant, equilibrium lies far to the right and very little osmium(VIII) will be present due to the complexation reaction. Therefore, the former contention is true, the straight line obtained in Figure 8.2 is valid and the second step of the reaction has a fractional dependence on osmium concentration. Simply the fact that this plot returned a straight line is further support for the significance of the result.

### 8.3.2 Varying the ionic strength

Figures 8.3 and 8.4 show the reactions of osmium tetroxide with ethanol in constant hydroxide concentrations but under varying ionic strengths. The figures give the specific reaction conditions.

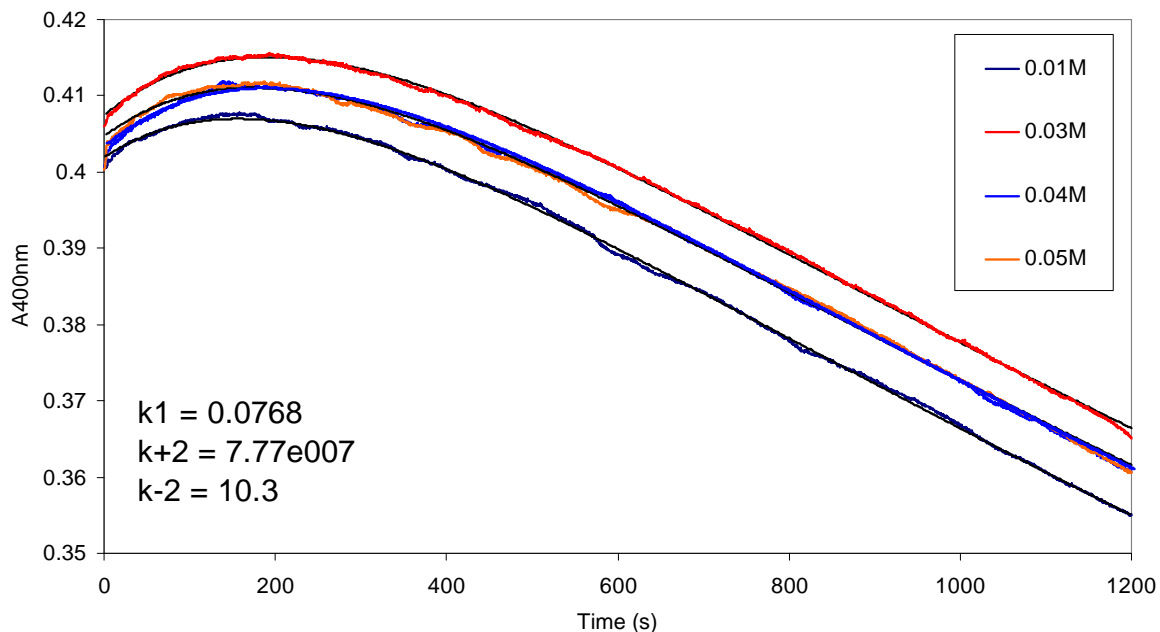


**Figure 8.3:** Progress curves of  $4.23 \times 10^{-4}$  M osmium tetroxide with 0.0095 M ethanol in 0.05 M hydroxide matrix. Increasing concentrations of sodium perchlorate (0.01 M to 0.05 M) were added to each reaction without affecting the rates of the reactions. The complexation reaction model 1.2 was fitted to each progress curve using the rate constants shown in the figure. The fits to the experimental data are shown in black. The fits were so good that it is difficult to see the fitted curves.

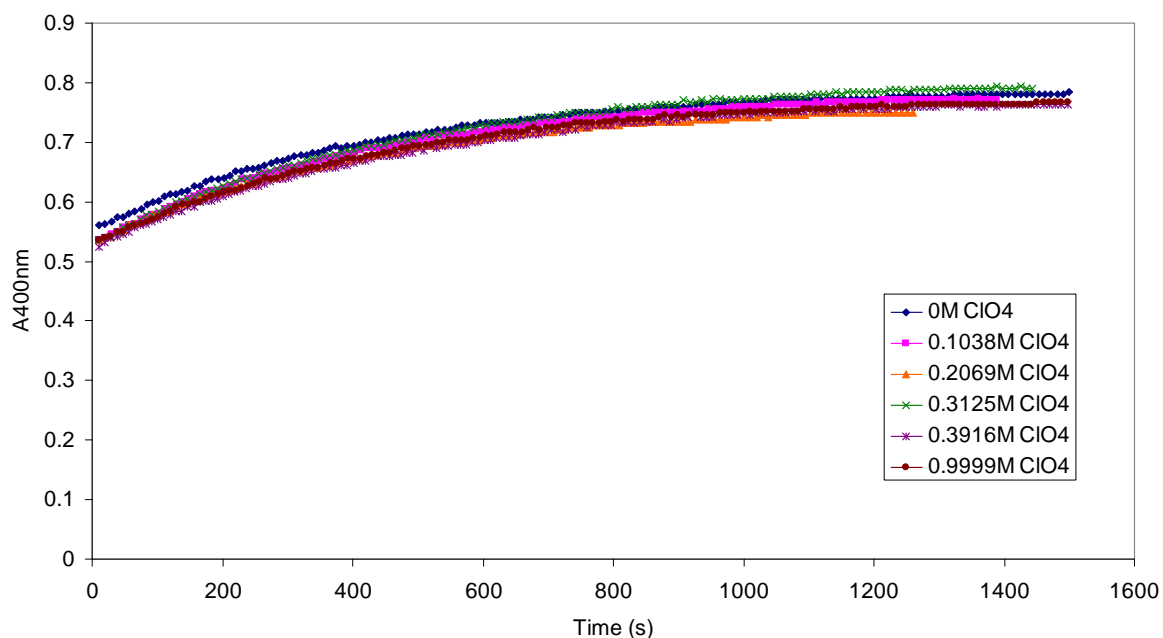


**Figure 8.4:** Progress curves of 0.00248 M osmium tetroxide with 0.01 M ethanol in a 0.1 M hydroxide matrix. Increasing concentrations of sodium perchlorate were added to the reactions without affecting the rates.

It is evident from Figures 8.3 and 8.4 that the rates of the reactions are unaffected by ionic strength. Figure 8.3 features low hydroxide and sodium perchlorate concentrations. Dynafit Model 1.2 returned a perfect fit for the experimental data using the same set of rate constants for each perchlorate concentration. Figure 8.4 shows that this observation holds true at higher perchlorate concentrations as well. The reactions were not modelled since it is abundantly clear from a simple scrutiny of the figure that there is no change in the progress curves of the reactions, which range in perchlorate concentration from zero to 1M.

No further information could be extracted from this data for the reason that the solutions could not be made dilute enough to conform to the Debye-Huckel limiting law as discussed in Section 8.1.2.

### **8.3.3 Varying the hydroxide concentration**

Figure 8.5 shows the progress curves of the same concentrations of osmium(VIII) and ethanol reacting under varying concentrations of sodium hydroxide. Qualitatively, it is clear to see that the rate of the reaction increases dramatically with an increase in hydroxide concentration. Equally clearly, it can be seen that no reaction occurs for any solution with a hydroxide concentration of 0.01M or less. Slow reactions begin occurring in hydroxide concentrations of 0.05M and the rate of the reactions continue to increase up to the final concentration investigated, which was 3M hydroxide.

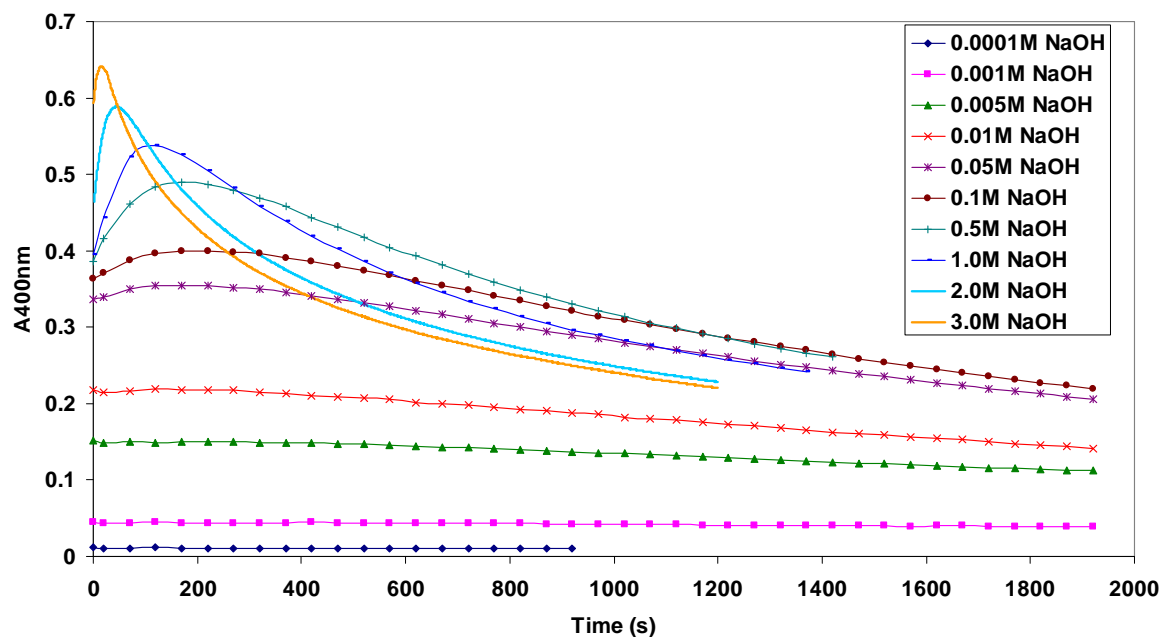
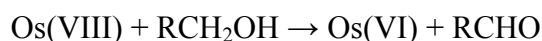


**Figure 8.5: Progress curves of the reactions of  $4.37 \times 10^{-4}$  M osmium tetroxide with 0.0098 M ethanol in varying concentrations of sodium hydroxide.**

The initial rate of the first step was determined as previously by determining the slope of the tangent to the progress curve at the start of the first step. In this case, it was not deemed appropriate to plot the initial rate of the second step versus the hydroxide concentration. At high hydroxide concentrations, there would be such a large excess that the initial hydroxide concentration would also be the initial concentration at the start of the second step. This, however, would not be the case at low hydroxide concentrations.

The initial rate shows a linear dependence on the hydroxide concentration. It follows, therefore, that a plot of log hydroxide concentration versus log rate (Figure 8.6) results in a linear curve, which has a slope of 0.86. The slope of the curve is close enough to unity to imply that the first step is first order in hydroxide concentration. As discussed in Section 8.3.1, this implies that the reaction



is first order in hydroxide concentration.

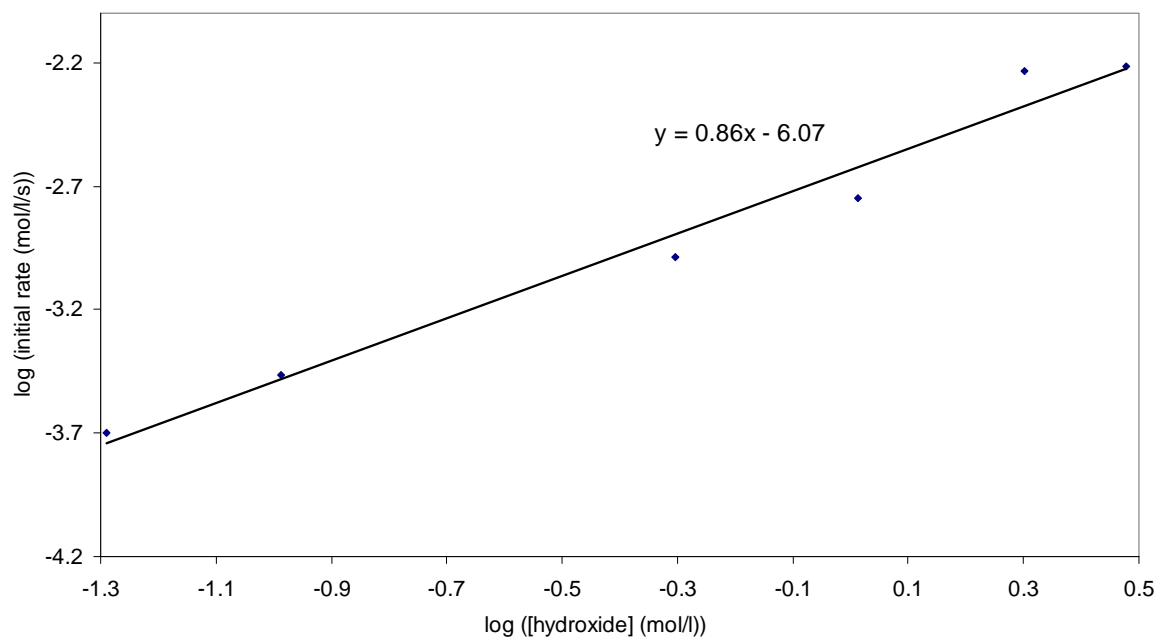


**Figure 8.6: log initial rate plotted versus log hydroxide concentration for the reactions of ethanol with osmium tetroxide in varying hydroxide concentrations.**

Figure 8.7 shows the progress curves of the reaction of osmium tetroxide with methyl ethyl ketone (MEK) under increasing concentrations of sodium hydroxide. As for the same reactions with ethanol, the increase in the rate of the reaction with increasing hydroxide concentration is plain to see. Also similarly to the ethanol reactions, there is no reaction in solutions with a hydroxide concentration of less than 0.025M. Figure 8.8 is a plot of log initial rate versus log hydroxide concentration. It has a slope of 1.13, which implies a first order dependence on hydroxide concentration.

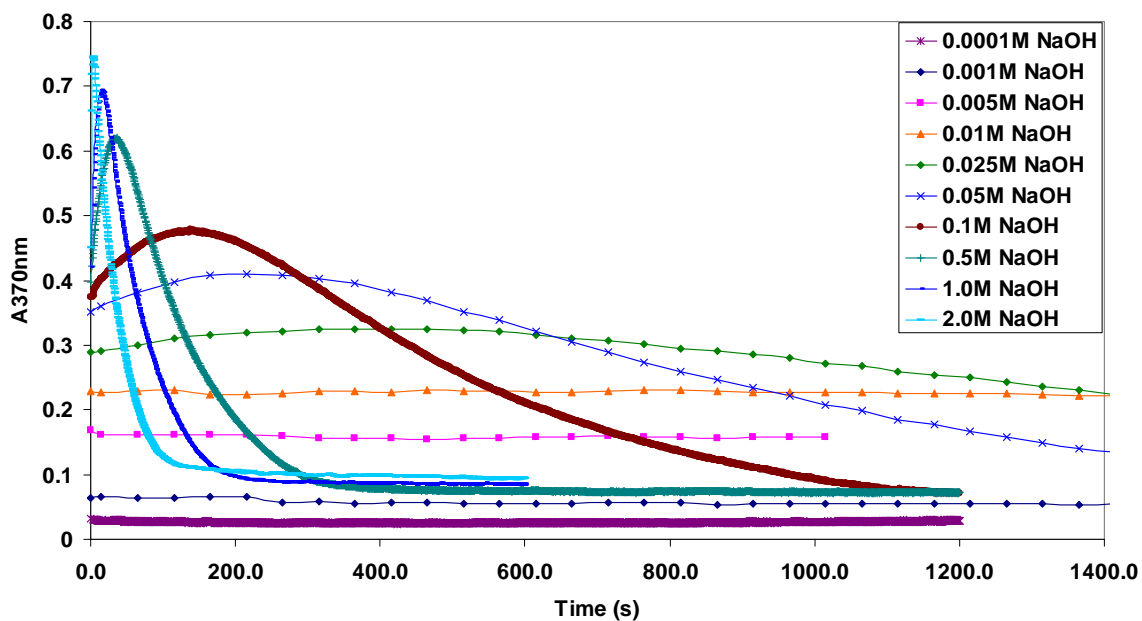


Figure 8.7: Progress curves of the reactions of  $3.45 \times 10^{-4} \text{M}$  osmium tetroxide with  $3.2 \times 10^{-4} \text{M}$  MEK in varying concentrations sodium hydroxide.

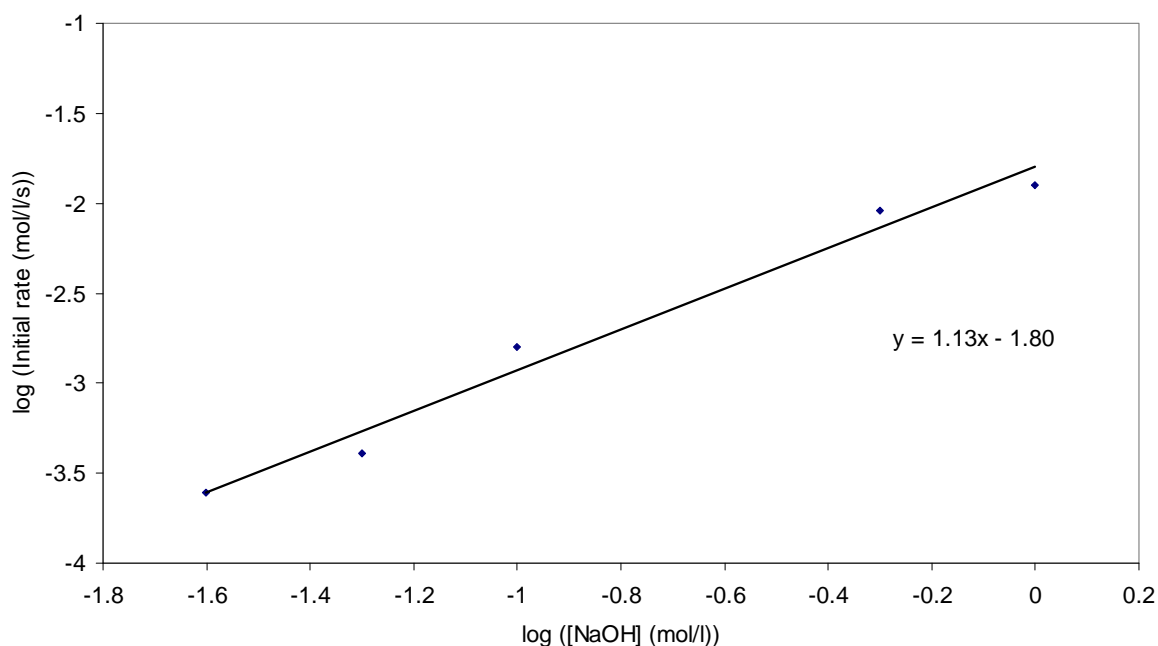
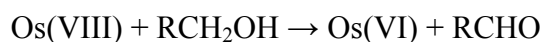
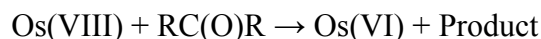


Figure 8.8:  $\log$  hydroxide concentration versus  $\log$  initial rate for the reactions of MEK with osmium tetroxide in varying hydroxide concentrations.

In summary, it is possible to say that the rate of both the alcohol and ketone reactions increases with increasing hydroxide concentration. Both of the initial rate limiting reactions:



and



are first order in hydroxide concentration.

This is in keeping with the findings of other workers <sup>(10, 5, 2, 4)</sup>. However, there is no agreement as to the range of hydroxide concentrations at which this holds true. No reaction was observed in hydroxide concentrations below 0.025M, whereas others report first order kinetics for hydroxide concentration in the  $10^{-4}$  mol/l region for primary alcohols <sup>(10)</sup>, acetone and MEK <sup>(5)</sup>. Others report first order kinetics for hydroxide up to about 0.01 mol/l hydroxide (which is more in keeping with this study), but zero order thereafter, using the organic substrates 2-propanol and 1-propanol <sup>(2)</sup> or tartrate and malate <sup>(4)</sup>. It is possible that the discrepancies have some basis in the fact that these studies make use of osmium tetroxide as a catalyst and not in stoichiometric quantities.

Further related to these observations is the fact that no reaction was observed in this study in aqueous solutions (no hydroxide present), acidic solutions or in organic matrices.

The kinetic Complexation Reaction Model was fitted to the experimental data and the rate parameters were generated. This is interesting for the sake of comparison of the conditional\* rate constants,  $k_1$ , of the MEK versus the ethanol reactions (Table 8.2). This is the only case in which the rate constants can be directly compared since in all other experiments the hydroxide concentrations of the alcohol and the ketone reactions were different. Thus we see that the MEK reaction is approximately 35 to 40 times faster than the ethanol reaction. This is quantitative confirmation of the empirical observations made earlier.

---

\* Rate constants are conditional on hydroxide concentration.



**Table 8.2:** Rate constants,  $k_1$ , generated by kinetic modelling software using the Complexation Reaction Model for the reactions of ethanol or MEK with osmium tetroxide in varying concentrations of hydroxide.

[NaOH] (mol/l)	Ethanol $k_1$ ( $M^{-1}s^{-1}$ )	MEK $k_1$ ( $M^{-1}s^{-1}$ )
0.025	-	2.03
0.05	0.116	4.12
0.1	0.112	7.94
0.5	0.214	30.35
1	0.505	55.96
2	2.323	96.87

### 8.3.4 Varying the dielectric constant

Figures 8.9 and 8.10 show the progress curves of the reactions of the same concentration of osmium tetroxide and ethanol in the presence of varying concentrations of tertiary butanol and acetonitrile, respectively. Table 8.3 gives the rate constant,  $k_1$ , obtained from the best fits to the experimental data, while keeping both the  $K_{eq}$  and the molar extinction coefficients constant.

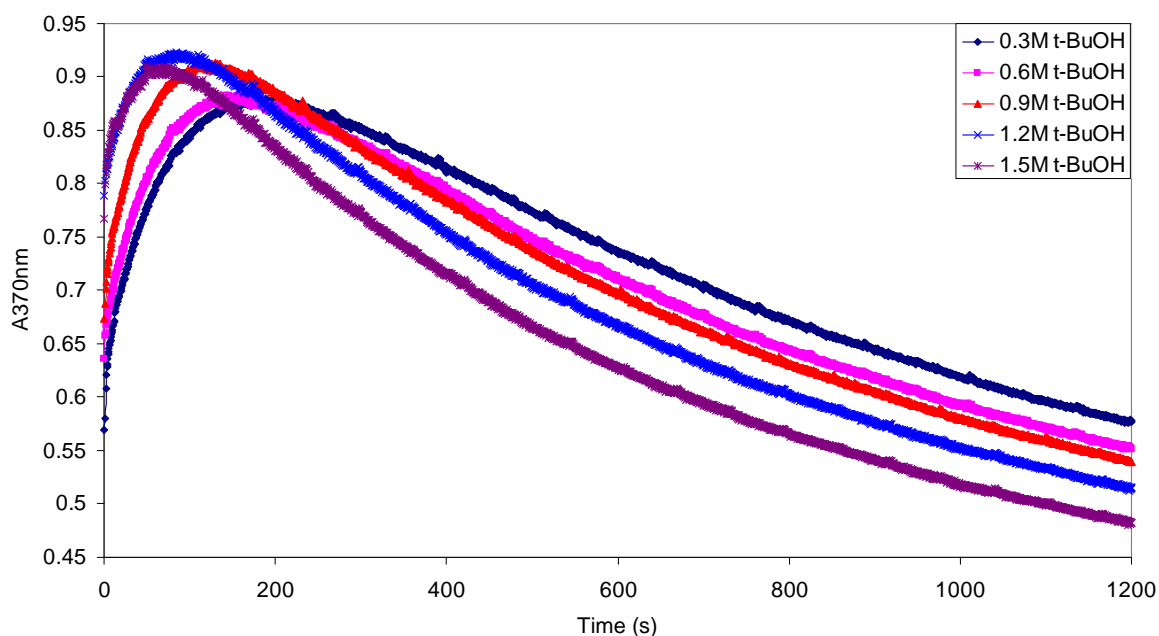


**Figure 8.9:** Progress curves of the reaction of  $4.48 \times 10^{-4} M$  osmium tetroxide with  $0.01 M$  ethanol in a  $0.1 M$  hydroxide matrix with varying tertiary butanol concentrations.

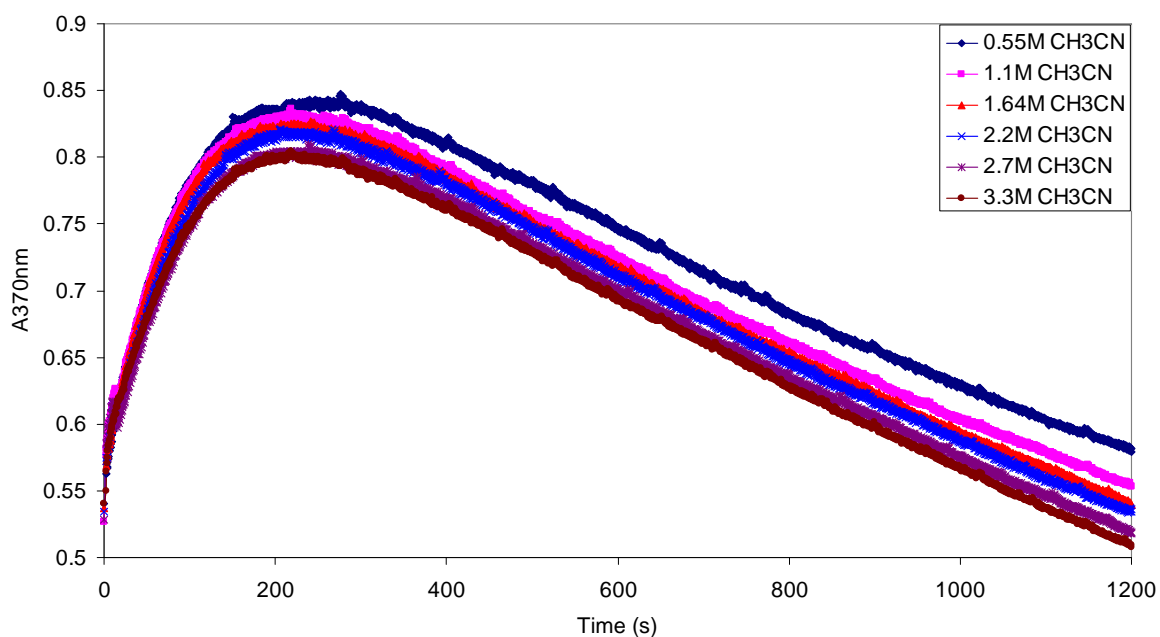


**Figure 8.10:** Progress curves of the reaction of  $4.48 \times 10^{-4}$  M osmium tetroxide with 0.01 M ethanol in a 0.1 M hydroxide matrix with varying acetonitrile concentrations.

**Table 8.3:** Rate constants,  $k_1$ , calculated for varying concentrations of *t*-butanol and acetonitrile. All other parameters are constant:  $[\text{OsO}_4] = 4.48 \times 10^{-4}$  M;  $[\text{ethanol}] = 0.01$  M;  $[\text{hydroxide}] = 0.1$  M.

[ <i>t</i> -Butanol] (mol/l)	$k_1$ ( $\text{M}^{-1}\text{s}^{-1}$ )	$[\text{CH}_3\text{CN}]$ (mol/l)	$k_1$ ( $\text{M}^{-1}\text{s}^{-1}$ )
0.3	0.447	0.55	0.2513
0.6	0.501	1.1	0.2791
0.9	0.528	1.64	0.2914
1.2	0.595	2.2	0.2977
1.5	0.694	2.7	0.3146
		3.3	0.3266

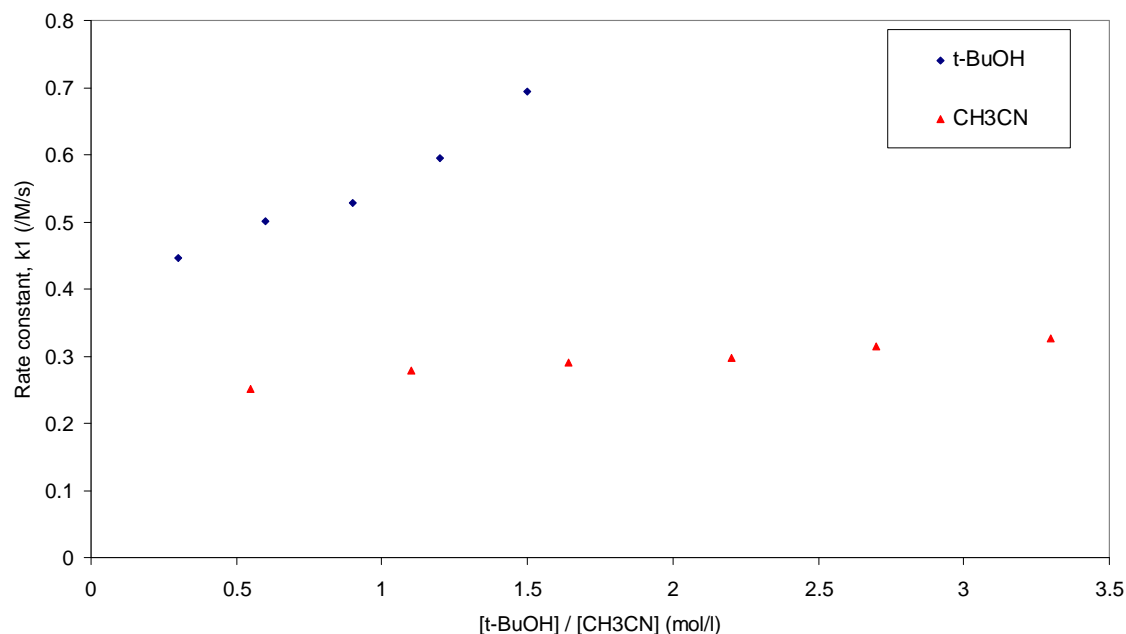


**Figure 8.11: The rate constant,  $k_1$ , as a function of tertiary butanol and acetonitrile concentration, respectively.  $[\text{OsO}_4] = 4.48 \times 10^{-4} \text{M}$ ;  $[\text{Ethanol}] = 0.01 \text{M}$ ;  $[\text{Hydroxide}] = 0.01 \text{M}$ .**

From the figures above it is clear that there is an increase in the rates of the reactions with increasing concentrations of both *t*-butanol and acetonitrile. However, the increase is not as marked for acetonitrile as it is for *t*-butanol. The actual values of the rates constants are also less for acetonitrile than for *t*-butanol. The dielectric constant decreases in the order water > acetonitrile > *t*-butanol. The rate constant,  $k_1$ , for the same reaction in 0.1M hydroxide with only osmium tetroxide and ethanol present is  $0.120 \text{M}^{-1} \text{s}^{-1}$ . Therefore, it can be said from the experimental data above that the rate of the reaction increases with decreasing dielectric constant. This would imply that more highly charged reactants come together in a low charge transition state. Solvents with a higher dielectric constant solvate the reactants very well and they have difficulty in coming together to react. Solvents with a lower dielectric constant do not solvate the reactants as well, but do solvate the lower charge transition state well, speeding the formation of the products.

At this stage it should be mentioned that it was experimentally determined that *t*-butanol does not take part in the reaction in the sense that it is not transformed during the reaction. This was determined by NMR and reported in Chapter 5.

The results obtained above are in contrast to those of Uma *et al*<sup>(10)</sup> who found that the rates of the reactions decreased with increasing *t*-butanol concentration. Their study was conducted in a 0.005M hydroxide matrix using catalytic quantities of osmium tetroxide. The conditions were not that dissimilar to those used in this study and the reason for this discrepancy cannot be accounted for. However, the case for an increase in reaction rate with a decrease in dielectric constant is given further credibility by the results of the HMPA reactions, which are presented below.

Although the HMPA experiments were not conducted under the same conditions as the previous ones and, as such, cannot be compared to them, it is also a participant in the reactions which does not, itself, undergo any change. This was established by NMR and reported in Chapter 5. Figure 8.12 shows the progress curves at various concentrations of HMPA with no ethanol or other reducing agent present, in 2M hydroxide. It was reported in Chapter 4 that osmium(VIII) could undergo precisely the same reduction process in a basic medium with no other reducing agent present. The rate of the reaction was just considerably slower. It seems that adding HMPA to the reaction can dramatically increase the rate of the reaction, without the HMPA itself taking part in the reaction. Table 8.4 shows the rate constants,  $k_1$ , for the HMPA reactions, together with the rate constant for the reaction of osmium(VIII) in hydroxide only. It seems that the HMPA acts in the same manner as the *t*-butanol and acetonitrile, by lowering the dielectric constant of the medium and so facilitating the formation of the low charge transition state. It does not seem as if there is complex formation between the HMPA and the osmium tetroxide to form an activated complex, since there is no change in the spectrum of the osmium tetroxide upon addition of the HMPA. There is also no change in the characteristic spectra throughout the reduction of the osmium(VIII) to osmium(VI).

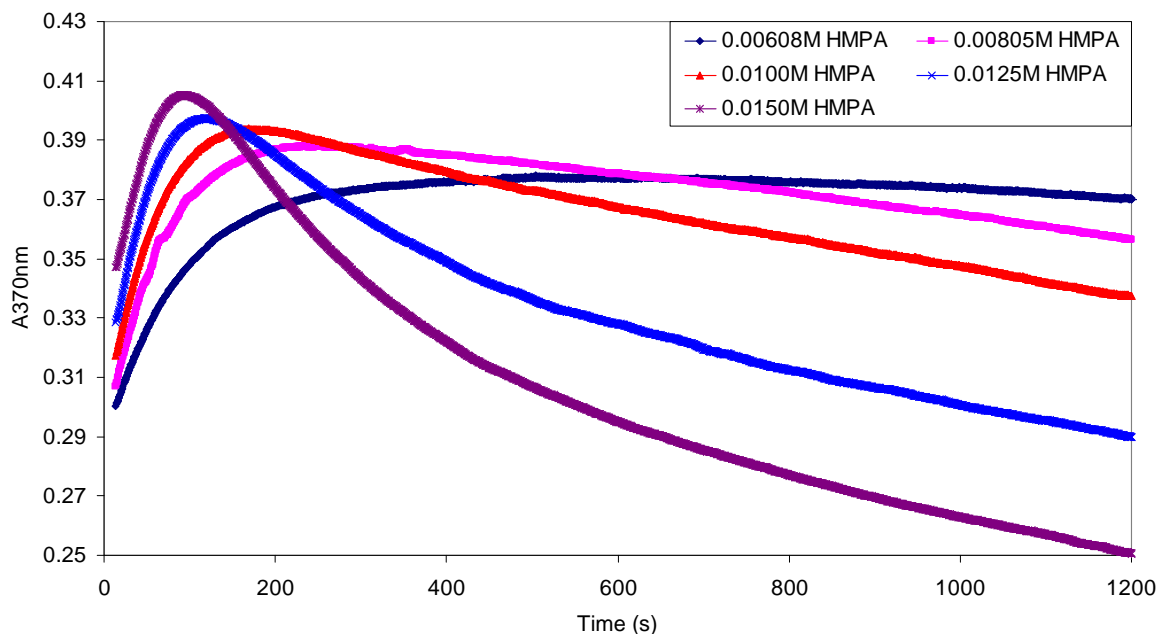


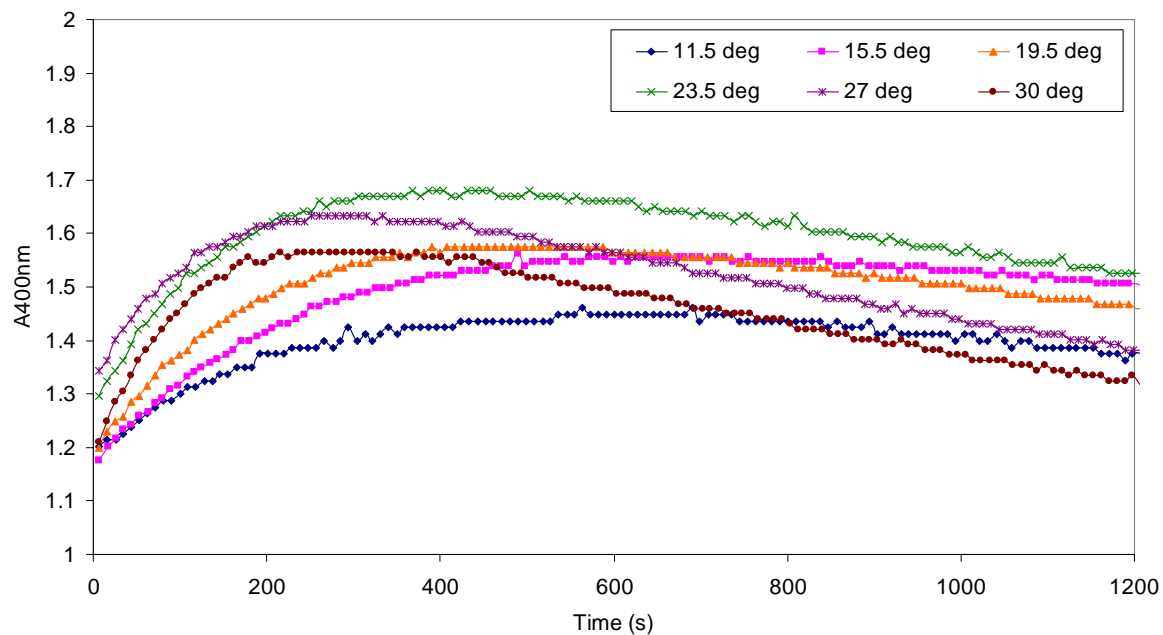
**Figure 8.12:** Progress curves of the reaction of  $2.92 \times 10^{-4}$  M osmium tetroxide with no ethanol present in a 2M hydroxide matrix with varying HMPA concentrations.

**Table 8.4:** Rate constants,  $k_1$ , for varying concentrations of HMPA. All other parameters are constant.  $[\text{OsO}_4] = 2.92 \times 10^{-4}$  M;  $[\text{hydroxide}] = 2$  M. Also given is the rate constant for reaction of  $4.93 \times 10^{-4}$  M osmium tetroxide in 2M hydroxide.

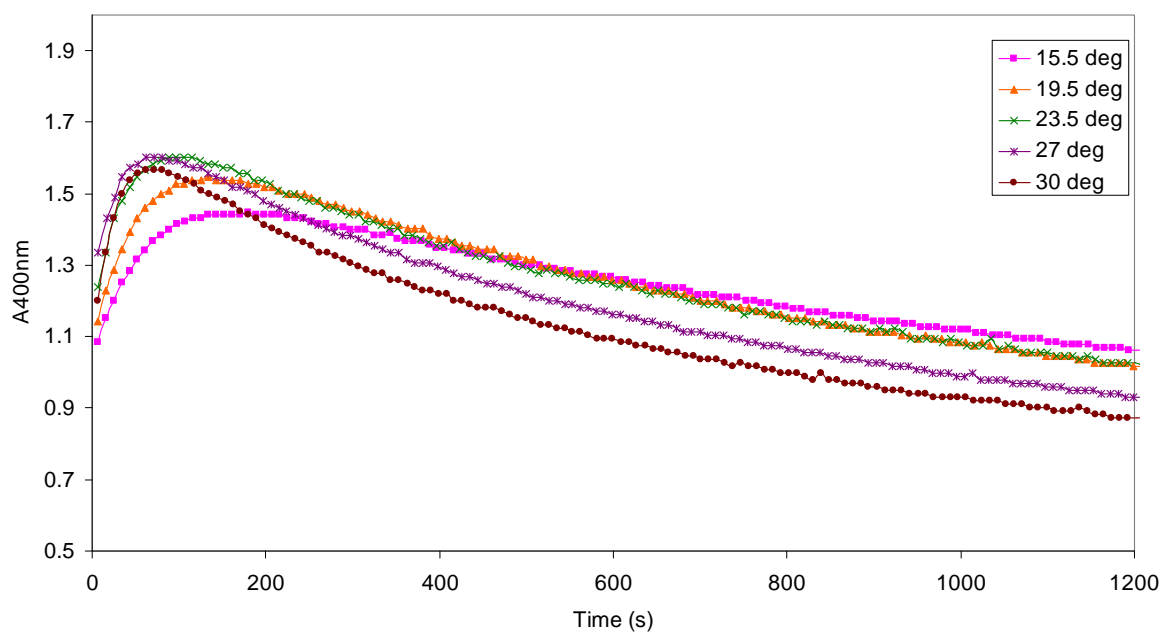
[HMPA] (mol/l)	$k_1$ ( $\times 10^{-3} \text{s}^{-1}$ )
No HMPA	0.0103
0.00608	0.997
0.00805	1.65
0.0100	2.20
0.0125	4.20
0.0150	6.87

### 8.3.5 Varying the temperature

Figures 8.13 to 8.15 show the progress curves for the reactions of the various alcohols with osmium tetroxide in a 2M hydroxide matrix at various temperatures. Qualitatively, it is clear to see that the rates of the reactions increase with increasing temperature. This is seen more clearly in Figure 8.16, which shows the rate constant,  $k_1$ , as a function of temperature. Also shown is the equilibrium constant,  $K_{eq}$ , as a function of temperature. This, however, shows no clear trend and there is a fair amount of scatter among the points. The theoretical Complexation Reaction Model was fitted to the experimental data. The rate constants returned by the best fits to the data are given in Table 8.5. These were then used to plot the Arrhenius plot in Figure 8.18, which gave reasonably good straight lines for each of the alcohols. The slopes of these straight lines are equal to  $-(E_a / R)$ . Therefore, using these slopes and Equations 8.5 and 8.6, it is possible to calculate the thermodynamic activation parameters which are given in Table 8.6.

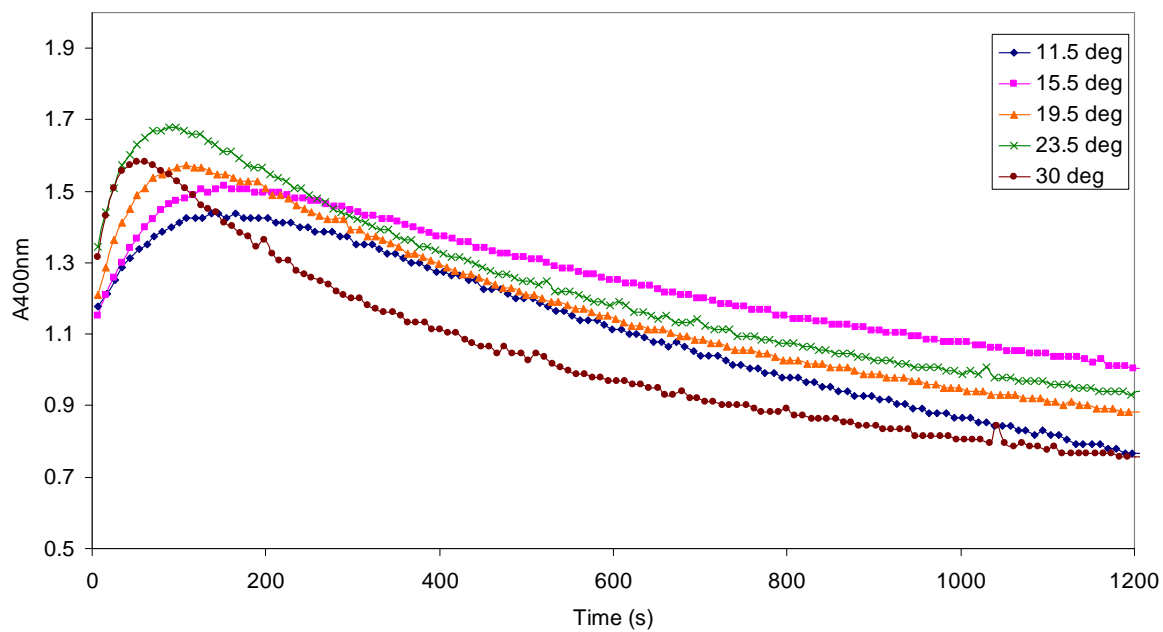


(a)

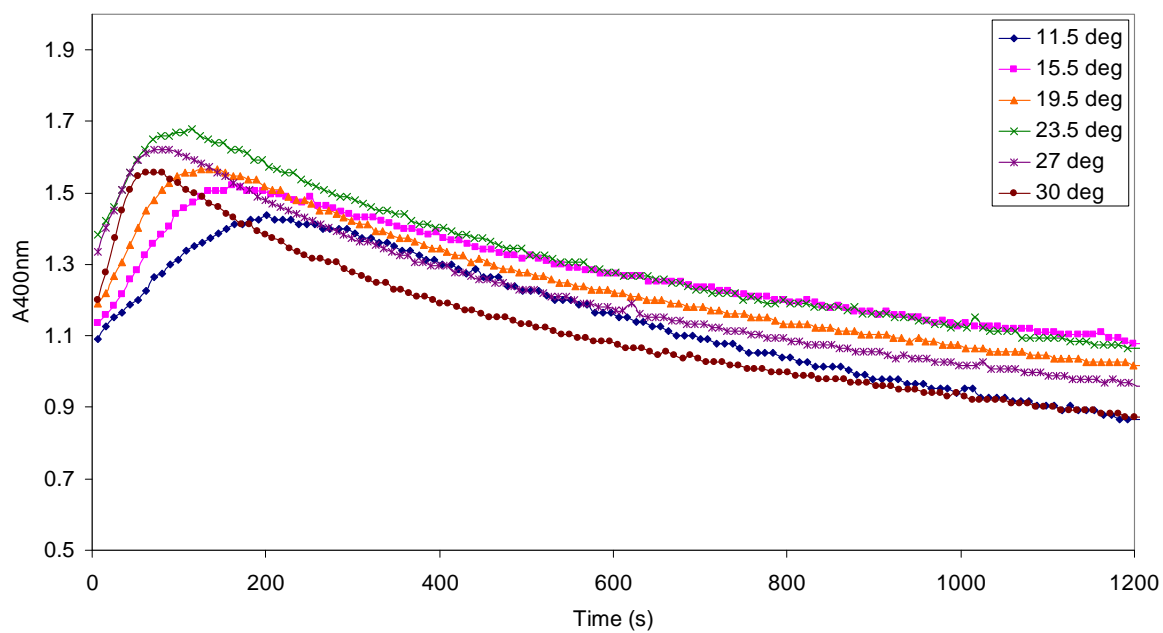


(b)

Figure 8.13: Progress curves of the reaction of  $5.59 \times 10^{-4} \text{M}$  osmium tetroxide with 0.01M (a) methanol and (b) ethanol; in 2M hydroxide at various temperatures.



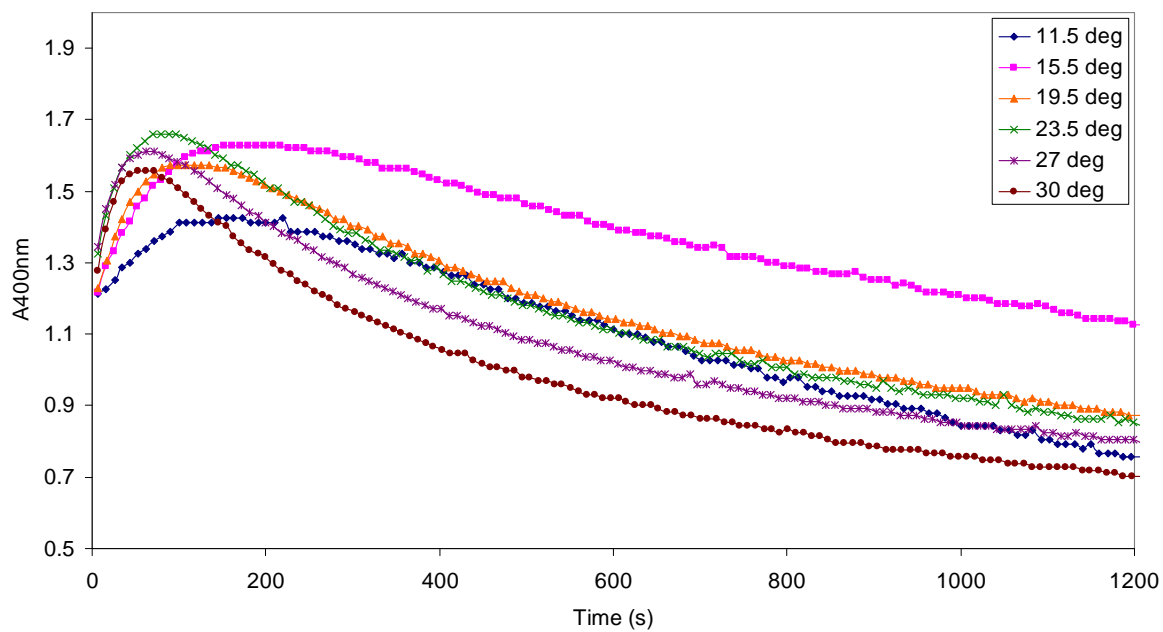
(a)



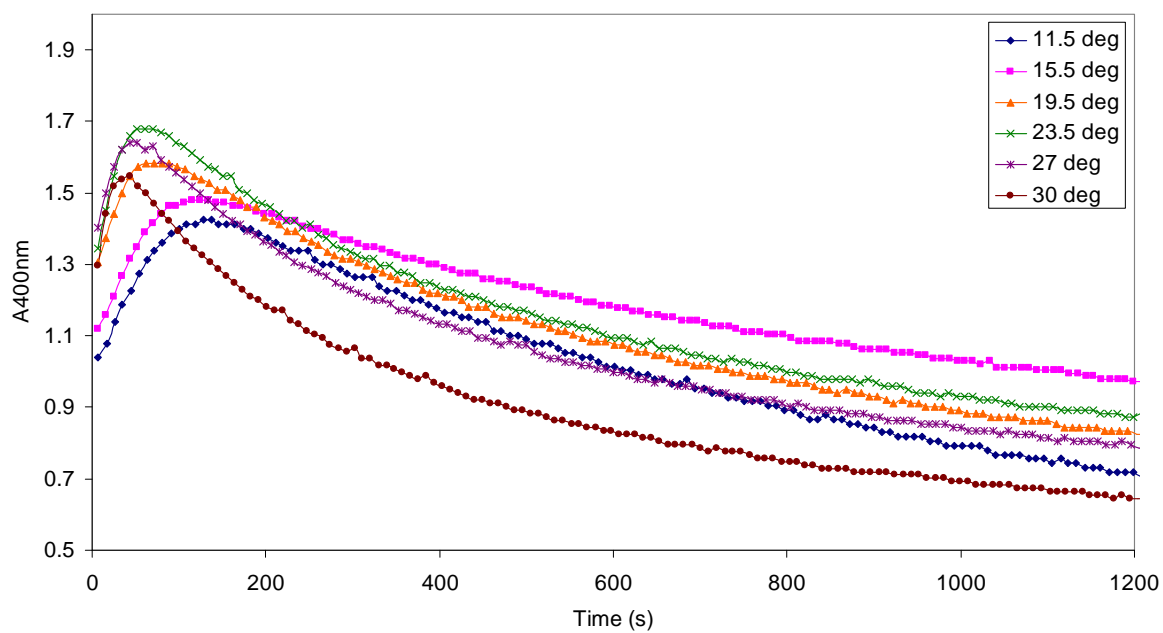
(b)

**Figure 8.14: Progress curves of the reaction of  $5.59 \times 10^{-4} \text{ M}$  osmium tetroxide with  $0.01 \text{ M}$  (a) 1-propanol and (b) 2-propanol; in  $2 \text{ M}$  hydroxide at various temperatures.**





(a)



(b)

**Figure 8.15:** Progress curves of the reaction of  $5.59 \times 10^{-4}$  M osmium tetroxide with 0.01 M (a) 1-butanol and (b) 2-butanol; in 2 M hydroxide at various temperatures.

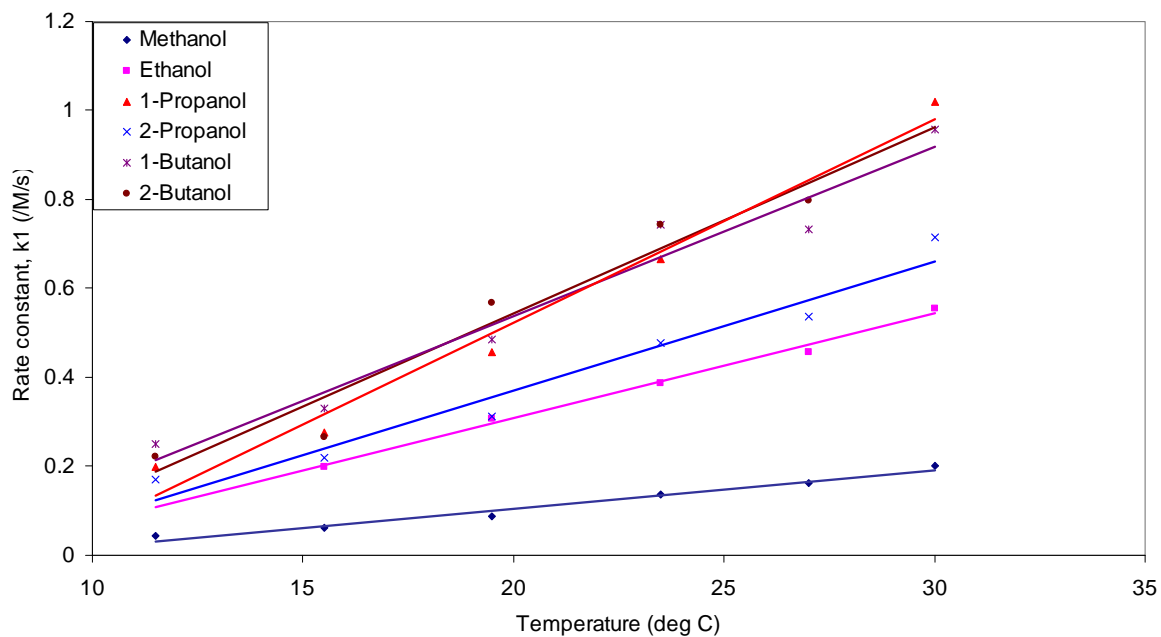


Figure 8.16: The rate constants,  $k_1$ , as a function of temperature.

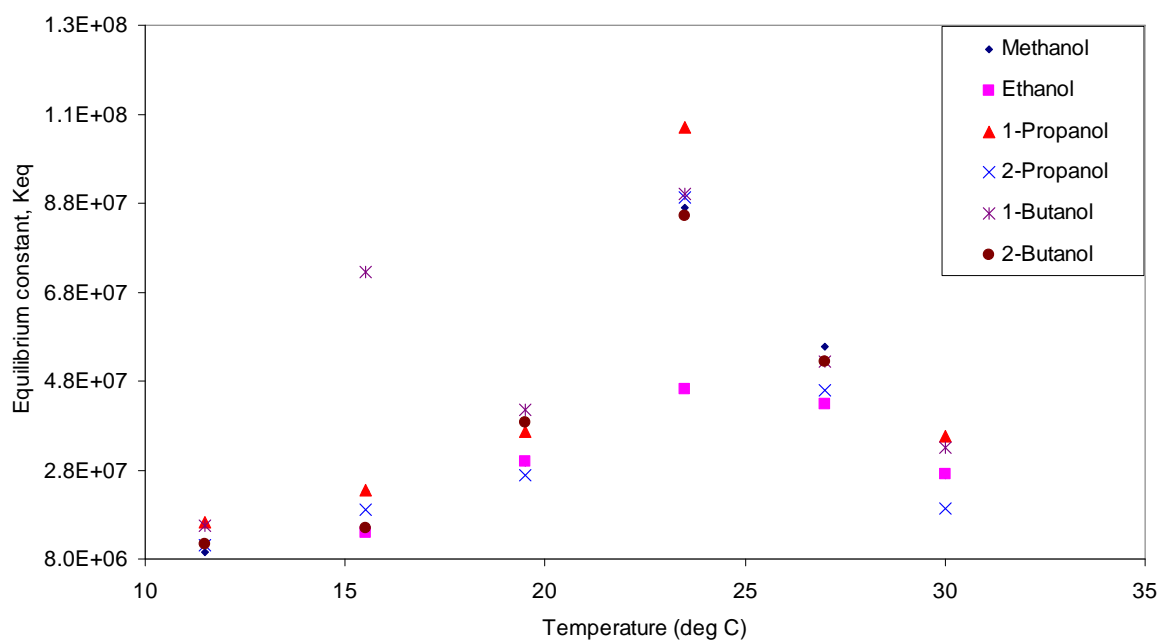


Figure 8.17: Equilibrium constant,  $K_{eq}$ , as a function of temperature.

**Table 8.5: Rate constant,  $k_1$  and equilibrium constant,  $K_{eq}$ , obtained from the best fit of the rate modelling software. Molar extinction coefficients were held constant.**

<b>Methanol</b>				
Temperature (°C)	$k_1$ ( $M^{-1}s^{-1}$ )	$k_{+2}$ ( $\times 10^8 M^{-1}s^{-1}$ )	$k_{-2}$ ( $M^{-1}s^{-1}$ )	$K_{eq}$ ( $\times 10^7 M^{-2}$ )
11.5	0.0437	2.18	23	0.948
15.5	0.0615	3.26	14	2.33
19.5	0.088	3.56	12	2.97
23.5	0.136	5.91	6.8	8.69
27	0.162	4.62	8.3	5.57
30	0.200	3.23	12	2.69
<b>Ethanol</b>				
Temperature (°C)	$k_1$ ( $M^{-1}s^{-1}$ )	$k_{+2}$ ( $\times 10^8 M^{-1}s^{-1}$ )	$k_{-2}$ ( $M^{-1}s^{-1}$ )	$K_{eq}$ ( $\times 10^7 M^{-2}$ )
15.5	0.200	2.25	16	1.41
19.5	0.306	3.28	11	2.98
23.5	0.388	3.87	8.4	4.61
27	0.457	3.76	8.8	4.27
30	0.556	3.25	12	2.71
<b>1-Propanol</b>				
Temperature (°C)	$k_1$ ( $M^{-1}s^{-1}$ )	$k_{+2}$ ( $\times 10^8 M^{-1}s^{-1}$ )	$k_{-2}$ ( $M^{-1}s^{-1}$ )	$K_{eq}$ ( $\times 10^7 M^{-2}$ )
11.5	0.198	2.61	16	1.63
15.5	0.276	3.05	13	2.35
19.5	0.458	3.67	10	3.67
23.5	0.666	5.77	5.5	10.5
30	1.02	3.41	9.6	3.55
<b>2-Propanol</b>				
Temperature (°C)	$k_1$ ( $M^{-1}s^{-1}$ )	$k_{+2}$ ( $\times 10^8 M^{-1}s^{-1}$ )	$k_{-2}$ ( $M^{-1}s^{-1}$ )	$K_{eq}$ ( $\times 10^7 M^{-2}$ )
11.5	0.171	1.65	15	1.10
15.5	0.220	2.10	11	1.91
19.5	0.311	4.03	15	2.69
23.5	0.478	6.97	7.8	8.94
27	0.536	5.06	11	4.60
30	0.715	3.27	17	1.92

1-Butanol				
Temperature (°C)	$k_1$ ( $M^{-1}s^{-1}$ )	$k_{+2}$ ( $\times 10^8 M^{-1}s^{-1}$ )	$k_{-2}$ ( $M^{-1}s^{-1}$ )	$K_{eq}(\times 10^7 M^{-2})$
11.5	0.251	2.80	18	1.56
15.5	0.330	5.30	7.3	7.26
19.5	0.485	3.70	8.9	4.16
23.5	0.743	6.40	7.1	9.01
27	0.733	4.20	8	5.25
30	0.958	3.30	10	3.30
2-Butanol				
Temperature (°C)	$k_1$ ( $M^{-1}s^{-1}$ )	$k_{+2}$ ( $\times 10^8 M^{-1}s^{-1}$ )	$k_{-2}$ ( $M^{-1}s^{-1}$ )	$K_{eq}(\times 10^7 M^{-2})$
11.5	0.223	1.92	17	1.13
15.5	0.266	2.10	14	1.50
19.5	0.567	3.29	8.5	3.87
23.5	0.743	3.75	4.4	8.52
27	0.797	2.94	5.6	5.25
30	1.30	15.5	64	2.42

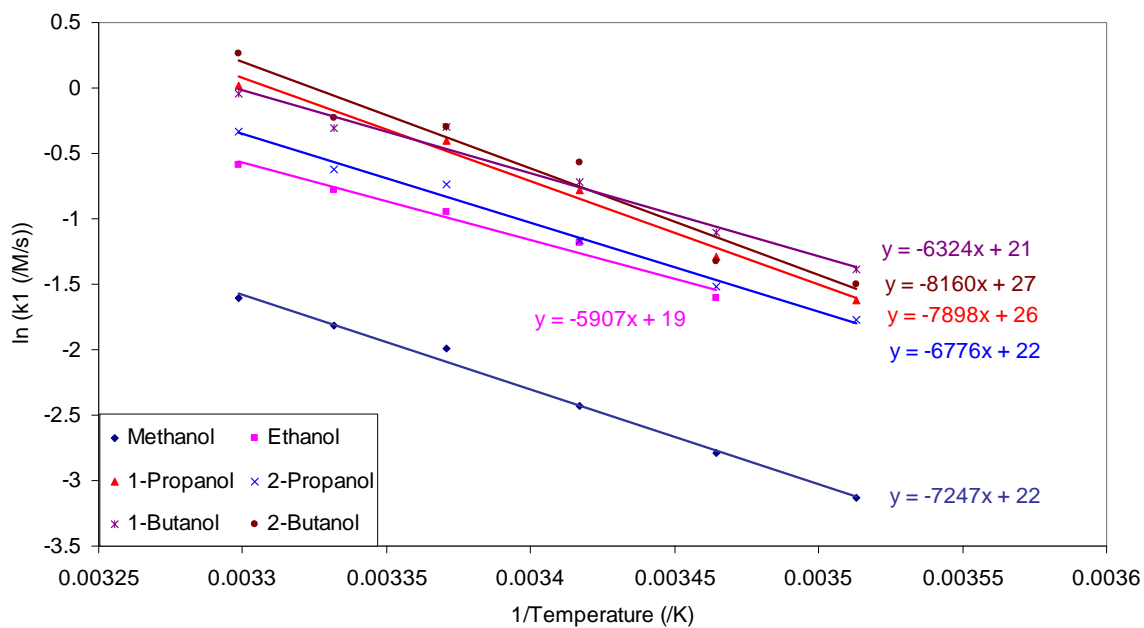
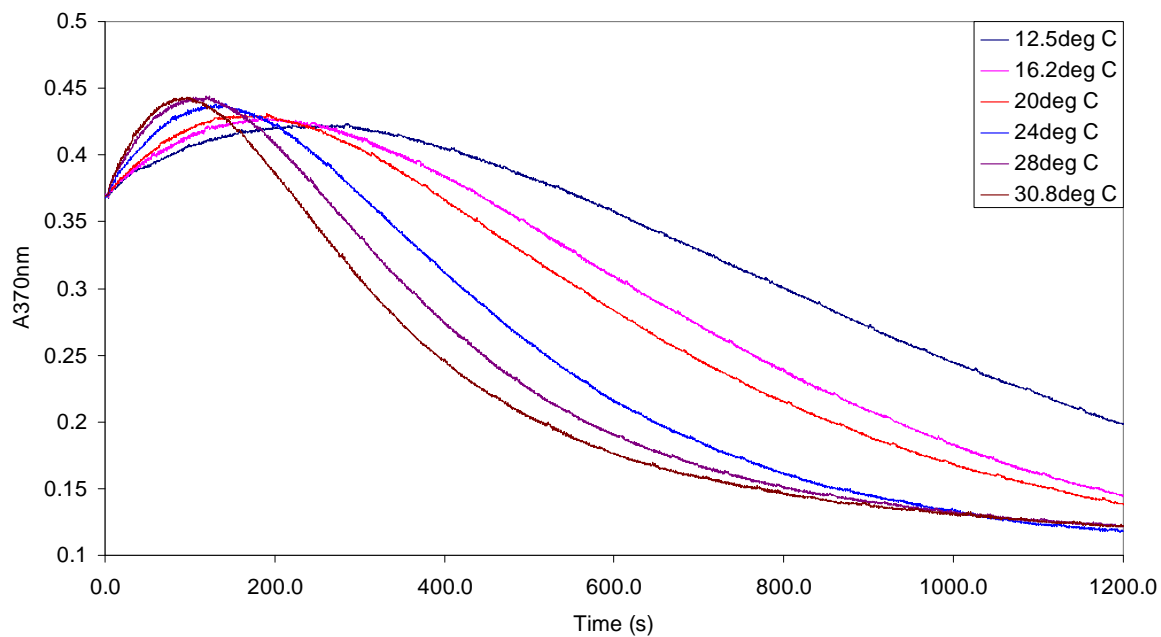


Figure 8.18: Arrhenius plots for the various alcohols in 2M hydroxide medium.

**Table 8.6: Activation parameters for the reduction of Os(VIII) by various alcohols in alkaline medium**[Os(VIII)] =  $5.59 \times 10^{-4}$ M; [alcohol] = 0.01M; [OH<sup>-</sup>] = 2M; 296.65K

	Methanol	Ethanol	1-Propanol	2-Propanol	1-Butanol	2-Butanol
$E_{a1}$ (kJ/mol)	60.3	49.1	65.7	56.3	52.6	67.9
$\Delta H^*_1$ (kJ/mol)	57.8	46.7	63.2	53.9	50.1	65.4
$\Delta S^*_1$ (JK <sup>-1</sup> mol <sup>-1</sup> )	-24.0	-28.9	-17.3	-24.0	-25.6	-15.7
$\Delta G^*_1$ (kJ/mol)	66.5	57.2	69.5	62.6	59.5	71.1

Figures 8.19 to 8.21 show the progress curves for the reactions of the three ketones with osmium tetroxide in a 0.1M hydroxide matrix at various temperatures. Qualitatively, it is clear to see that the rates of the reactions increase with increasing temperature. This is confirmed by the plot of the rate constant,  $k_1$ , as a function of temperature. There is a linear relationship between the increase in rate constant with temperature. Figure 8.23 shows the relationship between  $K_{eq}$  and temperature. There is some scatter for the acetone values but, in general, the equilibrium constant is fairly constant over the range of temperatures. The theoretical Complexation Reaction Model was fitted to the experimental data. The rate constants returned by the best fits to the data are given in Table 8.7. These were then used to plot the Arrhenius plot in Figure 8.24, which gave reasonably good straight lines for each of the alcohols. The slopes of these straight lines are equal to  $-(E_a / R)$ . Therefore, using these slopes and Equations 8.5 and 8.6, it is possible to calculate the thermodynamic activation parameters which are given in Table 8.8.



**Figure 8.19: Progress curves of the reaction of  $3.91 \times 10^{-4}$  M osmium tetroxide with  $6.22 \times 10^{-4}$  M acetone in a 0.1M hydroxide medium at various temperatures.**

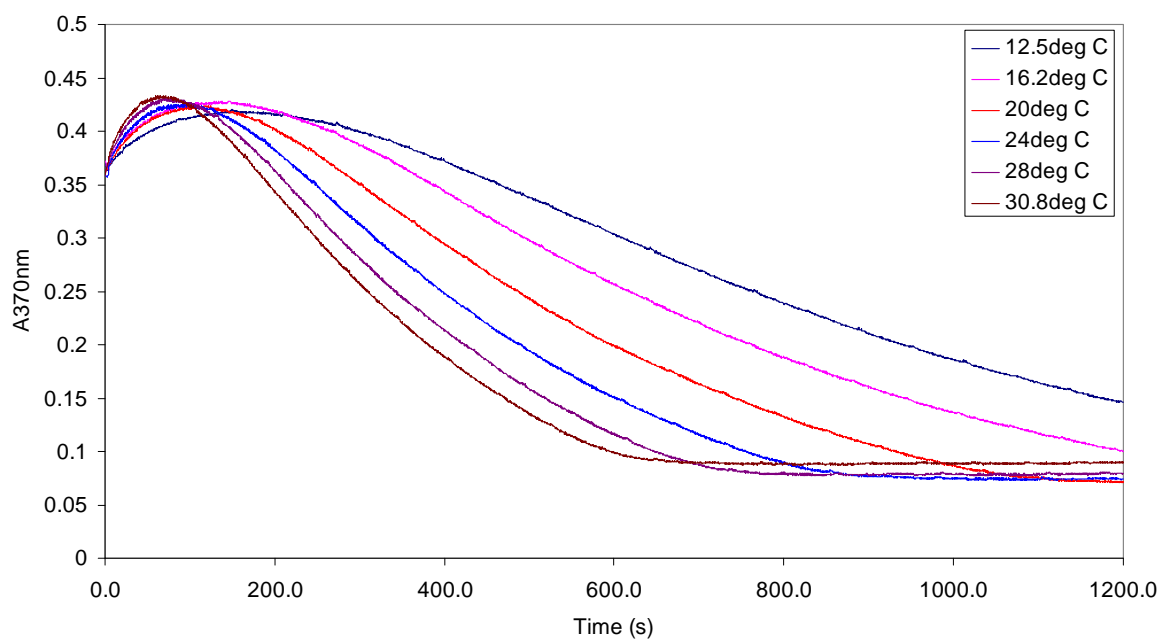


**Figure 8.20: Progress curves of the reaction of  $3.91 \times 10^{-4}$  M osmium tetroxide with  $3.50 \times 10^{-4}$  M MEK in a 0.1M hydroxide medium at various temperatures.**

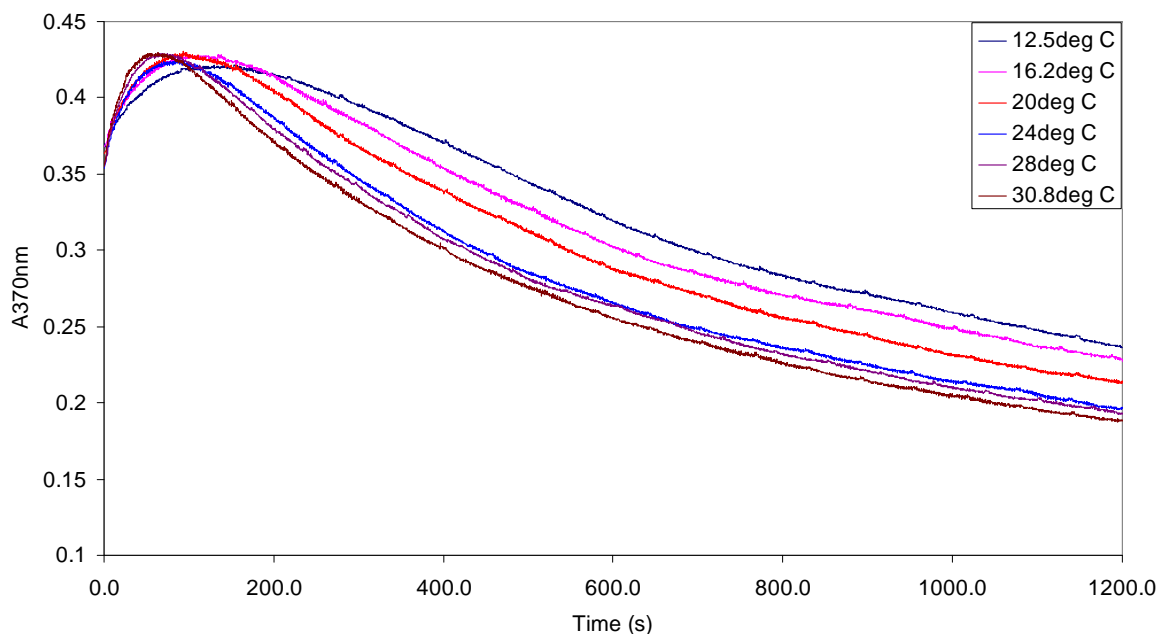


**Figure 8.21:** Progress curves of the reaction of  $3.91 \times 10^{-4} \text{M}$  osmium tetroxide with  $1.59 \times 10^{-4} \text{M}$  acetophenone in a  $0.1 \text{M}$  hydroxide medium at various temperatures.

**Table 8.7:** Rate constant,  $k_1$  and equilibrium constant,  $K_{\text{eq}}$ , obtained from the best fit of the rate modelling software. Molar extinction coefficients were held constant.

Acetone				
Temperature (°C)	$k_1$ ( $\text{M}^{-1}\text{s}^{-1}$ )	$k_{+2}$ ( $\times 10^4 \text{M}^{-1}\text{s}^{-1}$ )	$k_{-2}$ ( $\text{M}^{-1}\text{s}^{-1}$ )	$K_{\text{eq}} (\times 10^6 \text{M}^{-2})$
16.2	4.18	2.05	0.0065	3.15
20	4.19	2.74	0.010	2.74
24	5.98	3.52	0.011	3.20
28	5.95	6.68	0.027	2.47
30.8	6.22	12.09	0.057	2.12
MEK				
Temperature (°C)	$k_1$ ( $\text{M}^{-1}\text{s}^{-1}$ )	$k_{+2}$ ( $\times 10^8 \text{M}^{-1}\text{s}^{-1}$ )	$k_{-2}$ ( $\text{M}^{-1}\text{s}^{-1}$ )	$K_{\text{eq}} (\times 10^6 \text{M}^{-2})$
12.5	4.66	1.04	55	1.89
16.2	6.15	1.10	51	2.16
20	8.06	1.10	51	2.16
24	10.04	1.12	49	2.29
28	11.69	1.13	48	2.35
30.8	12.66	0.98	44	2.23

Acetophenone				
Temperature (°C)	$k_1$ ( $M^{-1}s^{-1}$ )	$k_{+2}$ ( $\times 10^8 M^{-1}s^{-1}$ )	$k_{-2}$ ( $M^{-1}s^{-1}$ )	$K_{eq}(\times 10^6 M^{-2})$
12.5	11.55	0.49	36	1.36
16.2	12.99	4.51	330	1.37
20	14.76	4.50	330	1.36
24	17.65	4.36	338	1.29
28	18.41	5.24	404	1.30
30.8	19.70	7.52	595	1.26

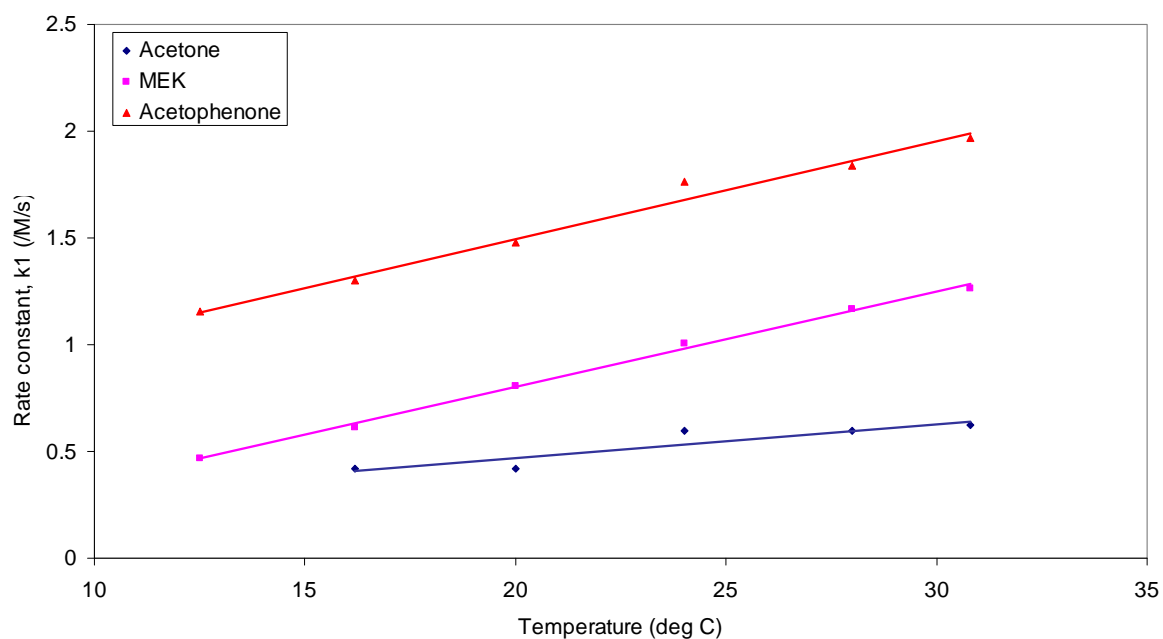


**Figure 8.22: The relationship between the rate constant,  $k_1$ , and temperature for the three ketones, acetone, MEK and acetophenone, in 0.1M hydroxide medium.**



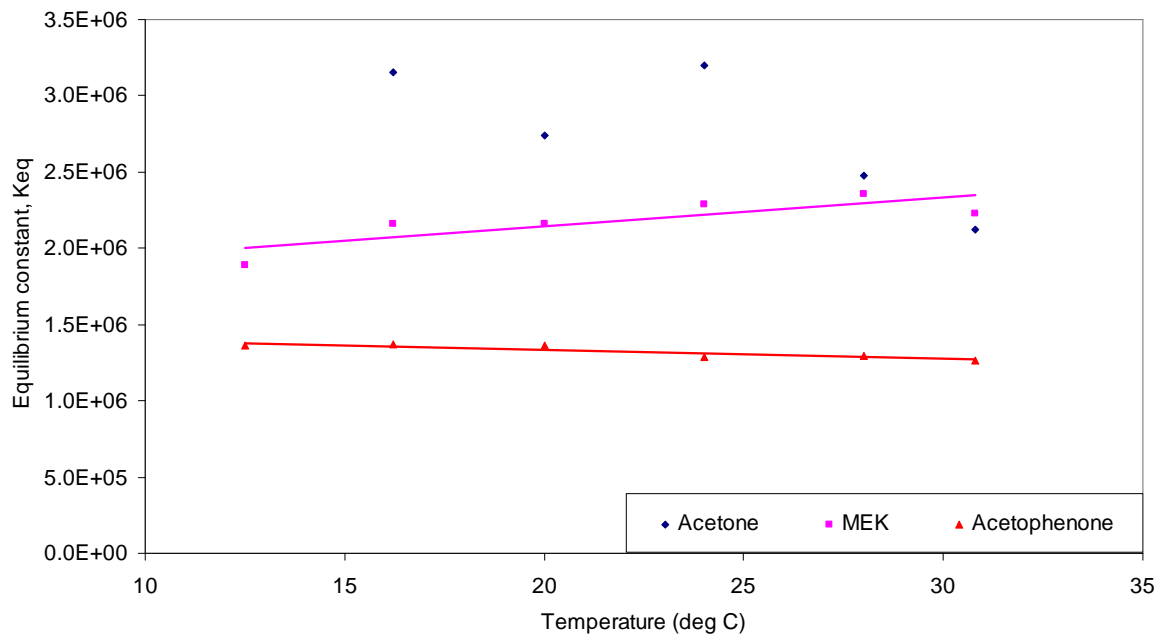


**Figure 8.23:** The relationship between the equilibrium constant,  $K_{eq}$ , and temperature for the three ketones, acetone, MEK and acetophenone, in 0.1M hydroxide medium.

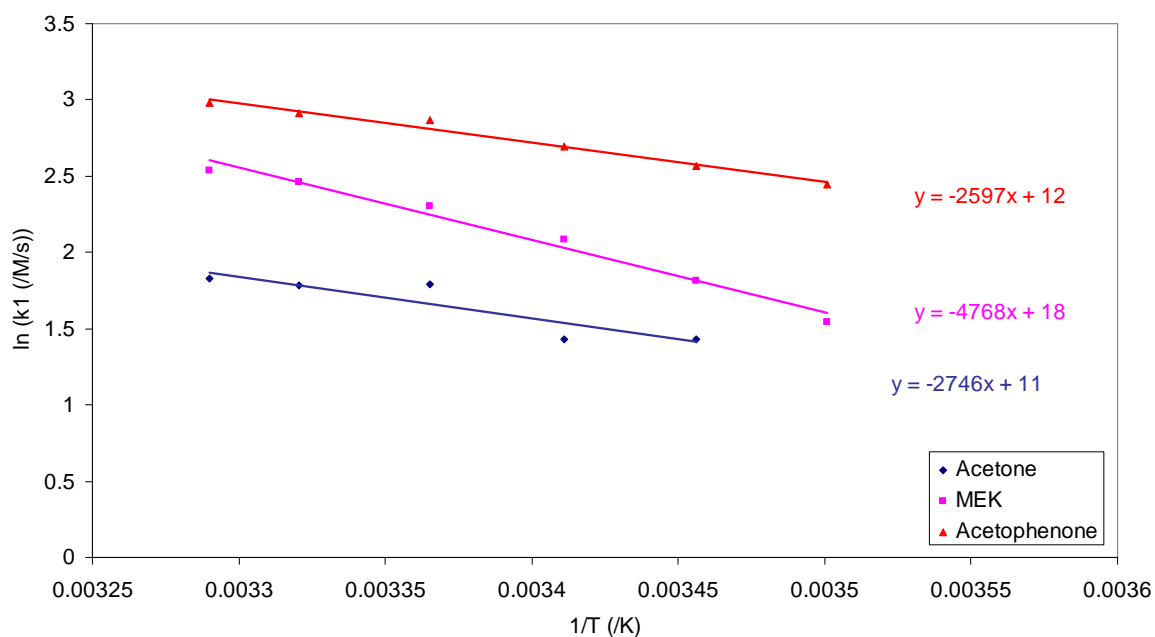


**Figure 8.24:** Arrhenius plot for acetone, MEK and acetophenone in 0.1M hydroxide medium.

**Table 8.8: Activation parameters for the reduction of Os(VIII) by various ketones in alkaline medium**[Os(VIII)] =  $3.91 \times 10^{-4}$  M; [ketone] = various; [OH<sup>-</sup>] = 0.1 M; 296.65 K

	Acetone	MEK	Acetophenone
$E_a$ (kJ/mol)	22.8	39.6	21.6
$\Delta H^*$ (kJ/mol)	20.4	37.2	19.1
$\Delta S^*$ (JK <sup>-1</sup> mol <sup>-1</sup> )	-42.2	-30.6	-40.5
$\Delta G^*$ (kJ/mol)	35.8	48.4	33.9

Thus, the dependence of the osmium tetroxide–alcohol and ketone reactions on temperature was established. The thermodynamic activation parameter  $E_a$  for the alcohols was within the typically expected limits, which are generally between 40 kJ/mol and 150 kJ/mol for an organic reaction<sup>(38)</sup>. The lower the activation energy, the faster the rate of the reaction, since almost all collisions between molecules occur with enough energy to surmount the transition state barrier. Reactions with an activation energy of less than 80 kJ/mol occur at or below room temperature, while those with an activation energy above 80 kJ/mol require heat energy to proceed. It should be clear from the preceding discussion that the calculated activation energies for the alcohols can not be entirely correct. It is empirically evident that the methanol reactions are certainly slower than the others. This should mean that the activation energy for the methanol should be the highest, necessitating the slowest reaction. This is not borne out by the results. There is much scatter in the  $E_a$  values and no clear trend is discernible. However, the values are all fairly close. This is especially true if one looks at the Gibbs free energy of activation,  $\Delta G^*$ , where the values are all very similar.

What does follow is the fact that the ketone activation energies are a lot smaller than those for the alcohols. This is empirically borne out by the fact that the ketone reactions are so much faster than those for the alcohols. This holds true even considering the fact that the rate constants are conditional on the pH of the medium and the ketone reactions were conducted in a twenty times less concentrated hydroxide medium.

Another comparison that should be drawn is that between the temperature dependence of the rate constants as opposed to the complex equilibrium constant. Although it was

difficult to get any clear results in the case of the alcohols, nevertheless the trend appears to be (and certainly is for the ketones) that the equilibrium constant,  $K_{\text{eq}}$ , is remarkably insensitive to temperature changes. The changes in the rates of the reactions appear to be entirely due to changes in the rate of the osmium(VIII) – substrate redox reaction and not the osmium(VIII) – osmium(VI) complexation reaction.

Naturally, the activation enthalpies and Gibbs activation energies have positive values since the transition state will be higher in energy than either the reactants or the products and will therefore require an input of energy. The negative values for the activation entropies,  $\Delta S^*$ , indicate a transition state that has a greater degree of order than the reactants. That is, there has been a decrease in entropy. In chemical terms, entropy decreases during associative processes<sup>(45)</sup>. A decrease in entropy may also be due to an increase in the polarity of the transition state, which causes an increase in the degree of solvation. Conversely, entropy will increase during dissociative processes such as the solution of crystals, mixing of reagents and breaking of bonds. It was seen in Section 8.3.4 that there is an increase in the rate with a decrease in the dielectric constant. It was inferred by that result that the transition state was a molecule of decreased charge. It therefore makes perfect sense that the negative activation entropy is attributed to an associative process caused by the coming together of two reactant molecules to form a transition state of low charge.

### 8.3.6 Varying the substrate and substrate concentration

The progress curves for the reactions of all the various substrates are shown in Figures 8.25 to 8.37. Shown firstly are the alcohols in Figures 8.25 to 8.32. Thereafter, the ketones in Figures 8.33 to 8.36 and, finally, the progress curves of the reaction of maleic acid ( $\text{HOOCCH}=\text{CHCOOH}$ ) with osmium tetroxide in Figure 8.39. All of these reactions were fitted to the Complexation reaction model and the best fits to the data generated rate constants, which are reported in Table 8.9.

#### ALCOHOLS

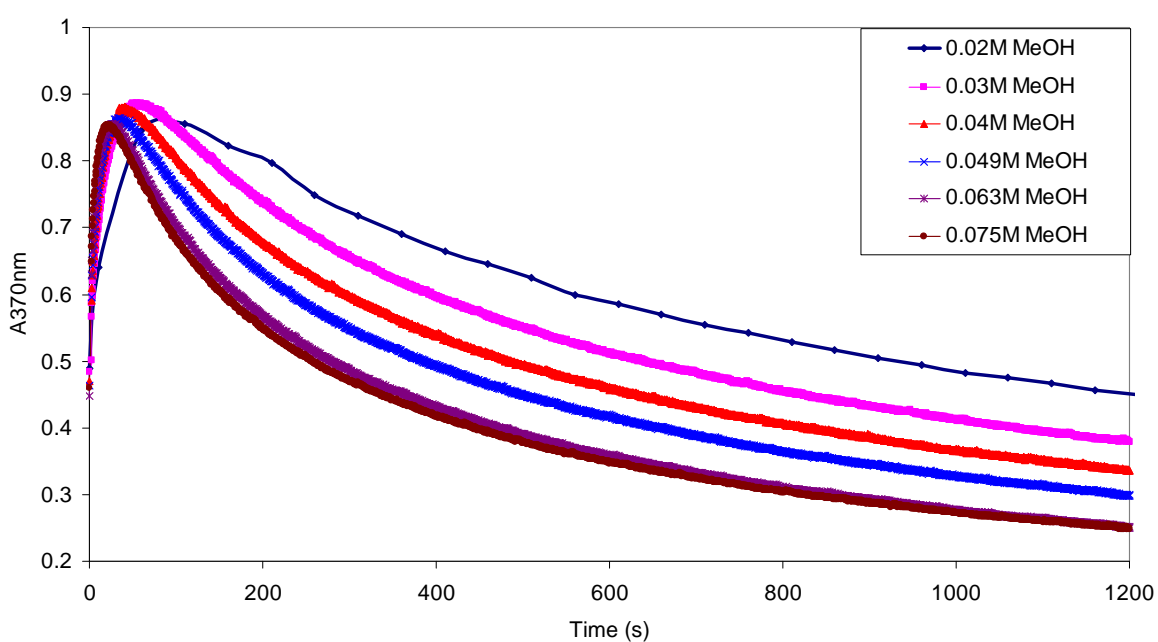


**Figure 8.25: Progress curves of the reaction of  $3.80 \times 10^{-4}$  M osmium tetroxide with increasing concentrations METHANOL in 2M hydroxide matrix.**

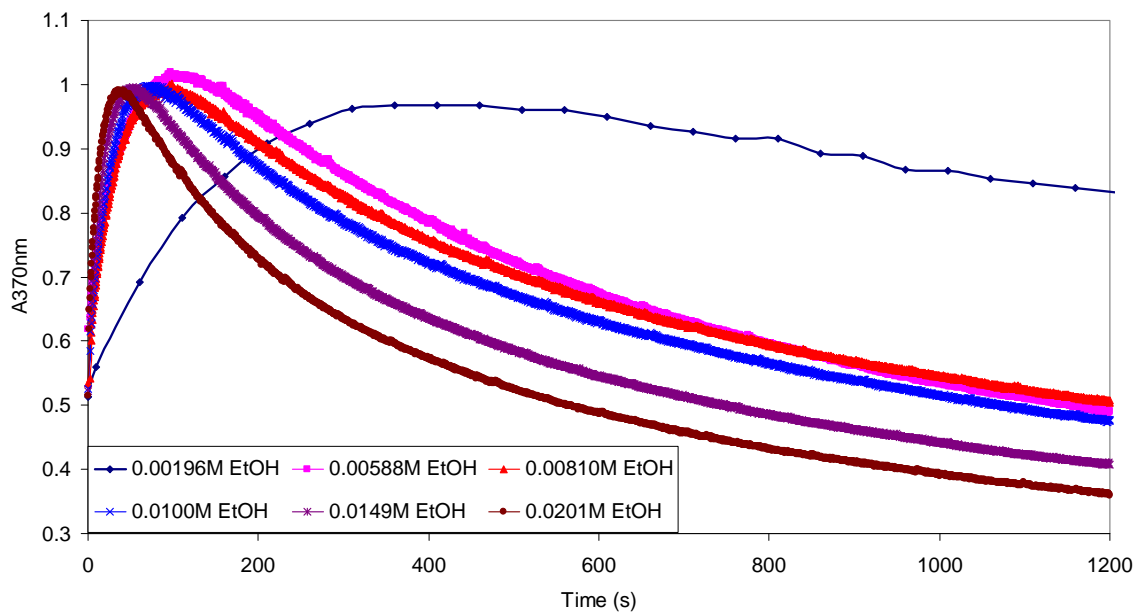


**Figure 8.26:** Progress curves of the reaction of  $4.32 \times 10^{-4}$  M osmium tetroxide with increasing concentrations ETHANOL in 2M hydroxide matrix.

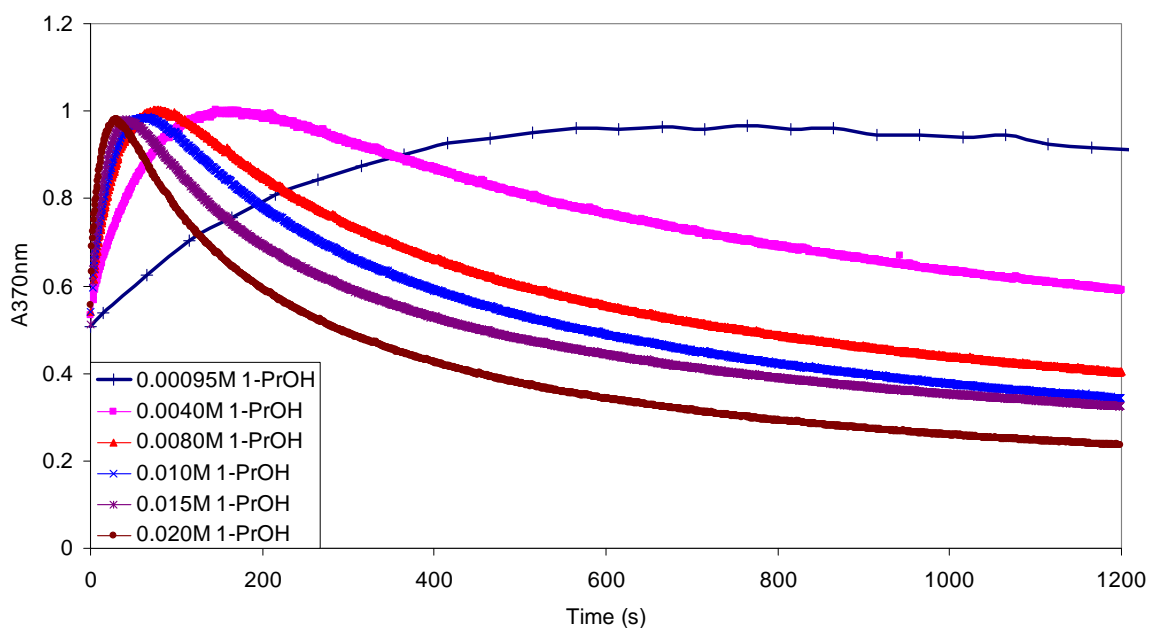


**Figure 8.27:** Progress curves of the reaction of  $4.32 \times 10^{-4}$  M osmium tetroxide with increasing concentrations 1-PROPANOL in 2M hydroxide matrix.

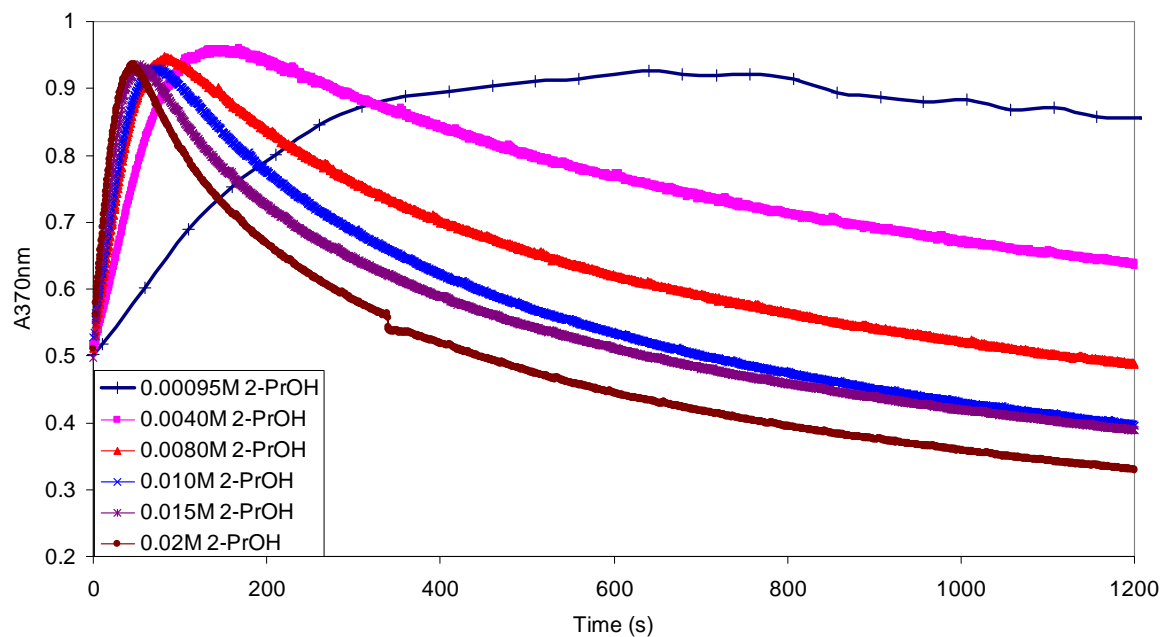


**Figure 8.28:** Progress curves of the reaction of  $4.32 \times 10^{-4}$  M osmium tetroxide with increasing concentrations 2-PROPANOL in 2M hydroxide matrix.

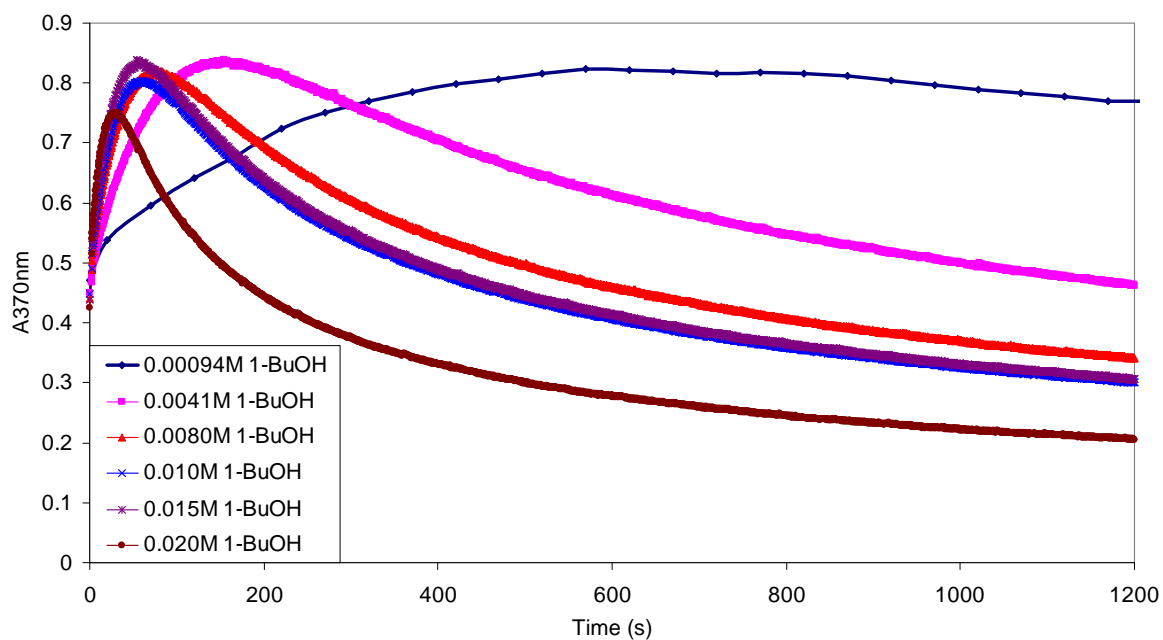


**Figure 8.29:** Progress curves of the reaction of  $3.80 \times 10^{-4}$  M osmium tetroxide with increasing concentrations 1-BUTANOL in 2M hydroxide matrix.

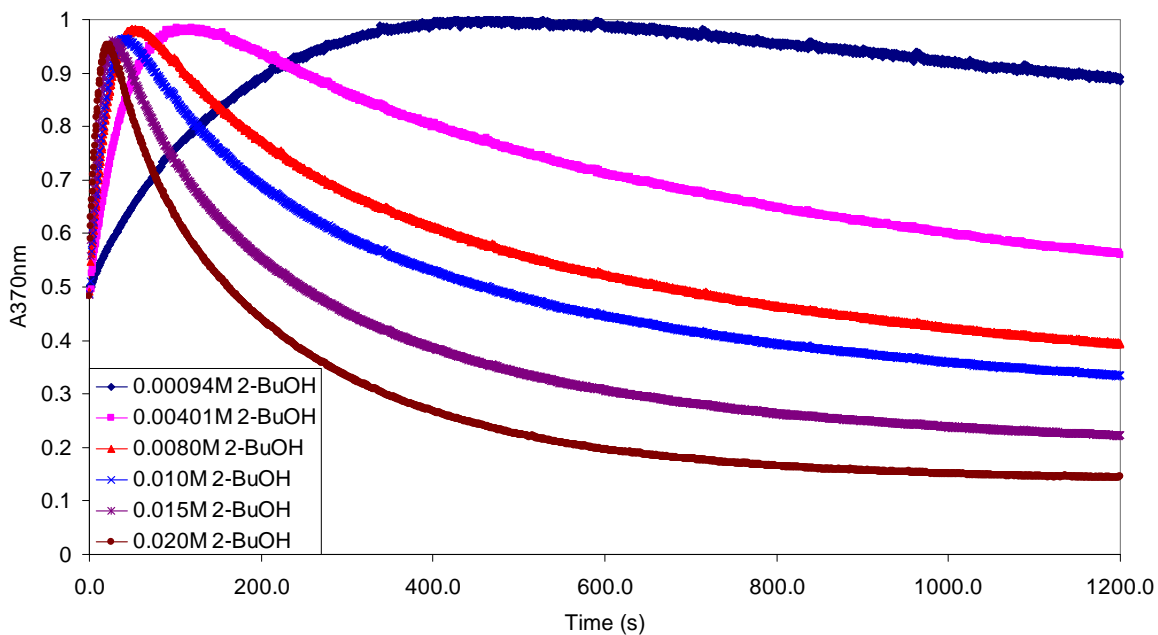


Figure 8.30: Progress curves of the reaction of  $4.80 \times 10^{-4}$  M osmium tetroxide with increasing concentrations 2-BUTANOL in 2M hydroxide matrix.

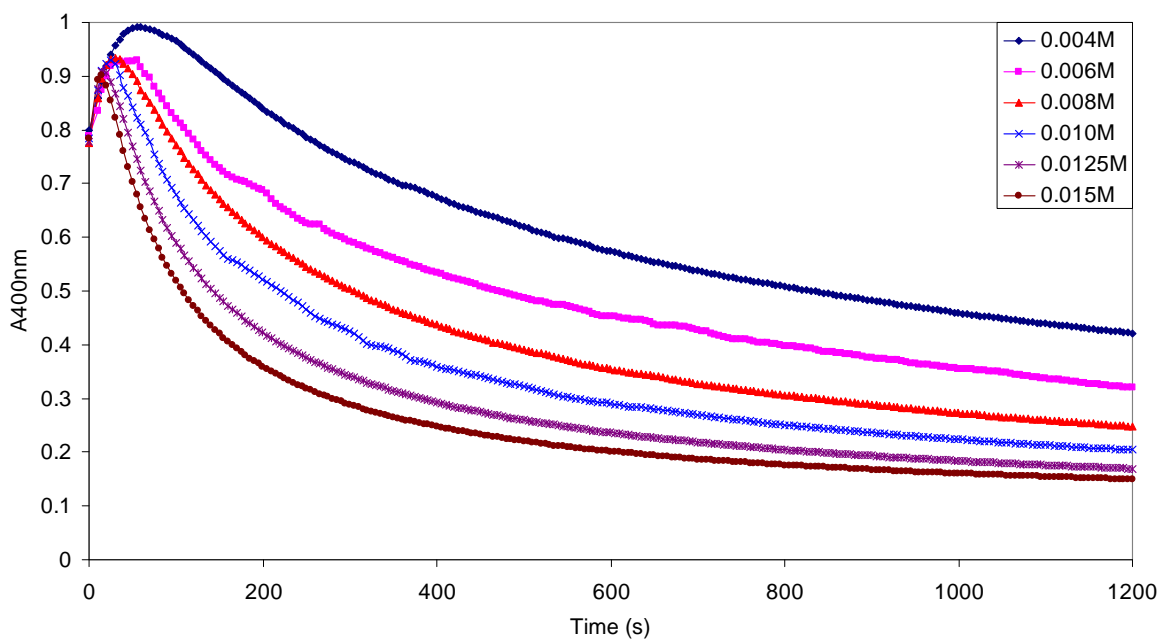


Figure 8.31: Progress curves of the reaction of  $8.54 \times 10^{-4}$  M osmium tetroxide with increasing concentrations 2-CHLOROETHANOL in 2M hydroxide matrix.

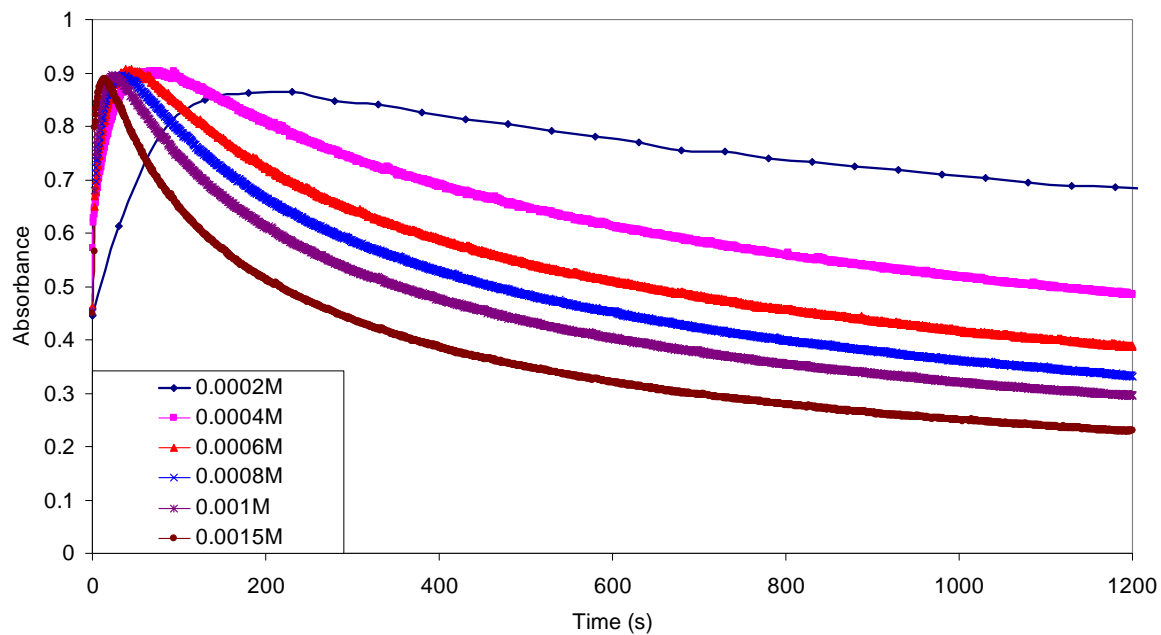


Figure 8.32: Progress curves of the reaction of  $3.71 \times 10^{-4}$  M osmium tetroxide with increasing concentrations BENZYL ALCOHOL in 2M hydroxide matrix.

### KETONES

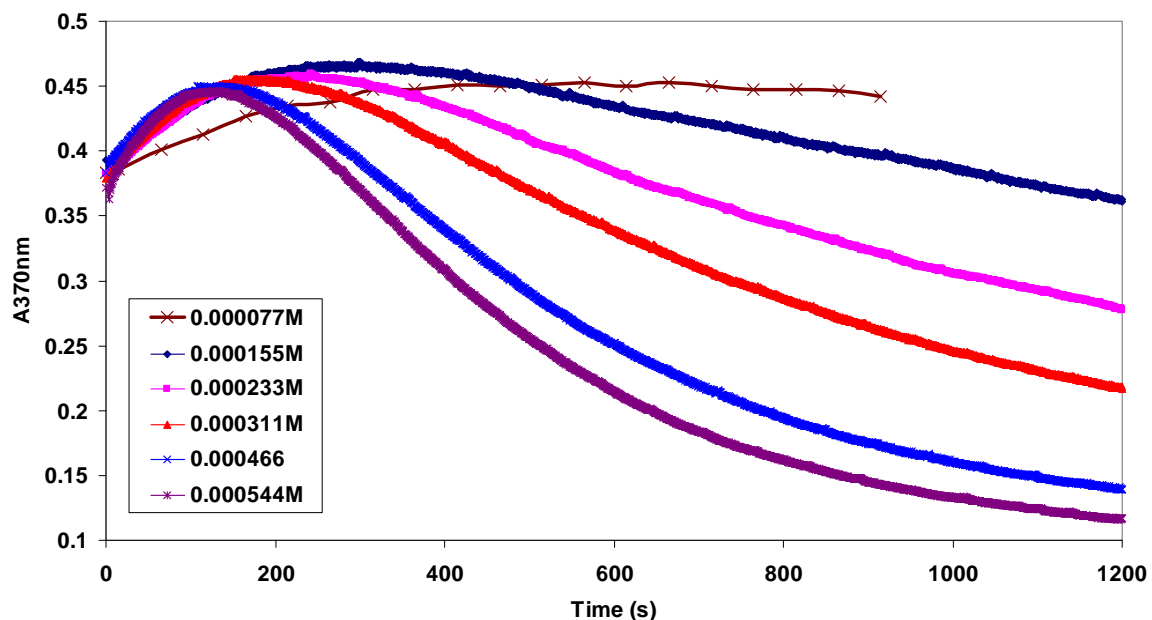


Figure 8.33: Progress curves of the reaction of  $3.45 \times 10^{-4}$  M osmium tetroxide with increasing concentrations ACETONE in 0.1M hydroxide matrix.



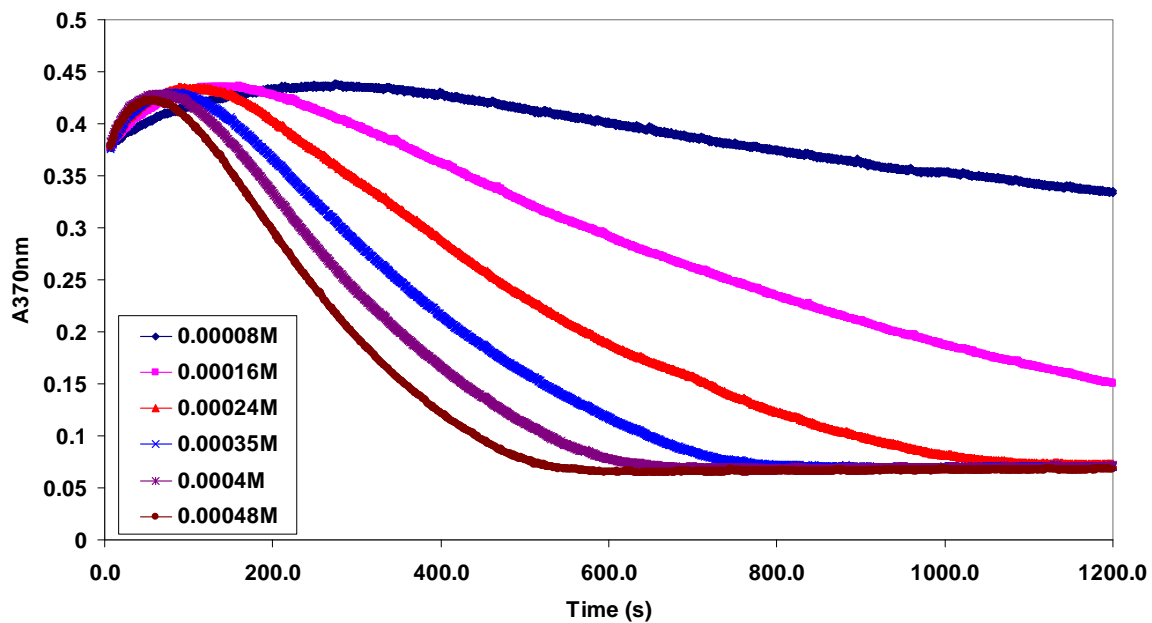


Figure 8.34: Progress curves of the reaction of  $3.76 \times 10^{-4}$  M osmium tetroxide with increasing concentrations MEK in 0.1M hydroxide matrix.

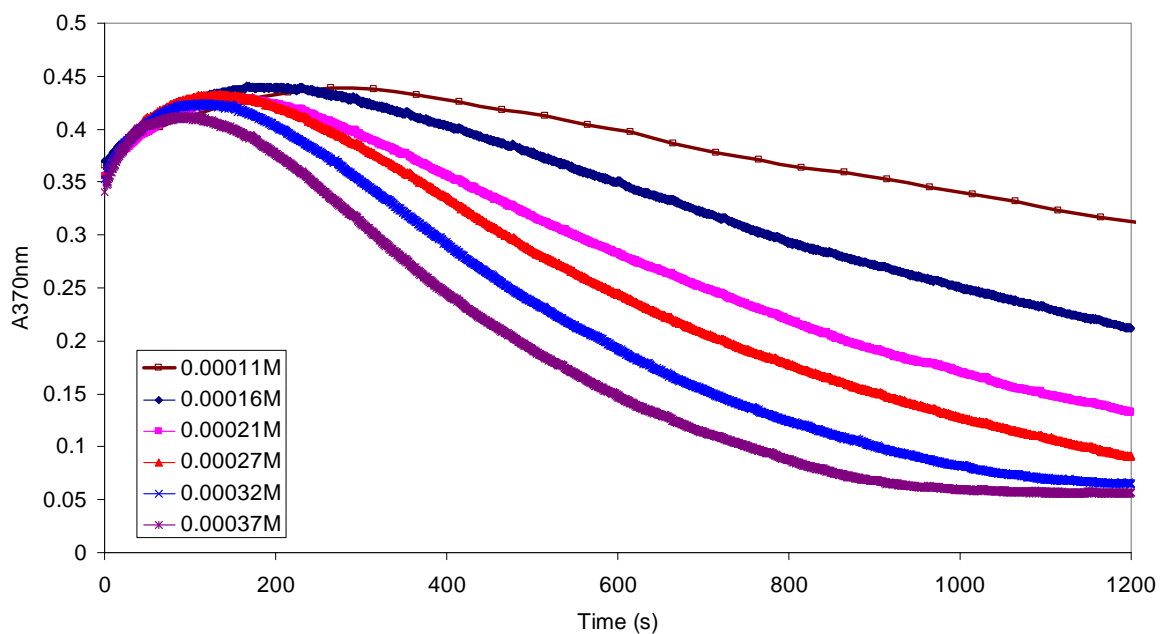
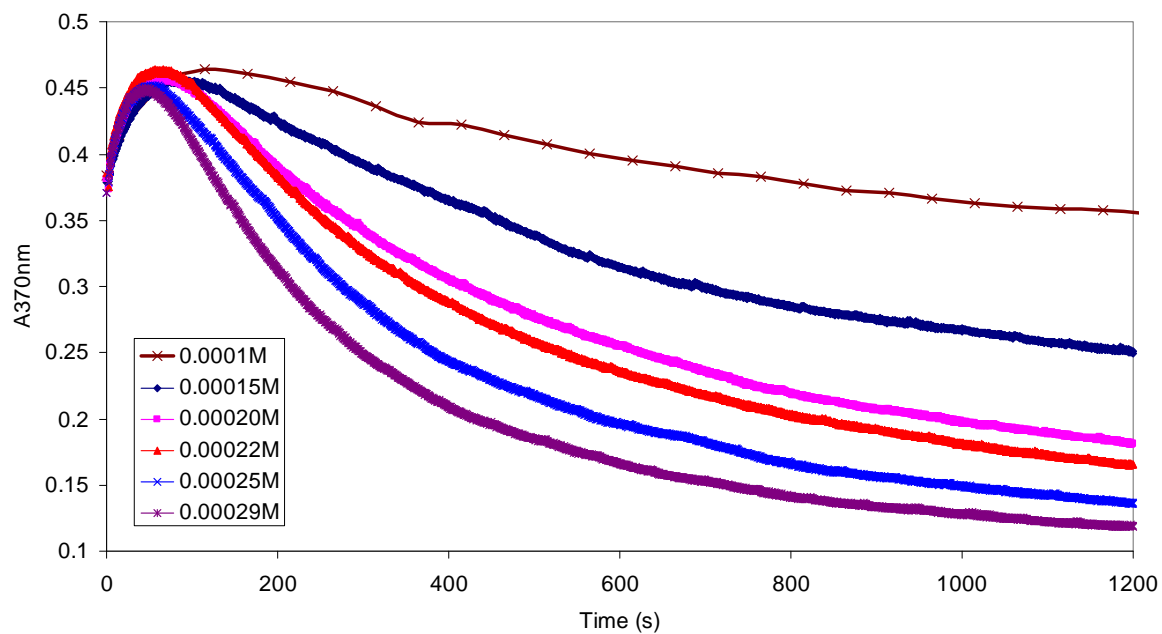
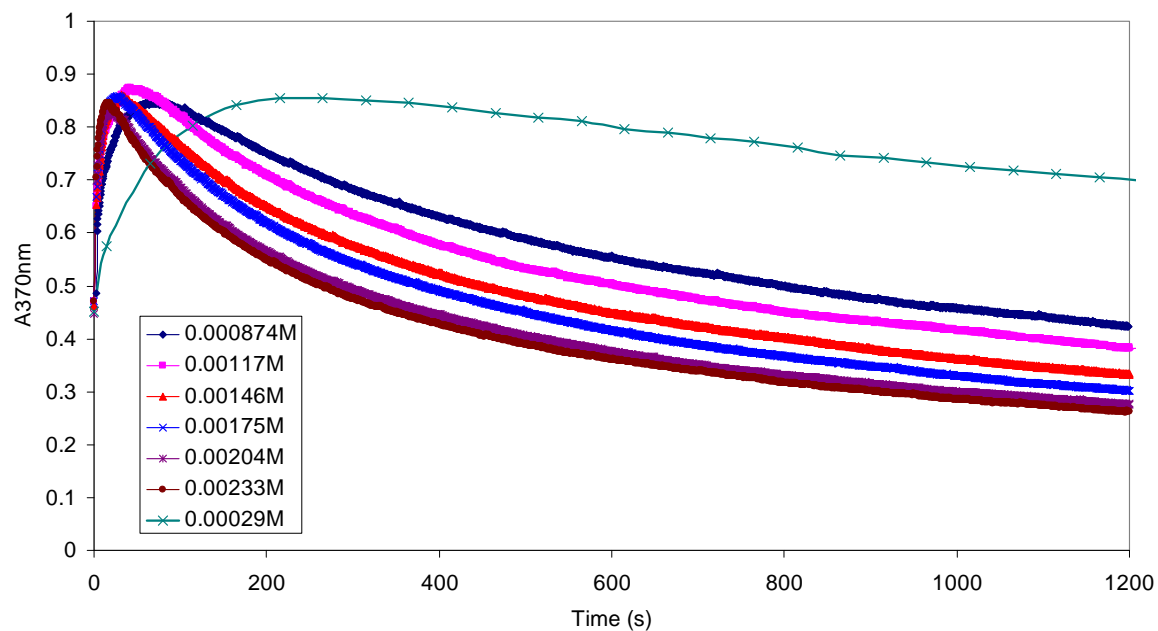


Figure 8.35: Progress curves of the reaction of  $3.76 \times 10^{-4}$  M osmium tetroxide with increasing concentrations 2-PENTANONE in 0.1M hydroxide matrix.



**Figure 8.36:** Progress curves of the reaction of  $3.97 \times 10^{-4} \text{M}$  osmium tetroxide with increasing concentrations ACETOPHENONE in 0.1M hydroxide matrix.

**ALKENE**



**Figure 8.37:** Progress curves of the reaction of  $3.89 \times 10^{-4} \text{M}$  osmium tetroxide with increasing concentrations MALEIC ACID in 2M hydroxide matrix.

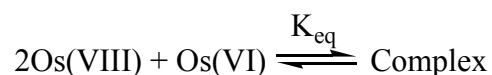
**Table 8.9: Parameters determined by rate modelling software for the reaction of osmium tetroxide with various substrates. [Hydroxide] (alcohols, maleic acid and no substrate) = 2M; [Hydroxide] (ketones) = 0.1M; Temperature = 25°C**

Alcohol	$k_1$ ( $M^{-1}s^{-1}$ )	$K_{eq}$ ( $\times 10^8 M^{-2}$ )	$\epsilon_{Os(VIII)}$ ( $M^{-1}cm^{-1}$ )	$\epsilon_{Complex}$ ( $M^{-1}cm^{-1}$ )	$\epsilon_{Os(VI)}$ ( $M^{-1}cm^{-1}$ )
Methanol	0.353	9.99	1210	8180	889
Ethanol	1.288	9.99	1317	8180	1034
1-Propanol	1.406	9.99	1210	8180	909
2-Propanol	1.624	9.99	1210	7425	1058
1-Butanol	1.600	9.99	1210	7445	808
2-Butanol	1.986	9.99	1210	6855	697
Benzyl alcohol	30.12	9.99	1210	8180	965
2-Chloroethanol <sup>a</sup>	3.430	9.99	918	3304	217
<b>Maleic acid</b>	11.64	9.99	1210	8090	935
<b>No substrate</b>	$1.03 \times 10^{-5}$ <sup>b</sup>	0.352	964	8556	815
Ketone	$k_1$ ( $M^{-1}s^{-1}$ )	$K_{eq}$ ( $\times 10^6 M^{-2}$ )	$\epsilon_{Os(VIII)}$ ( $M^{-1}cm^{-1}$ )	$\epsilon_{Complex}$ ( $M^{-1}cm^{-1}$ )	$\epsilon_{Os(VI)}$ ( $M^{-1}cm^{-1}$ )
Acetone	6.48	9.13	1072	8180	414
Methyl ethyl ketone	14.01	7.87	882	8180	209
2-Propanone	8.88	7.54	906	8180	160
Acetophenone	18.95	6.79	952	8180	440

<sup>a</sup> Molar extinction coefficients at 400nm

<sup>b</sup>  $s^{-1}$

Table 8.9 above gives the parameters for the reactions of osmium tetroxide with all the various substrates. The reactions with the alcohols, maleic acid and with no substrate at all (that is, in pure sodium hydroxide) were all performed in a 2M hydroxide matrix. It should be noted that having no substrate present implies a first order rate reaction. The complexation reaction

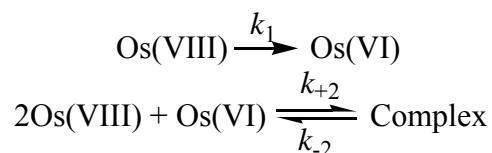


should yield the same equilibrium constant at the same hydroxide concentrations, since it is not dependent on the type of substrate used. Therefore,  $K_{eq}$  was held constant for all alcohols in order that the rate constant,  $k_1$ , did not become distorted by varying  $K_{eq}$  values. When  $K_{eq}$  was allowed to shift, the modelling programme returned rate constants that were inconsistent with the observed rates across the range of substrates. It was not possible to

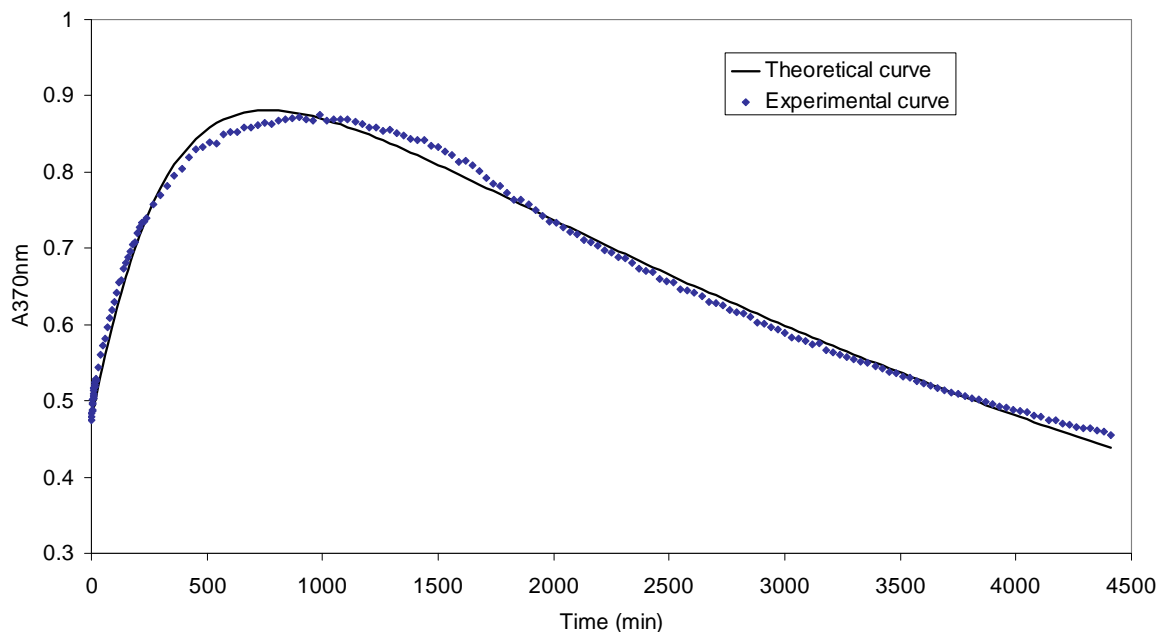
keep this value constant for the reaction of osmium tetroxide with hydroxide since the fit of the reaction model to the experimental data became too poor. Likewise,  $K_{\text{eq}}$  was allowed to shift in fitting the reaction model to the ketone data in order to obtain a good fit. However, the variation in  $K_{\text{eq}}$  is not too great.

Obviously molar extinction coefficients for the osmium species should also remain constant. The easiest of the osmium molar extinction coefficients to simulate is that of the osmium(VIII) species since that should be the only absorbing species present at the start of the reaction. Remembering that the osmium(VIII) species is pH dependent, there is some variation in the values, even at the same pH. Therefore it is not surprising that there should be some variations in the molar extinction coefficients of the other osmium species. Most important to keep reasonably constant, is the complex molar extinction coefficient since large variations in this will cause distortions in the equilibrium constant. The values are fairly consistent across the range of substrates and constant in the case of the ketones. Although in no way constrained to that value, they return values that are remarkably close to the value predicted in Chapter 5.3.1.4 by  $A_x$  versus  $A_y$  plots ( $7283 \text{ L}\cdot\text{mol}^{-1}\cdot\text{cm}^{-1}$ ).

A first order rate constant was determined for the reaction of osmium(VIII) in a pure hydroxide medium. This was done by fitting the model



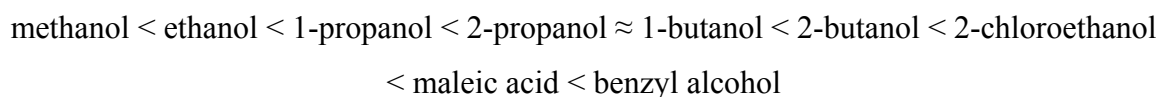
The best fit is given below in Figure 8.38. The rate constant,  $k_1$ , is extremely small at  $1.03 \times 10^{-5} \text{ s}^{-1}$ .



**Figure 8.38: Best fit of the theoretical complexation model to the reaction of  $4.93 \times 10^{-4}$  M osmium tetroxide in 2M hydroxide**

Figure 8.39 compares all the first order rate constants of reactions performed in 2M hydroxide while Figure 8.41 shows the rate constants of the ketone reactions performed in 0.1M hydroxide medium. What is immediately apparent from Figure 8.39 is the very large value for the benzyl alcohol reaction. If we compare just the simple alcohols, methanol to butanol (Figure 8.40), we find that, in general, there is an increase in the rate of the reaction with an increase in the length of the carbon chain. There is a rather large increase in the rate from methanol to ethanol. Thereafter, there is a small increase to the average propanol and, again, to the average butanol rate constant. In comparing isomers, 2-propanol has a larger rate constant than 1-propanol and, similarly, 2-butanol has a larger rate constant than 1-butanol.

Thus, the rate of the reaction increases in the order:



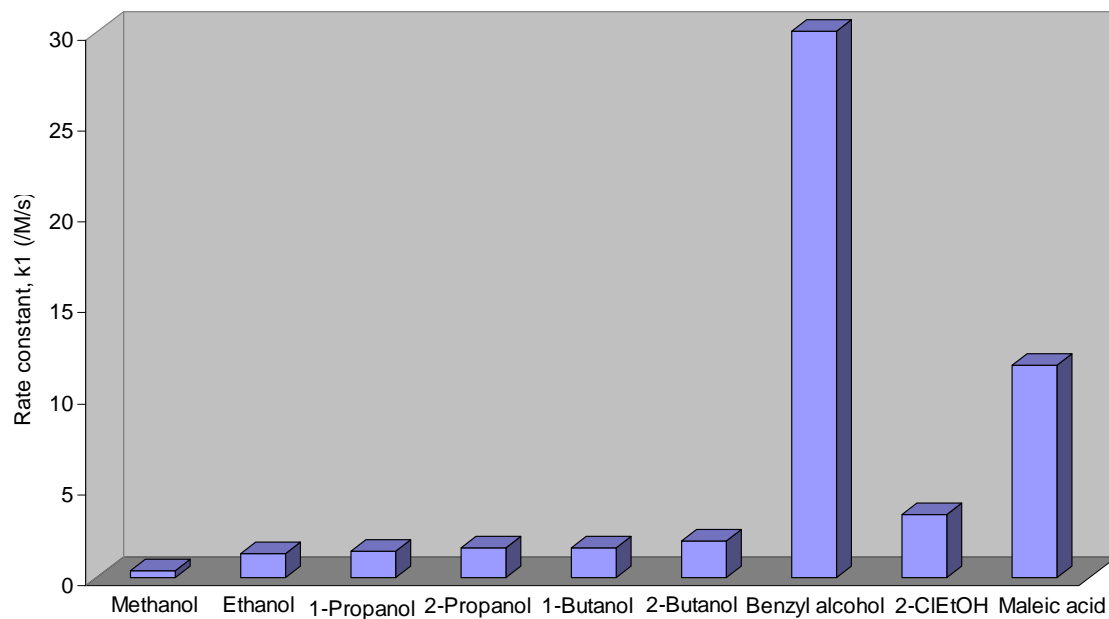


**Figure 8.39:** Comparison of the rate constants,  $k_1$ , for the reaction of osmium tetroxide with alcohols and maleic acid in a 2M hydroxide matrix.

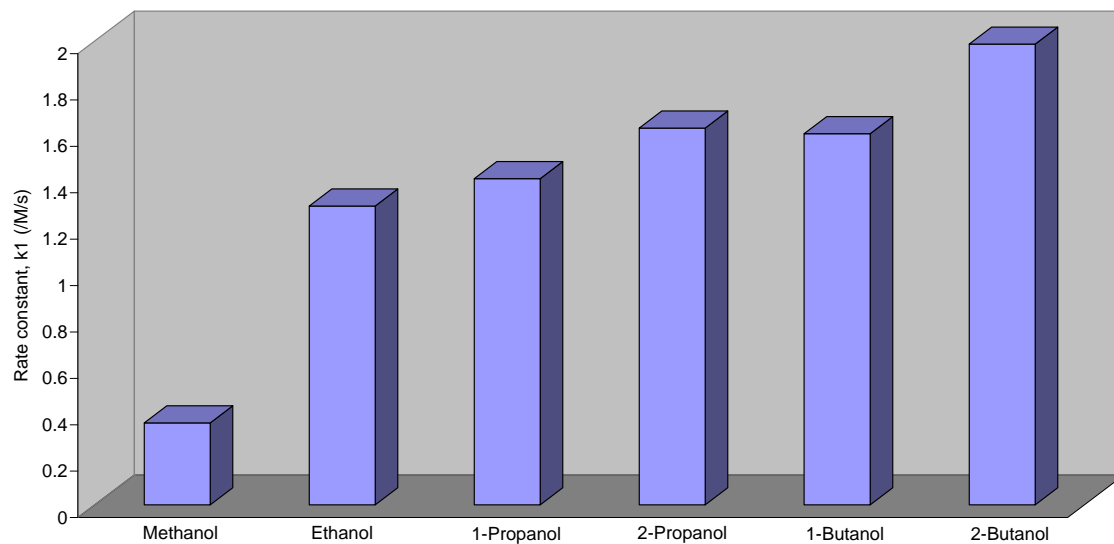


**Figure 8.40:** Comparison of the rate constants,  $k_1$ , for the reaction of osmium tetroxide with the simple alcohols, methanol to butanol, in a 2M hydroxide matrix.

In comparing the ketone reactions, approximately the same trend is seen except for the anomalous 2-pentanone, which has a smaller rate constant than the shorter chain MEK. Although not possible to make a direct comparison in the rate constants for the reactions with alcohols compared to ketones because of the differing pH's of the solutions, it is entirely evident that the reactions of the ketones are faster than those for the alcohols. This was also discussed in Section 8.33. MEK, for example has a rate constant of  $96.9\text{M}^{-1}\text{s}^{-1}$  in 2M hydroxide.

Maleic acid, at a rate constant of  $11.64\text{M}^{-1}\text{s}^{-1}$  in 2M hydroxide, is somewhere between those of the ketones and the alcohols. This is reasonable, since it will be argued that it has a similar mechanism to those of the ketones.

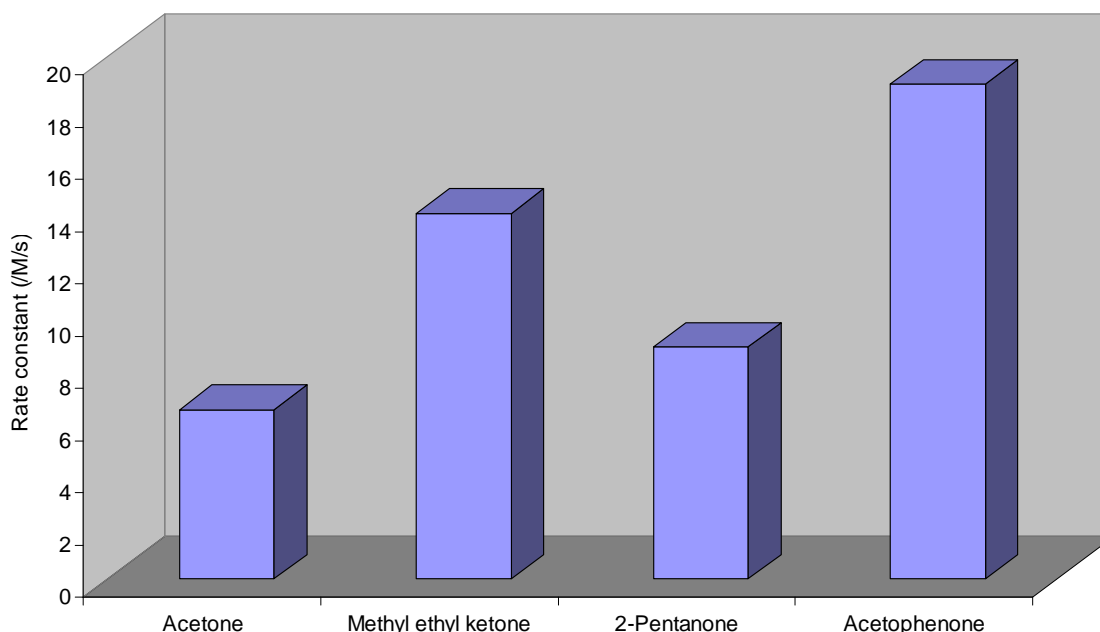


**Figure 8.41:** Comparison of the rate constants,  $k_1$ , for the reaction of osmium tetroxide with ketones in a 0.1M hydroxide matrix.

In order to compare the reactions in a systematic way, a Taft plot was constructed (Figure 8.42). This is done by choosing a reference reaction and by comparing the rates of closely similar reactions with this reference reaction.

$$\log \frac{k_1}{k_0} = \rho^* \sigma^*$$

Methanol was considered as the reference reaction with a rate constant,  $k_0$ . The other, variously substituted, alcohols have rate constants,  $k_1$ , as reported in Table 8.9. Figure 8.42 shows the Taft plot for the alcohols ethanol, 1-propanol, 2-propanol, 1-butanol and 2-butanol. The  $\sigma^*$  values for the substituents, defined as X in X-OH, were obtained from Hine<sup>(47)</sup> (for ester hydrolysis). The inclusion of benzyl alcohol and 2-chloroethanol in the Taft plots results in a reversal of the slope of the plot (Figure 8.43). This type of deviation from linearity may be due to a change in the mechanism of the reaction or due to a change in the rate-determining step of a multi-step reaction<sup>(45)</sup>. A discontinuity in the Taft plot concave downwards is indicative of a change in the rate-determining step, whereas a change in slope concave upwards is indicative of a change in mechanism. Since these are changes of the latter variety, it may indicate that there is a change in mechanism when using benzyl alcohol or 2-chloroethanol as the reducing agent. Alternatively, the Taft equation only takes into account contributions to the rate due to the inductive effect of substituents to the functional group. Steric effects and resonance are not taken into account. Therefore, there may be contributions to the rate of the benzyl alcohol reaction from resonance structures that stabilise the transition state. These aspects will be covered in more detail in Chapter 9.

Apart from experimental errors in rate constants, one may expect the experimental points to lie some 10 to 15% off the best straight line<sup>(45)</sup>. This is the limit to which the relationship holds due to minor variations in solvation and other unrelated factors. This accounts for the scatter in Figure 8.42.

The slope of the Taft plot is the reaction constant,  $\rho^*$ . This is a measure of the sensitivity of the reaction to electronic perturbation. If  $\rho^*$  is positive then the rate of the reaction will be increased by adding electron-withdrawing substituents to the substrate. Conversely, if  $\rho^*$  is negative then the rate of the reaction will be increased by adding electron-donating substituents to the substrate<sup>(45)</sup>. In other words, there is the development of some positive charge on the transition state, which is stabilised by electron-donating substituents. The



negative value for  $\rho^*$  in Figure 8.42 suggests that the rates of the reactions undergo an increase upon the addition of electron donating substituents. It also correlates quite well with previously published results using the alcohols methanol, ethanol, 1-propanol, 1-butanol, isobutanol and 1-pentanol and reporting a  $\rho^*$  value of -1.91<sup>(14)</sup>.

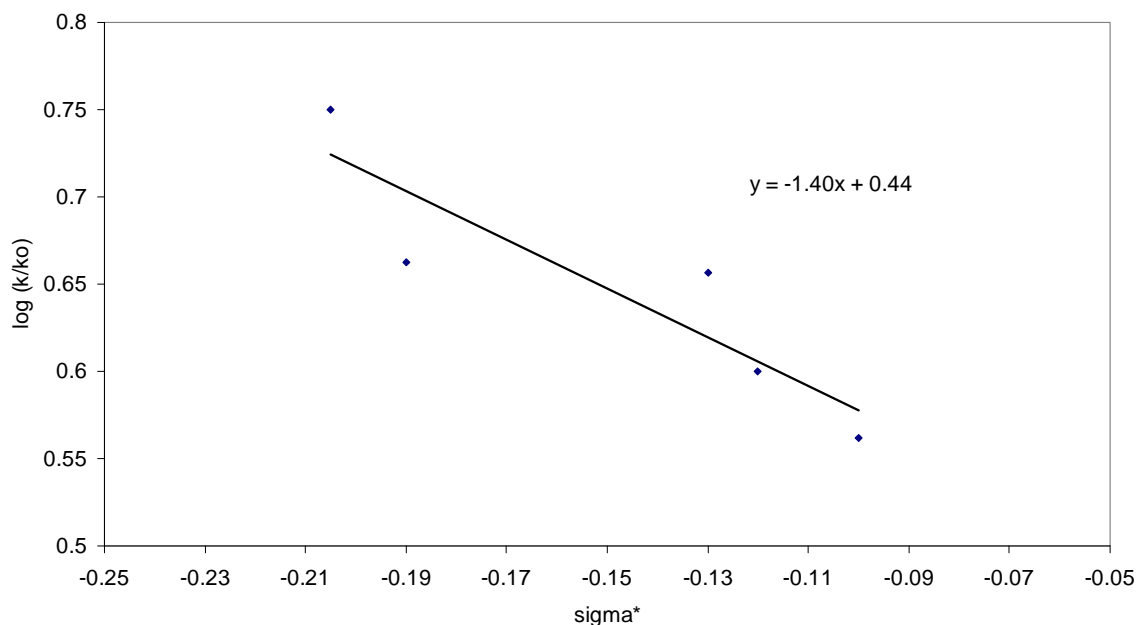


**Figure 8.42:** Taft plot, incorporating the alcohols ethanol, 1-propanol, 2-propanol, 1-butanol and 2-butanol.

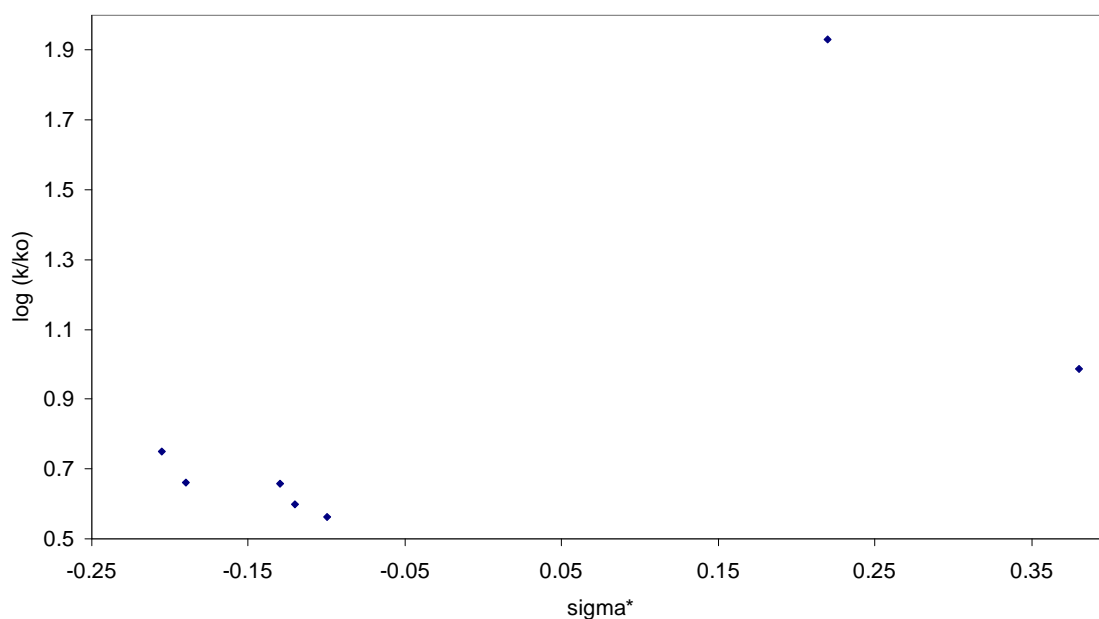


**Figure 8.43:** Taft plot, incorporating all of the alcohols from Figure 8.46, as well as benzyl alcohol and 2-chloroethanol.

## 8.4 SUMMARY

1. The initial osmium-ethanol reaction is first order with respect to osmium concentration.
2. The initial osmium-ethanol and osmium-MEK reactions are first order with respect to hydroxide concentration.
3. No reaction occurs below a threshold hydroxide concentration of approximately 0.025M.
4. No reaction occurs in water, acidic or organic matrices.
5. Above threshold hydroxide concentrations, further ionic strength perturbations make no difference to the rates of the reactions.
6. A decrease in dielectric constant results in an increase in the rate of the reaction, which implies that more highly charged reactants come together in a low charge transition state.
7. There is an Arrhenius-dependent increase in the rate of the reactions (alcohols and ketones) with increasing temperature.
8. Thermodynamic parameters were calculated.
9. Negative values for the activation entropies,  $\Delta S^*$ , indicate a transition state that has a greater degree of order than the reactants. This is caused by an associative process, which forms a transition state of low charge.
10. The rates of the osmium tetroxide-alcohol reactions increase with a variation in the substrate in the following manner:  
methanol < ethanol < 1-propanol < 2-propanol  $\approx$  1-butanol < 2-butanol <  
2-chloroethanol  $\ll$  benzyl alcohol
11. The rates of the osmium tetroxide-ketone reactions increase with a variation in the substrate in the following manner:  
acetone < 2-pentanone < methyl ethyl ketone < acetophenone
12. A Taft plot of the alcohols methanol to 2-butanol gives a straight line with a slope,  $\rho^*$ , of -1.40. This indicates an increase in the rate with an increase in the electron-donating properties of the substituents to the hydroxide functional group.
13. Benzyl alcohol and 2-chloroethanol show discontinuities in the Taft plot indicating either a change in the mechanism of the reaction, or the incorporation of factors into the rate that are not accounted for in the Taft plot (e.g. resonance, steric hindrance).

## CHAPTER 9

---

---

### CONCLUSION

---

---

The aim of this final chapter is to take all the data discussed in the other chapters and tie it together into a coherent whole with the view to proposing the reaction mechanism for the reaction series. Much of the reaction scheme has already been determined by the stoichiometric and kinetic reaction models and all that remains is to tie these schemes together into a reaction mechanism. The progress of the alcohol molecule will be followed through the reaction. Firstly, the oxidation of the alcohol to an aldehyde or ketone will be discussed, and then its further oxidation to the final products. The osmium(VIII)-osmium(VI) interaction will be discussed, and finally a single proposal for the mechanism of the reaction of osmium(VIII) with an alcohol will be put forward.

It was established in Chapters 7 and 8 that the osmium(VIII)-alcohol reaction is first order in osmium, alcohol and hydroxide. The reaction mechanism shown in Figure 9.1 is broken down into three parts: A, B and C. Concentrating firstly on part A, there must be consensus as to the osmium(VIII) species that takes part in the reaction. It has mostly been referred to as osmium(VIII) up until now. In Chapter 4, however, the ratios of the three osmium(VIII) species were given. Most of the alcohol reactions were conducted in a 2M hydroxide matrix at which hydroxide concentration the osmium(VIII) species is in the ratio 40%  $[\text{OsO}_4(\text{OH})]^-$  to 60%  $[\text{OsO}_4(\text{OH})_2]^{2-}$ . However, it has been established that there is an increase in the rate of the reaction with increasing hydroxide concentration, and that at 3M hydroxide concentration, the osmium(VIII) species are in the ratio 29.5%  $[\text{OsO}_4(\text{OH})]^-$  to 70.5%  $[\text{OsO}_4(\text{OH})_2]^{2-}$ . Therefore, it seems that the higher the concentration of  $[\text{OsO}_4(\text{OH})_2]^{2-}$ , the faster the rate of the reaction. This does not necessarily mean that there is a correlation between the two. It seems more likely, that the hydroxide participates in some other area of the reaction, thus enhancing the rate of the reaction. The reasons that the addition of the hydroxide ligands to osmium tetroxide

may not enhance, and possibly even slows, the rate of the reaction are twofold. Firstly, the osmium(VIII) centre now has octahedral geometry, a geometry favoured by osmium. This makes the addition of the alcohol or ketone in an associative transition state species less favourable (although the osmium(VIII), being a large 3d species, should be able to accommodate a 7-coordinate geometry). Secondly, the addition of hydroxide ligands to the osmium tetroxide shifts electron density onto the osmium(VIII) centre, making the osmium(VIII) a less effective electrophile. This may slow the rate of the redox reaction. However, the fact remains that the rate of the reaction is increased by increasing hydroxide concentration and  $[\text{OsO}_4(\text{OH})_2]^{2-}$  will be the osmium(VIII) species depicted as taking part in the reaction mechanism.

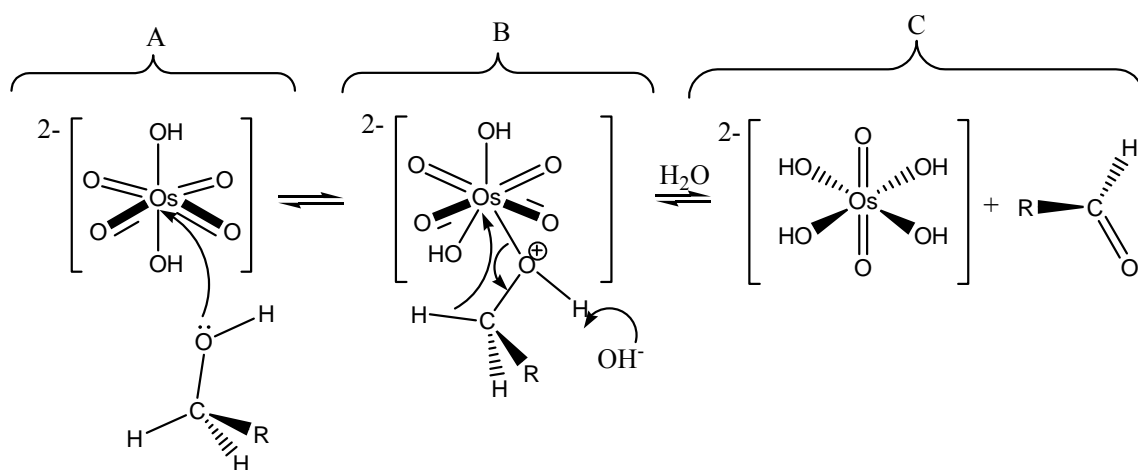


**Figure 9.1: Part 1 of the hydride transfer model – from the associative reaction of the primary or secondary alcohol molecule with the osmium(VIII), to formation of the osmate ion and the aldehyde or ketone.**

The next aspect of the reaction that must be decided is whether the reaction is initiated by C-H bond cleavage (as shown in Figure 9.2) or O-H bond cleavage (as shown in Figure 9.1). On the face of it, there are several aspects that impact negatively on the latter route. Firstly, the species  $\text{RO}^-$  will be far more reactive towards the osmium(VIII) centre than the species  $\text{ROH}$ .  $\text{CH}_3\text{O}^-$  is about 20 000 times more reactive as a nucleophile than  $\text{CH}_3\text{OH}$ . Thus, there is a definite correlation between the rate of a

reaction and the acidity of the reacting nucleophile. The more acidic a nucleophile (in this case the alcohol), the faster the reaction. In other words, since the acidity of the alcohols increases in the order, secondary alcohol < primary alcohol < methanol, the rate of the reaction should increase in the same manner. In fact, the observed rates are quite the opposite, and the methanol reaction is by far the slowest.

A second aspect initially thought to impact negatively on the associative complexation of the osmium and alcohol, was that of steric hindrance. It seems reasonable that a hindered, bulky substrate should prevent easy approach to the osmium molecule, making bond formation difficult. Once again, we see the opposite result, with the larger alcohol molecules having the fastest rates.

For the above two reasons, it was initially thought that the reaction may proceed by C-H bond cleavage as depicted in Figure 9.2. The osmium(VIII) centre, being a  $d^0$  species and a strong electrophile, abstracts a hydride ion from the alcohol in an E2 reaction. There is instant rearrangement of the hydrogen atom to an oxygen atom in the second step and then further interaction with water in the last step to form the osmium(VI) product.

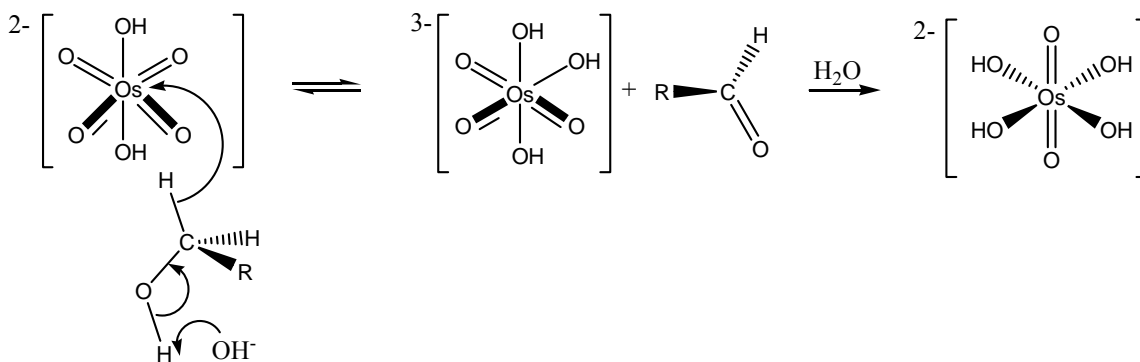


**Figure 9.2: The E2 C-H bond cleavage model**

However, there is one important aspect that the E2 mechanism does not satisfy. That is the associative formation of a low charge transition state. This was implied in two ways. Firstly, by the negative value for the activation entropy, which implied an associative

process and, secondly, by the increase in the rate with decreasing dielectric constant, which implied the stabilisation of a low charge intermediate by the less polar solvents acetonitrile and tertiary butanol. In addition, oxygen is a very good ligand for the  $d^0$  osmium(VIII) and the initial association of the alcohol through the oxygen atom is far more favourable than through a hydrogen atom.

The means of reconciling the formation of a low charge intermediate with an increase in rate despite the decreasing acidity and increasing steric hindrance of the substrates, is quite simple if part A in Figure 9.1 is not the rate limiting step in the reaction mechanism. If part B is the rate limiting step, then the parameters governing its rate will be manifest in the empirical studies. Part B of the O-H bond cleavage model depicts the association of the osmium(VIII) with the alcohol molecule through an Os-O bond to form a large, low-charge molecule in keeping with empirical evidence. This molecule undergoes hydride ion transfer in which the hydride attached to the  $\alpha$ -carbon is transferred to the osmium with the resultant formation of a C-O double bond and the reduction of the osmium(VIII) to osmium(VI). There is rapid rearrangement of the hydrogen atom to an oxygen atom in the second step and then further interaction with water in the last step to form the osmium(VI) product.

Since the transfer of the hydride ion is rate-limiting, the more stable the molecule in the absence of the hydride ion, the faster the rate of the reaction. The removal of the hydride ion results in the development of a positive charge on the  $\alpha$ -carbon. The more large and polarisable alkyl groups attached to the  $\alpha$ -carbon, the more the electron density can shift towards that transient positive charge. This results in a lower energy transition state. This explains the increase in rate with the increasing numbers of alkyl groups attached to the  $\alpha$ -carbon. Also explained by this reaction scheme is the fact that tertiary alcohols with no hydrogen attached to the  $\alpha$ -carbon cannot undergo oxidation.

A greater susceptibility to substituent effects is linked to a larger slope for the Taft plot,  $\rho^*$ . A large  $\rho^*$ -value thus implies a large charge *change* on the  $\alpha$ -carbon during the rate-limiting step<sup>(49)</sup>. The slope of the Taft plot,  $\rho^*$ , in this instance is fairly

small (-1.40)<sup>(48)</sup>. This implies that the rate-limiting hydride transfer is linked to the synchronous removal of the hydroxyl proton, which lowers the positive charge on the  $\alpha$ -carbon. This explains the rate dependence of the reaction on the hydroxide concentration and is illustrated in part B of the reaction scheme. The hydroxide ion is integral in removing the hydroxyl proton. In solutions where no strong base is present, no reaction will occur since there will be no driving force if the hydroxyl proton is not removed. This explains why no reaction occurred in acidic solutions, pure water and organic solvents.

The Taft plot confirmed that for an increase in electron-donating substituents, one could expect an increase in the rate of the reaction. The inclusion of benzyl alcohol into the Taft plot resulted in deviation from linearity. The rate of that reaction was dramatically faster than the rates of the other alcohols. This may be explained by the fact that the Taft equation only takes into account induction and not resonance or steric hindrance. It was argued above that steric effects do not impact on this reaction. However, there may be considerable resonance stabilisation of the benzyl alcohol transition state as demonstrated in Figure 9.3 below. This may account for the disproportionate increase in the rate of the benzyl alcohol reaction. Figure 9.3 also clearly demonstrates the development of the positive charge with removal of the hydride ion.

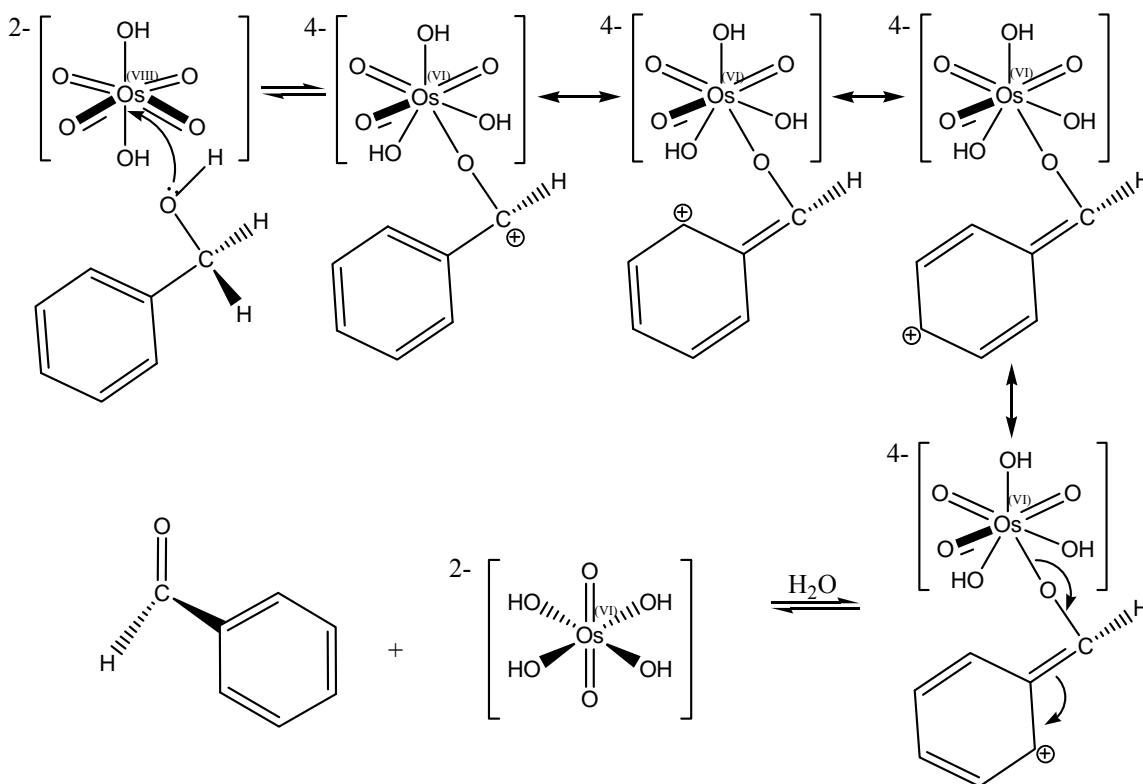


**Figure 9.3: The hydride transfer model for benzyl alcohol showing the resonance stabilisation of the associative transition state.**

The rate of the reaction with 2-chloroethanol was completely contrary to that predicted by the Taft plot. The reaction showed an increase in the rate, even though the substituents were electron-*withdrawing*. This discontinuity in the Taft plot could not be explained by resonance, but can be explained by a change in the reaction mechanism. The reaction mechanism in Figure 9.4 was initially thought to be a very elegant and simple solution to the reaction mechanism for all substrates. However, it cannot explain the empirical increase in rate with an increase in positively inductive substituents. The removal of the  $\alpha$ -hydrogen as a proton and not as a hydride ion, results in the development of a transient *negative* charge on the  $\alpha$ -carbon. This would be stabilised by electron-withdrawing substituents and accounts for the increase in rate when using 2-chloroethanol as a substrate. It is an area that requires further investigation with other substrates with electron-withdrawing substituents. If this mechanism is, indeed, an alternative to the hydride ion transfer mechanism, then the Taft plot should show two



clearly distinct portions – a straight line with negative slope for the hydride transfer mechanism and a second straight line with positive slope for the proton abstraction mechanism.

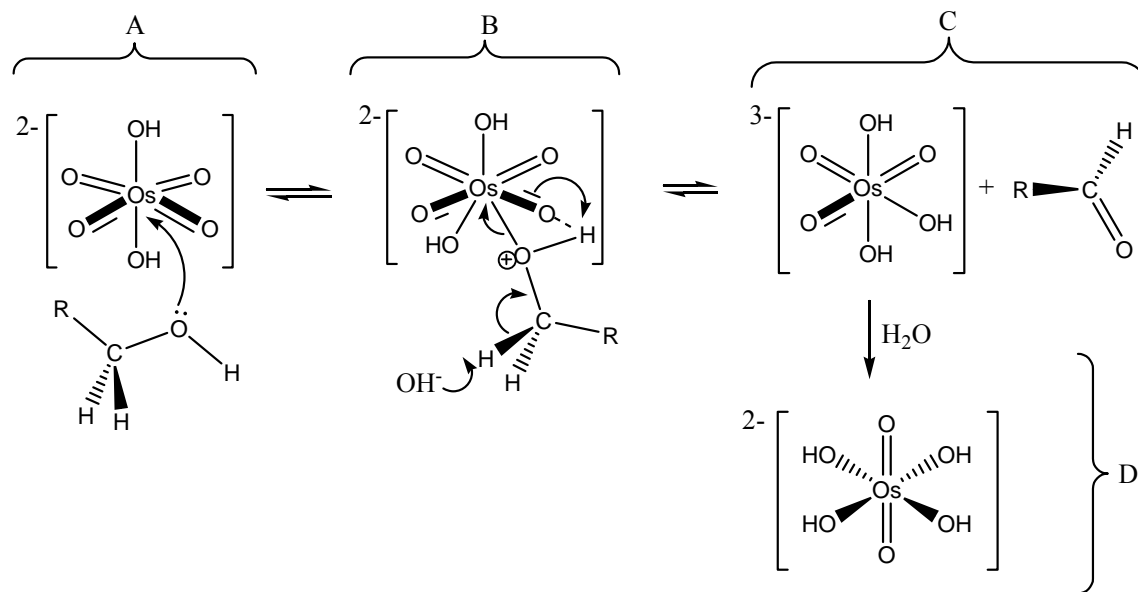


**Figure 9.4: Proton abstraction mechanism for the reaction of 2-chloroethanol with osmium tetroxide in basic medium.**

Up to this stage, the primary or secondary alcohol has been oxidised to an aldehyde or ketone. However, this is not the end of the reaction for the organic substrate. Chapter 5 showed that alcohols were oxidised through to carboxylic acids and Chapter 8 confirmed that the reaction of osmium(VIII) with MEK was 35 to 40 times faster than that with ethanol. It is feasible for an aldehyde, as the product of the reaction between osmium tetroxide and a primary alcohol, to react in a similar way to the alcohols. The aldehyde goes through an associative process initiated by a nucleophilic addition reaction of the hydroxide to the carbonyl carbon, followed by hydride ion transfer, resulting in reduction of osmium(VIII) to osmium(VI) and C-O double bond formation. This results in the formation of a carboxylic acid – the major product observed for the reaction of osmium(VIII) with primary alcohols.

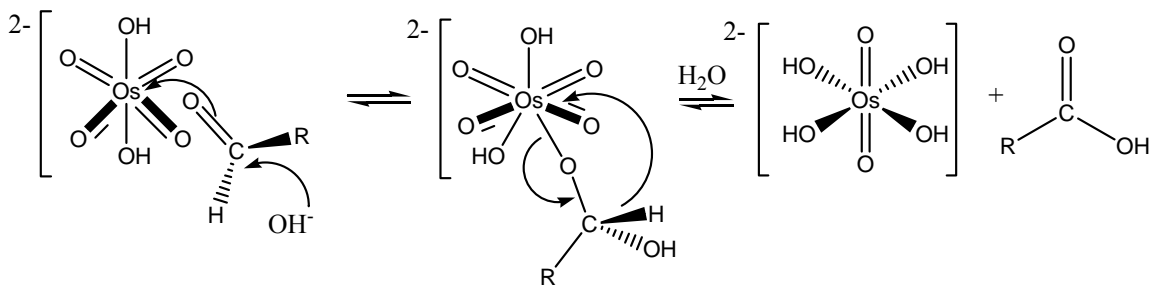


**Figure 9.5: Part 2 of the hydride transfer model for primary alcohols. The reaction mechanism for the reaction of an aldehyde with osmium(VIII) in basic medium.**

However, the situation is not so straightforward for the reaction of secondary alcohols with osmium(VIII). According to Figure 9.1, this results in the production of osmium(VI) and a ketone. A ketone does not have a hydrogen atom attached to the carbonyl carbon and, just like tertiary butanol, cannot undergo the hydride transfer mechanism that is the driving force for the oxidation of alcohols and aldehydes. However, experiments with ketones clearly show that the ketone is highly reactive towards osmium(VIII) and causes osmium(VIII) to undergo precisely the same changes in its absorbance spectrum as does the reaction of the osmium(VIII) with alcohols. Therefore, there must be another mechanism at work. Ketones (and aldehydes) undergo a range of reactions in basic medium that were discussed in Chapter 4. They undergo carbonyl condensation reactions, the formation of gem diols and enolates. However, none of these reactions produces a product that contains an  $\alpha$ -hydrogen. Enolates, however, contain a C-C double bond and, as was demonstrated in Chapter 8 and was discussed in Chapter 3, alkenes are highly reactive towards osmium(VIII). The mechanism in Figure 9.6 is an adaptation of the standard, accepted osmium(VIII)-alkene reaction.

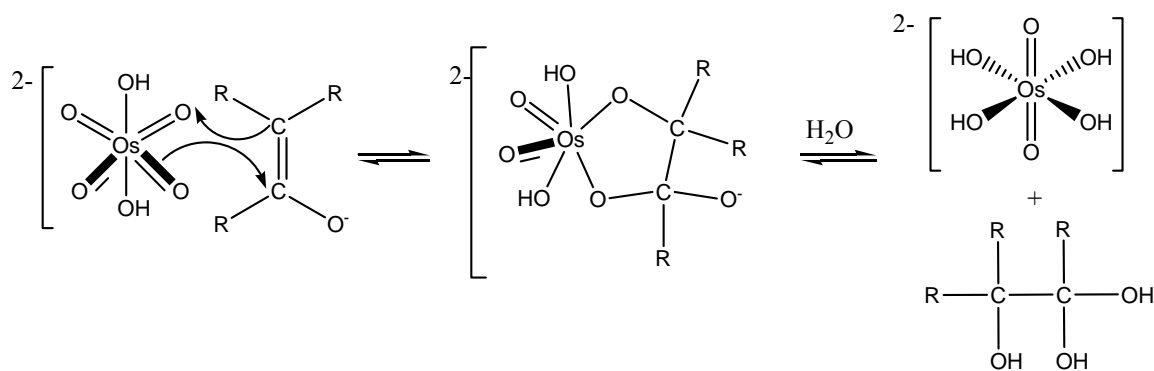


**Figure 9.6: Part 2 of the hydride transfer model for secondary alcohols. The reaction mechanism for the reaction of an ketone with osmium(VIII) in basic medium. Note that the reactive organic species is the enolate ion.**

Figure 9.6 above shows that the enolate ion is the reactive organic species. This forms a five-membered ring with the osmium(VIII) according to conventionally accepted studies<sup>(11, 13, 38)</sup>. This ring is under steric strain and rapidly hydrolyses to the osmate ion and a tri-substituted alcohol. Naturally, being an alcohol, this organic molecule will undergo further oxidation to form the products reported in Chapter 5 for each of the different substrates. Since the aldehydes are also capable of undergoing enol formation, it is feasible that it, too, undergoes the reaction mechanism depicted in Figure 9.6. However, since the major products in the oxidation of primary alcohols are their respective carboxylic acids, it seems that the mechanism in Figure 9.6 would be a minor pathway.

This concludes the discussion of the organic substrate reaction with osmium(VIII). However, another interesting and novel reaction was observed during this study. That was the interaction between the osmium(VIII) and the osmium(VI). This resulted in the increased absorbance observed on the progress curve during reaction with all the substrates. It was subsequently confirmed by titration of osmium(VIII) with osmium(VI), and from the stoichiometry and kinetic modelling, that there was complex formation between the osmium(VIII) and osmium(VI) in the ratio 2 to 1. The tendency of osmium to form polymeric species, particularly with oxo, nitrido or carboxylato bridges is documented<sup>(16)</sup>. Dimeric osmium(VI) and osmium(VIII) species are common

and the *syn*- and *anti*-dimeric monoesters of osmium(VI) and alkenes were discussed in Chapter 3. The species  $\text{Na}_2[\text{Os}_2\text{O}_6(\text{OH})_4]n\text{H}_2\text{O}$  was reported as being the product of a reaction between osmium tetroxide and sodium hydroxide in water-ethanol <sup>(16)</sup>. However, there are few documented trimers and few mixed-oxidation state polymeric compounds. This is an aspect of the research that certainly deserves further study. However, on the basis of the evidence thus far it is possible to postulate the following reaction between osmium(VIII) and osmium(VI).

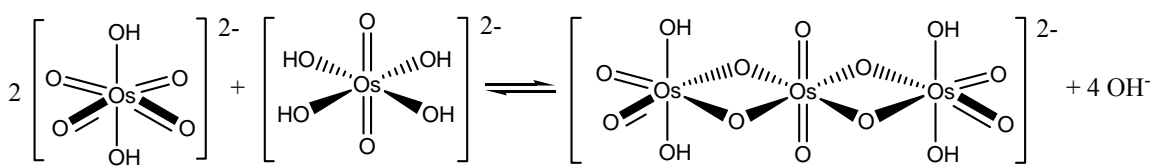


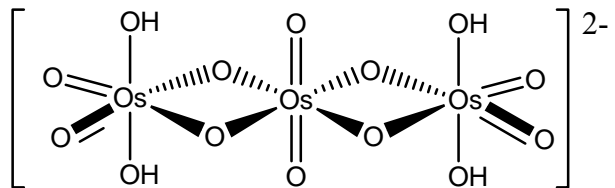
**Figure 9.7: Trimer formation between osmium(VIII) and osmium(VI)**

The trimer formation proceeds with the evolution of four hydroxide molecules. In effect this would increase the rate of the reverse reaction at increasing hydroxide concentrations. At the same time it would slow the rate of the forward reaction. However, the concentration of osmium(VI) is increasing more rapidly at increasing hydroxide concentrations because of the increase in the rate of the alcohol-osmium(VIII) reaction. Therefore the two reactions are working antagonistically, as far as hydroxide dependence is concerned.

This concludes the discussion on the mechanism of the osmium(VI)-alcohol reaction. The salient points can be summarised as follows:

1. Primary and secondary alcohols are oxidised to their respective aldehydes and ketones.
2. The  $\rho^*$ -value obtained is consistent with rate-limiting hydride transfer coupled with synchronous removal of the hydroxyl proton.
3. The reaction products suggest that aldehydes are oxidised via the same hydride transfer mechanism to their respective carboxylic acids in the major pathway.

4. Ketones (and aldehydes as a minor pathway) are oxidised via electrophilic attack on the C-C double bond of the enolate reactive intermediate.
5. Osmium(VIII) and osmium(VI) react to form a trimer:



in a side-reaction which is in dynamic equilibrium with the main osmium(VIII)-alcohol reaction.

6. Discontinuity in the Taft plot suggests that resonance plays a role in stabilising the intermediate in the benzyl alcohol reaction, thereby increasing the rate of the reaction.
7. Similarly a reversal in the Taft plot for 2-chloroethanol suggests that a change in mechanism to a proton abstraction mechanism is responsible for the increase in the rate of the reaction.

## REFERENCES

---

1. Rankin, K.N., Qing Liu, J.H., Henry Yee, Nazih A. Noureldin and Lee, D.G. *Tetrahedron Letters*. 1998, 39, 1095-1098.
2. Singh, H.S., Singh, S.P., Singh, S.M., Singh, R.K. and Sisodia, A.K. *The Journal of Physical Chemistry*. 1975, 79(18), 1920-1924.
3. Singh, N.P., Singh, V.N. and Singh, M.P. *Aust. J. Chem.* 1968, 21, 2913-8.
4. Singh, N.P., Singh, V.N., Singh, H.S., Singh, M.P. *Aust. J. Chem.* 1970, 23, 921-8.
5. Singh, V.N., Singh, H.S and Saxena, B.B.L. *J. Am. Chem. Soc.* 1969, 91(10), 2643-8.
6. Singh, Bharat, Singh, B.B. and Singh, R.P. *J Inorg. Nucl. Chem.* 1981, 43, 1283-6.
7. Subbaraman, L.R., Subbaraman, J. and Behrman, E.J. *Inorganic Chemistry*. 1972, 11(11), 2621-7.
8. Sharpless, K.B, Teranishi, A.Y. and Backvall, J.E. *J. Am. Chem. Soc.* 1976, 99(9), 3120-7.
9. Jordan, R.B. Reaction mechanisms of inorganic and organometallic systems. 2<sup>nd</sup> ed. 1998. Oxford University Press, Oxford.
10. Uma, K.V. and Mayanna, S.M. *Journal of Catalysis*. 1980, 61, 165-9.
11. Singh, H.S. Oxidation of Organic Compounds with Osmium Tetroxide. In: Organic synthesis by oxidation with metal compounds. 1986. Ed. W.J. Mijs & C.R.H. de Jonge. Plenum Press, New York.
12. Subbaraman, L.R., Subbaraman, J. and Behrman, E.J. *J. Org. Chem.* 1973, 38(8), 1499-1504.
13. Veerasomaiah, P., Reddy, K.B., Sethuram, B. and T. Navaneeth Rao. *J Indian Chem. Soc.* 1989, 66, 755-8.
14. Veerasomaiah, P., Reddy, K.B., Sethuram, B. and T. Navaneeth Rao. *J Indian Chem. Soc.* 1988, 27A, 876-9.
15. Menger, F.M, Ladika, M. *J. Am. Chem. Soc.* 1987, 109, 3145.
16. Griffith W.P. Osmium. In: Comprehensive Coordination Chemistry. The synthesis, reactions, properties and applications of coordination compounds. 1987. Vol 4. Ed. G. Wilkinson. Pergamon Press, Oxford.

17. Lay, PA and Harman, WD. *Recent advances in inorganic chemistry*. 1991, 37, 219-379
18. Griffith, WP. In: *The Chemistry of the Rarer Platinum Metals (Os, Ru, Ir & Rh)*. Chapter 3. 1967, Interscience.
19. [www.cns.uni.edu/](http://www.cns.uni.edu/)
20. Griffith, W.P. *Platinum Metals Review*. 2004, 48(4), 182-189.
21. Aldrich Chemical Company, Inc. Osmium tetroxide material safety and data sheet, 2001.
22. Brunot, F.R. *J Ind. Hyg. & Tox.* 1933, 136-143.
23. McLaughlin, AIG, Milton, R and Perry, KMA. *British J of Ind. Med.* 1946, 183-186.
24. <http://www.webelements.com/webelements/elements/text/Os/>
25. Criegee, R. *Liebigs Ann. Chem.* 1936, 522.
26. [http://www.acros.com/\\_Rainbow/pdf/AO\\_Oxidation\\_OSMIUM\\_DEF.pdf](http://www.acros.com/_Rainbow/pdf/AO_Oxidation_OSMIUM_DEF.pdf).
27. The Royal Swedish Academy of Sciences. Advanced information on the Nobel Prize in Chemistry 2001. [http://nobelprize.org/nobel\\_prizes/chemistry/laureates/2001/chemadv.pdf](http://nobelprize.org/nobel_prizes/chemistry/laureates/2001/chemadv.pdf).
28. Thomas, S and Zalbowitz, M. Fuel cells – Green Power. Los Alamos National Laboratory, New Mexico. Published by US Department of Energy.
29. Owen, J.R. Ion conducting polymers. In: *Electrochemical Science and Technology of Polymers – 1*. 1987. Ed. Linford, R.J. Elsevier Applied Science Publishers, Salem, Massachusetts.
30. Senapati, S; Ray, US; Santra, PK; Sinha, C; Slawin, AMZ and Woollins, JD. *Polyhedron*. 2002, 21, 753-762.
31. McFadzean, B.J. MSc Thesis. 2004, University of Port Elizabeth, South Africa.
32. Galbacs, ZM, Zsednai, A and Csanyi, LJ. *Transition metal chemistry*. 1983, 8, 328-332.
33. Krauss, F. & Wilken, D. *Z. Anorg. Allg. Chem.* 1925, 145, 151.
34. Chugaev, L. & Gritzmann, E. *Z. Anorg. Allg. Chem.* 1928, 172, 213.
35. Lott, KAK and Symons, MCR. *J. Chem. Soc.* 1960, 973.
36. Mouchel, B and Bremard, C. *J. Chem. Research (S)*. 1978, 312-313.
37. Collin, R.J., Jones, J. and Griffith, W.P. *J. Chem. Soc., Dalton Trans.* 1974. 1094.

38. McMurray, J. *Organic Chemistry* – 4<sup>th</sup> ed. 1996. Brooks/Cole Publishing Company, Pacific Grove, USA.
39. Bales, B.C., Brown, P., Dehestani, A. and Mayer, J.M. *J. Am. Chem. Soc.* 2005, 127(9). 2832-3.
40. Chugaev, L. & Gritzmann, E. *Z. Anorg. Allg. Chem.* 1928, 172, 213.
41. Sauerbrunn, RD and Sandell, EB. *J. Am. Chem. Soc.* 1953, 75, 3554.
42. Lee, JD. 1991. *Concise inorganic chemistry*. 4<sup>th</sup> ed. Chapman and Hall, London.
43. Kuzmic, P. 1996. “Program DYNAFIT for the analysis of enzyme kinetic data: Application to HIV proteinase.” *Anal. Biochem.* 237, 260-273.
44. House, J.E. *Principles of Chemical Kinetics*. 1997. Wm. C. Brown Publishers, London.
45. Isaacs, N.S. *Physical Organic Chemistry*. 2<sup>nd</sup> Ed. 1995. Addison Wesley Longman Ltd., Harlow.
46. Atkins, P.W. *Physical Chemistry*. 5<sup>th</sup> ed. 1994. Oxford University Press, Oxford.
47. Hine, J. *Physical Organic Chemistry*. 2<sup>nd</sup> Ed. 1962. McGraw-Hill Book Company, Inc, New York.
48. Blackwell, L.F. and Hardman, M.J. *Eur. J. Biochem.* 1975, 55, 611-615.
49. Johnson, C.D. *The Hammett Equation*. 1980. Cambridge University Press, Cambridge.
50. Cotton, FA and Wilkinson, G. *Advanced Inorganic Chemistry*. 4<sup>th</sup> ed. 1980, Wiley-Interscience, New York.
51. Cotton, S. *Chemistry of Precious Metals*. 1<sup>st</sup> ed. 1997, Blackie Academic and Professional, London.